

# Research and Development of a Combined Fuel Cell and Satellite Thruster System

Using Novel Hydrogen Peroxide Decomposition Techniques

Pieter Pinson

Master of Science Thesis





# Research and Development of a Combined Fuel Cell and Satellite Thruster System

Using Novel Hydrogen Peroxide Decomposition Techniques

by

Pieter Pinson

to obtain the degree of Master of Science,  
in the field of Aerospace Engineering,  
at the Delft University of Technology,  
to be defended publicly on June 22, 2022 at 9.30 am.

|                   |                                |          |                    |
|-------------------|--------------------------------|----------|--------------------|
| Student number:   | 4268687                        |          |                    |
| Project duration: | August 2, 2021 – June 22, 2022 |          |                    |
| Thesis committee: | Dr. J. Guo                     | TU Delft | <i>Chairholder</i> |
|                   | Dr. B.V.S. Jyoti               | TU Delft | <i>Supervisor</i>  |
|                   | Ir. J. Quesada Mañas           | SolvGE   | <i>Supervisor</i>  |
|                   | Dr. R. Noomen                  | TU Delft | <i>Committee</i>   |

This thesis is confidential and cannot be made public until June 22, 2023.

An electronic version of this thesis is available at <http://repository.tudelft.nl/>.

The work in this thesis was supported by SolvGE. Their cooperation is hereby gratefully acknowledged.



Copyright © Delft Department of Space Engineering



All rights reserved.



---

# Preface

This MSc thesis report shows the effort that has been put in researching the subjects of hydrogen peroxide, fuel cells and satellite thrusters. With it I conclude my study Spaceflight Engineering at the faculty of Aerospace Engineering (AE) and my time at the Delft University of Technology (TU Delft) in general. It has been a great privilege and honour to receive this education and go through the whole learning process. The project was conducted in collaboration with SolvGE, who provided me with the hydrogen peroxide and support throughout the period. The research itself has been conducted in the various labs in the aircraft hall of the faculty.

Firstly, I would like to thank my thesis committee, R. Noomen and J. Guo and my supervisors Botchu Jyoti and Jaime Quesada Mañas. Jyoti for her endless enthusiasm, close involvement and feedback on the project. Jaime for his critical feedback and advise on the thesis and experiments itself. Also, much appreciation to the SolvGE team for the all the tips and tricks on the subject and constantly showing interest in what I had to tell. Working together with Rinus and Emre on the different setups was really nice, helpful and mostly a lot of fun. Thank you to Larissa, Pranav and Nico who were there to help in the whole process. Of course many thanks to my girlfriend on helping and joining me in all the adventures during the studies and life. Lastly, a lot of gratitude to my friends and family for their support on which I could always rely.

Despite some setbacks during the MSc thesis study, a positive vibe predominates this period, in which a lot of skills were attained and experiences were gained. Mainly a better understanding of how all of the lessons are related to real life situations. I cannot wait to apply the knowledge I obtained during my studies to contribute to a better future by means of engineering similarly as I tried to do already during this project.

*Pieter Pinson*  
*Delft, June 9, 2022*



---

# Abstract

Various different challenges are being faced in the space industry, concerning the increased difficulty level of missions that are planned, down-scaling of the satellites and especially considering the toxicity of fuels used in the spacecraft. To systematically tackle these problems, requirements are set for a 'CubeSat' sized satellite for which a sustainable and environmental friendly power and propulsion system has to be developed. Many 'green' propellant options are there to deliver the power, of which mainly Hydrogen Peroxide ( $H_2O_2$ ) is considered a suitable option, because of its high energy density and reaction products being only water and oxygen. Besides being used in the propulsion system as propellant, the  $H_2O_2$  could then also be used as fuel and oxidizer to generate electric power in a fuel cell system.

The exothermic decomposing liquid is currently under investigation to provide thrust and electricity using catalyst materials, which experiences degradation of performance over time. Therefore, different long-lasting solutions have been experimented with, based on thermal decomposition of the  $H_2O_2$  and improved electro-reduction methods. This way, a green solution would be present to undertake various missions using small spacecraft that need around  $1N$  of thrust, while simultaneously delivering up to  $60W$  of extra power during its operation. Multiple Proof of Concept (PoC)'s were therefore developed to understand the processes and acquire the voltage, current and temperature data, generated and required by the systems. The energy required for decomposition of the  $H_2O_2$  using various resistance wires was recorded visually and with thermocouples. A drop test study was done for better understanding first, after which a safe injection setup was constructed where different conditions could be looked into. Various fuel cell structures were tested in a different experimental setup before this, to try and reach the extra power the thermal decomposition requires. A demonstration of the various ways this system could be optimized was then done, mainly by changing input parameters. Cooperation of the systems was looked into by checking the feasibility of combining them and incorporation in a CubeSat. Several electrochemical related properties prove to have large effects on the power density and potential and a maximum of  $4.5mW$  was reached. Similarly, the decomposition conditions of the propellant will have to be looked into more, since the  $24.8W$  currently needed for small mass flow rate decomposition, is excessive already.

This makes the incorporation in a combined system design difficult, but worth investigating, because of the many possibilities it brings forth. Based on the study performed so far it is concluded that providing enough sustainable electrochemical power for an efficient thermal decomposition is challenging, but feasible. To continue the research it is advised to improve the experimental setup instruments and robustness, such that effects of changes to the systems core components and cooperation can be looked into more closely. The required conditions and achieved results with  $H_2O_2$  will be presented in this research as well as recommendations to future work on this upcoming field of study.



---

# Table of Contents

|   |             |
|---|-------------|
| <b>Preface</b>  | <b>i</b>    |
| <b>Abstract</b>   | <b>iii</b>  |
| <b>List of Figures</b>                                      | <b>xi</b>   |
| <b>List of Tables</b>                                       | <b>xiii</b> |
| <b>Glossary</b>   | <b>xvii</b> |
| List of Acronyms . . . . .                                  | xvii        |
| List of Symbols . . . . .                                   | xviii       |
| <b>1 Introduction</b>                                       | <b>1</b>    |
| 1-1 Satellite Challenges . . . . .                          | 1           |
| 1-2 Satellite Power & Propulsion . . . . .                  | 1           |
| 1-3 Research Goals . . . . .                                | 3           |
| 1-3-1 Research Questions . . . . .                          | 3           |
| 1-3-2 Research Objectives . . . . .                         | 4           |
| 1-4 Report Outline . . . . .                                | 5           |
| <b>2 Literature Study</b>                                   | <b>7</b>    |
| 2-1 H <sub>2</sub> O <sub>2</sub> Thermochemistry . . . . . | 7           |
| 2-1-1 Decomposition . . . . .                               | 7           |
| Catalytic . . . . .   | 9           |
| 2-1-2 Safety Regulations . . . . .                          | 10          |
| 2-2 Satellite Thruster Theory . . . . .                     | 10          |

|          |   |           |
|----------|---|-----------|
| 2-2-1    | Ideal Rocket Equations . . . . .                            | 10        |
| 2-2-2    | Spacecraft Propulsion . . . . .                             | 12        |
|          | Mono-propellant . . . . .                                   | 12        |
|          | Bi-propellant . . . . .                                     | 13        |
| 2-2-3    | Decomposition Methods . . . . .                             | 14        |
|          | Electrothermal . . . . .                                    | 14        |
|          | Hypergolic & Pyrotechnic . . . . .                          | 15        |
| 2-3      | Fuel Cell Fundamentals . . . . .                            | 15        |
| 2-3-1    | Electric Power Generation . . . . .                         | 15        |
|          | Electric Power Performance . . . . .                        | 16        |
| 2-3-2    | H <sub>2</sub> O <sub>2</sub> Electrochemistry . . . . .    | 18        |
| 2-3-3    | Direct Liquid Fuel Cells . . . . .                          | 19        |
| 2-3-4    | H <sub>2</sub> O <sub>2</sub> Cell System Summary . . . . . | 20        |
| 2-4      | Conclusion . . . . .  | 22        |
| <b>3</b> | <b>Project Baseline</b> . . . . .                           | <b>23</b> |
| 3-1      | Satellite Requirements . . . . .                            | 23        |
| 3-2      | System Selection . . . . .                                  | 25        |
| 3-2-1    | Igniter Trade Off . . . . .                                 | 26        |
| 3-2-2    | Fuel Cell Trade Off . . . . .                               | 27        |
| 3-2-3    | Reference Systems . . . . .                                 | 29        |
|          | Thermal Decomposition Reference . . . . .                   | 29        |
|          | Fuel Cell Reference . . . . .                               | 30        |
| 3-3      | Engineering Challenges . . . . .                            | 31        |
| 3-3-1    | Material Compatibility . . . . .                            | 31        |
| 3-3-2    | Experiment Safety . . . . .                                 | 32        |
| 3-4      | Verification & Validation . . . . .                         | 33        |
| 3-4-1    | Instrumentation . . . . .                                   | 34        |
|          | General . . . . .   | 34        |
|          | Potentiostat . . . . .                                      | 34        |
|          | SEM & XRD . . . . .   | 35        |
|          | Digital Multimeter . . . . .                                | 35        |
|          | Thermocouples . . . . .                                     | 35        |

---

|          |   |           |
|----------|---|-----------|
| 3-4-2    | H <sub>2</sub> O <sub>2</sub> Concentration . . . . . | 36        |
| 3-5      | Analytical Models . . . . .                           | 36        |
| 3-5-1    | Fuel Cell Polarization . . . . .                      | 36        |
| 3-5-2    | Thermal Decomposition Capacity . . . . .              | 38        |
| 3-6      | Conclusion . . . . .                                  | 39        |
| <b>4</b> | <b>Fuel Cell System</b>                               | <b>41</b> |
| 4-1      | Fuel Cell Manufacturing . . . . .                     | 41        |
| 4-1-1    | Electrode Production . . . . .                        | 41        |
|          | Gas Diffusion Layer . . . . .                         | 42        |
|          | Catalyst Material . . . . .                           | 42        |
| 4-1-2    | Membrane . . . . .                                    | 45        |
| 4-1-3    | Membrane Electrode Assembly Production . . . . .      | 45        |
|          | Current Collectors . . . . .                          | 46        |
|          | Gaskets . . . . .                                     | 46        |
| 4-1-4    | Cell Structure Production . . . . .                   | 47        |
|          | Passive Construction . . . . .                        | 47        |
|          | Active Construction . . . . .                         | 48        |
| 4-2      | Test Preparation . . . . .                            | 48        |
| 4-2-1    | MEA Validation . . . . .                              | 49        |
| 4-2-2    | Instrumentation . . . . .                             | 51        |
| 4-2-3    | Test Setup . . . . .                                  | 51        |
| 4-2-4    | Experiments Overview . . . . .                        | 53        |
| 4-2-5    | Initial Results . . . . .                             | 53        |
| 4-3      | Fuel Cell Experiments . . . . .                       | 54        |
| 4-3-1    | Test Measurements . . . . .                           | 54        |
| 4-3-2    | Polarization Curve Procedure . . . . .                | 55        |
| 4-3-3    | Stability & Repeatability Procedures . . . . .        | 56        |
| 4-3-4    | Passive Cell Results . . . . .                        | 57        |
| 4-3-5    | Active Cell Results . . . . .                         | 58        |
| 4-3-6    | Fuel Cell Overview . . . . .                          | 59        |
| 4-4      | Performance Optimization Tests . . . . .              | 60        |
| 4-4-1    | Surface Area Results . . . . .                        | 60        |

|          |  |           |
|----------|--|-----------|
| 4-4-2    | Electrolyte Ratio Results . . . . .    | 61        |
| 4-4-3    | Flow Rate Increase . . . . .           | 61        |
|          | Flow Rate Results . . . . .            | 62        |
| 4-4-4    | Cell Stacking . . . . .                | 62        |
|          | Cell Stack Results . . . . .           | 63        |
| 4-4-5    | Electrolyte Composition . . . . .      | 64        |
| 4-5      | Discussion & Recommendations . . . . . | 65        |
| 4-5-1    | Reaction Kinetics . . . . .            | 65        |
| 4-5-2    | Setup Improvements . . . . .           | 67        |
| 4-6      | Conclusion . . . . .                   | 68        |
| <b>5</b> | <b>Decomposition Thruster</b>          | <b>69</b> |
| 5-1      | Experimental Preparation . . . . .     | 69        |
| 5-1-1    | Instrumentation . . . . .              | 70        |
|          | Thermocouples . . . . .                | 70        |
|          | Recordings . . . . .                   | 71        |
|          | Other Parameters . . . . .             | 71        |
| 5-1-2    | Heating Wire . . . . .                 | 72        |
| 5-2      | Drop Test Study . . . . .              | 72        |
| 5-2-1    | Experimental Setup . . . . .           | 72        |
| 5-2-2    | Results & Discussion . . . . .         | 73        |
|          | Injection . . . . .                    | 75        |
|          | Insulation . . . . .                   | 76        |
|          | Drop Decomposition . . . . .           | 76        |
|          | Solution Summary . . . . .             | 77        |
| 5-3      | Injected Flow Study . . . . .          | 78        |
| 5-3-1    | Injection Setup . . . . .              | 79        |
|          | Injector Specifications . . . . .      | 80        |
| 5-3-2    | Decomposition Results . . . . .        | 81        |
|          | Experimental Outcomes . . . . .        | 83        |
|          | Heating Wire Results . . . . .         | 87        |
| 5-4      | Plasma Arc Decomposition . . . . .     | 92        |
| 5-4-1    | Electrical Discharge . . . . .         | 92        |



---

|  |            |
|--|------------|
| High Voltage Generator . . . . .           | 93         |
| 5-4-2 Arc Drop Test . . . . .              | 93         |
| Arc Experimental Setup . . . . .           | 94         |
| Discharge Drop Results . . . . .           | 94         |
| 5-4-3 Injection Arc Experiments . . . . .  | 96         |
| 5-5 Discussion & Recommendations . . . . . | 97         |
| 5-5-1 Heating Wire Improvements . . . . .  | 97         |
| 5-5-2 Arc Improvements . . . . .           | 98         |
| 5-6 Conclusion . . . . .                   | 99         |
| <b>6 Combined Satellite System</b>         | <b>101</b> |
| 6-1 Cooperative System . . . . .           | 101        |
| 6-1-1 Performance Evaluation . . . . .     | 101        |
| Propulsion System . . . . .                | 101        |
| Power System . . . . .                     | 102        |
| 6-1-2 Propellant Combination . . . . .     | 103        |
| Reaction Products . . . . .                | 103        |
| 6-1-3 Effectiveness Increase . . . . .     | 104        |
| Heat Loss Minimizing . . . . .             | 104        |
| Other Applications . . . . .               | 104        |
| 6-2 Spacecraft Incorporation . . . . .     | 104        |
| 6-2-1 Thruster System . . . . .            | 105        |
| Inlet & Injection . . . . .                | 105        |
| Decomposition Chamber . . . . .            | 106        |
| 6-2-2 Fuel Cell System . . . . .           | 106        |
| Propellant Supply . . . . .                | 107        |
| 6-3 Conclusion . . . . .                   | 107        |
| <b>7 Summary</b>                           | <b>109</b> |
| 7-1 Conclusions . . . . .                  | 109        |
| 7-2 Recommendations . . . . .              | 111        |
| <b>Bibliography</b>                        | <b>113</b> |

---

|   |            |
|---|------------|
| <b>Appendices</b>                               | <b>125</b> |
| -1 SEM, EDS & XRD Manual . . . . .              | 125        |
| -2 Keithley Measurement Manual . . . . .        | 132        |
| -3 High-Speed Recording Camera Manual . . . . . | 133        |
| -4 Thermocouple Measurement Manual . . . . .    | 134        |
| -5 Material Compatibility Sheet . . . . .       | 135        |
| -6 90% Hydrogen Peroxide Safety Sheet . . . . . | 145        |

---

## List of Figures

|      |  |    |
|------|--|----|
| 1-1  | Thrust vs Specific Impulse for Various Micro-Propulsion Systems [86]                 | 2  |
| 1-2  | Power vs Duration of Various Satellite Power Source Possibilities [81]               | 3  |
| 2-1  | H <sub>2</sub> O <sub>2</sub> Decomposition Properties [68]                          | 8  |
| 2-2  | Concentration vs Heat for Self-Accelerated Decomposition [117]                       | 8  |
| 2-3  | High Concentration H <sub>2</sub> O <sub>2</sub> Safety Concerns                     | 10 |
| 2-4  | Mono-propellant System Design [60]   | 12 |
| 2-5  | Bi-propellant System Design [60]   | 13 |
| 2-6  | Bi-propellant Combination Performance [42]   | 13 |
| 2-7  | Resistojet Thruster Design [22]  | 14 |
| 2-8  | Schematic Fuel Cell System Design [49]   | 16 |
| 2-9  | Polarization Curve [109]   | 17 |
| 2-10 | Current Density vs (Mixed) Potential [4]   | 19 |
| 2-11 | Direct Liquid Fuel Cell (DLFC) System Structure [93]                                 | 19 |
| 3-1  | Dry Mass vs Specific Impulse for Various Micro-propulsion Systems [22]               | 24 |
| 3-2  | Power vs Thrust for Various Electric Micro-propulsion Systems [22]                   | 25 |
| 3-3  | Heating Wire, a) Model, b) Picture, c) Double Coil Example [80]                      | 29 |
| 3-4  | Active Cell Reference From Literature [132]  | 30 |
| 3-5  | Material Chemical Compatibility Test Examples  | 31 |
| 3-6  | Performance Results From Polarization Model  | 37 |
| 3-7  | Power & Temperature vs H <sub>2</sub> O <sub>2</sub> Concentration                   | 38 |
| 3-8  | Power vs Temperature Increase of High-Test Peroxide (HTP) Taken From Literature [36] | 39 |

|      |   |    |
|------|---|----|
| 4-1  | Soaking Deposition Process With Carbon Paper (CP)                                   | 43 |
| 4-2  | CP Spraying Setup   | 44 |
| 4-3  | Nickel Foam Electrodeposition Setup   | 45 |
| 4-4  | Hot Press Plate Filled With Various Membrane Electrode Assembly (MEA)'s             | 46 |
| 4-5  | MEA With Copper Current Collectors  | 47 |
| 4-6  | Passive Fuel Cell Structural Design   | 48 |
| 4-7  | Microscopic Images of the Palladium Deposited on Carbon Fiber Cloth (CFC)           | 49 |
| 4-8  | Microscopic Image & Energy Dispersive X-Ray Spectroscopy (EDS) of Nickel Deposition | 50 |
| 4-9  | X-Ray Diffractometry (XRD) Analysis of Electrodes                                   | 50 |
| 4-10 | Fuel Cell Test Setup Infrastructures  | 52 |
| 4-11 | H <sub>2</sub> O <sub>2</sub> Fuel Cell Experimental Setup                          | 52 |
| 4-12 | Fuel Cell Functioning and MEA Setup   | 53 |
| 4-13 | Passive Fuel Cell Failed Experiment Outcomes  | 54 |
| 4-14 | Fuel Cell Procedure Raw Current & Voltage Data                                      | 55 |
| 4-15 | Fuel Cell Manual Polarization Test Close-up   | 56 |
| 4-16 | Fuel Cell Circuit 220Ω Resistance Stability Test                                    | 57 |
| 4-17 | Passive Cell Refill Stability Test  | 57 |
| 4-18 | Passive Cell Polarization Test Results  | 58 |
| 4-19 | Active Cell Polarization Test Results   | 59 |
| 4-20 | Experimental Fuel Cell Results Overview   | 59 |
| 4-21 | Passive Cell Surface Area Tests   | 60 |
| 4-22 | Active Cell Electrolyte Concentration Test Results                                  | 61 |
| 4-23 | Fuel Cell High Flow Rate Setup  | 62 |
| 4-24 | Fuel Cell Flow Rate Results   | 63 |
| 4-25 | Active Cell Stack Setups  | 63 |
| 4-26 | Active Cell 'Stacked' Results   | 64 |
| 4-27 | Active Cell Electrolyte Results   | 65 |
| 5-1  | First Drop Test Study Setup Infrastructure  | 73 |
| 5-2  | Final Drop Test Study Setup Overview  | 74 |
| 5-3  | First Drop Test Setup Experimental Results  | 75 |
| 5-4  | Color Visual 97% H <sub>2</sub> O <sub>2</sub> Decomposition Recording              | 77 |
| 5-5  | High Speed 97% H <sub>2</sub> O <sub>2</sub> Decomposition Recording                | 77 |

---

|      |   |     |
|------|---|-----|
| 5-6  | Injection Setup Infrastructure . . . . .  | 79  |
| 5-7  | Final Injected Flow Study Setup Overview . . . . .  | 80  |
| 5-8  | Injected H <sub>2</sub> O <sub>2</sub> Propagation Experiment . . . . .                           | 81  |
| 5-9  | Heating Coil Configuration Test Recordings . . . . .  | 82  |
| 5-10 | Setup Failure Examples . . . . .  | 84  |
| 5-11 | Water Reference Test Results . . . . .  | 85  |
| 5-12 | H <sub>2</sub> O <sub>2</sub> Droplet Accumulating Inside Heating Wire . . . . .                  | 85  |
| 5-13 | Partial Decomposition Test Result Cases . . . . .   | 86  |
| 5-14 | Steady State Decomposition Test Results . . . . .   | 87  |
| 5-15 | Wire Type and Outcome Dependency . . . . .  | 88  |
| 5-16 | Power Range Outcome Classification . . . . .  | 88  |
| 5-17 | Concentration Outcome Classification . . . . .  | 89  |
| 5-18 | Power Range Decomposition Cases . . . . .   | 90  |
| 5-19 | Concentration Decomposition Cases . . . . .   | 90  |
| 5-20 | Power vs Temperature Filtered Decomposition Cases . . . . .                                       | 91  |
| 5-21 | Concentration vs Temperature Filtered Decomposition Cases . . . . .                               | 91  |
| 5-22 | Commercial Arc Generator . . . . .  | 93  |
| 5-23 | Thermocouple 1 Readings During Arc Discharge . . . . .  | 94  |
| 5-24 | Camera Recording of 3V, 1.72A Arc Discharge 97% H <sub>2</sub> O <sub>2</sub> Drop Test . . . . . | 95  |
| 5-25 | 6V, 2.91A, Arc Discharge During 97% H <sub>2</sub> O <sub>2</sub> Flow Injection . . . . .        | 96  |
| 6-1  | Combined Satellite System Infrastructure . . . . .  | 105 |



---

# List of Tables

|     |  |    |
|-----|--|----|
| 1-1 | Small Satellite Classification . . . . .   | 1  |
| 1-2 | Averaged Environmental Friendly Mono-propellant Options [91] . . . . .                         | 2  |
| 2-1 | H <sub>2</sub> O <sub>2</sub> Properties [90] . . . . .  | 7  |
| 2-2 | H <sub>2</sub> O <sub>2</sub> Fuel Cell Electrochemical Reactions and Potentials [6] . . . . . | 18 |
| 2-3 | Various DLFC Fuel Reactions [2] . . . . .  | 20 |
| 2-4 | Fuel Cell Systems Literature Overview . . . . .  | 20 |
| 2-4 | Fuel Cell Systems Literature Overview . . . . .  | 21 |
| 2-4 | Fuel Cell Systems Literature Overview . . . . .  | 22 |
| 3-1 | Requirements for the Satellite Power and Propulsion System . . . . .                           | 24 |
| 3-2 | Decomposition System Trade Off . . . . .   | 26 |
| 3-3 | Fuel Cell System Trade Off . . . . .   | 27 |
| 3-4 | Fuel Cell Study Reference Parameters Overview . . . . .  | 31 |
| 3-5 | Material, Chemical and Environmental Conditions Compatibility Overview . . . . .               | 32 |
| 3-6 | Fuel Cell Performance Constants . . . . .  | 37 |
| 4-1 | Keithley 2701 Measurement Specifications . . . . .   | 51 |
| 4-2 | Number Of Fuel Cell Experiments Performed . . . . .  | 53 |
| 4-3 | Fuel Cell Recommendations Overview . . . . .   | 68 |
| 5-1 | K-type Thermocouple Specifications . . . . .   | 70 |
| 5-2 | Nichrome 60 AWG 24 Specifications . . . . .  | 72 |
| 5-3 | Drop Experiment Settings Summary . . . . .   | 74 |
| 5-4 | Nebuliser Disc Injector Specifications . . . . .   | 81 |

|     |   |    |
|-----|---|----|
| 5-5 | Number Of Injected H <sub>2</sub> O <sub>2</sub> Experiments Performed (15-30W, 30-45W, 45-60W) . . . . . | 83 |
| 5-6 | Commercial Arc Generator Specifications . . . . .   | 94 |
| 5-7 | Decomposition System Recommendations Overview . . . . .   | 99 |



---

# Glossary

## List of Acronyms

|                                   |   |
|-----------------------------------|---|
| <b>ABS</b>                        | Acrylonitrile Butadiene Styrene   |
| <b>AE</b>                         | Aerospace Engineering   |
| <b>AEM</b>                        | Anion Exchange Membrane   |
| <b>AHP</b>                        | Analytical Hierarchy Process  |
| <b>AWG</b>                        | American Wire Gauge   |
| <b>CAD</b>                        | Computer Aided Design   |
| <b>CEM</b>                        | Cation Exchange Membrane  |
| <b>CFC</b>                        | Carbon Fiber Cloth  |
| <b>GC</b>                         | Gas Chromatography  |
| <b>CP</b>                         | Carbon Paper  |
| <b>CJC</b>                        | Cold Junction Compensation  |
| <b>CTC</b>                        | Charge Transfer Coefficient   |
| <b>DAQ</b>                        | Data Acquisition System   |
| <b>DDT</b>                        | Decomposition Delay Time  |
| <b>DLFC</b>                       | Direct Liquid Fuel Cell   |
| <b>DMM</b>                        | Digital Multi Meter   |
| <b>EDS</b>                        | Energy Dispersive X-Ray Spectroscopy                                    |
| <b>EPDM</b>                       | Ethylene Propylene Diene Monomer  |
| <b>GDL</b>                        | Gas Diffusion Layer   |
| <b>GHS</b>                        | Globally Harmonised System of Classification and Labelling of Chemicals |
| <b>H<sub>2</sub>O<sub>2</sub></b> | Hydrogen Peroxide   |
| <b>HPOR</b>                       | Hydrogen Peroxide Oxidation Reaction                                    |
| <b>HPRR</b>                       | Hydrogen Peroxide Reduction Reaction                                    |
| <b>HTP</b>                        | High-Test Peroxide  |
| <b>LEO</b>                        | Low Earth Orbit   |
| <b>NFPA</b>                       | National Fire Protection Association                                    |

|                 |                                  |
|-----------------|----------------------------------|
| <b>NI</b>       | National Instruments             |
| <b>NTO</b>      | Dinitrogen Tetroxide             |
| <b>MEA</b>      | Membrane Electrode Assembly      |
| <b>MMH</b>      | Monomethylhydrazine              |
| <b>MPL</b>      | Micro Porous Layer               |
| <b>MSDS</b>     | Material Safety Data Sheet       |
| <b>OAP</b>      | Orbit Average Power              |
| <b>OCP</b>      | Open Circuit Potential           |
| <b>ORR</b>      | Oxidation Reduction Reaction     |
| <b>PEM</b>      | Polymer Exchange Membrane        |
| <b>PLA</b>      | Poly Lactic Acid                 |
| <b>PoC</b>      | Proof of Concept                 |
| <b>PTFE</b>     | Polytetrafluoroethylene          |
| <b>PVC</b>      | Polyvinyl Chloride               |
| <b>PVDF</b>     | Polyvinylidene Fluoride          |
| <b>RPA</b>      | Rocket Propulsion Analysis       |
| <b>SMD</b>      | Sauter Mean Diameter             |
| <b>SEM</b>      | Scanning Electron Microscopy     |
| <b>SS</b>       | Stainless Steel                  |
| <b>TEG</b>      | Thermoelectric Generator         |
| <b>TPE</b>      | Thermoplastic Elastomer          |
| <b>TRL</b>      | Technology Readiness Level       |
| <b>TU Delft</b> | Delft University of Technology   |
| <b>XPS</b>      | X-Ray Photoelectron Spectroscopy |
| <b>XRD</b>      | X-Ray Diffractometry             |

## List of Symbols

### Roman

|                  |                        |              |
|------------------|------------------------|--------------|
| $\bar{R}$        | Universal gas constant | $J/(mol\ K)$ |
| $\bar{R}_{spec}$ | Specific gas constant  | $J/(kg\ K)$  |
| $\Delta G$       | Gibbs free energy      | $J$          |
| $\Delta H$       | Heat of reaction       | $J/mol$      |
| $\Delta P$       | Pressure drop          | $Pa$         |
| $\Delta S$       | Change in entropy      | $J/(mol\ K)$ |
| $\Delta v$       | Change in velocity     | $m/s$        |

---

|              |   |             |
|--------------|---|-------------|
| $\dot{m}$    | Mass flow rate  | $kg/s$      |
| $A$          | Surface area  | $m^2$       |
| $a$          | Empirical efficiency constant 1                       | —           |
| $a_c$        | Drop size constant                                    | —           |
| $A_e$        | Nozzle exit area                                      | $m^2$       |
| $a_k$        | Activity of species $k$                               | —           |
| $A_t$        | Nozzle throat area                                    | $m^2$       |
| $A_{emp}$    | Empirical constant                                    | —           |
| $A_{sat}$    | Saturation ionization constant                        | $1/(Pa\ m)$ |
| $B$          | Magnetic field strength                               | $A/m$       |
| $b$          | Empirical efficiency constant 2                       | —           |
| $B_{ex}$     | Excitation and ionization energy constant             | $V/(Pa\ m)$ |
| $C$          | Capacitance   | $F$         |
| $c$          | Molar concentration                                   | $mol/L$     |
| $c_v$        | Specific heat capacity at constant volume             | $J/(kg\ K)$ |
| $c_{pg}$     | Specific heat capacity at constant pressure of gas    | $J/(kg\ K)$ |
| $c_{pl}$     | Specific heat capacity at constant pressure of liquid | $J/(kg\ K)$ |
| $d$          | Distance  | $m$         |
| $d_{out}$    | Outer diameter  | $m$         |
| $E$          | Electric field strength                               | $V/m$       |
| $E_r^0$      | Reversible cell potential at standard conditions      | $V$         |
| $E_a$        | Activation potential losses                           | $V$         |
| $E_c$        | Concentration potential losses                        | $V$         |
| $E_o$        | Ohmic potential losses                                | $V$         |
| $E_r$        | Reversible cell potential                             | $V$         |
| $E_{cell}$   | Cell potential  | $V$         |
| $Ed$         | Energy density  | $J/m^3$     |
| $F$          | Faraday constant                                      | $A\ s/mol$  |
| $F_{thrust}$ | Thrust force  | $N$         |
| $g_0$        | Gravitational acceleration                            | $m/s^2$     |
| $I$          | Electric current                                      | $A$         |
| $I_0$        | Exchange current density                              | $A/m^2$     |
| $I_i$        | Fuel crossover and internal current losses            | $A$         |
| $I_m$        | Limiting cell current                                 | $A$         |
| $I_{cap}$    | Capacitance current                                   | $A$         |
| $I_{sp}$     | Specific impulse                                      | $s$         |
| $Id$         | Current density                                       | $A/m^2$     |
| $k$          | Reaction rate   | $1/s$       |
| $k_b$        | Boltzmann constant                                    | $J/K$       |
| $L$          | Length  | $m$         |

|            |                             |          |
|------------|-----------------------------|----------|
| $L^*$      | Characteristic length       | $m$      |
| $L_h$      | Latent heat of vaporization | $J/kg$   |
| $M$        | Molar mass                  | $kg/mol$ |
| $m$        | Mass                        | $kg$     |
| $m_0$      | Initial mass                | $kg$     |
| $m_1$      | Final mass                  | $kg$     |
| $Ma$       | Mach number                 | –        |
| $n$        | Number of electrons         | –        |
| $n_{ref}$  | Refractive index            | [–]      |
| $P$        | Power                       | $W$      |
| $p$        | Pressure                    | $Pa$     |
| $p_0$      | Ambient pressure            | $Pa$     |
| $p_c$      | Chamber pressure            | $Pa$     |
| $p_e$      | Nozzle exit pressure        | $Pa$     |
| $P_h$      | Heating power               | $W$      |
| $P_p$      | Hydraulic pump power        | $W$      |
| $Pd$       | Surface power density       | $W/m^2$  |
| $Q$        | Volumetric flow rate        | $m^3/s$  |
| $q$        | Electric charge             | $A s$    |
| $R$        | Resistance                  | $\Omega$ |
| $r$        | Location                    | $m$      |
| $R_c$      | Cell resistance             | $\Omega$ |
| $R_e$      | Electronic cell resistance  | $\Omega$ |
| $R_i$      | Ionic cell resistance       | $\Omega$ |
| $T$        | Temperature                 | $K$      |
| $t$        | Time                        | $s$      |
| $T_0$      | Starting temperature        | $K$      |
| $T_c$      | Chamber temperature         | $K$      |
| $T_{boil}$ | Boiling temperature         | $K$      |
| $T_{melt}$ | Melting temperature         | $K$      |
| $U$        | Voltage                     | $V$      |
| $U_b$      | Breakdown voltage           | $V$      |
| $u_f$      | Fuel utilization efficiency | –        |
| $u_r$      | Fuel reformer efficiency    | –        |
| $V$        | Volume                      | $m^3$    |
| $v$        | Velocity                    | $m/s$    |
| $V_c$      | Chamber volume              | $m^3$    |
| $v_e$      | Effective exhaust velocity  | $m/s$    |
| $v_s$      | Speed of sound              | $m/s$    |
| $v_{inj}$  | Injection velocity          | $m/s$    |

---

**Greek**

|               |                              |                 |
|---------------|------------------------------|-----------------|
| $\alpha$      | Charge transfer coefficient  | –               |
| $\epsilon$    | Electrical permittivity      | $F/m$           |
| $\eta_c$      | Power conditioner efficiency | –               |
| $\eta_p$      | Parasitic power efficiency   | –               |
| $\eta_{cell}$ | Cell efficiency              | –               |
| $\gamma$      | Heat capacity ratio          | –               |
| $\gamma_{se}$ | Second Townsend coefficient  | –               |
| $\mu$         | Dynamic viscosity            | $Pa\ s$         |
| $\nu$         | Stoichiometric coefficient   | –               |
| $\rho$        | Density                      | $kg\ m^3$       |
| $\rho_r$      | Electrical resistivity       | $\Omega\ m$     |
| $\sigma$      | Electrical conductivity      | $1/(\Omega\ m)$ |
| $\sigma_s$    | Surface tension              | $N/m$           |



---

# Chapter 1

---

## Introduction

Satellite power and propulsion is a field of study that is constantly changing due to technological advances. More challenging missions are being planned which each require their own special needs [54]. Besides this, there is an increase in down-scaling of the satellites nowadays [14]. Finally, a turnaround is necessary concerning the toxicity of fuels used in the space industry [26]. In this master thesis report, the subject of using Hydrogen Peroxide ( $H_2O_2$ ) decomposition for fuel cell and thruster applications in satellites is researched. This chapter will elaborate on why this is necessary and what exactly are the goals of the research.

### 1-1 Satellite Challenges

Depending on the mission type and mass of the satellite, the requirements regarding power and propulsion for the spacecraft are specified [84] [85]. An increasingly popular type of satellite that is being launched is the ‘CubeSat’, which varies from 1U up to 32U or more. Each U represents a  $10 \times 10 \times 10 \text{ cm}$  unit building block, weighing around  $1 - 2 \text{ kg}$ , meaning this type falls within the range of nano- and micro-satellites in Table 1-1 [62] [116]. Due to its relatively low costs and countless possibilities [20], research is done by universities such as the Delft University of Technology (TU Delft), where there is a lot of knowledge available already from developing CubeSats [115]. For the purpose of developing novel techniques within this thesis research, the focus will thus be on nano- or micro-satellite sized systems.

**Table 1-1:** Small Satellite Classification

| Class     | Femto | Pico  | Nano | Micro  | Mini    |
|-----------|-------|-------|------|--------|---------|
| Mass [kg] | <0.1  | 0.1-1 | 1-10 | 10-100 | 100-500 |

### 1-2 Satellite Power & Propulsion

A propulsion system is needed to control the small satellite and can be of any type shown in Figure 1-1. The amount of thrust required is dependent on the type of manoeuvre, but for Low Earth Orbit (LEO) maintenance, a continuous thrust to weight ratio of  $10^{-5} \text{ N/kg}$  should

suffice [30]. With ambitious lunar and interplanetary missions, requirements are higher and a higher specific impulse and change in velocity are needed [51]. Currently, the smaller sized satellites mostly have simple cold gas and mono-propellant thruster, utilizing inert gasses and hydrazine. Therefore, the area of research will be a similar compact system which provides around 1N of thrust, aiming for high specific impulse.

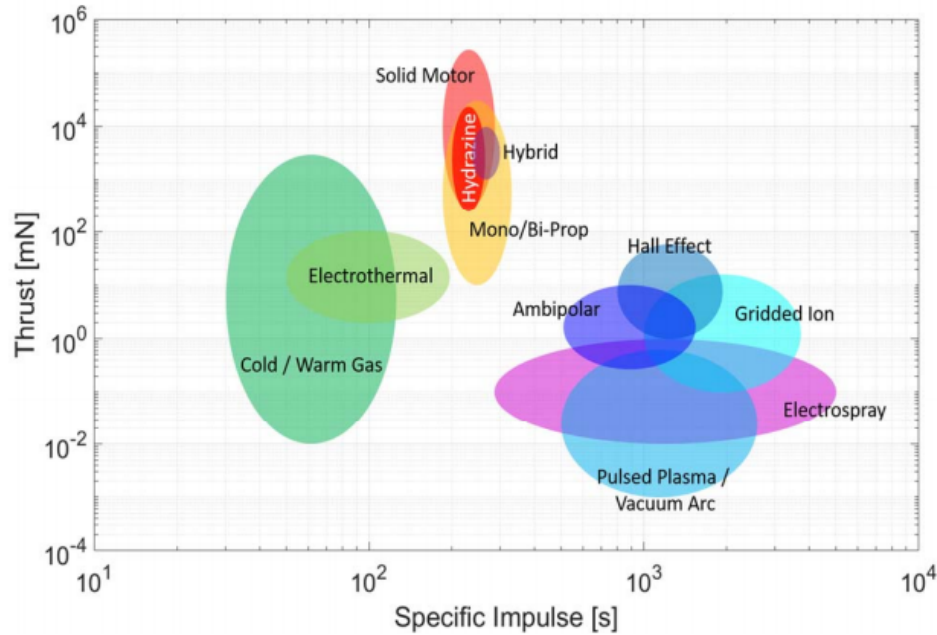


**Figure 1-1:** Thrust vs Specific Impulse for Various Micro-Propulsion Systems [86]

Research is required to solve the problem of the toxic propellants currently used and to improve the sustainability of this propulsion type [41]. Instead of decomposing the liquid hydrazine with a catalyst, a different propellant and thruster should be used. Since CubeSats are often piggybacking on larger satellite missions, this propellant can not be under high pressure or be easily self-ignited. A lot of research has been done to find this ‘greener’ solution, resulting in the options shown in Table 1-2 [27]. The most suited regarding its benign properties, high energy density liquid state and reaction products would be to use high concentration  $H_2O_2$  [123].  $H_2O_2$  is essentially water with an extra oxygen atom into which it will also decompose exothermically if triggered. This choice is also based on its availability during this graduation project and its possibilities for usage within the space industry [100] [42] [124]. The chemical is namely already being used in rocketry applications and when above 70% concentration it is referred to as High-Test Peroxide (HTP). It is definitely not the propellant with the highest specific impulse, but this can be improved when it is used as an oxidizer with various other fuels in a bi-propellant system.

**Table 1-2:** Averaged Environmental Friendly Mono-propellant Options [91]

| Propellant type      | HAN              | ADN              | $NO_x(l)$        | $H_2O_2$         |
|----------------------|------------------|------------------|------------------|------------------|
| Specific Impulse [s] | $\bar{x} = 256$  | $\bar{x} = 255$  | $\bar{x} = 296$  | $\bar{x} = 170$  |
| Density [ $g/cm^3$ ] | $\bar{x} = 1.35$ | $\bar{x} = 1.31$ | $\bar{x} = 0.87$ | $\bar{x} = 1.40$ |



The method of decomposition can also be improved since currently there is a degradation in performance because of the catalyst used. A more long-lasting solution would be to use an electrothermal way of decomposing, such as conductive heating, running the propulsion through an arc or electromagnetic radiation. This would however impose additional power requirements on the system, which would ideally be solved without a severe increase in system mass. Several options are there to provide this power shown in Figure 1-2, of which batteries and solar arrays are mostly being used at the moment.

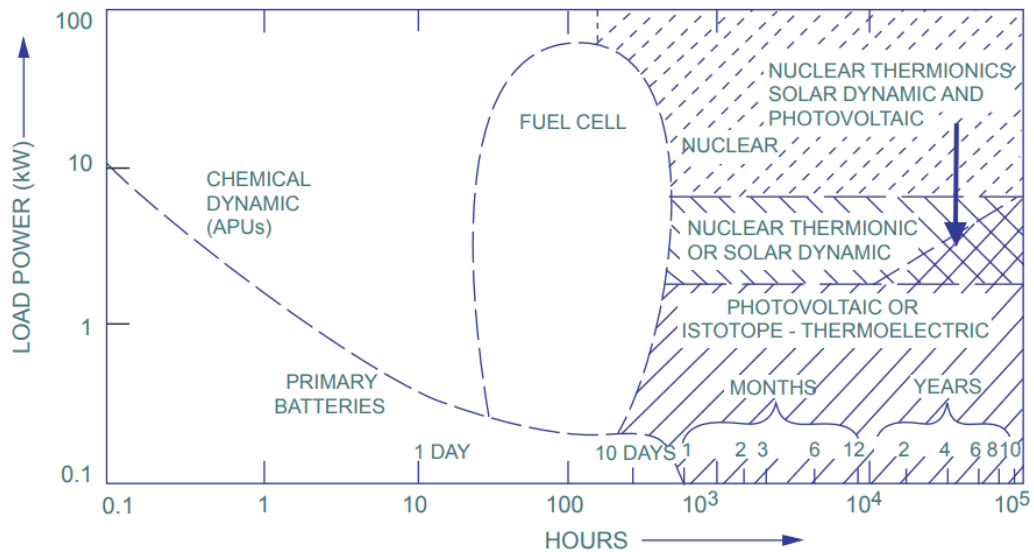


**Figure 1-2:** Power vs Duration of Various Satellite Power Source Possibilities [81]

When solar power is less available due to the type of mission or the satellite being in an eclipse; nuclear energy, thermal conversion or fuel cells can provide a solution. For usage in space, fuel cells have the highest efficiency and a very high energy density, meaning the system can stay compact [109] [18]. Because no air is available in space to use as an oxidizer in the fuel cell, liquid  $H_2O_2$  could be used here as well, since it has the appropriate properties. The Technology Readiness Level (TRL) of this technique is however still low and further research is required for the development of such a system.

## 1-3 Research Goals

To be able to structurally tackle the challenges mentioned in Section 1-2, several objectives and questions are set out as guidance throughout this research. A concrete solution to the problems related to satellite power and propulsion and the use of  $H_2O_2$  should come forth from reaching those goals in the end.

### 1-3-1 Research Questions

The area of interest for this thesis project is mainly the actual development of a Proof of Concept (PoC) system. The field of research related to  $H_2O_2$  is so large that it has to be

well specified what the exact functions are going to be. The aim is not to tackle encountered problems using subsequent research, but to solve them by trying different system designs. This is thus incorporated into the main question, which goes as follows:

*How can  $H_2O_2$  be used in a satellite system to provide power as well as thrust most effectively and what would be the performance parameters?*

Since there are many cumbersome ways of providing power and thrust to a satellite, the 'effectively' statement is added, which is intended to scale down the options. This general question is then split up into more specific sub questions:

- What thermal decomposition system uses the least power per volume and mass to decompose HTP?
- What  $H_2O_2$  fuel cell structure and composition provides the most power and can easily be incorporated in a large CubeSat?
- Can the fuel cell and thruster designs be adjusted to fit one another and benefit from additional modifications?
- How can the systems be incorporated to function in a satellite, working together as much as possible?

It is expected that combining the  $H_2O_2$  power and propulsion systems is feasible and will be more beneficial than each system on its own.

### 1-3-2 Research Objectives

The main research objective of this thesis is related to the questions above and goes as follows:

*To investigate and develop a  $H_2O_2$  satellite fuel cell and thruster using novel decomposition techniques that are applied in a combined system, by researching the possibilities, designing the systems, setting up the tests and analyzing the experimental results.*

The goal of this research is thus to check the feasibility of such a combined system, by developing both individual systems first. Only then it can be investigated whether or not the energy required by the thermal decomposition system of the thruster can be generated from the same propellant by a fuel cell in the power system. To reach the general objective described above, some more specific sub-goals have been set up as well:

- Thermally decompose  $H_2O_2$  without a catalyst, by applying different decomposition methods in an experimental setup.
- Generate electricity via electroreduction of  $H_2O_2$  in a fuel cell setup, by applying different cell structures.

- Increase performance of the standard systems, by testing both under different conditions and compositions.
- Integrate both systems in a satellite architecture, using the PoC's to make a combined design.
- Report on the system, by evaluating its results to use for later recommendation re-considerations.

Although these are quite large tasks to fulfil, with the knowledge obtained from literature and experiments, the systems are expected to progress quickly. Each individual objective will add new knowledge to the research community since such tests have not yet been found to be performed.

## 1-4 Report Outline

The purpose of this report is to gain insight into the functionality of  $\text{H}_2\text{O}_2$  decomposition, fuel cells and satellite thrusters. Knowledge obtained from an experimental campaign, together with the research on existing applications, can be used to develop a combined system that is more sustainable. The goal of this report is thus to show the most suitable options for a combined  $\text{H}_2\text{O}_2$  power and propulsion system and describe how it functions and performs, based on the developed PoC's.

Before actually going into the lab, a literature study has been performed, shown in Chapter 2. In there, some fundamentals regarding  $\text{H}_2\text{O}_2$ , fuel cells and satellite thrusters are explained, followed by a study on experiments with these systems found in literature. After those are summarized, a system selection is made in Chapter 3, such that a clear project plan can be made based on several reference papers. The general aspects of the research are discussed there as well and some guidelines are set with the help of analytical models, before delving into the experiments of each individual system. First, the fuel cell campaign is described in Chapter 4, going through it chronologically; from preparation to tests and its results. Subsequently, the same is done for the thruster in Chapter 5, with a focus on creating a universal and safe setup. Then the two come together in Chapter 6, where the incorporation of each PoC in a CubeSat is discussed as well as how they can be combined into a single more efficient design. Finally, a conclusion is drawn and recommendations are set up in Chapter 7, referring back to the research goal that was set up in this chapter.



---

# Chapter 2

---

## Literature Study

Before the actual thesis project started, a period of over three months has already been spent on finding out how exactly fuel cells, thrusters and Hydrogen Peroxide ( $\text{H}_2\text{O}_2$ ) decomposition works. This information, together with additional knowledge obtained during the experimental campaign of the thesis is discussed in this chapter.

### 2-1 $\text{H}_2\text{O}_2$ Thermochemistry

The properties of  $\text{H}_2\text{O}_2$  make it a wanted substance that is widely used in industry for disinfecting and bleaching purposes [118]. It is composed of a water molecule with an additional oxygen atom, which is usually produced on a large scale with the help of an anthraquinone process [96] [57]. The reason to choose High-Test Peroxide (HTP) above other options in this study besides its truly harmless reaction products, is its availability during this research. In Table 2-1 the most relevant properties of pure  $\text{H}_2\text{O}_2$  are listed such as molar mass  $M$ , the density  $\rho$ , the melting and boiling temperature  $T_{\text{melt}}$  &  $T_{\text{boil}}$  and the latent heat of vaporization  $L_h$  (at 320K).

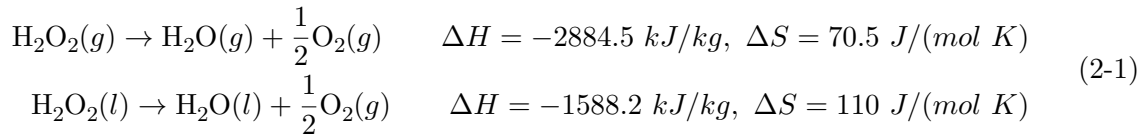
| $M$ [g/mol] | $\rho$ [g/m <sup>3</sup> ] | $T_{\text{melt}}$ [K] | $T_{\text{boil}}$ [K] | $c_{p_l}$ [J/(gK)] | $c_{p_g}$ [J/(gK)] | $L_h$ [J/g] |
|-------------|----------------------------|-----------------------|-----------------------|--------------------|--------------------|-------------|
| 34.01       | 1450                       | 272.7                 | 423.3                 | 2619               | 1267               | 1426        |

**Table 2-1:**  $\text{H}_2\text{O}_2$  Properties [90]

Other interesting quantities are the dynamic viscosity's  $\mu$ , which are  $1.249\text{mPa} \cdot \text{s}$  at 293 K and  $19\text{mPa} \cdot \text{s}$  at 573K in vapor. Compared to water,  $\text{H}_2\text{O}_2$  is heavier and stays in the liquid state longer when heated. Also, the specific heat capacity at constant pressure  $c_{p_l}$  &  $c_{p_g}$  of  $\text{H}_2\text{O}_2$  is lower for both liquid as gas, meaning less energy is required for heating.

#### 2-1-1 Decomposition

The thermal decomposition of  $\text{H}_2\text{O}_2$  is an exothermic reaction, as shown in Eq. (2-1). The amount of energy released, is dependent on its state, which will be primarily in gaseous form when HTP is used in thruster applications.



Here,  $\Delta H$  stands for the heat of reaction and  $\Delta S$  for the change in entropy, calculated according to Hess's law. The intermediate processes however, are somewhat more complex and contain many intermediate radical species each with their own rate constants [107]. The linear relations of the decomposition reaction products are visually shown in Figure 2-1, where an increase in  $\text{H}_2\text{O}_2$  concentration causes a rise in temperature and oxygen percentage.

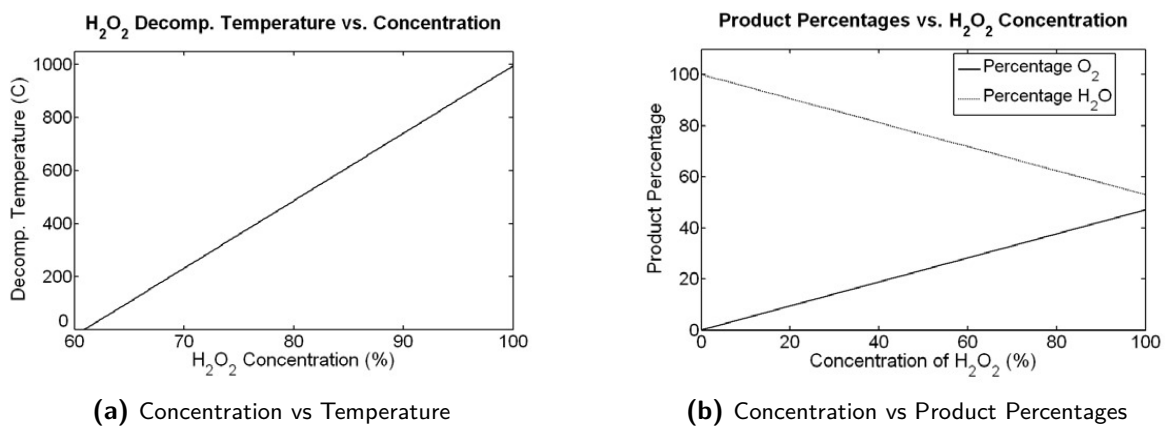


**Figure 2-1:**  $\text{H}_2\text{O}_2$  Decomposition Properties [68]

As soon as the temperature reaches a certain threshold, the decomposition reaction can self-accelerate due to the heat production. The amount of heat released and required in this process is captured in Figure 2-2, which shows that the reaction can become self-sustaining at around 64% concentration.

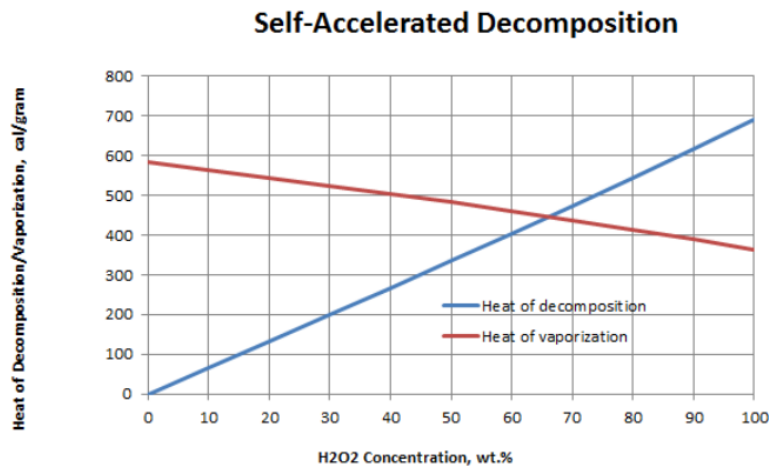


**Figure 2-2:** Concentration vs Heat for Self-Accelerated Decomposition [117]

Besides concentration and temperature, an increased pH value also causes the H<sub>2</sub>O<sub>2</sub> to be more unstable and the decomposition reaction rate  $k$  to increase [134]. In general, the reaction rate for vapor at low pressure,  $\approx 1000Pa$  changes according to Eq. (2-2), depending on temperature  $T$  and the universal gas constant  $\bar{R}$ , taken here specifically as  $1.987cal/(K mol)$  [39].

$$k = 10^{13} \cdot \exp\left(\frac{-48000}{\bar{R} \cdot T}\right) \quad (2-2)$$

Finally, impurities in the liquid, contact time and surface area specifications are also important parameters for the decomposition [106]. Mixing the liquid with other chemicals can cause a more stable H<sub>2</sub>O<sub>2</sub> solution, when for example gelling agents or stabilizers are added to increase the viscosity and stop the liquid from slowly decomposing over time. Or it can cause a chemical reaction to happen, which is unwanted in the case of contamination, but it can also be used for good when controlled.

In general there are several ways to achieve the decomposition; by adding photo, electric or thermal energy. Various ways of heating can be used, such as an arc, conductive or radiative, but mainly convective methods of initiating decomposition are used in literature. In the case of H<sub>2</sub>O<sub>2</sub>, the exothermic reaction can also be caused chemically, by using various catalysts.

### Catalytic

Due to its high reactivity, the easiest way to trigger a decomposition reaction is to use a type of catalyst; enzymes, hetero- and homogeneous substances. Systems utilizing H<sub>2</sub>O<sub>2</sub> mostly use a heterogeneous material, namely metals from the transition group. When in contact with each other, the decomposition reaction is initiated and heat is released. This means that next to the material used, the contact area is very influential. Commonly used catalysts in rocket engines are platinum, silver and manganese compounds, but also nickel, palladium and gold can be used, depending on the reaction kinetics required [44]. Metals such as iron, cause hydroxyl radicals to be formed and even non metallic substances such as potassium combinations, cause very fast reactions [98]. Ideally, a catalyst is not consumed and only acts as an activator, meaning the system should work as long as H<sub>2</sub>O<sub>2</sub> is present. In reality however, the currently used catalysts are degrading, meaning the performance of the above systems will go down over time as well. This is one of the reasons to research the other possibilities of decomposition activation or to optimize the catalyst.

The type of catalyst is selected on its function, which is in this case either as an electrode in a fuel cell or as an igniter in a thruster. Besides the discussed thermal activation, which is suitable in a propulsion system, there is also an electric reduction and oxidation process. The reaction caused by the catalyst can namely be electroreducing, in which it creates electric current without additional heat, which is ideal for the power application. The redox properties depend mainly on the pH of the solution and the catalyst used. The more precise reaction with H<sub>2</sub>O<sub>2</sub> in this process is explained later in Section 2-3-2. A third option would be the less desirable corroding reaction. This can cause for example rust and should thus for both applications be prevented. In any of the reactions described above the chemical products with H<sub>2</sub>O<sub>2</sub> are the same, being water and oxygen.

## 2-1-2 Safety Regulations

Overall, the usage of  $H_2O_2$  comes along with many improvements over other currently used substances in the space industry. There are however some drawbacks to its use, mainly related to explosive hazards [46]. Those are obviously caused by the decomposition reaction discussed in Section 2-1-1, which can cause thermal runaway when accidentally triggered. Related to this is the storage in a confined space, since  $H_2O_2$  will also slowly continuously decompose, where the oxygen gas can cause a pressure build up. Some more straightforward hazards are related to the handling of the liquid due to its corrosive nature. This is also recorded with the National Fire Protection Association (NFPA) diamond and Globally Harmonised System of Classification and Labelling of Chemicals (GHS) symbols shown in Figure 2-3a [88]. Careful operation of the chemical is thus necessary, as a tiny drop of high concentration can already cause painful bleaching stains, as shown in Figure 2-3b. The Material Safety Data Sheet (MSDS) of 90%  $H_2O_2$  is added as appendix -6 for further reference.



(a) GHS Symbols & NFPA Diamond



(b) Bleached Finger Skin

Figure 2-3: High Concentration  $H_2O_2$  Safety Concerns

## 2-2 Satellite Thruster Theory

In this section the system in which  $H_2O_2$  is most commonly used in the space industry is explained. This could either be as mono-propellant after catalytic decomposition, or as an oxidizer in a bi-propellant system. The basic equations taken from Zandbergen [137] and Sutton [113] are explained first, after which the decomposition methods of  $H_2O_2$  propellant is looked into in more detail.

### 2-2-1 Ideal Rocket Equations

In the case of chemical rockets as is investigated in this research, the ideal rocket theory can be used. Therefore, the standard rocket equations shown in Eq. (2-3) apply, from which the thrust force  $F_{thrust}$ , change in velocity  $\Delta v$ , specific impulse  $I_{sp}$  and effective exhaust velocity  $v_e$  can be obtained.



$$F_{thrust} = \dot{m} \cdot v_e + A_e (p_e - p_0) \quad \& \quad \Delta v = g_0 \cdot I_{sp} \cdot \ln \frac{m_0}{m_1} \quad (2-3)$$

$$\text{where } I_{sp} = \frac{v_e}{g_0} \quad \& \quad v_e = \sqrt{\frac{2 \cdot \gamma}{\gamma - 1} \cdot \bar{R}_{spec} \cdot T_c \cdot \left(1 - \left(\frac{p_e}{p_c}\right)^{\frac{\gamma-1}{\gamma}}\right)}$$

Where  $\dot{m}$  is the mass flow rate,  $A_e$  the nozzle exit area,  $p_e$  the nozzle exit pressure and  $p_0$  is the ambient pressure, which can be assumed to be  $0Pa$  in the vacuum conditions of space.  $g_0$  is the gravitational acceleration, which has a value of  $9.80665m/s^2$ . In the natural logarithm the initial mass of the rocket  $m_0$  is divided by its final mass  $m_1$ , which will be the initial mass minus the expelled propellant in the case of the thruster.  $\gamma$  is the heat capacity ratio,  $\bar{R}_{spec}$  is the specific gas constant and  $T_c$  is the chamber temperature. Finally there is the ratio between the nozzle exit and chamber pressure  $p_c$ , which can also be replaced by the density or temperature ratio at a different location according to the Poisson relation. Important in Eq. (2-3) are the assumptions that apply, shown in the four points listed below, which makes the use of this ideal rocket theory possible.

1. The gas at the exhaust is homogeneous and constant in composition.
2. The expelled gas mixture obeys the ideal gas law from Eq. (2-4).
3. The gas heat capacity is constant despite changing temperature and composition.
4. The flow through the nozzle is isentropic, one-dimensional and remains steady.

As can be seen in all the assumptions from the list, the propellant is ideally in a gaseous state within the combustion chamber and nozzle, hence the ideal gas law shown in Eq. (2-4) can be used.

$$p \cdot V = m \cdot \bar{R}_{spec} \cdot T \quad \text{or} \quad \frac{p}{\rho} = \bar{R}_{spec} \cdot T \quad \text{where } \bar{R}_{spec} = \frac{\bar{R}}{M} = c_p - c_v \quad (2-4)$$

Standard gas parameters are used here, being: pressure  $p$ , volume  $V$ , mass  $m$ , temperature  $T$  and density  $\rho$ . The previously shown values are obtained with the help of the universal gas constant  $\bar{R}$ , which has a value of  $8.314 J/(K mol)$ , molar mass  $M$  and  $c_p$  and  $c_v$  are the heat capacities at constant pressure and volume respectively. Additionally the parameters shown in Eq. (2-5) are helpful, where  $Ma$  is the mach number,  $v_s$  is the speed of sound and  $v$  &  $A$  are the velocity and surface area.

$$Ma = \frac{v}{v_s} \quad \& \quad \dot{m} = \rho \cdot A \cdot v = \text{constant} \quad \text{where } v_s = \sqrt{\gamma \cdot \bar{R}_{spec} \cdot T} \quad (2-5)$$

Lastly, a helpful expression can be a rewritten form for the mass flow rate shown in Eq. (2-6), in which  $A_t$  stands for nozzle throat area.

$$\dot{m} = \frac{p_c \cdot A_t}{\sqrt{\bar{R}_{spec} \cdot T_c}} \cdot \Gamma \quad \text{with} \quad \Gamma = \sqrt{\gamma} \cdot \left( \frac{2}{\gamma + 1} \right)^{\frac{\gamma+1}{2(\gamma-1)}} \quad (2-6)$$

Related to the design of the liquid rocket motor are some extra consideration that should be taken into account, certainly in smaller sized systems. One of which is the significant amounts of heat that is released in the combustion chamber depending process. The other is the pressure drop that is induced by the accelerating flow and the contact surfaces in the reaction chamber. Additionally the chamber should be designed having a characteristic length  $L^*$  large enough to make sure the combustion can run completely, depending on the reaction kinetics. It is determined by the chamber volume and nozzle throat area ratio;  $V_c/A_t$ .

### 2-2-2 Spacecraft Propulsion

There are many ways to use the propellant in a thruster system, but the only two relevant methods for use of  $H_2O_2$  would be either as mono- or bi-propellant.

#### Mono-propellant

Besides cold & warm gas thrusters, mono-propellants are a commonly used type in the nano- and micro-satellite class, due to their simplicity. They consist of a pressurant that pushes the propellant through a catalyst bed where it decomposes and further expands in the nozzle. Additionally, a regulator and valve are required for control, as shown in Figure 2-4.

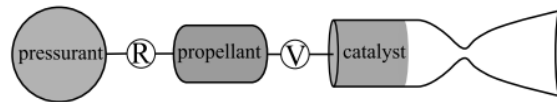


**Figure 2-4:** Mono-propellant System Design [60]

Currently the most utilized propellant is hydrazine and the catalyst aluminum oxide, providing up to 250s of specific impulse. When  $H_2O_2$  is used as propellant the system works the same way, but gives only around 150s of specific impulse [23]. Then there is the group of liquified gasses such as carbon and nitrous oxides, which still only have a specific impulse of around 65s [123]. In most cases these gasses are used in cold gas systems, but in this system helium and nitrogen would be used as a pressurant. The pressure required can become quite high due to the pressure drops present from running the propellant through the catalytic beds [7].

One of the problems with mono-propellant thrusters is the life-span of catalytic beds, since performance degrades due to poisoning and thermal cycling [33]. Therefore, research is performed on ways to improve this catalytic bed and overall thruster performance with new green propellants, materials and structures [23] [12]. A solution would be to print the monolithic catalyst beds using additive manufacturing [32]. Even better would be to replace it with another method to initiate decomposition as discussed later in Section 2-2-3, which will however require extra power [37].

**Bi-propellant**

The other option would be to use  $H_2O_2$  as an oxidizer in a bi-propellant thruster. Next to the high energy density  $Ed$ , it namely consists of good oxidizing properties due to its molecular composition. This system works by mixing the oxidizer with a fuel in a combustion chamber, where it is ignited and accelerated through the nozzle, as shown in Figure 2-5.

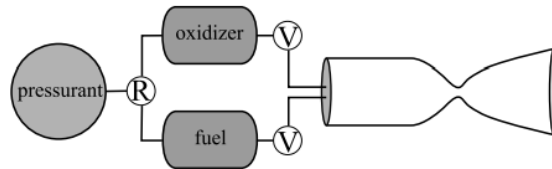


**Figure 2-5:** Bi-propellant System Design [60]

In comparison to mono-propellant systems, bi-propellants are somewhat more complex and heavy and provide higher thrust, which is why they are not used on small satellites yet [125]. As fuel, another toxic variant is commonly used; Monomethylhydrazine (MMH) in combination with Dinitrogen Tetroxide (NTO) as oxidizer, which gives thrust levels of over  $10N$  and specific impulse of around  $300s$ . The theoretical performances of some bi-propellant combinations are shown in Figure 2-6, but many more are possible [8].

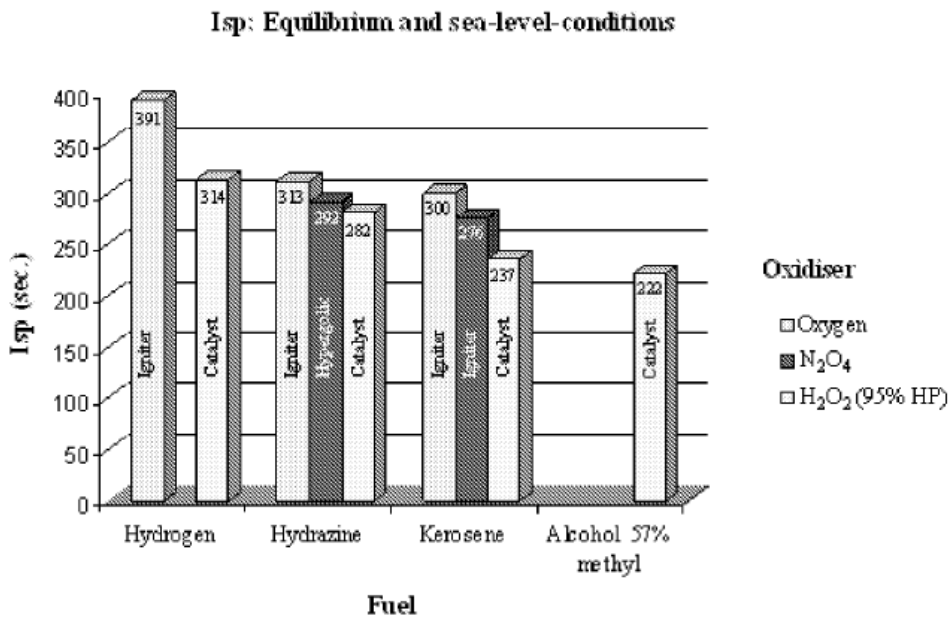


**Figure 2-6:** Bi-propellant Combination Performance [42]

As can be seen, the method of ignition is to first catalytically decompose  $H_2O_2$ , to subsequently inject this with the fuel in the combustion chamber. Therefore, research is again being done on the catalyst, also for smaller bi-propellant structures [61]. The reason for decomposing the  $H_2O_2$  before injection is because of the vapor formed which causes auto-ignition with the hydrocarbon fuels.

### 2-2-3 Decomposition Methods

As mentioned,  $H_2O_2$  is thus currently decomposed using catalysts, in both thruster systems. There are however different methods possible to decompose the propellant, depending on the situation.

#### Electrothermal

Some thrusters that are currently being developed operate in a similar fashion as the mono-propellant system, but require electric input. A resistojet is the most similar option, which uses a heating element to add energy to the propellant that flows through it, as shown in Figure 2-7.

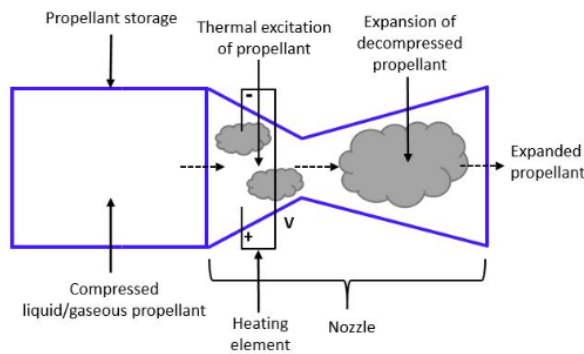


**Figure 2-7:** Resistojet Thruster Design [22]

Another, more electric system is the an arcjet, which forms a propellant plasma with an arc between two electrodes. It does so with electrical discharges, which at a low frequency would be a less energy consuming solution. These spark plugs are also used in cars engines and work in the same way at high voltage intervals, but might not be able to transfer enough heat to the propellant. Lastly, an electromagnetic radiating igniter could be used to ionize and subsequently accelerate the propellant, for example with a laser. Similarly to the arcjet however, a laser system is not much looked into yet, can become quite complicated and most likely requires too much energy. With these ignition methods, a catalytic bed is not needed anymore, since the  $H_2O_2$  temperature will now rise to the point at which the decomposition self-accelerates.

The resistojet is the most promising one for the application with  $H_2O_2$  due its thermal decomposition properties. It works by heating the propellant using conductive heating, which will degrade less as a system, but imposes other challenges. One problem that holds for all of the electrothermal options is the heat and thus power required to initiate the decomposition for the high heat capacity property of  $H_2O_2$ . Some experiments for small scale resistojets with Xenon show already a usage of  $30W$  for just  $18mN$  of thrust and  $48s$  specific impulse [25]. This heating power  $P_h$  in such a system is an important parameter and is shown in Eq. (2-7).

$$P_h = \dot{m} \left( c_{pl} (T_{boil} - T_0) + c_{pg} (T_c - T_{boil}) + L_h \right) \quad (2-7)$$

Here,  $L_h$  is the latent heat of vaporization,  $T_0$ ,  $T_c$  &  $T_{boil}$  are the initial, chamber and boiling propellant temperature and  $c_{p_g}$  &  $c_{p_l}$  are the specific heat at constant pressure of the gaseous and liquid phase propellant. When inserting the mass flow rate from Eq. (2-6) in Eq. (2-7), the dependency of the required power on chamber temperature and pressure is visible [22].

### Hypergolic & Pyrotechnic

Some propellant combinations do not require ignition via an external source, but ignite when coming into contact with each other, ideal for a bi-propellant system. For  $H_2O_2$  quite some combinations for this method are possible, but the green fuels would be the preferred options [122] [79] [43]. Many of the options are mixtures that include the metal catalysts used for the decomposition as well, but in this way a lot more heat will be released during the reaction [92]. With regards to safety, this auto-ignition is momentarily only done with the vapor after catalytic decomposition, so the contact area is large and the temperature is already elevated, causing high performance. Other methods could be looked into as well, such as premixing and subsequent heating, which would however drastically decrease the safety. These pyrophoric properties are less wished for since spontaneous ignition is hard to prevent and safety and control are then at risk.

Besides mono- and bi-propellants there are also solid rocket motors. For bigger thruster or launchers, this ignition system where the propellant in a solid state is often used, being a pyrogen igniter or torch igniter [137]. Those function in a similar fashion as fireworks and thus need to be ignited their selves as well. This is often done using one of the methods described before, after which the reaction can not be put to stop. All this makes it very unsuitable for use in smaller satellites.

## 2-3 Fuel Cell Fundamentals

This section will cover the basics of fuel cells and dive deeper in the theory of how they can generate power with  $H_2O_2$ . Then, some other state of the art options are discussed to get an overview of what could be used in a satellite system.

### 2-3-1 Electric Power Generation

The purpose of a fuel cell is to generate power by directly converting the chemical energy to electricity. Required in this process are thus a fuel, oxidizer, electrodes, being an anode and cathode, and an electrolyte. A general schematic representation of a simple hydrogen-oxygen fuel cell is shown in Figure 2-8. The system works by transferring ions and electrons generated at the anode in a catalytic oxidation reaction with the fuel. These products will then react again at a catalyst cathode with the oxidizer to form the waste products. The generated electrons travel via an external circuit to be used in a power system and the free ions go through an electrolyte.

In general, the fuel and oxidizer are the most defining aspects, around which the rest of the system is designed. The anode and cathode catalysts are selected based on their ability to perform the electrochemical reaction with the fuel and oxidizer. These can either form

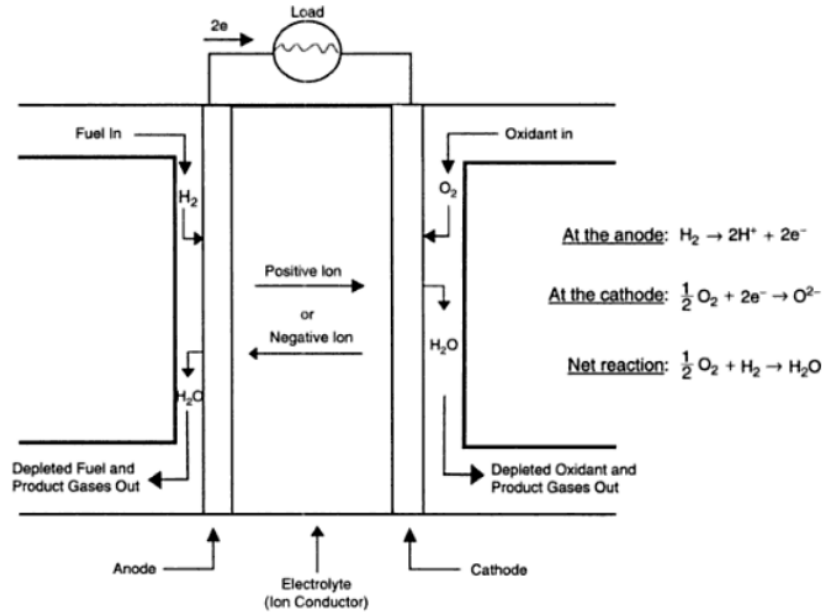


Figure 2-8: Schematic Fuel Cell System Design [49]

the electrode on their own or be deposited on a support structure, also referred to as the Gas Diffusion Layer (GDL). The electrolyte that is used with the chemicals is usually a Polymer Exchange Membrane (PEM), based on the liberated ions. This can either be a Cation Exchange Membrane (CEM) which is negatively charged and only lets through positive ions, or an Anion Exchange Membrane (AEM) which does the opposite. The electrolyte can however also be liquid only and not require a membrane, as long as oxidation and reduction reactions happen at the electrodes with a reactant. The performance does drastically increase though, when a membrane is used to make it into two compartments, each having a specific anolyte and catholyte.

### Electric Power Performance

The performance of a fuel cell can be evaluated by its voltage  $U$  and current  $I$ , resulting in a certain power  $P$ . This relation is captured by the Nernst equation, which is shown in Eq. (2-8) [64].

$$E_{cell} = \underbrace{\left[ E_r^0 + A_{emp} \ln \left( \prod_k a_{k_r}^{\nu_k} \right) \right]}_{\text{Reversible cell voltage } E_r} - \underbrace{\left[ \frac{A_{emp}}{\alpha} \ln \left( \frac{I_i + I}{I_0} \right) \right]}_{\text{Activation losses } E_a} - \underbrace{[I(R_c)]}_{\text{Ohmic losses } E_o} + \underbrace{\left[ A_{emp} \ln \left( 1 - \frac{I}{I_m} \right) \right]}_{\text{Concentration losses } E_c} \quad (2-8)$$

In this equation, cell potential  $E_{cell}$  is calculated, using either current or current density  $Id$  in multiple terms that affect the performance of the fuel cell system. The starting parameter is  $E_r^0$ , which is a tabulated reversible cell potential at standard conditions, calculated using the

Gibbs free energy  $\Delta G$ . Its value represents the voltage that is obtained when no current runs through the cell, also known as the Open Circuit Potential (OCP). The second term takes into account the reaction rate of the chemical species  $k$ , which together with the first becomes the reversible cell voltage  $E_r$ . It includes the stoichiometric coefficient  $\nu$  and the activity of species  $k$ ,  $a_k$ , for which mostly partial pressures are used. In Eq. (2-8), empirical constant  $A_{emp}$  is used, which is calculated using universal gas constant  $\bar{R}$  and Faraday constant  $F$  shown in Eq. (2-9).

$$A_{emp} = \frac{\bar{R}T}{nF} \quad \text{with } \bar{R} = 8.314 \text{ J/(K mol)} \quad \& \quad F = 96485 \text{ s A/mol} \quad (2-9)$$

The losses terms that follow in Eq. (2-8), cause the actual cell potential to be lower than the reversible cell voltage. The first are activation losses  $E_a$ , caused by energy required to make the reaction go at low current densities. In there, you have the Charge Transfer Coefficient (CTC)  $\alpha$ , which is defined by the electrochemical reaction rate and the electrode material. This term also includes the fuel crossover and internal current losses  $I_i$ . As the name suggests, they are cell characteristics caused by fuel as well as electrons that can pass through to the other side, causing the OCP to be substantially lower than in theory. Lastly, it has a term for exchange current density  $I_0$ , which is a standard 'reference' current, intrinsic to the electrode material, structure and its environment. Then there are the Ohmic losses  $E_o$ , which depends on cell resistance  $R_c$ . This actually comes from several sources, being electronic resistance  $R_e$  from cell components and ionic resistance  $R_i$  coming from the electrolyte. Finally, the last term are the concentration losses  $E_c$ , which are caused by a decrease in reactant at the surface of the electrodes, since it is being used to quickly. The associated variable is the limiting current density  $I_m$ , which shows at high current densities depending on the reactant and reaction.  $E_a$  and  $E_c$  should be taken into account for both the anode as well as cathode, each having its own independent variables depending on the electrode.

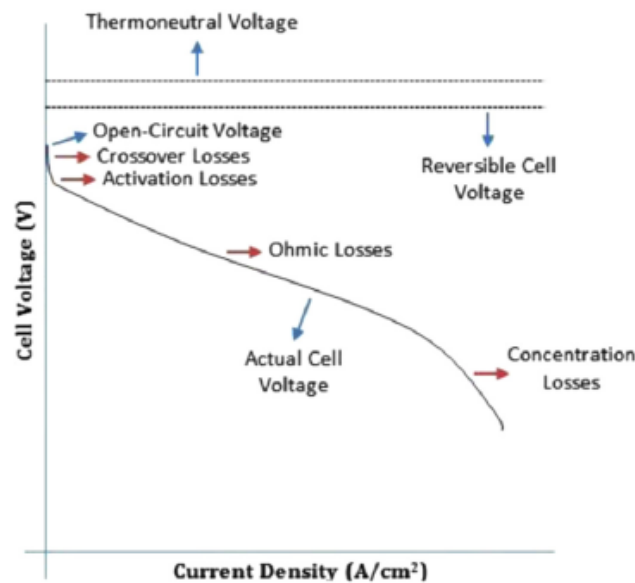


Figure 2-9: Polarization Curve [109]

The resulting cell potential is captured in the so called polarization curve, which visualises the performance of the fuel cell as shown in Figure 2-9. This plot often also contains the corresponding power density  $Pd$  of the cell. This parameter is calculated by multiplying potential with current density. It indicates clearly the load at which the cell works optimally, being the peak of the parabola.

Compared to other power systems, the efficiency of a fuel cell can theoretically be far higher and reaches up to 80% and over [47]. This efficiency is depending mostly on the fuel from which it converts the energy of which the equation is shown in Eq. (2-10)[109].

$$\eta_{cell} = \frac{nFE}{\Delta H} (u_f u_r \eta_c \eta_p) \quad \text{with} \quad \eta_p = 1 - a - \frac{b}{EI} \quad (2-10)$$

The left fraction is based on known voltage and reversible efficiency which determine the efficiency of the cell itself, which can be multiplied by some auxiliary system losses on the right.  $u_f$  is the mass ratio of reacted to input fuel in the cell,  $u_r$  is the reformer efficiency and  $\eta_c$  is the power conditioner efficiency.  $u_p$  is the parasitic power efficiency present in subsystems, calculated with empirical constants  $a$  &  $b$ .

### 2-3-2 H<sub>2</sub>O<sub>2</sub> Electrochemistry

Operation of H<sub>2</sub>O<sub>2</sub> within a fuel cell can be divided according to the reactions that happen at the cathode and anode. These are dependent on the pH value and happen via the processes shown in Table 2-2.

**Table 2-2:** H<sub>2</sub>O<sub>2</sub> Fuel Cell Electrochemical Reactions and Potentials [6]

| Acid  |                     | Alkaline<br>(H <sub>2</sub> O <sub>2</sub> + OH <sup>-</sup> → HO <sub>2</sub> <sup>-</sup> + 2H <sub>2</sub> O) |                     |
|---|---------------------|--|---------------------|
| H <sub>2</sub> O <sub>2</sub> + 2H <sup>+</sup> + 2e <sup>-</sup> → 2H <sub>2</sub> O | $E_{c_1}^0 = 1.78V$ | HO <sub>2</sub> <sup>-</sup> + H <sub>2</sub> O + 2e <sup>-</sup> → 3OH <sup>-</sup>                             | $E_{c_1}^0 = 0.87V$ |
| H <sub>2</sub> O <sub>2</sub> → O <sub>2</sub> + 2H <sup>+</sup> + 2e <sup>-</sup>    | $E_a^0 = 0.69V$     | HO <sub>2</sub> <sup>-</sup> + OH <sup>-</sup> → O <sub>2</sub> + H <sub>2</sub> O + 2e <sup>-</sup>             | $E_a^0 = 0.15V$     |
| O <sub>2</sub> + 4H <sup>+</sup> + 4e <sup>-</sup> → 2H <sub>2</sub> O                | $E_{c_2}^0 = 1.23V$ | O <sub>2</sub> + 2H <sub>2</sub> O + 4e <sup>-</sup> → 4OH <sup>-</sup>  | $E_{c_2}^0 = 0.40V$ |

Notable is the high H<sub>2</sub>O<sub>2</sub> oxidation potential of 1.78V in acid solutions, making the chemical one of the most powerful oxidizers [11]. An additional anode and cathode reaction can however also take place, that creates a so called mixed potential which lower the cell performance [4]. Together with the Hydrogen Peroxide Reduction Reaction (HPRR)  $E_{c_1}^0$ , a Hydrogen Peroxide Oxidation Reaction (HPOR)  $E_a^0$  can occur at the same electrode, from which oxygen is released, causing a Oxidation Reduction Reaction (ORR)  $E_{c_2}^0$  to take place subsequently. This process causes the actual voltage obtained to be only  $\approx 0.85V$  in acid and  $\approx 0.15V$  in alkaline media, which is far lower than the maximum theoretical value as shown in Figure 2-10.

The selectivity of different electrocatalysts determine to what degree the HPRR or HPOR are favoured [6], which means the electrodes should be carefully selected. Also, having an alkaline anodic and an acid cathodic environment causes the potential of the HPRR and HPOR to be optimal. When taking into account the temperature and concentration influences as well, the potential loss is minimized, certainly with electrochemical reactions at higher current density, where the mixed potential has little influence.



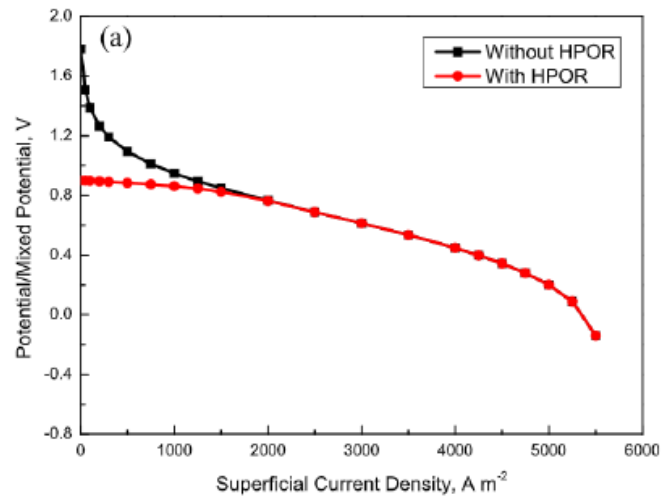


**Figure 2-10:** Current Density vs (Mixed) Potential [4]

### 2-3-3 Direct Liquid Fuel Cells

Since the electrochemical reactions are applied to  $\text{H}_2\text{O}_2$  in a liquid state, a higher energy density is reached and different applications are possible. The working principles are the same for this so-called Direct Liquid Fuel Cell (DLFC), but different fuels and oxidizers can now be used in the system. The complete setup will consist of multiple components leading to a setup as shown in Figure 2-11, which can then again be stacked to reach a higher voltage. Usually, the two electrodes are also covered with a patterned plate, through which the solutions flow at a certain rate following a path.

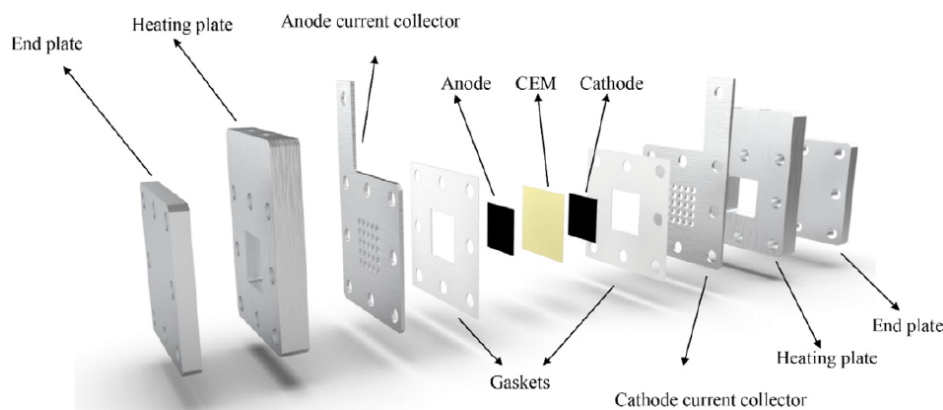


**Figure 2-11:** DLFC System Structure [93]

Various fuels could be used in a DLFC in combination with  $\text{H}_2\text{O}_2$  as oxidizer, similarly to the thruster bi-propellants. Additionally, the ions can now also be transferred with an electrolyte mixed in the liquids for better transport of the charge. This was also visible in the performance difference of  $\text{H}_2\text{O}_2$  between acid and alkaline solutions. The most promising fuels added at the anode are summarized in Table 2-3. The reactions involving carbon fuels can however also form  $\text{CO}_2$  as product, making the system inherently less environmental friendly.

**Table 2-3:** Various DLFC Fuel Reactions [2]

| Fuel               | u [Wh/L] | Overall Reaction   | $E_{rev}^0$ [V] |
|--------------------|----------|--|-----------------|
| Hydrazine          | 5400     | $N_2H_4 + 4OH^- + 4H^+ + 2H_2O_2$<br>$\rightarrow N_2 + 4H_2O$                           | 2.13            |
| Sodium Borohydride | 9946     | $BH_4^- + 4H_2O_2 + 8OH^- + 8H^+$<br>$\rightarrow BO_2^- + 14H_2O$                       | 3.01            |
| Ethylene Glycol    | 5800     | $C_2H_6O_2 + 4H_2O_2 + 8H^+ + 10OH^-$<br>$\rightarrow (COO^-)_2 + 16H_2O$                | 2.47            |
| Ethanol            | 6280     | $CH_3CH_2OH + 2H_2O_2 + 5NaOH + 2H_2SO_4$<br>$\rightarrow CH_3COONa + 8H_2O + 2Na_2SO_4$ | 2.52            |

### 2-3-4 H<sub>2</sub>O<sub>2</sub> Cell System Summary

A clear method of distinguishing the fuel cell type is by its structure, which can either be one or two compartment. Together with the fuel and oxidizer used, this parameter has the largest effect on performance. Catalysts, other cell components and fuel and oxidizer conditions define the cell as well and should thus be taken into account when comparing the systems. A list of the most relevant fuel cells found in literature that utilize H<sub>2</sub>O<sub>2</sub> has therefore been set up, along with the above parameters. This results in Table 2-4, where the maximum power density  $Pd$  and OCP are shown at the noted temperature. Electrode and electrolyte at both the anode and cathode are displayed above each other, with the Nafion membrane type and flow rate added as remarks if applicable.

**Table 2-4:** Fuel Cell Systems Literature Overview

| Ref. & Remark   | Electrodes (A&C)   | Electrolytes (A&C)  | Performance                     |
|---|--|---|---------------------------------|
| <b>One compartment - H<sub>2</sub>O<sub>2</sub></b>           |  |   |                                 |
| Yamazaki 2008 [52]  | 100% Au sheet<br>100% Ag sheet                                   | 0.3M H <sub>2</sub> O <sub>2</sub> +0.1M NaOH   | 0.08mW/cm <sup>2</sup><br>0.12V |
| Shaegh 2012 [108]   | Ni mesh<br>PB/CP   | 0.5M H <sub>2</sub> O <sub>2</sub> +0.1M HCl  | 1.55mW/cm <sup>2</sup><br>0.6V  |
| Yamada 2014 [127]   | Ni mesh<br>FePt  | 0.3M H <sub>2</sub> O <sub>2</sub> +0.1M NaCl   | 4.2mW/cm <sup>2</sup><br>0.74V  |
| Nguyen 2020 [89]  | Ni mesh<br>C <sub>32</sub> H <sub>18</sub> FeNe <sub>8</sub> /CP | 0.5M H <sub>2</sub> O <sub>2</sub> +0.1M HCl  | 3.41mW/cm <sup>2</sup><br>0.56V |
| Martins 2020 [78]   | Ni mesh<br>Cu <sub>4</sub> Fe(CN) <sub>6</sub> /CFC              | 0.5M H <sub>2</sub> O <sub>2</sub> +0.1M HCl  | 8.3mW/cm <sup>2</sup><br>0.72V  |
| <b>Passive - Two compartment - H<sub>2</sub>O<sub>2</sub></b> |  |   |                                 |
| Sanli 2011 [103]<br>N117                                      | 0.4mg Ni/CP<br>4mg Pt/CP   | 1M H <sub>2</sub> O <sub>2</sub> +6M KOH<br>2M H <sub>2</sub> O <sub>2</sub> +1.5M H <sub>2</sub> SO <sub>4</sub> | 3.9mW/cm <sup>2</sup><br>0.9V   |
| Sanli 2013 [104]<br>N117                                      | 0.4mg Ni/CP<br>PbSO <sub>4</sub> /CP                             | 1M H <sub>2</sub> O <sub>2</sub> +3M KOH<br>1M H <sub>2</sub> O <sub>2</sub> +1.5M H <sub>2</sub> SO <sub>4</sub> | 10mW/cm <sup>2</sup><br>1V      |
| Continued on next page...                                     |  |   |                                 |

**Table 2-4:** Fuel Cell Systems Literature Overview

| Ref. & Remark   | Electrodes (A&C)                      | Electrolytes (A&C)   | Performance                          |
|---|---------------------------------------|--|--------------------------------------|
| Pan 2019 [93]<br>N211, (+fuel)                                      | 1mg Pd/CFC<br>2.66mg Au/CFC           | 5M C <sub>2</sub> H <sub>6</sub> O <sub>2</sub> +9M KOH<br>4M H <sub>2</sub> O <sub>2</sub> +1M H <sub>2</sub> SO <sub>4</sub> | 30.3mW/cm <sup>2</sup><br>1.58V      |
| Lu 2020 [73]<br>N115, (+fuel)                                       | 3mg PtRu/CFC<br>6.7mg PB/CFC          | 6M CH <sub>3</sub> OH<br>30% H <sub>2</sub> O <sub>2</sub> +2M H <sub>2</sub> SO <sub>4</sub>                                  | 3mW/cm <sup>2</sup><br>0.4V (40°C)   |
| <b>Active - Two compartment - H<sub>2</sub>O<sub>2</sub></b>        |                                       |  |                                      |
| Yang 2012 [130][129]<br>N115, 10mL/min                              | 0.3mg Pd/CFC                          | 1M H <sub>2</sub> O <sub>2</sub> +4M KOH<br>2M H <sub>2</sub> O <sub>2</sub> +2M H <sub>2</sub> SO <sub>4</sub>                | 14.3mW/cm <sup>2</sup><br>0.9V       |
| Yang 2013 [131]<br>N115, 10mL/min                                   | Ni/Ni mesh<br>0.3mg Pd/CFC            | 1M H <sub>2</sub> O <sub>2</sub> +4M KOH<br>2M H <sub>2</sub> O <sub>2</sub> +2M H <sub>2</sub> SO <sub>4</sub>                | 19.4mW/cm <sup>2</sup><br>0.9V       |
| Yang 2014 [132]<br>N115, 15mL/min                                   | Ni/CFC<br>0.3mg Pd/CFC                | 1M H <sub>2</sub> O <sub>2</sub> +4M KOH<br>2M H <sub>2</sub> O <sub>2</sub> +2M H <sub>2</sub> SO <sub>4</sub>                | 21.6mW/cm <sup>2</sup><br>0.9V       |
| Ye 2015 [135]<br>N115, 10mL/min                                     | Ni-Nas/Ni mesh<br>0.3mg Pd/CFC        | 0.9M H <sub>2</sub> O <sub>2</sub> +4M KOH<br>2M H <sub>2</sub> O <sub>2</sub> +2M H <sub>2</sub> SO <sub>4</sub>              | 48.7mW/cm <sup>2</sup><br>0.9V       |
| Yang 2016 [128]<br>N115, 20mL/min                                   | Ni/Ni mesh<br>AuPd-NP/CFC             | 1M H <sub>2</sub> O <sub>2</sub> +4M KOH<br>2M H <sub>2</sub> O <sub>2</sub> +2M H <sub>2</sub> SO <sub>4</sub>                | 22.8mW/cm <sup>2</sup><br>0.86V      |
| Xiao 2017 [126]<br>N115, 10mL/min                                   | Ni/Ni mesh<br>NiFe-HCF/CFC            | 1M H <sub>2</sub> O <sub>2</sub> +4M KOH<br>2M H <sub>2</sub> O <sub>2</sub> +2M H <sub>2</sub> SO <sub>4</sub>                | 36mW/cm <sup>2</sup><br>1.09V        |
| <b>Active - Two compartment - H<sub>2</sub>O<sub>2</sub> - Fuel</b> |                                       |  |                                      |
| An 2011 [3]<br>N211, 2mL/min  | 1mg PdNiC/Ni foam<br>60% Pt/CFC       | 3M EtOH+5M NaOH<br>4M H <sub>2</sub> O <sub>2</sub> +1M H <sub>2</sub> SO <sub>4</sub>   | 360mW/cm <sup>2</sup><br>1.6V (60°C) |
| Li 2015 [70]<br>N115, 2, 10mL/min                                   | 2mg Pd/CP<br>2mg Pt/CP                | 1M HCOONa+3M NaOH<br>1M H <sub>2</sub> O <sub>2</sub> +1M H <sub>2</sub> SO <sub>4</sub>                                       | 330mW/cm <sup>2</sup><br>1.6V        |
| Li 2016 [69]<br>A201, 1, 3mL/min                                    | 2mg Pd/CP<br>2mg Pt/CP                | 7M HCOOK<br>15% H <sub>2</sub> O <sub>2</sub>  | 37mW/cm <sup>2</sup><br>0.72V (40°C) |
| Ma 2010 [56]<br>N212, 5mL/min                                       | NiPt/CFC<br>Pd/CFC                    | 10% NaBH <sub>4</sub> +20% NaOH<br>2M H <sub>2</sub> O <sub>2</sub> +1.5M H <sub>2</sub> SO <sub>4</sub>                       | 327mW/cm <sup>2</sup><br>1.7V        |
| Ma 2011 [75]<br>PHME, 10mL/min                                      | 5mg NiPd/CFC<br>Au/CFC                | 10% NaBH <sub>4</sub> +20% NaOH<br>2M H <sub>2</sub> O <sub>2</sub> +2M H <sub>2</sub> SO <sub>4</sub>                         | 81.8mW/cm <sup>2</sup><br>1.85V      |
| Abdolmaleki 2017 [1]<br>N117, 2.5mL/min                             | 1mg NiPt/CFC<br>0.5mg Pt/CFC          | 1.5M NaBH <sub>4</sub> +2M NaOH<br>2M H <sub>2</sub> O <sub>2</sub> +0.5M H <sub>2</sub> SO <sub>4</sub>                       | 65mW/cm <sup>2</sup><br>1.7V         |
| Lee 2017 [65]<br>Nafion, 20mL/min                                   | 1mg Pt/GF                             | 5.3M NaBH <sub>4</sub> +10M NaOH<br>2.9M H <sub>2</sub> O <sub>2</sub> +3.4M H <sub>2</sub> SO <sub>4</sub>                    | 240mW/cm <sup>2</sup><br>1.7V        |
| Yi 2018 [136]<br>N117, -mL/min                                      | 4.5mg PtFe/CFC<br>4.5mg Pt/CFC        | 1M NaBH <sub>4</sub> +3M NaOH<br>2M H <sub>2</sub> O <sub>2</sub> +0.5M H <sub>2</sub> SO <sub>4</sub>                         | 65mW/cm <sup>2</sup><br>1.7V         |
| Hjelm 2019 [50]<br>N117, 10mL/min                                   | 0.3mg Pd/C glass<br>0.31mg Pt/C glass | 0.1M NaBH <sub>4</sub> +1M NaOH<br>0.4M H <sub>2</sub> O <sub>2</sub> +1M H <sub>2</sub> SO <sub>4</sub>                       | 211mW/cm <sup>2</sup><br>1.72V       |
| Wang 2019 [120]<br>N117, 2mL/min                                    | 1mg Pd/Ni foam<br>1mg Pt/CP           | 1.5M NaBH <sub>4</sub> +3M KOH<br>15% H <sub>2</sub> O <sub>2</sub> +1.5M H <sub>2</sub> SO <sub>4</sub>                       | 300mW/cm <sup>2</sup><br>1.8V (70°C) |
| Braesch 2020 [16]<br>N117, 2mL/min                                  | 0.7mg Ni eNFT<br>1mg Pt               | 1.5M NaBH <sub>4</sub> +3M KOH<br>15% H <sub>2</sub> O <sub>2</sub> +1.5M H <sub>2</sub> SO <sub>4</sub>                       | 446mW/cm <sup>2</sup><br>2V (70°C)   |
| <b>Miscellaneous - H<sub>2</sub>O<sub>2</sub></b>                   |                                       |  |                                      |
| Continued on next page...   |                                       |  |                                      |

**Table 2-4:** Fuel Cell Systems Literature Overview

| Ref. & Remark                                       | Electrodes (A&C)           | Electrolytes (A&C)   | Performance                           |
|---|----------------------------|--|---------------------------------------|
| Brodrecht 2003 [19]<br>Semi-flow cell<br>55.7mL/min | 100% Al flakes<br>Au mesh  | 10% H <sub>2</sub> O <sub>2</sub> +1M KOH  | 57.6mW/cm <sup>2</sup><br>1.53V       |
| Shu 2012 [112]<br>Semi-flow cell<br>N115, 110mL/min | AZ61 Mg<br>Pd/Ti mesh      | 0.68M NaCl<br>0.5M H <sub>2</sub> O <sub>2</sub> +0.5M H <sub>2</sub> SO <sub>4</sub>  | 110mW/cm <sup>2</sup><br>2.1V         |
| An 2014 [5]<br>RedOx Couple<br>N117, 2mL/min        | 1mg PdNiC/Ni foam<br>3x CP | 3M EtOH+5M NaOH<br>1M VO <sub>2</sub> <sup>+</sup> +2.5M H <sub>2</sub> SO <sub>4</sub><br>4M H <sub>2</sub> O <sub>2</sub> +1M H <sub>2</sub> SO <sub>4</sub> | 450mW/cm <sup>2</sup><br>2.07V (60°C) |

## 2-4 Conclusion

H<sub>2</sub>O<sub>2</sub> is known mainly within the space industry as the oxidizing agent in launch systems. This exothermic decomposing chemical has similar characteristics to water, but is far more useful as propellant due to the extra oxygen atom. At concentrations of 64% and over, the high energy density liquid is prone to start a self-accelerated decomposition when ignited. This reaction is currently mainly initiated with catalysts, but can be achieved by applying electric or thermal energy as well. Despite its environmental friendly reaction products, being water and oxygen, safety is a crucial aspect and handling should always be done with caution. Despite having somewhat lower standard rocket parameters in comparison with hydrazine, it is a good alternative to replace the hazardous chemical in a mono-propellant system. Also in bi-propellant systems H<sub>2</sub>O<sub>2</sub> is advantageous due to its properties which make it react with various other fuels. This can happen hypergolic or pyrotechnic, but more often requires an electrothermal or catalytic ignition method beforehand. Then there are the electrochemical energy properties of H<sub>2</sub>O<sub>2</sub> which make it an ideal power source in situations where no oxygen is available, as is the case in space. This can be done with a fuel cell, where an anode and cathode catalysts cause a decomposition reaction which makes electrons flow through the system. The amount of energy released this way is calculated with the Nernst equation, resulting in a polarization curve which shows voltage versus current density. When using H<sub>2</sub>O<sub>2</sub>, the potential which can be build up is quite high, but lowered due to various concurrent reactions and standard system losses. The gained power can however be increased when the liquid is used in a cell system with other liquid fuels, on which a lot of research is still being performed.

---

## Chapter 3

---

# Project Baseline

Before diving directly into tackling the research objectives, a clear overview of the challenges along the way is needed. Therefore, the exact requirements are determined as well as a selection of what system fits best to meet them. To make this even more evident a reference system is taken as a baseline, corresponding with the set goals of this research. This way an idea is obtained of the challenges and an impression of performance can be formed using simple analytical models.

### 3-1 Satellite Requirements

To research the possibilities of satellite power and propulsion systems in a more structured way, some guidelines have to be set out. This is partly done in Chapter 1 by defining that the development will be for a CubeSat sized satellite, which can still range from 1U to 32U. The best way of checking the propulsion requirements is with the  $\Delta v$  budget, which is optimally formed by the product of low dry mass with high specific impulse. This function of specific impulse and mass ratio is captured in Figure 3-1 for various CubeSats and orbital periods.

Typical values for Low Earth Orbit (LEO) station keeping at 500km altitude are 25m/s per year, with missions aiming for five years of operation. With current knowledge, only large size CubeSats would be able to do orbit maintenance for the set thruster type, which should also be the focus in early stages of development [66]. Since this combined Hydrogen Peroxide ( $\text{H}_2\text{O}_2$ ) system is designed to replace current toxic mono-propellants, satellite requirements for that type are taken as a reference. From Figure 1-1 one can see that thrust levels should thus be around 1N and the specific impulse is determined to reach approximately 170s with  $\text{H}_2\text{O}_2$  propellant according to Table 1-2. An example is a 10kg micro-satellite, that requires 1N thrust, 230s specific impulse for a  $\Delta v$  of 452m/s [67]. Another example would be the requirements set for a 30kg 16U spacecraft in a Mars mission, utilizing both chemical as well as electrical propulsion [77]. Having the same  $\Delta v$ , specific impulse and 3N thrust at max, but also a system weight constraint of 7.5kg. Considering  $\text{H}_2\text{O}_2$  propellant performance is lower, more propellant has to be taken into space, increasing the overall satellite mass. Together with the technology for both the power and propulsion system being less far developed, the combined system will most likely be heavier. So when setting the same  $\Delta v$  budget as requirement, a more relaxed requirement regarding the mass should be applied.

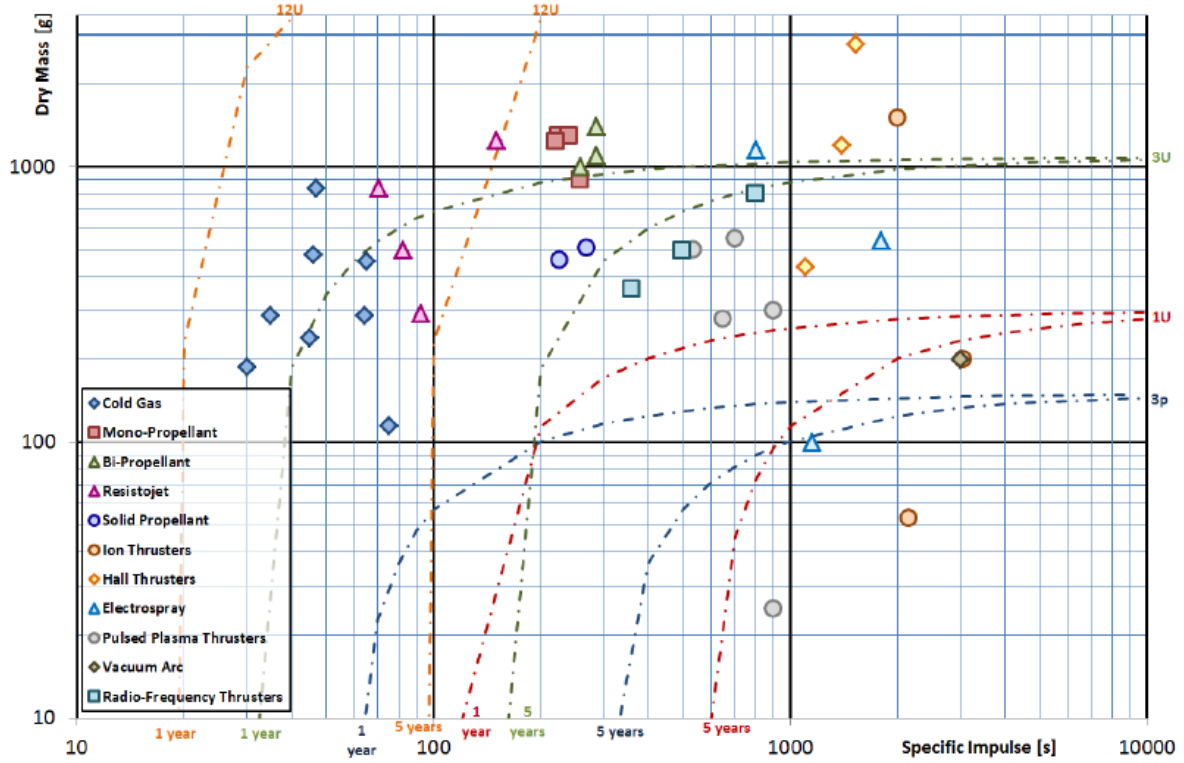


Figure 3-1: Dry Mass vs Specific Impulse for Various Micro-propulsion Systems [22]

Additionally, the power consumption of the satellite in nominal operation has to be defined, which is done according to the power budget. Typical values for the nano- and micro-satellites are around 10W, but these can go up drastically during peak operation, for example when the thruster is active. Also the type of payload has a large effect and communication to distant places requires high consumption, so wide margins should be taken into account [76]. With the 10kg & 30kg previous examples, normal power usage would be around 15W & 24W, with additionally 60W due to electrical propulsion [77]. Decreasing in satellite size and mass in a LEO would result in Orbit Average Power (OAP) of 4.24W as required for Delfi ‘N3xt’ and 4W for the even the smaller ‘PQ’ which utilizes a resistojet [13] [99]. The relation between thrust and power is illustrated for different type of thrusters in Figure 3-2, with resistojet systems falling within the range of most CubeSats.

Since this research will experiment with propulsion systems that requires electrical energy in a similar way as a resistojet, the power required will thus go up with 2 to 30W depending on the thrust required [22]. To stay safe in budget a peak power boundary is taken and doubled, since a thrust of higher than 1N could be required. To restrict size and mass of the combined system, the aim is not to go over 10kg, leading to the overall satellite requirements shown in Table 3-1.

Table 3-1: Requirements for the Satellite Power and Propulsion System

| REQ-1                       | REQ-2          | REQ-3              | REQ-4                    | REQ-5                  |
|-----------------------------|----------------|--------------------|--------------------------|------------------------|
| $\Delta v \approx 0.45km/s$ | $F \approx 1N$ | $I_{sp} \geq 170s$ | $P_{system} \approx 60W$ | $m_{system} \leq 10kg$ |

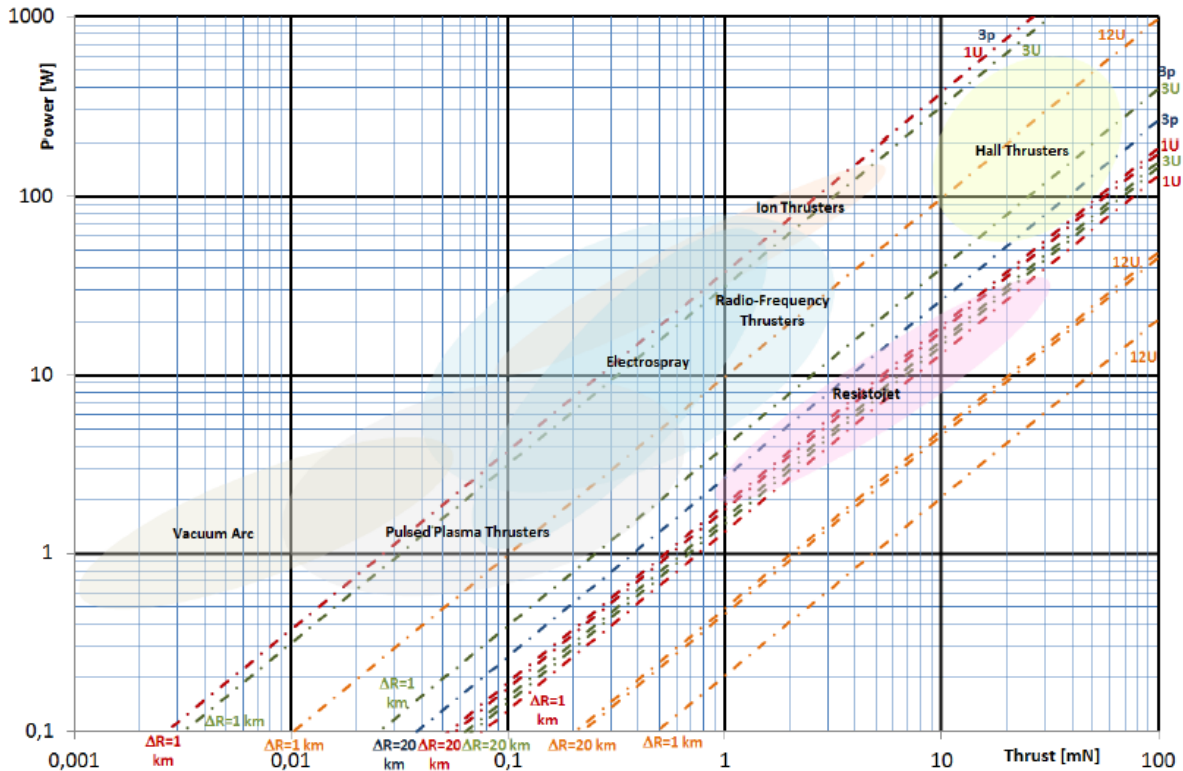


Figure 3-2: Power vs Thrust for Various Electric Micro-propulsion Systems [22]

## 3-2 System Selection

Now the satellite system requirements are set, a match can be made with the most suitable design options to fulfil them. The options to do so for propulsion are limited when  $H_2O_2$  is required as the propellant. Many electric propulsion methods namely drop out and mainly an ignition type remains to choose from. The ignition system is called ‘igniter’, because it is usually used for that cause, whilst it will hereafter also be referred to as ‘decomposition system’ due to its use with  $H_2O_2$  only. The igniter should be selected first since the power generation systems or fuel cell types working with  $H_2O_2$  differ quite a lot and depend on the power required for propulsion.

The selection of the system type was done using the Analytical Hierarchy Process (AHP) Trade-off Tool analysis [102]. This method uses objective and subjective input to assign scores to criteria and the options to select from. The numerical outcome of each criterion and option is based on the analysis in which all aspects are pairwise compared. The first criterion is feasibility; whether or not such a system can be realized within the thesis study. This depends of course on the complexity of the system, but also on the availability of instruments and components, budget restrictions and time wise considerations. Secondly, there is sustainability, which is measured by how ‘green’ the system is and also if it is durable and hence does not degrade much over time. Then there is compatibility, which looks at the possibilities of incorporating each system in a satellite and the ability to combine the thruster with the fuel cell. Lastly, safety plays a large role mainly when executing the experiments themselves, but also related to the general operation of the system.

### 3-2-1 Igniter Trade Off

The propulsion system that can be used in combination with  $H_2O_2$  are either mono- or bi-propellant or a variant of the resistojet. In the mono- case, a catalyst bed is the igniter, which is found to degrade, should be replaced and is thus not selected. In the bi-propellant case, a hypergolic reaction with an additional fuel is the way to go. However, this also requires an initial decomposition system to get the  $H_2O_2$  oxidizer at a temperature which will ignite the other fuel, often done using catalysts. So only the resistojet decomposition variant options remain, from which a distinction between three methods can be made. All those options rely on electricity, being resistance heating, arc discharge and electromagnetic radiation. Each transfer the energy to the propellant differently which hugely affects their use case and efficiency. As mentioned in Section 2-2-3, resistance heating is the most straightforward and has been experimented with already, but the other methods probably work as well and should thus not be excluded. This results in the decomposition system trade off for utilization in this project as shown in Table 3-2.

**Table 3-2:** Decomposition System Trade Off

| Criteria                  | Feasibility | Sustainability | Compatibility | Safety | Total |
|---------------------------|-------------|----------------|---------------|--------|-------|
| <b>Weight</b>             | 0.486       | 0.153          | 0.114         | 0.248  | 1.000 |
| Resistance (heating wire) | 0.59        | 0.23           | 0.45          | 0.48   | 0.494 |
| Electric (discharge arc)  | 0.28        | 0.38           | 0.32          | 0.29   | 0.302 |
| Radiation (laser pulse)   | 0.13        | 0.38           | 0.23          | 0.23   | 0.204 |

The main trade off criterion is the feasibility of the igniter, which in the case of resistance heating is easy since only a power source and resistance wire are required, all available already. The electricity is simply led through a wire that heats up and transfers that energy to the propellant. This is the main reason this decomposition method scores high and is selected to first conduct experiments. Making a setup that works with electrical discharge decomposition is more complex already since more electrical components are required. The difficulties depend on the frequency of the discharge and current type but are mainly attributed to conditions in the experimental thruster set-up that have to be suitable. A laser system is hard to obtain and difficult to work with if it is not the full focus of the project. The system would have to be fully rebuilt to fit the setup and be used as an igniter, which is not something that is easily possible. The laser is a whole system on its own which depends on many aspects and is quite complex already.

Regarding the sustainability of the igniters, all systems perform better already than the catalyst decomposition method. Using a heating wire most resembles the catalyst since there is direct contact between the components and the  $H_2O_2$ . This will thus cause corrosion slightly and the materials will have to be selected and shielded accordingly, hence it scores less well in this category. The electrodes present in the discharge system could erode because of impact, similar to the laser impact location. Also, these systems rely fully on the additional electrical components which are likely to degrade over time as well.

Also, its compatibility with  $H_2O_2$  propellant and the space environment is taken into account, which is dependent mainly on the material type as shown later in Section 3-3-1. Since the electrodes and even more so, the laser system has non-direct contact, they might degrade less but do need additional room for placement and protection of the components. This



makes incorporation in the satellite less favorable. In contrary to resistance wire which would simply replace the catalyst bed in the decomposition chamber. Also regarding the power usage compatibility of the wire is higher, since slowly heats up over time whilst the other two require instant high power to operate. This makes potentially combining them with the fuel cell power source lower.

Lastly, the resistance heating system is relatively safe and easy to work with, and only high temperatures should be taken into account. Electrical discharges, however, also come along with high voltages and are somewhat more difficult to control. Radiative decomposition using lasers should be done with caution in specially adapted environments, for example, because of the risk of damage to the eyes. This makes the latter not suitable for experimentation during this project, whilst if time allows, electrical discharge decomposition experiments will be tested.

As one might have noticed, performance is not yet taken into account when choosing the method of decomposition during the experiments. This is primarily because it is difficult to obtain the parameters that define this for each individual method. Only little data on power usage for the igniters themselves is available through literature and the data on the actual transfer of heat to the propellant differs for each case. Besides this, there are no studies found in which only the decomposition system differs and the other parameters inside the thruster such as propellant and mass flow rate used, are the same, which makes it difficult to compare. Besides this, the energy needed to decompose should always be the same in the case of 100% efficiency, since this is defined by the characteristics of the propellant and not the igniter. The exact numbers on how much energy is being transferred to the  $H_2O_2$  should come from actual experimental results later in Section 5-3-2.

### 3-2-2 Fuel Cell Trade Off

Similarly to the decomposition method trade off, an overview is given of the fuel cell systems in Table 3-3, again sorted based on their structure. However, a better understanding is present here of multiple aspects of the power systems, due to the many experiments already performed, as summarized earlier in Section 2-3-4. Therefore, it was possible to take performance into account here, which is based on an objective comparison of power density output between the best presentable cells of each class.

**Table 3-3: Fuel Cell System Trade Off**

| Criteria        | Power | Feasibility | Compatibility | Sustainability | Safety | Total |
|-----------------|-------|-------------|---------------|----------------|--------|-------|
| <b>Weight</b>   | 0.176 | 0.402       | 0.090         | 0.132          | 0.200  | 1.000 |
| 1 Compartment   | 0.02  | 0.40        | 0.23          | 0.38           | 0.33   | 0.304 |
| 2 Comp. passive | 0.05  | 0.20        | 0.2           | 0.25           | 0.26   | 0.191 |
| 2 Comp. active  | 0.08  | 0.12        | 0.28          | 0.16           | 0.19   | 0.146 |
| 2 Comp. fueled  | 0.32  | 0.12        | 0.1           | 0.06           | 0.06   | 0.131 |
| Semi flow cell  | 0.16  | 0.12        | 0.13          | 0.1            | 0.12   | 0.125 |
| RedOx coupled   | 0.37  | 0.05        | 0.06          | 0.05           | 0.04   | 0.103 |

The power output is clearly higher whenever a fuel is added to the system, as is the case in the fueled and RedOx coupled cell. Furthermore, the performance of a one compartment cell

is insufficient to meet the power requirements set for the satellite. Apart from the passive two compartment cell, the others show power densities that are good enough and can easily be enhanced. The absence of a propellant flow rate thus appears to be the bottleneck for the passive case. It should however not yet be excluded, since some tricks are there to boost its output.

Similarly, as with the decomposition trade off, the feasibility of the system is one of the main criteria for its selection. Here the score is the opposite of performance with a one compartment cell being very basic and not requiring many components. Whilst the RedOx coupled cell is very complex and dependent on many aspects. No previous experience or materials are present to build this  $\text{H}_2\text{O}_2$  cell, so the start will be from scratch. Building a RedOx coupled cell, therefore, becomes very difficult and the road there is too long to fit in this project. Building a one compartment cell should be easy, but is considered as lost effort when it is known in advance that the performance is insufficient. A passive two compartment cell, therefore, seems to be a good starting point despite the many steps that have to be taken to obtain a first working system. Whenever a first prototype of the two compartment cell is manufactured, the active class differ very little in complexity and can thus be developed without too many alterations to the setup.

Regarding compatibility with the satellite environment, all systems score fairly well, each having its own pros and cons. Active systems require extra room to operate, with the benefit of having more control over the output which is the opposite of the passive systems. The pumps could for example also be used to drive the thruster. The semi and RedOx cell's overkill in these aspects, taking in a lot of room and operating at very high flow speeds only. Having only one compartment also means only one electrolyte is required, which matches better with the monopropellant environment of the thruster.

Sustainability wise, all of the systems use a catalyst for electrochemical reduction but in a more protected environment. At low temperatures and flow rates, the catalyst namely experiences far less degradation over time than it would in a thruster catalytic bed. Hence, the semi flow cell and active systems score worse in this category. Simultaneously, combining the  $\text{H}_2\text{O}_2$  with a fuel could also create an unwanted reaction product, making these systems less 'green'. Therefore the passive and  $\text{H}_2\text{O}_2$  only systems score best. Ideally, the electrolytes used in the cell would be removed as well to decrease corrosion effects, but this will probably drastically lower performance.

Lastly, safety can become an issue, mainly when performing experiments. The chemicals used here are often quite dangerous to work with, but inevitable to obtain the desired levels of performance. A good separation of the compartments is crucial in this and if done properly, some fuels that are also used in a bi-propellant system could be used as well. However, the more different chemicals are added the more dangerous the system thus becomes. Having high flow rates, concentrations and temperatures should also be prevented, hence the top three structures score best in the analysis.

The structures that will be developed during this project are thus the two compartments passive and subsequently active cell systems, despite the higher score of the one compartment cell. This is because the one compartment will never achieve enough power to provide for the thruster, whilst a lot of additional modifications can be done to the other systems to make them score higher. This includes changes that are expected to benefit all criteria in both categories at once and make the systems more suitable for use in a satellite. Additionally,

combining it not only with the propulsion system but also adding a thermoelectric generator to obtain even more power from the otherwise accompanied lost heat [133] could be helpful.

### 3-2-3 Reference Systems

Next to the set requirements from Section 3-1, additional guidelines will help to accelerate the development of a combined fuel cell and satellite thruster system. Therefore, a reference system from literature is selected for both the power and propulsion experiments, so the obtained results can be compared with the existing data. These systems are thus chosen from the categories as discussed in the trade off from Section 3-2.

#### Thermal Decomposition Reference

The thruster will thus be based on a heating wire decomposition system and in the case of spare time, arc decomposition is attempted as well. There was only one study found to try the resistojet approach in this thrust range for decomposing the High-Test Peroxide (HTP), which is therefore taken as the reference [80].

However, since developing an accompanied thrust stand, nozzle and decomposition chamber is out of scope of this research, mainly the decomposition system itself and obtained data is being looked into. A heater was used for this, consisting of a resistance wire (3), shielded by an MgO electrical insulator (2), surrounded by an inconel case (1), as shown in Figure 3-3.

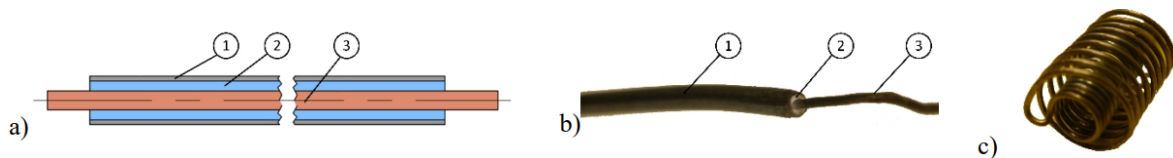


**Figure 3-3:** Heating Wire, a) Model, b) Picture, c) Double Coil Example [80]

Two thermocouples and a pressure sensor were installed to measure the corresponding parameters as the HTP was injected into the chamber with a mass flow rate of  $1.3g/s$ . The wire was set at a temperature of  $600^{\circ}C$  using an external power supply, resulting in a decomposition of the HTP with over  $900^{\circ}C$  and  $4.5bar$ . The thrust almost reached  $1N$  in this configuration, but the power input to achieve this is left unmentioned and should thus be explored via own research. A related study from the same research group however, showed  $200$  to  $250W$  was needed, unfortunately using a gaseous propellant at lower mass flow rates [58].

The discharge plasma arc reference study gives a more clear answer on the power required, being  $0.95mN/W$ , unfortunately again using a different for this case hydroxylammonium nitrate based propellant [111]. The experimental setup is however clearly displayed and could thus be used as a guideline in the case discharge decomposition is tested. The execution is fairly simple, as the propellant flows in between the electrodes, where it forms a plasma. A different study with a more advanced thruster setup, where nitrogen is first ignited into plasma to later decompose  $H_2O_2$  needed far more than  $1kW$  already [9].

## Fuel Cell Reference

The power system will utilize the electrochemical properties of the  $\text{H}_2\text{O}_2$ , as is done in several active two compartment structures before. Instead of starting with the highest scoring one compartment cell, the challenge of directly developing a two compartment cell is taken, trying a passive one first and continue with an active one subsequently. Predominantly the production of the cell itself is therefore helpful to have a guidance for, as well as what power output to expect. Two overarching research groups are there to provide this knowledge, both related to these two compartment cells. The first utilizing a passive structure, with a different electrode production method than the usual [103] [104]. The second one has carried out an even more elaborate research with better results using an active cell and is shown in Figure 3-4 [130] [129] [131] [132].

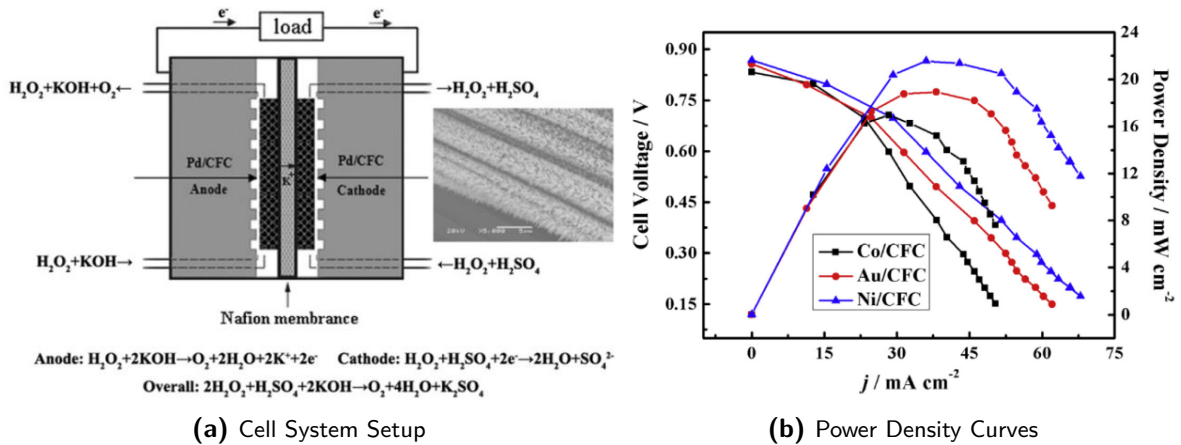


Figure 3-4: Active Cell Reference From Literature [132]

In the optimal case, a peak power density of over  $20\text{mW}/\text{cm}^2$  and Open Circuit Potential (OCP) slightly less than  $0.9\text{V}$  is reached with a nickel anode and palladium cathode, as shown in Figure 3-4b. The support structure of the electrodes also show to have an influence on the cell, where a mesh is taken as anode most commonly and a Carbon Fiber Cloth (CFC) as cathode. These two studies show how besides spraying and soaking, electroplating can be used to deposit the various catalysts on this base layer. Next, there should be a chemically activated Nafion membrane type hot pressed in between the anode and cathode, based on the electrolyte and how the cell will be used in general. The two studies also agree upon using potassium hydroxide (KOH) as anolyte and sulfuric acid ( $\text{H}_2\text{SO}_4$ ) as catholyte to obtain a good electrochemical environment for the  $\text{H}_2\text{O}_2$  as discussed in Section 2-3-2. The total active cell design is shown in Figure 3-4a, where a zoom of the electrodeposited catalyst surface structure is displayed on the right hand side. The passive cell looks very much alike this cell, but is constructed without the flow channels and uses different electrodes. A small overview of the achieved power density using various electrode catalyst materials added behind its performance of the reference systems is given in Table 3-4.

**Table 3-4:** Fuel Cell Study Reference Parameters Overview

| Cell Structure              | Passive (Ni anode)                 | Active (Pd cathode)  |
|-----------------------------|------------------------------------|----------------------|
| Power Density [ $mW/cm^2$ ] | 3.75 (Pt), 10 (PbSO <sub>4</sub> ) | 14.3 (Pd), 21.6 (Ni) |

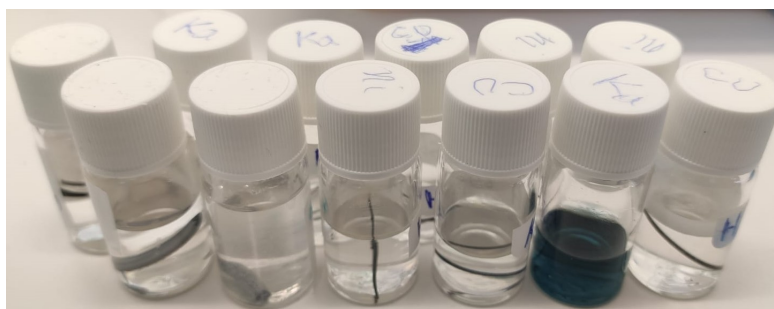
### 3-3 Engineering Challenges

In the development process of fuel cell and igniter systems, some notorious challenges will be encountered related to either the chemical characteristics or performing experiments in general. Mainly the issues regarding material compatibility and safety of chemicals that are used should be averted.

#### 3-3-1 Material Compatibility

Before the actual fuel cell and decomposition system is being set up, it has to be checked if the materials can actually withstand the chemicals that are being used in the system. Material selection is not only important for the material itself, but also needs to take into account the effects on the decomposition of H<sub>2</sub>O<sub>2</sub> and accompanied safety issues. Therefore, some information on the resistance of possible materials to the H<sub>2</sub>O<sub>2</sub>, acids and bases has been looked up, as can be seen in Appendix -5. Also temperature and electric resistance are important parameters to look into, since they can become a bottleneck in either system. Thus, some initial simple material compatibility tests have been performed to check degradation via observation. The material would be mainly used for the end plates, as containers, tubing, or the electrochemical features of the fuel cell Membrane Electrode Assembly (MEA) itself. Regarding the igniter, the heating wire materials are most important as well as the injection components and protective casing. The combined results from literature and experimental study for various materials with chemicals and conditions and are listed in Table 3-5. In here, unavailable materials or ones that are known to fail already have been left out.

During tests, a small piece of the material was examined by leaving it in a chemical and checking changes such as weight loss afterwards, as shown with some samples in Figure 3-5.

**Figure 3-5:** Material Chemical Compatibility Test Examples

Environmental condition effects were inspected with ovens, multi meters and by force, to validate the foreknown listed performance. A plus sign means the material works well with that criteria, a circle indicates possible use with caution and a minus means the material

**Table 3-5:** Material, Chemical and Environmental Conditions Compatibility Overview

| Material          | HTP | Acid | Base | Fuel | Temperature | Electricity | Pressure | Feasibility |
|-------------------|-----|------|------|------|-------------|-------------|----------|-------------|
| <b>Structural</b> |     |      |      |      |             |             |          |             |
| PLA               | +   | +    | o    | +    | o           | +           | o        | +           |
| ABS               | +   | +    | +    | +    | o           | +           | o        | +           |
| PVDF              | +   | +    | +    | +    | o           | +           | o        | o           |
| PVC               | +   | +    | +    | +    | o           | +           | o        | o           |
| PTFE              | +   | +    | +    | +    | o           | +           | -        | +           |
| TPE               | -   | -    | +    | o    | o           | +           | -        | +           |
| Glass             | +   | +    | +    | +    | +           | +           | +        | -           |
| SS 316            | +   | +    | +    | +    | +           | -           | +        | -           |
| Aluminum          | +   | -    | -    | o    | +           | -           | +        | -           |
| Ceramics          | +   | +    | +    | +    | +           | +           | +        | -           |
| <b>Functional</b> |     |      |      |      |             |             |          |             |
| Nafion            | +   | +    | +    | +    | o           | o           | -        | +           |
| Carbon            | o   | +    | +    | +    | +           | o           | +        | +           |
| Copper            | o   | o    | o    | -    | +           | +           | +        | +           |
| Nickel            | o   | o    | +    | o    | +           | +           | +        | +           |
| Iron              | -   | -    | -    | o    | +           | +           | +        | o           |
| Chromium          | o   | o    | +    | +    | +           | +           | +        | o           |
| Platinum          | o   | +    | o    | +    | +           | +           | +        | o           |
| Palladium         | +   | +    | o    | +    | +           | +           | +        | o           |

does not function well for some of the goals in mind. In some cases, there is a combination of materials, chemicals or effects present, which mostly has an unwanted negative effect on its objective. This for example occurs when  $H_2O_2$  and  $H_2SO_4$  are mixed and form an even more aggressive compound, or both pressure as well as high temperature are applied. This will predominantly negatively effect the materials that already score less than good on one of the criteria.

Plastic is the chosen to construct the fuel cell structure with, because of its availability within this project and additive manufacturing possibilities. From all types, Poly Lactic Acid (PLA) is cheapest and easiest to work with, but Acrylonitrile Butadiene Styrene (ABS) the most resistant yet still producible. This is why for structural causes, all prototypes can initially be made of PLA and then be upgraded to ABS, Polyvinylidene Fluoride (PVDF), Polyvinyl Chloride (PVC) up to Stainless Steel (SS) and eventually even glass or ceramics. The same holds for the decomposition structure, although this requires some more resistance materials to start with, safety wise. Polytetrafluoroethylene (PTFE) or Teflon is preferred above Thermoplastic Elastomer (TPE) to fulfill roles such as tubing or tape. Functionally, it seems that not many materials are uniformly deployable, but will have to be chosen for its use specifically, as with Nafion and palladium fulfilling roles in the MEA. For the heating wire, combined metals such as Inconel is the way to go, whilst alloys containing copper are thus less resistance due to its mismatching properties.

### 3-3-2 Experiment Safety

Since during this project many challenges regarding safety are encountered, extra attention is laid on this topic. The dangers are related firstly to the explosive nature of  $H_2O_2$  decompo-

sition, which involves high temperature that can cause burns. A chemical burn can however be created far more quickly due to the many acid, base and high concentration compounds used in this project. Lastly, operation of the instruments and components comes along with high electric currents, voltage and temperatures. Several precautions should thus be taken to minimize the chance on accidents, as listed below.

- **Study:** being aware in advance what the chemical properties and associated risks are, is essential. Similarly, knowing how to operate the necessary instruments can be helpful. Therefore, all Material Safety Data Sheet (MSDS) and instrument manuals were looked up to prevent cases of surprise.
- **Control:** manage the situation, by knowing what is the status of everything and making sure the environment and surroundings is optimal. Being in control of the setup and careful handling of the chemicals and setup is part of this, to prevent for example thermal runaway.
- **Prepare:** use a checklist to go by each device or component in advance and know what information is wanted from the experiment. Doing simpler, individual tests initially, leading up to the final desired experiment will help to get one familiar with the setup.
- **Downsize:** by keeping everything on a small scale, less damage can be caused in the case something goes. The same information will probably come forth from the smaller setups, just an additional extrapolation has to be done.
- **Minimize:** if less experiments involving hazardous situations need to be done, it can go wrong less often. Obtaining as much information as possible in each test will help in this.
- **Protect:** most obvious is probably to wear protection during experiments, so in the case something does go wrong, no one will get hurt. This is done of course by wearing a lab coat, glasses and gloves, but also by working inside a fume hood or protective casing.

### 3-4 Verification & Validation

The Technology Readiness Level (TRL) of both the fuel cell and thruster is around three to four during this project, which is basically experimental Proof of Concept (PoC) and validation in the lab. Hence, a physical prototype is already existing and the theoretical principles are known to function. The basic parameters which need to be measured to acquire the performance are thus known as well, being mainly temperature, current and voltage. There will however be many challenges related to obtaining the exact values in an experimental setup and checking whether these values are correct or not. This can be done firstly by comparing it with the predefined reference systems and information obtained in Section 2. Secondly, a model can be set up to place the theoretical results and the experimental ones side by side. This analytical model is however only a reflection of the final performance involving many assumptions, as is shown later in Section 3-5. Third, the experiments themselves can be used as validation, by repeating them several times whilst using the exact same settings.

Verification is achieved by performing tests which are known to not work and give a definite outcome. A final and more distinctive verification is done using specific instruments along the way of the system development processes which can confirm proper operation of the device used in the setup. This validation and verification has thus already partially been performed for the materials, as shown by Table 3-5.

### 3-4-1 Instrumentation

The instruments themselves however have to be validated as well on correct functioning. Hence, the required devices that will be used in the fuel cell and decomposition experiments are tested first and discussed hereafter.

#### General

Examining basic properties is done with standard tools such as a weighing scale, ruler, camera, thermo- and voltmeter. Mainly individual components are tested this way during intermediate steps leading up to the final system, to validate if the process goes correctly. Since there are multiple of them present in the lab checks are done first with one and then again with a second one to see if the same values are derived. Something similar was done with the high-speed camera and power supply used in the decomposition study of Section 5-2-1. A second handheld camera was used to see if it matched the high-speed recordings and a different power supply was sometimes attached to the setup to see if the same power was needed for the igniter.

Then there were some instruments during the MEA production process from Section 4-1 which could not be validated at all. Since the airbrush used for spray deposition did not have a manual or gauges during operation, its validity was low and the device had thereafter not been used any longer. The Joos 500kN hot press used in the making of the cell did however have a manual and a digital indication of the pressure and temperature during operation. This made it possible to at least monitor the procedure and register the possible offsets which could later be taken into account. Regardless of their simplicity both instruments required an instruction by the responsible lab employee beforehand to verify for correct operation.

Finally there were the pumps used in the fuel cell experiments which did not have a gauge to monitor its flow rate. Hence, this had to be determined for various liquids and quantities at set power inputs. Multiple tests were thus done in which a known amount of mass and volume was pumped through and the time it took was measured and vice versa.

#### Potentiostat

Then there was the first complex instrument which had to be used in the electrodeposit procedure as explained in Section 4-1. Before using the potentiostat (AUTOLAB PGSTAT302), an instruction was given on its operation by the responsible lab manager as well as the manual was walk through. Also, the required procedure was partially explained already by the reference study and some clarification on the steps of the process were inquired from the NOVA (2.1.5) potentiostat software manufacturers. The validation of the current and potential itself



came from sampling plots of the process afterwards. Before the actual MEA was used in this, it was attempted with a dummycell first. Using this dummycell, the complete process could be monitored and validated on correct operation.

## **SEM & XRD**

To verify whether or not the catalyst had been deposited correctly using the potentiostat, the Scanning Electron Microscopy (SEM) and X-Ray Diffractometry (XRD) could be used. These devices were both available at the Delft University of Technology (TU Delft) and were also able to perform an X-Ray Photoelectron Spectroscopy (XPS) and Energy Dispersive X-Ray Spectroscopy (EDS). An extensive instruction and clarification by the manual was required beforehand however, since they are quite expensive and complicated. Predominantly helpful to see changes in the material before and after usage, by first imaging the untreated and later deposited MEA and thus to validate correct deposition, as will be discussed in Section 4-2-1. These instruments are on its own backed up again by normal microscopes images which were taken beforehand and compared to see if the SEM images would match.

## **Digital Multimeter**

The digital multimeter was used in this study for the fuel cell current and voltage measurements. Two Keithley 2701's are the exact instrument types, of which the operation at the TU Delft was normally linked with two extremely cumbersome old fashioned measurement cars. This was found hard to use with the fuel cell set up, hence after the Digital Multi Meter (DMM) instruction it was connected to only one laptop with 'Kickstart' software. The manual was found to be very helpful by explaining all its functions and correct operation. Upon installation, the DMM's were tested first with various AA, AAA and 12V batteries having a known potential and current output to validate its measurement. Similarly a power supply was used to check its measurement range as well as resistances at known loads were added to the circuit to verify if the DMM reaction was correct. All of this proved the instrument functioned properly, still a handheld voltmeter was sometimes attached before, during and after experiments to see if the same values were obtained.

## **Thermocouples**

For the decomposition study, the most important component which needed to be checked was the thermocouple. On its own, this thin K-type wire was just two different metals connected at its ends. Hence, a Data Acquisition System (DAQ) was needed to measure the potential difference that arises when heating it up, for which the National Instruments (NI)-9219 was a perfect fit. When connected to a Labview or Flexlogger program, its results are automatically read and stored on the laptop. The associated wire and measurement conditions needed to be imported first to have a matching recording scale. The DAQ and wire descriptions indicate clearly already the accuracy and installation, but validation had to be performed anyway. Hence, the wires were taken from the known ambient temperature and immersed in boiling water of 100°C. During these tests a lab thermometer was used simultaneously to see if the values corresponded. Over time, this test was repeated to check if potential corrosion on the wires caused misreading.

### 3-4-2 H<sub>2</sub>O<sub>2</sub> Concentration

Since the H<sub>2</sub>O<sub>2</sub> that is available in chemical labs is either 30% or 50% and the rest water, it has to be diluted or concentrated to obtain other ratios. Diluting goes the same way as with other chemicals that have to be lowered in concentration during the project. Water or the accompanied chemical is added to the H<sub>2</sub>O<sub>2</sub> after having carefully calculated and measuring its quantity. This step is performed predominantly during tests with the fuel cell, where often low molar concentration  $c$  of only a few molar  $M$ , is required. Measuring the exact concentrations afterwards is difficult, but due to the high accuracy of the weighing scale when preparing the solutions, it is assumed that deviations are negligibly small.

The upgrading of H<sub>2</sub>O<sub>2</sub> concentration goes with a patented technology developed by SolvGE, the company at which the study is performed. This process makes it possible to work with HTP which is required in the decomposition test predominantly. The exact values of the concentrated H<sub>2</sub>O<sub>2</sub> do however need to be verified, which is done with the use of a handheld refractometer. This instrument measures the index of refraction of the inserted liquid in Brix. This unit can be converted to concentration of the H<sub>2</sub>O<sub>2</sub>, since its refractive index  $n_{ref}$ , is known to be 1.408. An inaccuracy of the measurements comes mainly from manual misreading, which go up to 0.4 Brix, as opposed to the instrument accuracy of  $\pm 0.1$  Brix. A digital refractometer was present and once used as well, used for verification of the handheld data, since its accuracy is up to  $\pm 0.01$  Brix. This results in a total inaccuracy of approximately 1% in tests where HTP is used.

## 3-5 Analytical Models

Another helpful tool in verifying the developed system is with analytical models which simulate their performance. To do so, calculations are done using Eq. (2-8) and Eq. (2-7) in Matlab. This is done first for the fuel cell's three most important parameters, being power density and voltage versus current density. Subsequently the thermal decomposition is analysed, to find the power needed to decompose H<sub>2</sub>O<sub>2</sub> and its accompanied decomposition temperature.

### 3-5-1 Fuel Cell Polarization

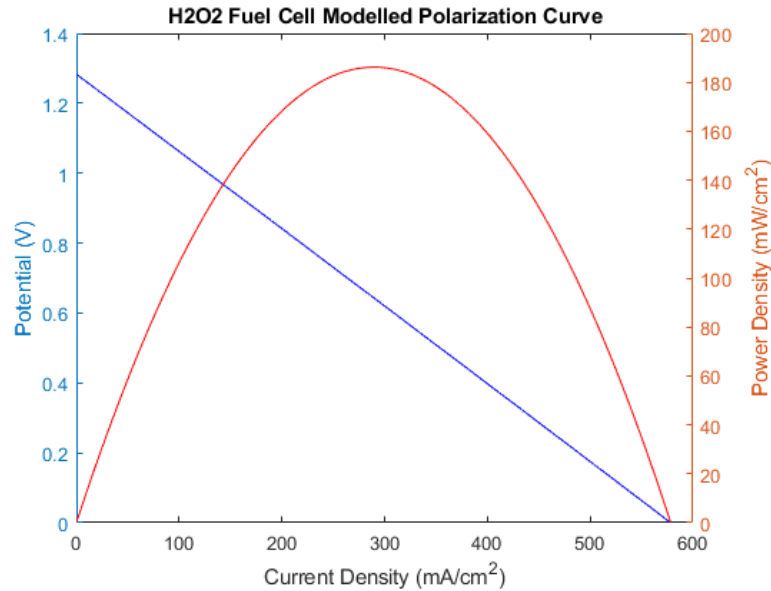
Fuel cell polarization is thus based on the Nernst equation shown in Eq. (2-8). It uses the basic properties of H<sub>2</sub>O<sub>2</sub> as shown in Table 2-1 and needs additional electrochemical specific parameters, displayed in Table 3-6. These constants were taken from literature and are based on the reference systems as described in Section 3-2-3.

The one unmentioned parameter here is electrical conductivity  $\sigma$ , which again depends on the resistivity  $\rho_r$  of the MEA components used. The Charge Transfer Coefficient (CTC), exchange current density  $I_d$  and electrical conductivity  $\sigma$  are unique for each anode ( $a$ ) and cathode ( $c$ ) material, hence influence the cell performance apiece. This CTC and exchange current density are the most defining parameters and determine mainly what current is achieved. They are not always properly defined in experimental data found in literature, but for this case taken either as an average or estimated value based on the material type and electrolyte combination used [40] [83]. The crossover losses are mostly reliant on the system conditions

**Table 3-6:** Fuel Cell Performance Constants

| Parameter                            | Value             | Remark             |
|--------------------------------------|-------------------|--------------------|
| $n$ [-]                              | 2                 | Electrons          |
| $\alpha_a$ [-]                       | 0.38              | Nickel             |
| $\alpha_c$ [-]                       | 0.2               | Palladium          |
| $I_{0a}$ [ $\frac{A}{cm^2}$ ]        | $10^{-6.1}$       | Ni in base         |
| $I_{0c}$ [ $\frac{A}{cm^2}$ ]        | $10^{-4}$         | Pd in acid         |
| $I_i$ [ $\frac{A}{cm^2}$ ]           | $3 \cdot 10^{-3}$ | Crossover          |
| $I_m$ [ $\frac{A}{cm^2}$ ]           | 1.4               | Limiting           |
| $\sigma_a$ [ $\frac{1}{\Omega cm}$ ] | 143000            | Nickel foam        |
| $\sigma_c$ [ $\frac{1}{\Omega cm}$ ] | 2.5               | Carbon fibre cloth |
| $\sigma_m$ [ $\frac{1}{\Omega cm}$ ] | 0.0564            | Nafion 117         |
| $d_m$ [cm]                           | 0.0183            | Nafion 117         |

itself and is selected to be fairly low due to the calm environment. The resistivity of the MEA materials are obtained from the technical specification sheets of the supplier. The mass transport present in concentration losses only comes into play at very high current densities when depletion of propellant goes fast. Similarly to the limiting current density, this performance will not be achieved with the system developed during this project, as its value does not show to have any influence on the model performance. The value of the empirical constant does not effect this system much either, since the operational conditions of the cell are kept constant. With the Hydrogen Peroxide Reduction Reaction (HPRR) set as standard state reversible voltage, a performance as shown in Figure 3-6 is achieved.

**Figure 3-6:** Performance Results From Polarization Model

In both reference studies, the achieved voltage and maximum current density are far below the shown value. This is expected to be induced by several sources of which the first is the

accompanied Hydrogen Peroxide Oxidation Reaction (HPOR), which instantly lowers the starting voltage. Almost always it is noticed that lowering the CTC will subsequently lower potential as well. This means that a lower partial current is present, because the flow of electrons from the electrode surface to a species in solution is less, hence the charge transfer is less. Besides these two, the resistance has a large influence on the maximum power density which is achieved which is why the conductivity of the electrodes used in the MEA and the current collectors should be maximized. Finally, more crossover losses than expected can be present in the cell, as the system and MEA wears over time and current is able to go from one side to the other due to membrane and structural deficiencies. Anyway, achieving the modelled polarization is the goal and should be possible, as since some of the losses are taken into account here already.

### 3-5-2 Thermal Decomposition Capacity

The power required to decompose  $H_2O_2$  can thus also be predicted, using the equation Eq. (2-7). The values that are of importance are mentioned before in Table 2-1 for  $H_2O_2$ , and are looked up as well for plain water [90]. Additionally there is the dependency of concentration on the power required, because of the more water being present. The ratio of water namely makes the heat capacity as well as heat of vaporization of the liquid higher. The assumption is made that the  $H_2O_2$  only needs to be raised  $130^\circ C$  in temperature to achieve decomposition at its boiling point. A mass flow rate of  $1.3g/s$  is taken as an input, based on the decomposition thruster reference study system. Finally, it is assumed that all of the energy input is transferred to the liquid, resulting in the input power required as shown in Figure 3-7.

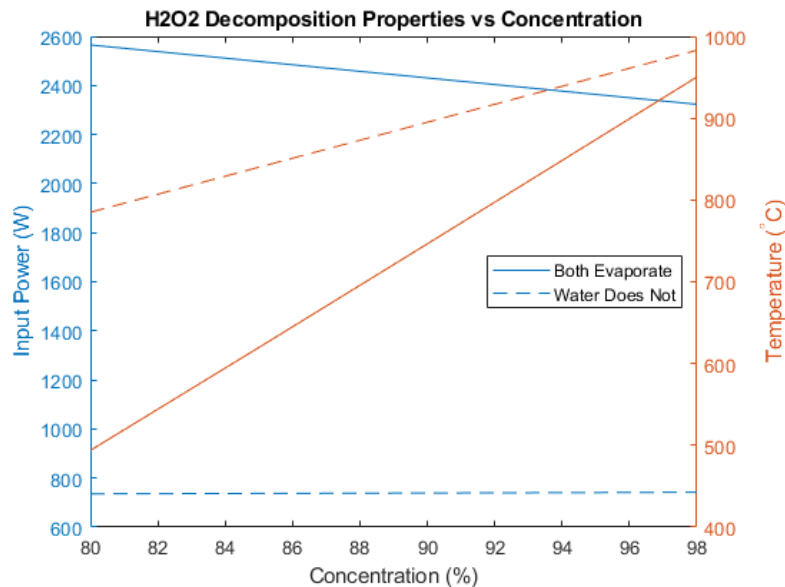
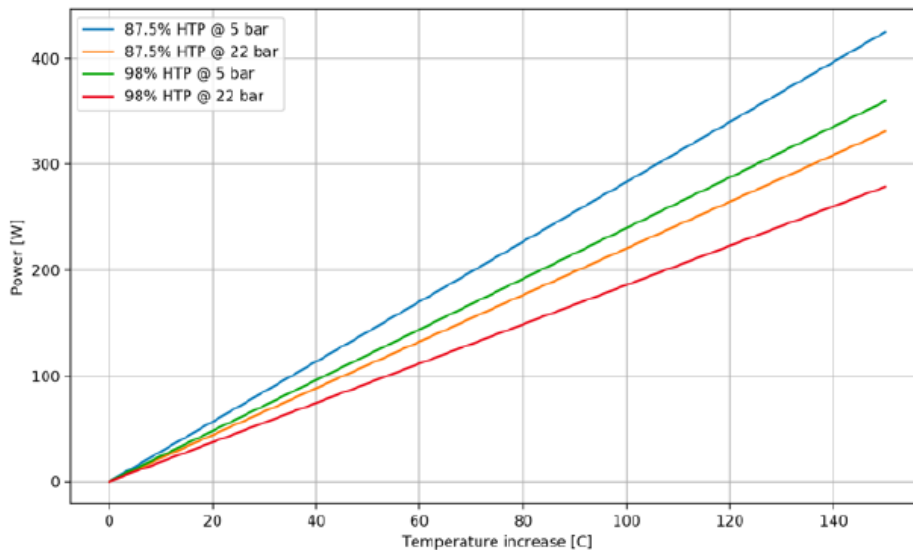


Figure 3-7: Power & Temperature vs  $H_2O_2$  Concentration

In this plot, maximum temperature reached is displayed as well, based on an ideal adiabatic process. These results were calculated using Rocket Propulsion Analysis (RPA) Lite and depend on similar conditions such as decomposition under atmospheric pressure and temperature. The required power turns out to be surprisingly high, mainly due to the contribution

of the latent heat of evaporation in the model. An attempt is done to lower this value by plotting the power in the case the share of water would not evaporate. The same has been done in a previous study for the temperature, resulting in the higher value shown [55]. This means the liquid water does take in energy to heat up but stays liquid after decomposition, as indicated by the dashed lines in Eq. (2-2). This would make the power required drop down drastically to approximately  $740W$ .



**Figure 3-8:** Power vs Temperature Increase of HTP Taken From Literature [36]

Figure 3-8 displays the temperature increase versus input power as recorded in a different study. This power required turns out to be far less, which can at least partially be attributed to the high pressure conditions. Their mass flow rate used is unknown, as well as the assumptions regarding evaporation, which both drastically influence the required power. The values however correspond more with the non-evaporating case, although the trend is more in line with the evaporating one.

Actual transfer of energy from the decomposition system to the propellant will however be far less, due to for example the heat loss present. Besides this, temperature increase required is predicted to be higher than just its boiling point. On the other hand however, heat released in the decomposition reaction will have a huge positive effect up until the point it is expected to become self-sustaining. Also, pre-heating of the chamber beforehand can be done at lower input power, as long as the temperature increase upon injection of the propellant is sufficient. Regardless, values of around  $2500W$  and over are expected to be needed to start decomposition in ambient conditions.

### 3-6 Conclusion

To be able to do a feasibility study and develop a PoC of a power and propulsion system, a project baseline is set up to aid the process. First, an indication of the satellite requirements is needed, from which  $60W$  peak power is the most defining one set for this study. The thruster

has to stay under this number and the fuel cell should produce it, whilst simultaneously meeting the other demands. To achieve this, the most suitable reference guideline from a system in literature is chosen after performing a trade off. The decision is based on achieving a certain level of performance and low complexity whereby the system can actually be safely realized within the project duration. The two compartment active cell and resistance coil decomposition system are selected to gradually build towards, for which several engineering challenges still lie ahead. Many of them are related to conducting repeatable experiments with  $\text{H}_2\text{O}_2$ , while keeping great attention to safety. Performing small scale tests with mainly plastic materials, should resolve this issue, as long as constant double checks are carried out during tests. Simple analytical models of the fuel cell polarization and power required for decomposition with the reference systems are made as a first impression. Similarly as the literature results it gives a clear indication of what results to expect and serve as a guideline throughout the development process itself.

---

## Chapter 4

---

# Fuel Cell System

With the knowledge gained from literature in Chapter 2, the project baseline and information provided in Chapter 3, it was then time to test a system of our own. The goal was to develop a Proof of Concept (PoC) fuel cell and find out if power generation using Hydrogen Peroxide ( $\text{H}_2\text{O}_2$ ) in such a system is indeed possible. This was done by developing prototypes of increased complexity, starting from scratch with production and optimizing its performance by various means along the way. The results from the experiments were then analyzed, so a conclusion could be drawn on ways to improve its output power. This chapter shows the development process in chronological order, addressing its findings and some important points that were run into to a further extent. Starting with the manufacturing of each component of the cell, then the experiments and the data that had come forth and finally recommendations based on all results.

### 4-1 Fuel Cell Manufacturing

Before the experiments could be performed, the fuel cell itself had to be produced. This meant each subcomponent had to be designed, manufactured and then assembled for testing. This was done based on the reference cases, available materials & instruments, safety precautions and further considerations mentioned in the project baseline of Chapter 3. First, the Membrane Electrode Assembly (MEA) and its elements are discussed and subsequently the cell and structure types that were developed and tested.

#### 4-1-1 Electrode Production

The design specifications of the anode as well as the cathode influence the performance of the fuel cell in various ways as seen before in Chapter 2. The first aspect is the material that is being used as a support structure and secondly the catalyst that could be deposited on there. The production process itself, however, plays a large role too and is a whole undertaking of its own. Therefore, several methods of fabrication are looked into, unfortunately taking up more time than initially planned due to their complexity. The reason why the production of the electrodes is done on site is that the ones required for this type of fuel cell were simply not commercially available. Most of those are only compatible with hydrogen and oxygen, whilst

they will not work with  $H_2O_2$  and other chemicals that are used here. The other reason for in situ production of the MEA is thus due to the deposition method, which has a very specific procedure that has not been performed with commercial ones. So instead of buying the ready made electrodes, only the individual materials are purchased to custom-build our own.

### Gas Diffusion Layer

One of these materials is for the support structures used in fuel cells which are mostly carbon based materials on which a catalyst is deposited. In our case this would be either Carbon Paper (CP) or Carbon Fiber Cloth (CFC), functioning as the cathode. It is however also possible that the Gas Diffusion Layer (GDL) itself is already functioning as a catalyst, as is the case with the nickel foam used as anode in this research. This does not rule out the possibility of an additional catalyst being deposited on there, as will be discussed later in Section 4-1-1. The support structures were cut to a size of  $2 \times 2 \text{ cm}$ , which is the area that is in contact with the electrolyte.

Before the GDL is used in the MEA it has to be pre-treated so no contamination is present on its surface and the material is activated. This cleansing, but mostly the activation of the material will eventually increase the power output of the cell depending on the chemicals. With CP for example, the power and current output become more than 1.5 times higher already in a different microfluidic cell type [71]. Since the rest of the process was not possible at the lab, only a part of the existing processes was followed [104]. Also, there were bigger concerns influencing the power generation process, hence this was not further investigated. CFC was not treated in any way before the deposition of the catalyst, in the contrary to nickel foam which was degreased beforehand [119].

The actual size and structure of the GDL directly influence the performance of the cell, since it affects the surface area. This characteristic is merely predefined by the type that was purchased. For the nickel anode foam structure, this was predefined mainly by the amount of pores and thickness (Beihai Composite Material Co, LTD). The main factor of influence for the carbon cathode would be the presence of a Micro Porous Layer (MPL) on either surface side. This is applied to improve the water management inside the cell, by making sure liquid does not get stuck in the GDL [121]. It also helps to reduce the resistance between the catalyst on it and the GDL itself. The same water resisting properties are possessed by Polytetrafluoroethylene (PTFE), which is why this is often included in the treatment of the GDL's as well (Fuel Cell Store). It was therefore decided to add one side of the carbon supports used in our fuel cells with such a layer and the treatment because it was expected to boost the performance.

### Catalyst Material

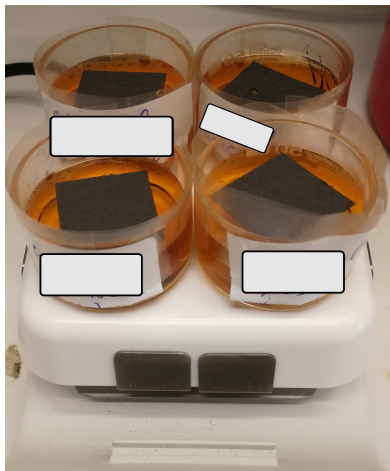
Then the most reactive element of the fuel cell is prepared, by making the catalyst and subsequently depositing it on the GDL. For the same catalyst elements palladium and nickel, there are different solutions needed depending on the method of deposition. Other materials that could have been used at either side of the MEA are Ag, Au, Pt,  $PbSO_4$  and Co, but these deemed less suitable. At the anode this is due to the bubble generation they create in the following order  $Ag > Pd > Pt > Au > Ni$  [103]. This affects clearly the system and its



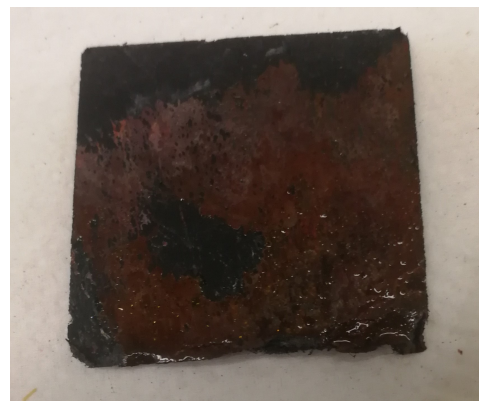
performance because the Oxidation Reduction Reaction (ORR) can take place more which is unwanted. At the cathode, these catalysts simply do not achieve as high Open Circuit Potential (OCP) and current density.

Deposition methods can thus be divided into three categories during this project. In the end, the electrodeposition is deemed most successful and suitable for long term operation and is therefore used to continue with in combination with the palladium cathode. The amount of catalyst on the GDL, or loading, was determined by simply weighing the GDL before and after deposition.

1. **Soaking:** in this method the GDL was submerged in the catalyst solution, similarly to during the pre treatment of the GDL itself. The solutions needed in this case consisted of multiple chlorides including the catalysts themselves [103] (Sigma Aldrich). CP was immersed in the stirred solution at a constant, elevated temperature, as shown in Figure 4-1a. Subsequently, the two were placed in an ultrasonicator to make the catalyst bond even better through vibrations.



(a) Multiple Electrodes in Setup



(b) Visible Uneven Catalyst Distribution

**Figure 4-1:** Soaking Deposition Process With CP

The soaking method was attempted in an early stage, when many things went wrong, such as the evaporation of the solution overnight. Also, the catalyst layer seemed to be distributed unevenly and was not bonding properly with the GDL, as can be seen in Figure 4-1b. Furthermore, despite being a quite simple process it takes a long time to bond and was attempted in literature only with CP. The lower performance resulting from this deposition, made it so that the method was not continued hereafter.

2. **Spraying:** this method is different from the others due to the catalyst composition, which is mixed to form an ink. This ink consisting of a solution with the catalyst and an ionomer binder and is prepared far in advance and subsequently sprayed on the GDL (Fuel Cell Store & Sigma Aldrich). This was done manually in a paint lab using a small airbrush set at low pressure. The GDL was placed and fixated on an aluminium sheet, covering the heating plate, as shown in Figure 4-2. The airbrush with the desired amount of catalyst is then simply sprayed on the GDL from the top at a close distance, in a zigzagging, mixed pattern.

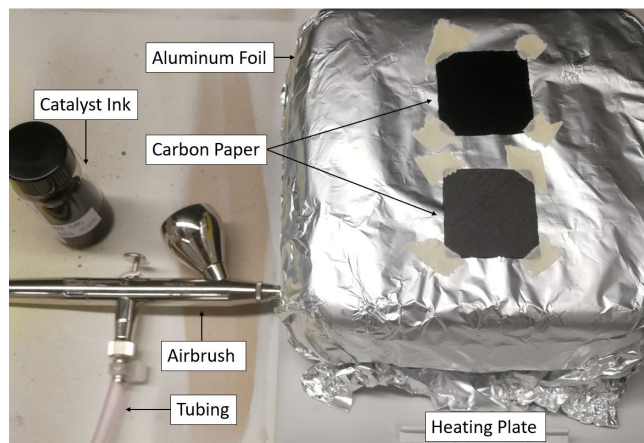


**Figure 4-2:** CP Spraying Setup

The spraying process was expected to be more quick, easy to execute and bond better in exchange for some extra effort. This turned out however to be far from ideal since many problems arose with the airbrush, which is a delicate instrument to operate. Usually, the spraying is performed in a more controlled environment by an automatic airbrush which can be set as desired [105]. Unfortunately, it was not possible to use this device since it was located at another faculty and unavailable at the time. This made the spray process unfavorable in the end as well, because of unequal distribution of the catalyst and difficult repeatability despite careful operation.

3. **Electric:** to be able to perform electrodeposition, a lot of time was invested in obtaining the materials required and getting to know the instruments used during the process. Similarly as with the soaking process chlorides are used here again, but now the GDL is treated in a voltammetry setup. In this three-electrode electrochemical cell, a circular platinum mesh counter electrode and a Silver chloride (Ag/AgCl) reference electrode ( $E = +0.197V$  in saturated KCl) is placed. The deposition of the catalyst happens through the reduction of cations by means of a direct electric current which is applied with a potentiostat (Autolab PGSTAT302N). This method was used for both CP and CFC with palladium, as well as nickel foam to boost performance with additional nickel deposition, as shown in Figure 4-3.

Electrodeposition was the most complicated option, which worked great with palladium on CFC whenever a specific potential pulse was applied to the three-electrode electrochemical cell [130]. Using this exact method, the catalyst would form dendrites on the CFC, which increased its surface area and prevented gas from building up in its layers so there would be better interaction with the electrolyte flow. When acquainted with the procedure and in possession of the required instruments, this would thus lead to optimal performance. Whether or not the process went according to expectations had to be verified hereafter, as explained later in Section 4-2-1. For nickel deposition, the procedure was unsuccessful, because the surface area of the foam was far too large in comparison with the counter electrode. Besides this, the foam on its own already proved to work perfectly fine and the additional nickel was deemed to be superfluous anyway.

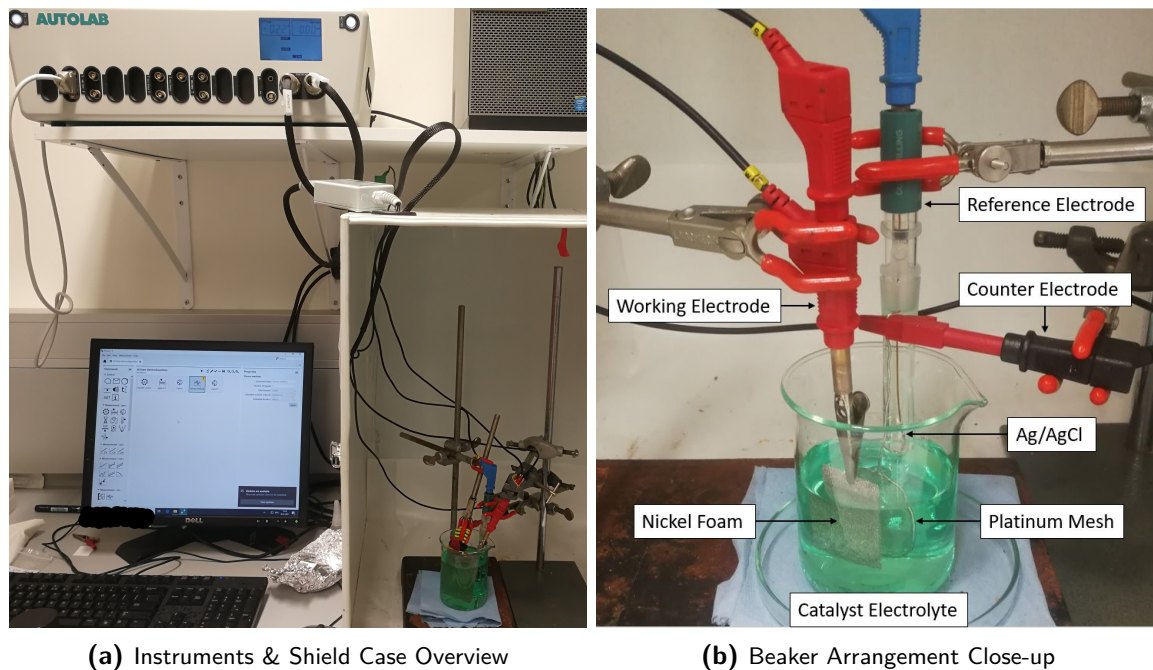


**Figure 4-3:** Nickel Foam Electrodeposition Setup

#### 4-1-2 Membrane

The type of membrane used in the  $\text{H}_2\text{O}_2$  liquid cell was a Polymer Exchange Membrane (PEM), for which often a commercial Nafion version is used. This is thus in solid state, functioned to let through only cations of a specific type. Similarly as with the GDL, the structure and treatment of this membrane have a large impact on the performance of the cell. Thickness is one of the first aspects to change and has a clear effect on crossover losses and its conductivity, according to literature [72]. But because the thinnest membranes are difficult to handle and might rupture upon assembly, mostly thicker ones are used. Similarly to the support structures, the membrane was cleansed beforehand and was also activated, by boiling it in the fuel and acid electrolyte used. In this case, the procedure was always applied, since a lot of literature addresses the fact that performance will increase from this, even when working with different electrolyte solutions [97] [94]. The membrane was cut to a slightly larger size than the GDL, to prevent the two electrodes from having direct contact and such that they could be clamped in between the cell structure.

#### 4-1-3 Membrane Electrode Assembly Production

Whenever the electrodes were finished, the treated membrane was sandwiched in between them to make the MEA fuse together using a hot press. The catalyst layers deposited on the MPL of the GDL were placed facing towards the inside to obtain the best conduction throughout the membrane [105]. Multiple MEA's, each with its own specifications, were placed on the aluminium plate to be subsequently compressed, as shown in Figure 4-4.

High temperature would cause the membrane to dry out, whilst applying too much pressure would cause the electrodes to be damaged. The deposited structures would namely break and



**Figure 4-4:** Hot Press Plate Filled With Various MEA's

the surface area would go down. But also the membrane could rupture causing the electrolyte to be able to pass through it.

### **Current Collectors**

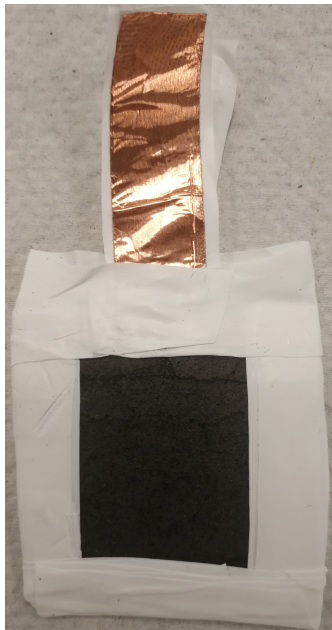
To measure and use the power produced by the fuel cell, current collectors needed to be added to the system. This is normally added as a metal bipolar plate in contact with the electrolyte and guiding outside the cell. This was however expensive, very heavy and did not fit with the rest of the cell structure. As instead current collector leads were connected directly to each electrode and extended to outside the system, where external cables could be clamped on them. Initially, applying copper tape at all edges of the GDL was used for this, as it was the most convenient solution during the project and a very good electrical conductor. Since it was known from evaluation in Section 3-3-1 to not be a perfect match with all chemicals and act as a slow catalyst for  $H_2O_2$ , it was fully covered with Teflon tape, as shown in Figure 4-5a.

A small extra strip at the top of the GDL on which no deposition had taken place, was used to secure the current collectors, such that it would not be in touch with liquids. Still, the copper strip as shown in Figure 4-5b could not be prevented from reacting inside and outside the cell structure and had to be replaced. This was later analysed in the Scanning Electron Microscopy (SEM) and found to be copper sulfate ( $CuSO_4$ ) as it reacts with the sulfuric acid in the electrolyte besides oxidizing from the  $H_2O_2$ . At a certain stage, the copper was substituted by a stainless steel wire which was forced on each electrode during the hot press procedure. Finally, the GDL's were extended in such a way, they could simultaneously serve as a current collector without the catalyst deposited on the electrode being affected.

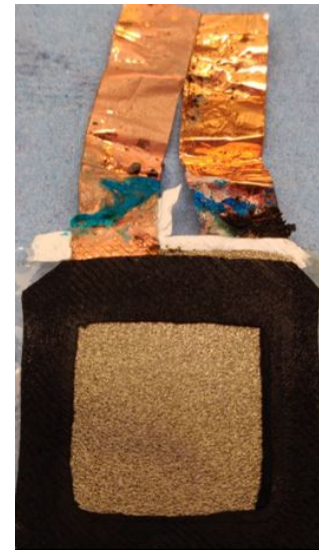
### **Gaskets**

Besides acting as a cover for the current collector, the Teflon as visible in Figure 4-5 also acted as an electric isolator. Finally, it had the function to serve as a gasket, which smooths out the pressure from clamping together the cell structure. This turned out not to work well enough as the cell kept breaking and leaking, so the Teflon was only applied locally from then on. Thereafter it only had the function to either electrically isolate the electrodes





(a) Teflon Covering the Edges



(b) Corrosion Effect &amp; Rubber Gasket

**Figure 4-5:** MEA With Copper Current Collectors

or act as a lubricant for better sealing of the tubes. Instead, an Ethylene Propylene Diene Monomer (EPDM) rubber foam of  $1\text{mm}$  thickness, as visible around the electrode in Figure 4-5b, would from then on serve as the gasket on either side. When applied in multiple layers and cut to the correct size, this helped in isolating and pressurizing the system quite well, but could not prevent the copper from being affected still. Additionally, a similar rubber ring was placed on one end of the gasket such that the cell could be sealed with high pressure and make it even more leakproof.

#### 4-1-4 Cell Structure Production

During the development process of the fuel cell, two types of constructions have been set up, depending on the way the electrolyte is supplied; active or passive. First, the passive structure was designed to see how much power it could deliver, which would subsequently form the basis of the active cell structure. As mentioned in Section 3-3-1, it was fully additive manufactured as changes could then easily be incorporated whenever a failure had taken place. These failures definitely occurred, as the Poly Lactic Acid (PLA) ruptured in the first few tests. Hence, the switch to Acrylonitrile Butadiene Styrene (ABS) was made, which turned out to be far more durable. The printing was done using an Ultimaker or Raise3D, after a Computer Aided Design (CAD) was made in Solidworks.

##### Passive Construction

In the case of a passive cell, the design was very straightforward, since it is primarily two compartments in between which the MEA is clamped. On the compartment end plate, the

two gaskets are placed and subsequently, a rubber ring is fixed in place by a groove on one end. Directly attached to the ends, are the compartments which could be filled with  $10mL$  liquid each. The two compartments are clamped firmly together using 11 M3 stainless steel bolts, with the current collectors exciting on the top. The complete MEA area is left open, with a sloped outward crossbeam at the upper side, which makes it possible for possibly generated gas to easily exit the system. This led to the final, compact design shown in Figure 4-6.

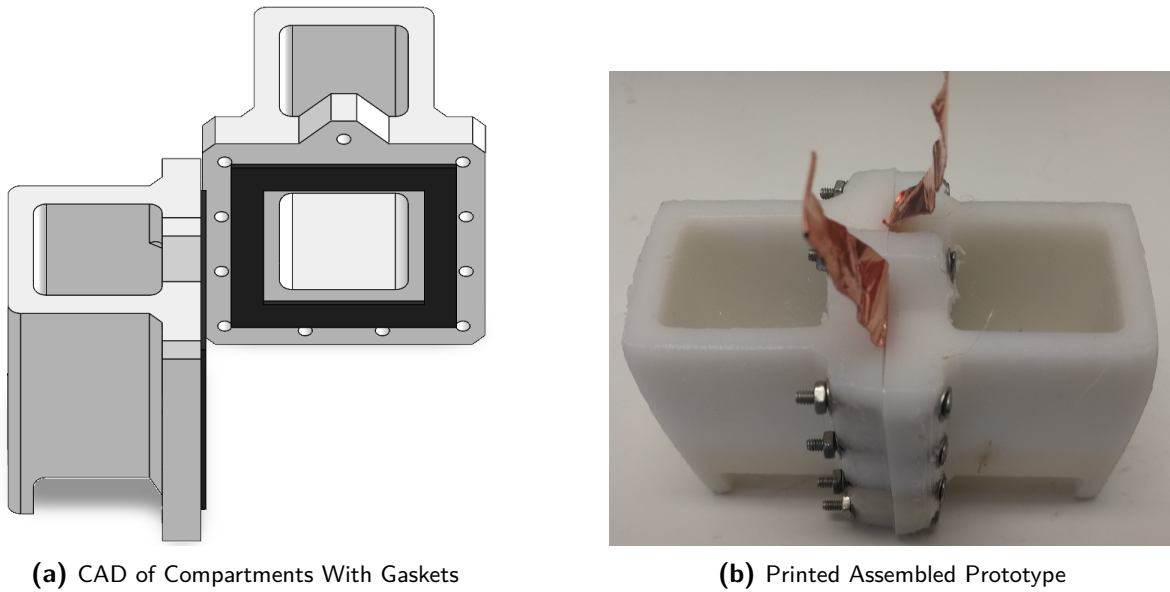


**Figure 4-6:** Passive Fuel Cell Structural Design

### Active Construction

The active construction thereafter was even more compact and included some more features. The first prototype namely included a glass window through which the liquid flow past the MEA was visible from the outside. Since no visible reactions were taking place and too much leakage was present due to difficult clamping, this part was stripped. Therefore the end plates were closed at the compartment area and included a serpentine flow pattern instead of an open MEA area at the other end in the final design. The clamping together with the bolts remained the same, but the way the gaskets and rubber ring were positioned was slightly altered. The big difference now was the addition of an in- and outlet where the tubes were attached. The liquid was subsequently forced through the flow field, which had an effective area of approximately  $3cm^2$  after having used an open area design first.

## 4-2 Test Preparation

After each individual component of the fuel cell had been manufactured, some preparation regarding the actual execution of the experiments has to be performed. To do so, the instruments used in the subsequent process as well as the specification of the components

manufactured are examined. Subsequent to installing the test setup, some exploratory tests were done such that it was known what to expect in the experimental campaign.

#### 4-2-1 MEA Validation

Since a large part of the performance of the fuel cell is dependent on the production method of the MEA and other components, it must be ensured these components functioned as intended. This mainly applied to the deposition of the catalyst and some other occurrences which happened during manufacturing. The first step in verifying this process was simply with visual confirmation and weighing of the GDL before and after decomposition as explained in Section 4-1-1.

A better picture could be obtained however through microscopic images since the concerning MEA is so small. A normal microscope elucidates already whether or not the process had been performed correctly, as can be seen in Figure 4-7a. Whether or not the dendritic palladium had formed had to be checked with a SEM, for which a manual was written, added in appendix -1. From the enlargements, as shown in Figure 4-7b, it was clear the deposition had been correctly executed.

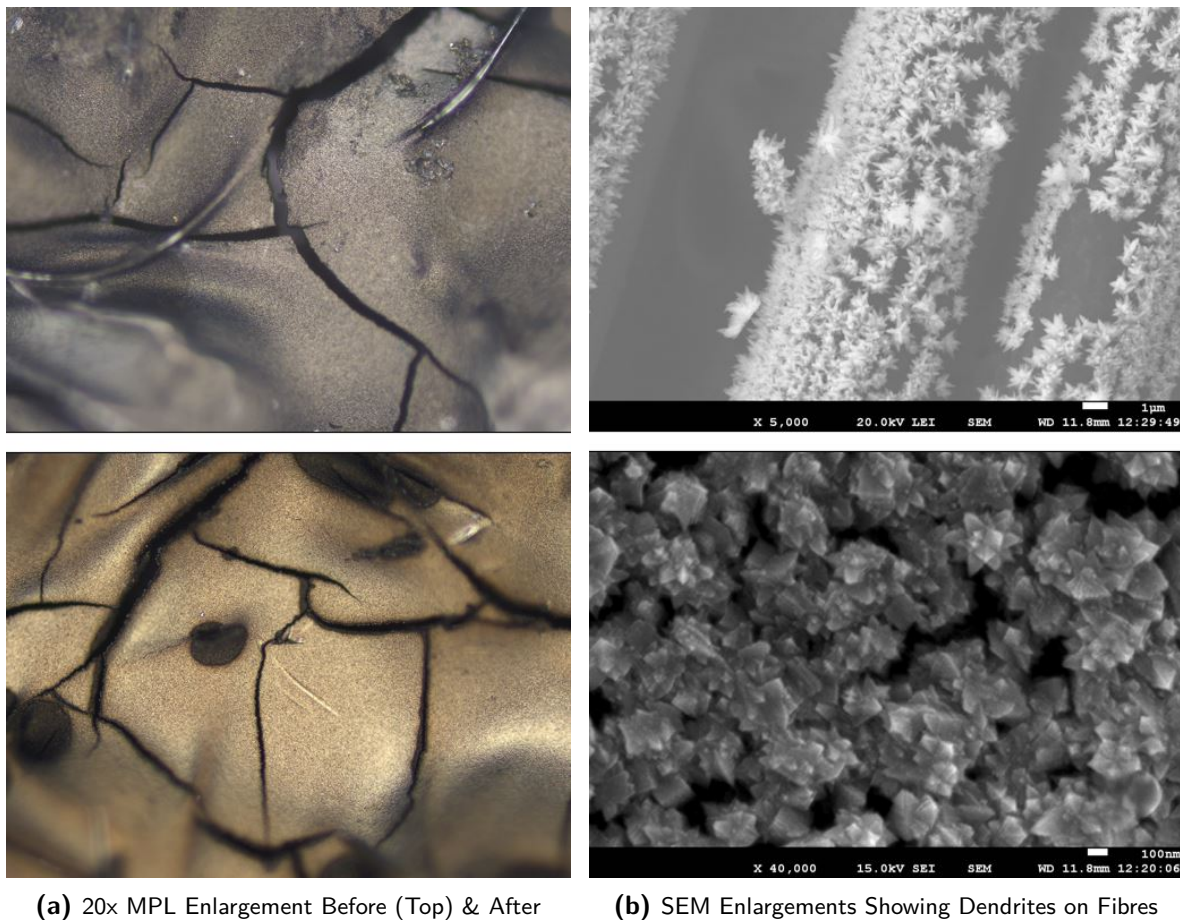


**Figure 4-7:** Microscopic Images of the Palladium Deposited on CFC

Additionally, Energy Dispersive X-Ray Spectroscopy (EDS) is performed on the electrode, to check if any unwanted compounds were formed. From this analysis, no elements other than the palladium were found on the CFC in comparison with the reference scan.

In the case of nickel foam, both analyses show clearly why additional nickel deposition did not work. The normally smooth surface of the metal now displayed lumps of green particles, whilst it should remain the same colour as the foam and be covered with cauliflower shaped structures [131]. The EDS clarifies what this could be, since oxygen and chlorine atoms are present, as shown in Figure 4-8.

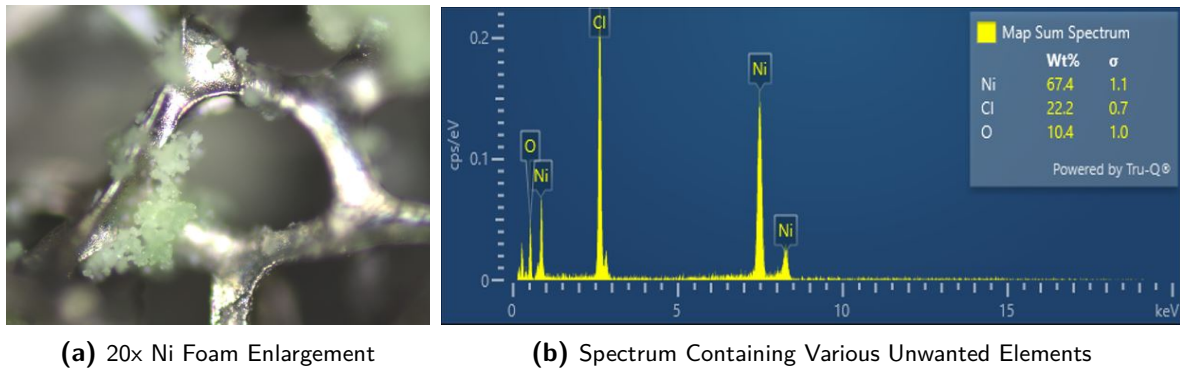


**Figure 4-8:** Microscopic Image & EDS of Nickel Deposition

To be certain that the palladium dendrites had the correct shape to prevent liquid from building up inside the GDL, an X-Ray Diffractometry (XRD) was used as well. With this machine, an X-Ray Photoelectron Spectroscopy (XPS) was performed such that the structure could be compared to that of the clean CFC as well as with the reference study results to check if it matches [130]. The results shown in Figure 4-9b, prove the correct compounds are obtained since the peaks have a clear correspondence.

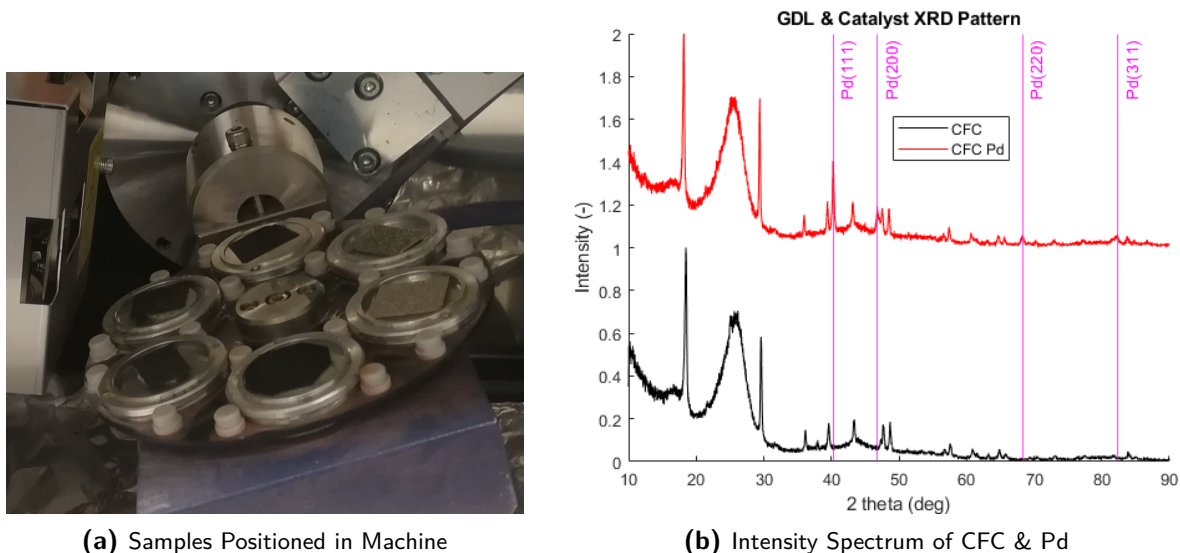


**Figure 4-9:** XRD Analysis of Electrodes

Subsequently, related more to obtaining the correct electric properties, a handheld multimeter



was used. With it, the resistance of multiple components was measured, to see if both electrodes are properly electrically isolated. Also to see if the current collectors are conducting well and if no other path is present between the two electrolytes, for example via the bolts. The measured resistance could subsequently be taken into account when calculating the losses and loads in the circuit.

### 4-2-2 Instrumentation

As mentioned before, the polarization curve is the best representation of the performance of the cell. To capture this, voltage and current at different loads need to be acquired, which can be done in a straightforward fashion using a Digital Multi Meter (DMM). Therefore, two Keithley's 2701 are attached to the current collectors, one in series and one parallel. They have a resolution of  $0.1\mu V$  and  $10nA$  and accuracy of  $15ppm$  and  $60ppm$  and are set to read at a frequency of  $1Hz$ . Unfortunately, both measurements could not be performed with only one Keithley, as they could only be attached to the circuit in one way. This caused a major error in the acquired data, as the actual measurement rate of the current turned out to be  $0.623Hz$  and that of voltage  $0.660Hz$ .

**Table 4-1:** Keithley 2701 Measurement Specifications

| Voltage & Current | Resolution          | Accuracy          | Frequency             |
|-------------------|---------------------|-------------------|-----------------------|
| Parallel & Series | $0.1\mu V$ & $10nA$ | $15ppm$ & $60ppm$ | $0.660Hz$ & $0.623Hz$ |

Loads are applied to the system mechanically, using a rack which included 13 different set resistances, ranging from  $270k\Omega$  to  $5\Omega$ . There is however a resistance present already measured to be approximately  $5\Omega$ , caused by the Keithley's, cables and current collectors. This value will thus be the resistance at short circuit and has to be added up to the loads that are applied.

The other measurement option could have been not only to use the potentiostat for electrodeposition, but also for the cause of obtaining the polarization curve. However, the fuel cell would have to be designed in such a way that the irregular shaped electrodes of the potentiostat would all fit inside. Also, the location of the potentiostat and type of attachments, made it so that using this instrument for performance measurements was not deemed possible during this project.

### 4-2-3 Test Setup

The electrical circuit of the experimental setup is quite simple and described in Figure 4-10a. The fuel cell acts as the power source and the variable resistances are the loads. The two are attached in series with the current measurement  $I$  and parallel with voltage measurement  $U$ . In the case of a passive cell, the appropriate amount of electrolyte is directly inserted into the corresponding compartment of the fuel cell. Before this, the recording is started already such that it can acquire all effects of the cell.

In the active infrastructure diagram of Figure 4-10b, the Data Acquisition System (DAQ)'s are indicated by a Keithley, measuring voltage (7) and current (8). The two are thus connected

to the fuel cell (3), with the resistance rack (4) in between as well as directly to the laptop (9), which contains the appropriate Kickstart software. The fuel and oxidiser are injected into the fuel cell using syringe pumps that are connected to an external power socket (10). The base anolyte is injected via pump (5) and after having passed through the cell, is collected again in a beaker (1). The same holds for the acid catholyte which has its pump (6) of which the reaction products are gathered in a beaker (2).

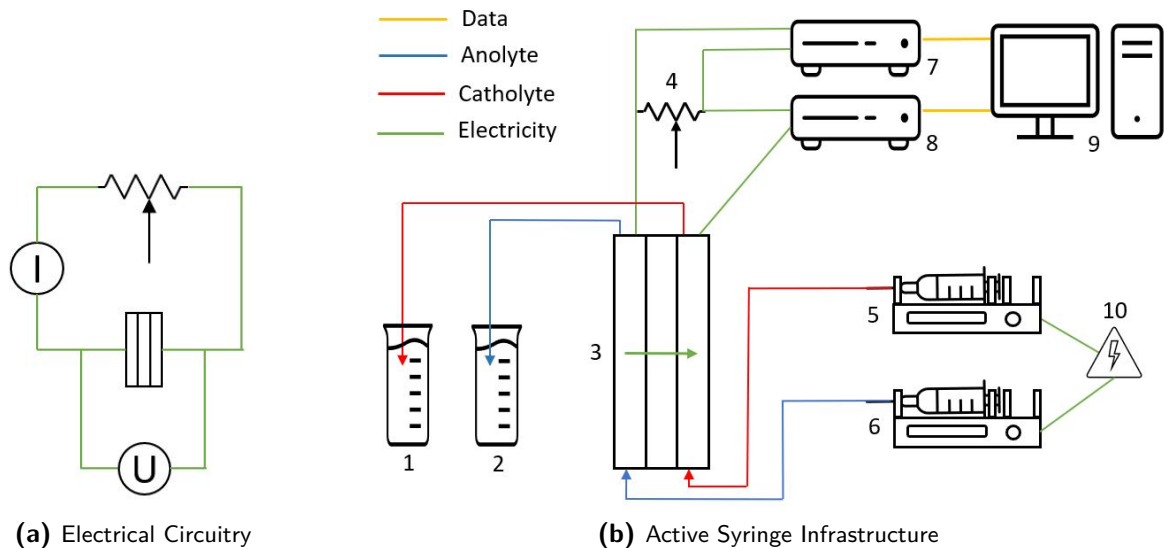


**Figure 4-10:** Fuel Cell Test Setup Infrastructures

The setup and how it was placed inside the fume hood for safety, is shown in Figure 4-11. Here it is visible how the standard setup as used in the passive cell in Figure 4-11a, can be upgraded with some pumps to form the active setup as shown in Figure 4-11b.

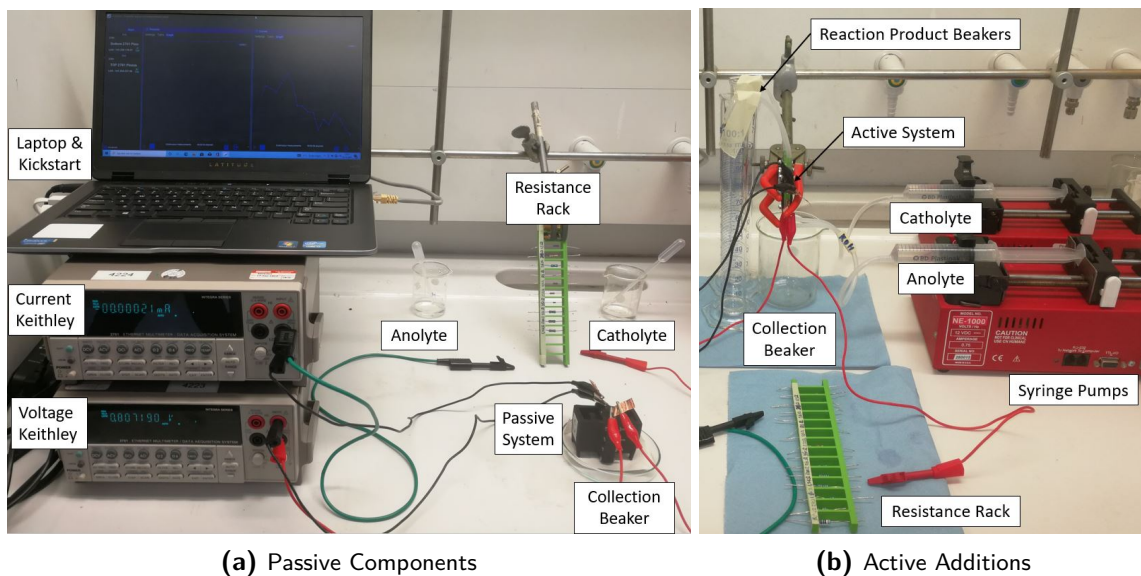


**Figure 4-11:**  $\text{H}_2\text{O}_2$  Fuel Cell Experimental Setup

#### 4-2-4 Experiments Overview

Even though the execution of the experiments slightly differed on each try due to changes to the cell components and test environment, the general design always remained the same and is displayed in Figure 4-12.

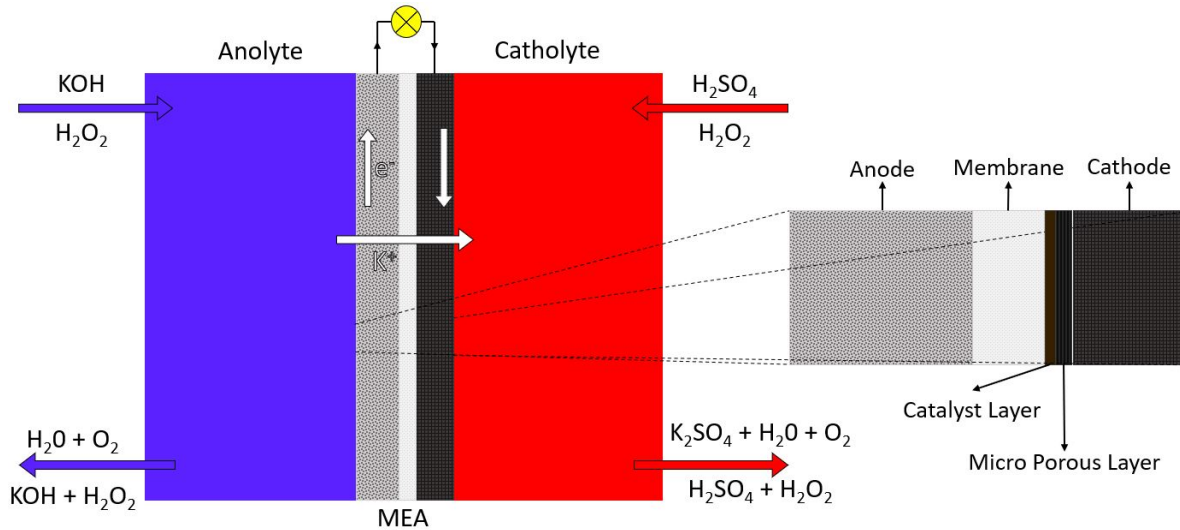


**Figure 4-12:** Fuel Cell Functioning and MEA Setup

An overview of the tests performed with what cell aspect is changed, is given in Table 4-2, in which the initial test as described in Section 4-2-5, are left out. The reason for having performed only 14 passive and more than double the amount of active tests has to do with additional experiments using the active structure as explained in Section 4-4.

**Table 4-2:** Number Of Fuel Cell Experiments Performed

| Category Changed | MEA |     | Flow Rate |     |      | Electrolyte                   |           | Other Tests |       |
|------------------|-----|-----|-----------|-----|------|-------------------------------|-----------|-------------|-------|
|                  | GDL | PEM | Low       | Med | High | H <sub>2</sub> O <sub>2</sub> | Acid/Base | Area        | Stack |
| Passive = 14     | 2   | 1   | 3         | 0   | 0    | 2                             | 1         | 5           | 0     |
| Active = 32      | 0   | 3   | 2         | 9   | 5    | 7                             | 3         | 0           | 3     |

#### 4-2-5 Initial Results

As mentioned in Section 4-1-4, the PLA compartments used in the first few passive cell test proved to react very bad on the anolyte mainly. Upon insertion of the liquid, the structure simply shattered, as shown in Figure 4-13a, leaving the anolyte behind in the collection beaker. Something was still to learn from the little data obtained in these tests, shown in Figure 4-13b. Mainly about how to improve the operation of the setup such that leakage and trapping of the formed gas bubbles would happen less. And secondly, a gist of how to enhance the performance of the cell by adding a mass flow past the GDL and reducing contact resistance.

After having minimized the leakage from the cell, actual procedures were set up to measure its performance. Recorded data was named according to the test performed: '[Flow Rate] -

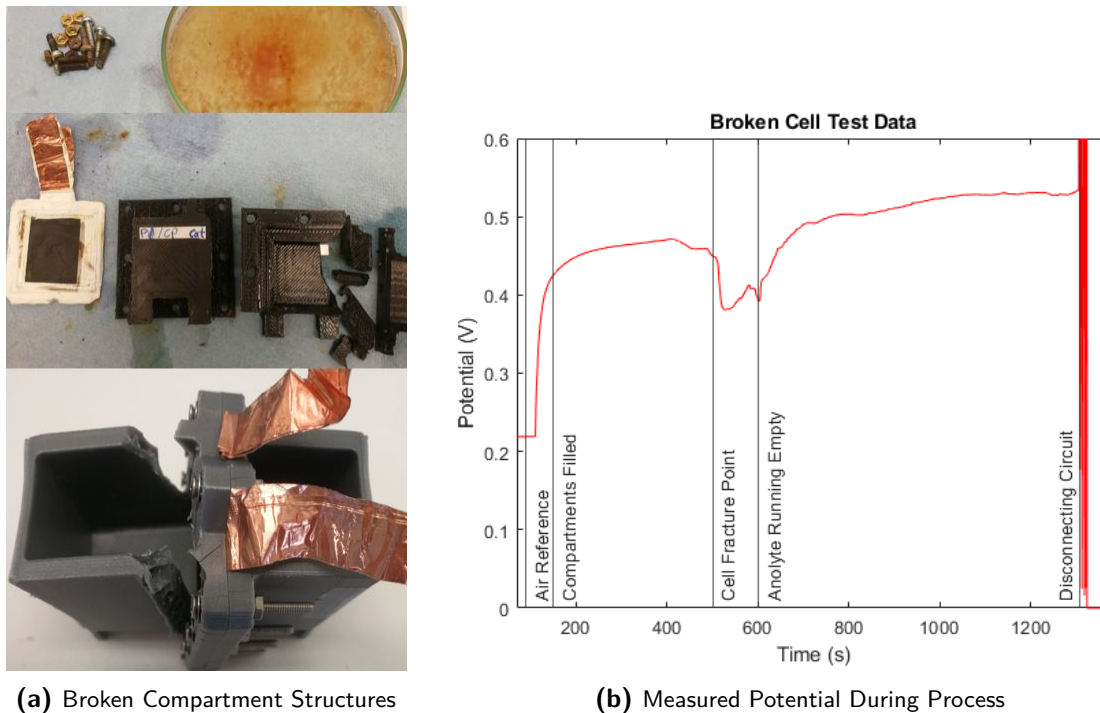


**Figure 4-13:** Passive Fuel Cell Failed Experiment Outcomes

[Anode] - [Loading, Cathode, Method] - [Membrane] - [Electrolyte]', with the method being either electro deposit 'EP' or spray deposit 'SP' and the electrolyte based on the catholyte concentration.

## 4-3 Fuel Cell Experiments

After finishing a set of MEA's and cell structures, arranging experimental setup and checking all on correct fabrication and operation, the test could be performed.

### 4-3-1 Test Measurements

Besides the maximum power produced by the cell, there are several other parameters of interest, that were looked for in the execution of the tests.

The OCP is the first one, as it indicates the maximum voltage and gives an indication of the losses present already in the system. Then there is the potential at a range of loads, from which a maximum power results via the polarization curve. Also interesting to know is the stability of the cell and thus the power output over time, by checking how quickly the potential and current decrease at a fixed resistance. Obtaining these parameters was done under different conditions such as MEA, concentration, mass flow rate and temperature to see how they can be optimized. The OCP test is repeated most commonly since this is the voltage the cell takes when it does not have a closed circuit. The polarization curve procedure was often performed twice to investigate the repeatability of the results.

During tests, first, the compartments were filled with the electrolyte until it had stabilized and reached a maximum OCP. At this point, the circuit was closed by connecting the resistance to the cell and the DMM clamps. Starting from the highest resistance, every five seconds a new lower resistance was connected, up to short circuit. This results in a stair shaped current and potential over time, as visible in the raw data in Figure 4-14. The process was repeated once the cell had recovered to its maximum OCP after disconnecting the clamps. Afterwards, a load was selected based on its maximum power to keep the cell operating for a while and to check its long term stability.

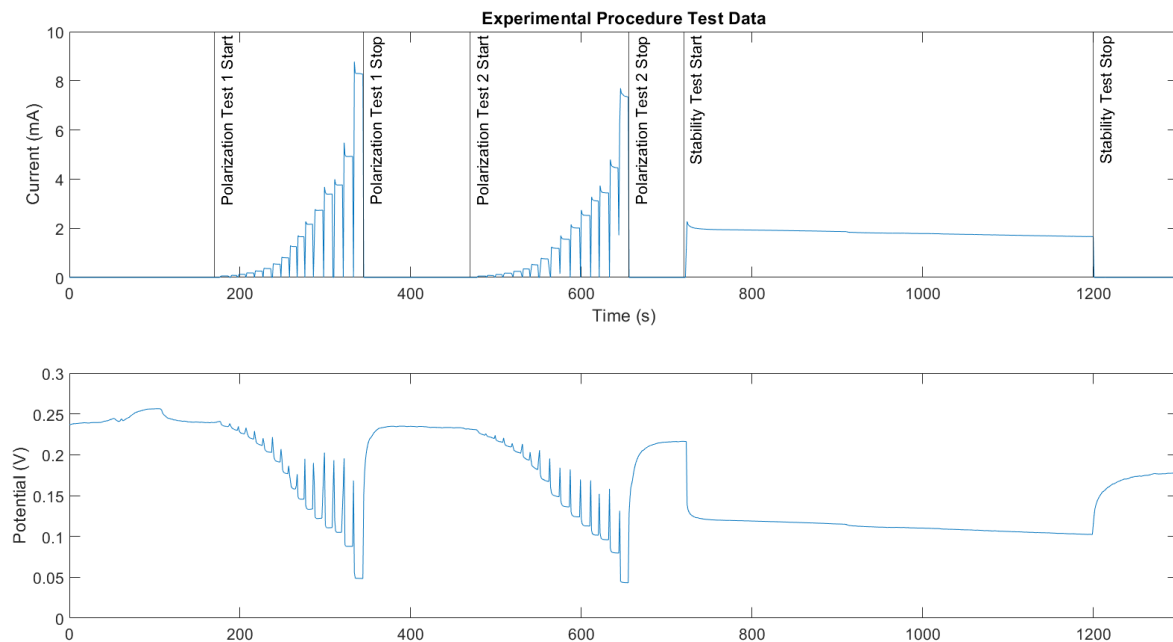
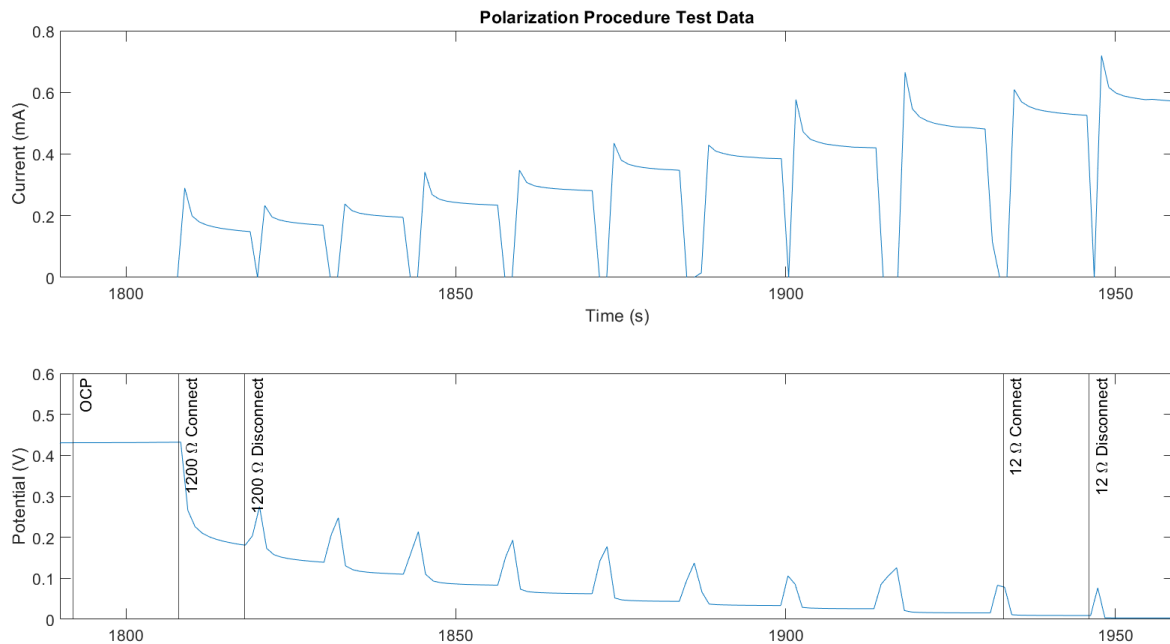


Figure 4-14: Fuel Cell Procedure Raw Current & Voltage Data

### 4-3-2 Polarization Curve Procedure

Analysing potential and current at different loads turned out to be quite a challenge, as the values tend to decrease rapidly after closing the circuit. This is visible in a data set in which a longer period of five minutes is taken before switching to a lower resistance. Hence it was decided to keep the operation of the cell at a set load short, up to approximately five seconds in the final few tests. At each step of the stair, a current and voltage are taken to be later used in the polarization curve. The manual interchanging of the resistances with the clamps was done in exactly one second every time. This expresses by the peaks and dips between the steps, as shown in Figure 4-15. The data was validated by checking if it matches with the set resistance via Ohm's law.

The product of a current and voltage value in each step is the next step from which the power curve is obtained. Both power and current are divided by the area of the MEA used in the test which is in contact with the fuel and oxidizer. This results in a graph as shown before in Figure 3-6. Despite several attempts to automate the data acquisition by writing a script, the results from the procedure turned out to be so inconsistent that the process of obtaining



**Figure 4-15:** Fuel Cell Manual Polarization Test Close-up

potential and current values at each step had to be done manually. This was partially due to an offset in the time-step's of approximately 0.01s between the current and voltage measurements and the rapid decrease of both parameters after attaching the resistance.

### 4-3-3 Stability & Repeatability Procedures

Since it was learned from the polarization test that the voltage and current go down quickly in the first few seconds, a closer look was taken at this occurrence. As the current gets higher, this initial decrease gets larger, which is not something that can be found back in the Nernst equation. It presumably has to do with the switching of resistance or measurement instrumentation delayed reaction, which makes it possible for the current that has built up on the electrodes to jump over more easily initially. Mainly current goes down at the start of each step, after which it settles. Resistance in the setup clarifies this, which is calculated by dividing the measured voltage by the current, as shown in Figure 4-16.

Over a longer period, the voltage and current would however stabilize and go towards an asymptote, making the resistance more constant after approximately 20s. Its response time turned out to be quite fast, as it always reaches 98% of its final value within five seconds. This is therefore the target time when taking the measurement value and passing it to the next resistance. Keeping the load on for longer could namely cause other effects which influence the curve, such as the build up of medium in the GDL. To be absolutely sure it had nothing to do with the depletion of the energy in the fuel and oxidiser, the concentration of the liquid is checked. This was done using the refractometer as discussed in Section 3-4-2, but since the  $\text{H}_2\text{O}_2$  is mixed in with other chemicals its Brix indication scale is different. Comparing with a reference measurement before usage of liquid in the cell however, gave no indication of depletion of the energy inside, as the reaction products indicated the same values.

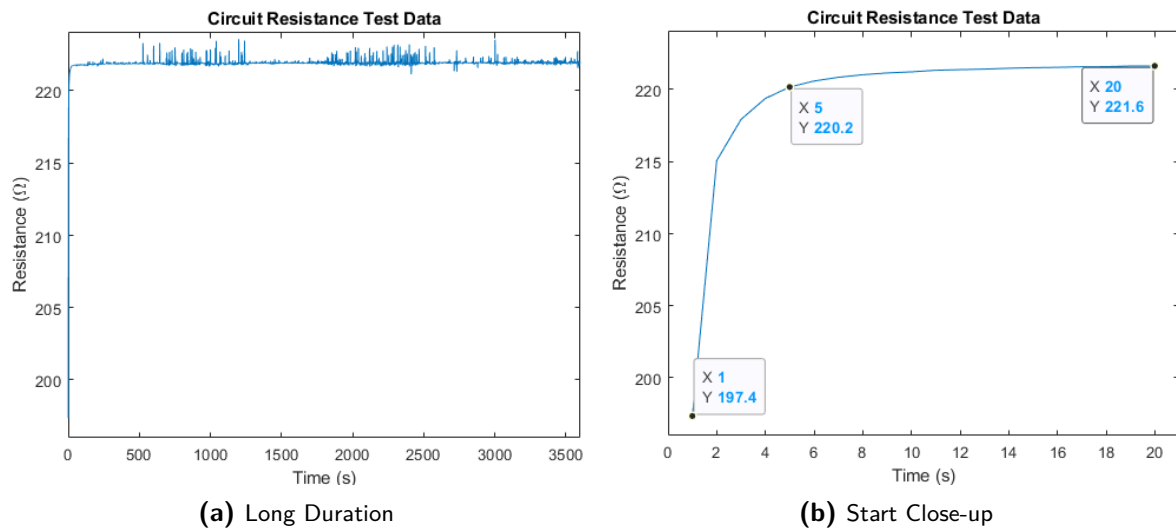


**Figure 4-16:** Fuel Cell Circuit 220Ω Resistance Stability Test

### 4-3-4 Passive Cell Results

The passive systems scored substandard on maximum power achieved, stability as well as repeatability. The power of the cell going down rapidly after the liquid being inside for some time appeared to have nothing to do with the depletion of the energy inside the liquid, however. This was proven after refreshing the fuel and oxidiser in each compartment after half an hour, as shown in Figure 4-17. Still, the transformation of  $H_2O_2$  to oxygen according to the electrochemical reaction as shown in Table 2-2 was visibly happening at the cathode compartment, since bubbles were forming on the CFC and floating up to the surface.

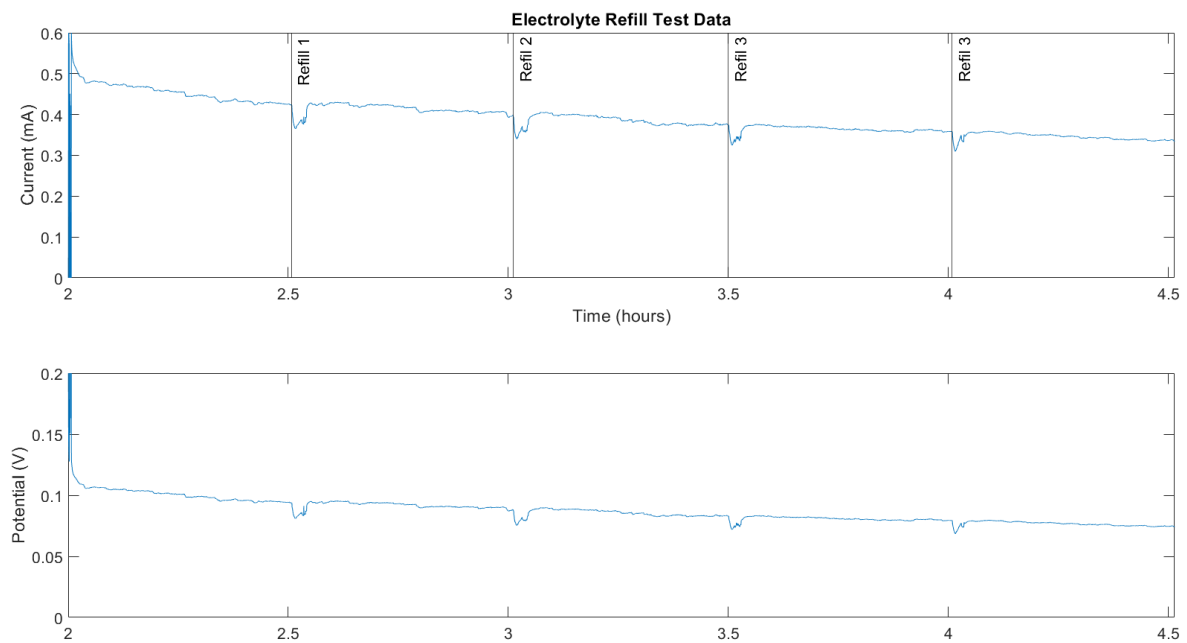


**Figure 4-17:** Passive Cell Refill Stability Test



The cell is used in a circuit with a constant load of  $220\Omega$  and achieves only such low values of potential and current because it has been used in some tests before, which heavily degrades its performance. This is visible in the repeatability of an early stage cell shown in Figure 4-18, where two subsequent polarization tests are compared via their curves.

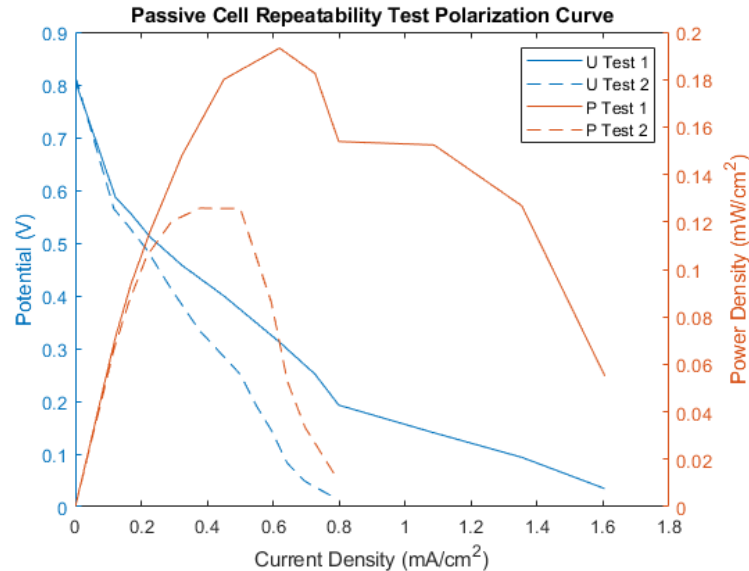


**Figure 4-18:** Passive Cell Polarization Test Results

There are thus some effects which affect the ability of electrons and cations to transfer to the other side over time in this cell. Presumably, this had to do with increased internal resistance, caused by a halt in the supply of fresh liquid to the electrode surface. Whenever the reaction had occurred, the liquid stays stuck there as no flow was present and the GDL could not properly be provided with a new electrolyte. This made it so, that predominately the first test carried out with the newly produced MEA gave legitimate results, such as a constant high OCP of maximally  $0.9204V$ . Therefore it was decided to continue with active cell systems hereafter, hoping their repeatability and stability were better. The highest power obtained was namely still far below the one obtained in literature, being  $0.5984mW/cm^2$  with the setup as described by Figure 4-12.

#### 4-3-5 Active Cell Results

Since the performance of the passive cell was found to be insufficient, the switch to the active system was made. It was expected that performance would go down less quickly after it has been in operation, due to flow at the electrode surfaces. As it turned out, this was indeed the case, since the repeatability showed to be higher, as can be seen in Figure 4-19.

In these tests, a flow rate of only  $0.3mL/min$  already proved to be sufficient, to have the cell recover to earlier OCP after a polarization test. Regarding short and longer stability, however, the active system gave similar results to the passive cell, as the current drops straight away at first, after which power keeps going down steadily. Increasing the flow rate to the maximum of the syringe pumps, which is  $1.28mL/min$ , causes the cell to return to values as before long duration operation even quicker.



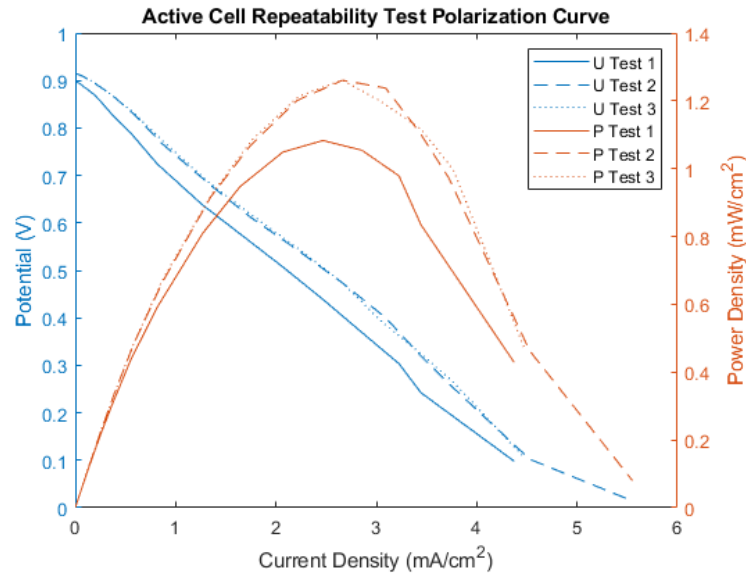


Figure 4-19: Active Cell Polarization Test Results

### 4-3-6 Fuel Cell Overview

An overview of all experiments done with the fuel cells is shown in Figure 4-20.

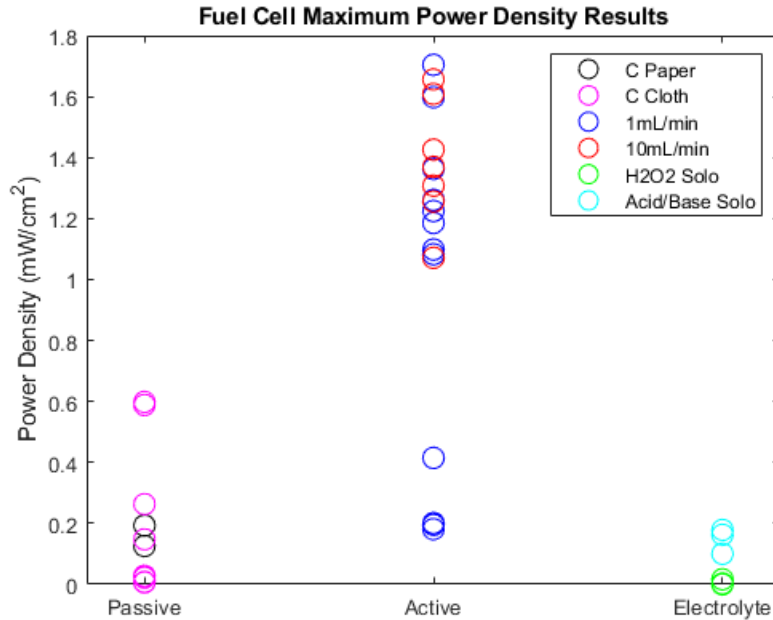


Figure 4-20: Experimental Fuel Cell Results Overview

Each category unfortunately still has differences compared to other cells within its class. These differences are related to changes made for testing other performance influences as discussed in Section 4-4. These can however not be compared because they do not have

enough data points to form a solid conclusion since not all parameters were kept constant. Hence aspects, such as loading, membrane and support structure and structural changes, are not taken into account but most definitely affect the power output.

## 4-4 Performance Optimization Tests

Besides having tested the different structures and various electrolyte concentrations in the active cell, there were some other effects noticeably affecting the performance. These were investigated throughout the project to learn more about the use-case of various cell changes.

### 4-4-1 Surface Area Results

To prove that obtaining a higher power due to current comes with an increase of reactant surface area, multiple MEA cell sizes were produced. The three cell structures are shown in Figure 4-21a, scaling from  $1\text{cm}^2$  to  $4\text{cm}^2$  and  $16\text{cm}^2$ . Apart from the  $4\text{cm}^2$  MEA having a slightly lower catalyst loading, they consist of the exact same components.

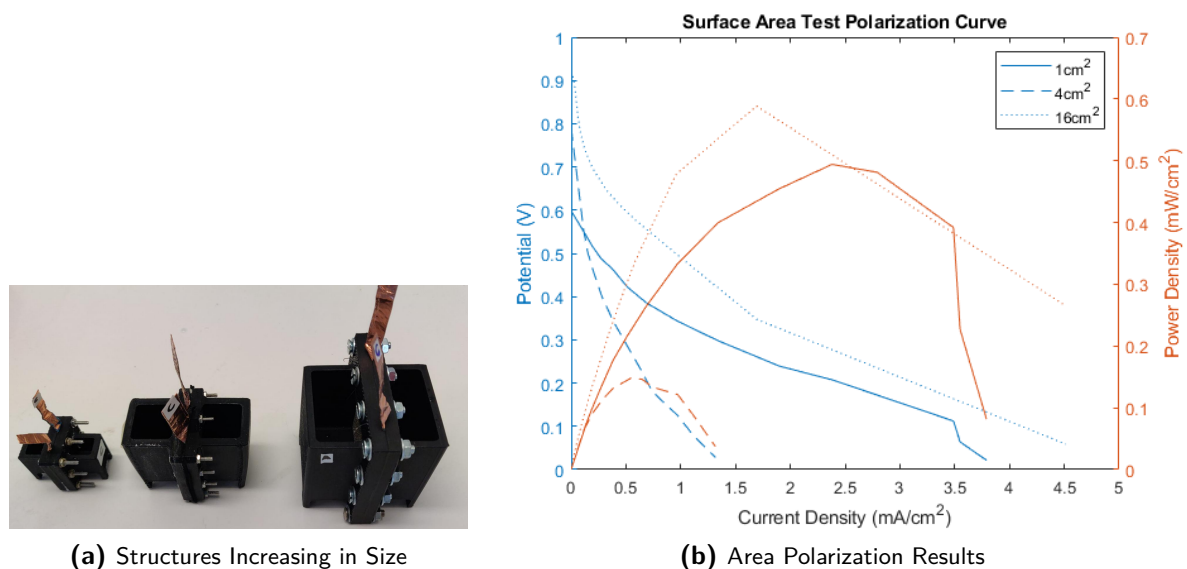


**Figure 4-21:** Passive Cell Surface Area Tests

Despite the middle sized cell's low performance, the cells showed an okay correspondence in power density, as shown in Figure 4-21b. The maximum power of the large cell namely turned out to be  $9.4157\text{mW}$  to  $0.4941\text{mW}$  for the small one, nineteen times as much. The reason for it being not sixteen might be due to inaccuracy of the actual liquid contact area as well as some standard cell system losses that have to be overcome. Too little and irregular results are there to prove so, but the trend of surface area increase with power should be linear.

### 4-4-2 Electrolyte Ratio Results

Some additional tests were done concerning the concentration to see whether or not a stoichiometric ratio in the electrolyte was really required. This led to the results as shown in Figure 4-22, where first KOH was increased and later the concentration of both  $H_2SO_4$  and  $H_2O_2$ .

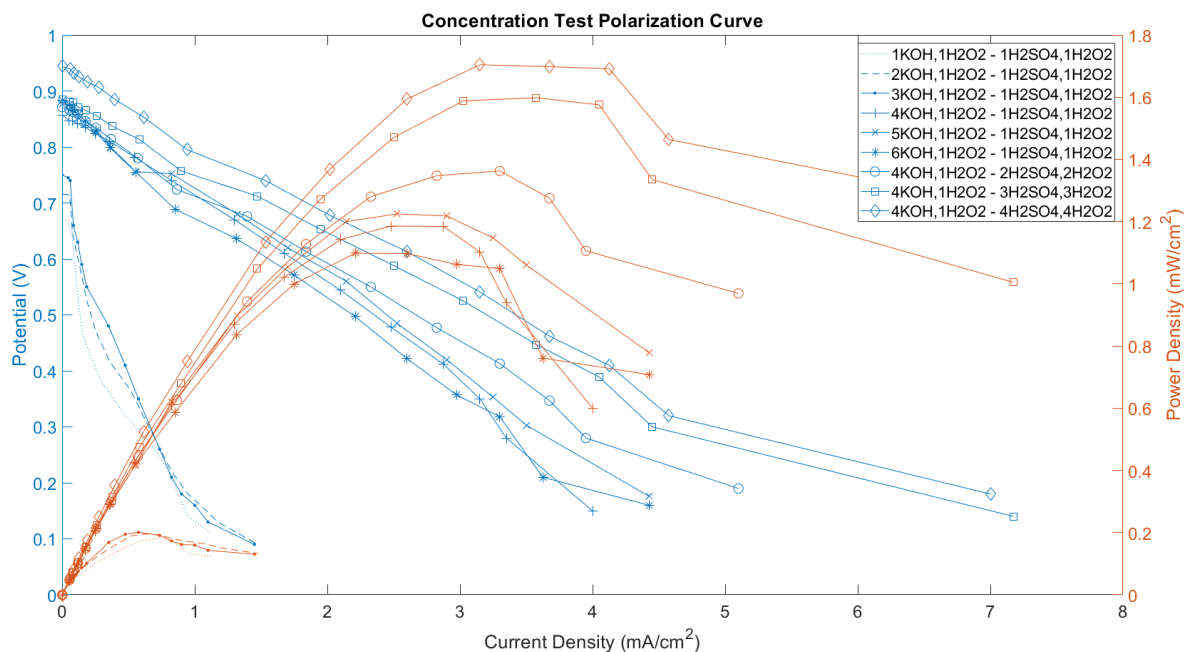


Figure 4-22: Active Cell Electrolyte Concentration Test Results

A huge increase is visible in the results between the 3M and 4M concentration KOH, which had only been noticed lately after doing the experiments. If these results are actually true, the difference is quite remarkable and stoichiometric ratios or higher concentrations are definitely worth using in the cell. There are however some doubts, since the  $H_2O_2$  used in the electrolyte was found to decompose on its own quite fast over time upon storage. This was learned hereafter as there was no more anolyte and a new solution was produced to continue the tests the following day. Hence far less than 1M could have been present in the first three experiments. Regardless of this aspect a clear trend is visible, showing the increase in maximum power up to the point of stoichiometric concentration and over.

### 4-4-3 Flow Rate Increase

Since the increase in flow rate turned out to work so well, the experimental setup was upgraded in several ways. Firstly to increase its flow rate to the  $10mL/min$  as used in the reference case and secondly to make electrolyte recycling and heating possible. Hence, peristaltic pumps were installed to replace the syringes, as shown in the infrastructure overview from Figure 4-23a.

The new elements in the setup for both anolyte and catholyte are indicated by the heating plates (2) and (11), and peristaltic pumps (4) and (7). The pump system actually consists

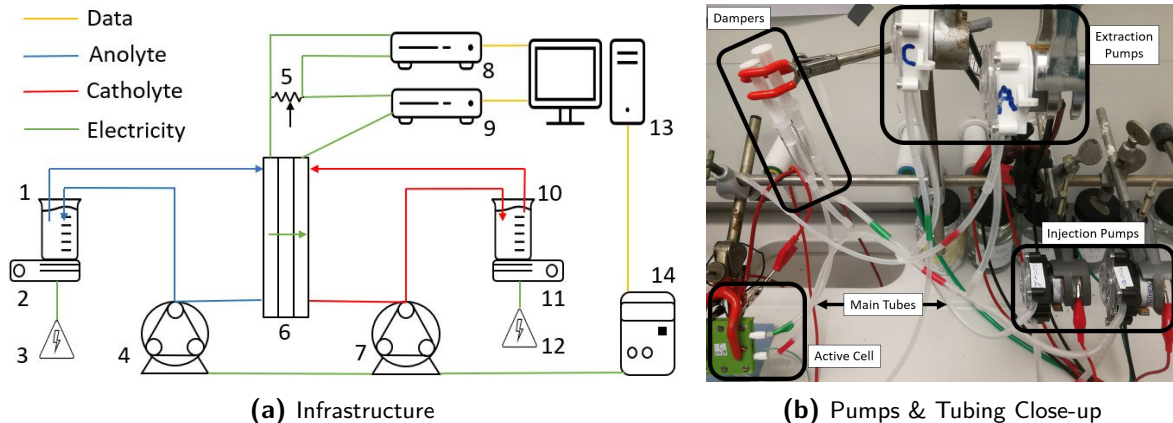


**Figure 4-23:** Fuel Cell High Flow Rate Setup

of four pumps and two power supplies (14) to resolve the problem of them having a minimal starting flow rate which is too high. To get to  $10\text{mL}/\text{min}$ , separation of flow was attempted first, with four tubes of which only one went through the cell, which was found to be very unstable and uncontrollable. Hence, two additional pumps were installed in such a way that they extract electrolyte from the main tube and recirculate it at a rate which makes the sum of the total flow equal to  $10\text{mL}/\text{min}$ . The setup is of course quite cumbersome as shown in Figure 4-23b, but the only possible solution at that time.

### Flow Rate Results

With the new flow rate, the maximum achieved power was even higher and the cell OCP stabilized almost instantly after the operation. A clear increase is visible in comparison with the passive and low flow rate, as shown in Figure 4-24. Compared to the  $19.4\text{mW}/\text{cm}^2$  from a similar cell study, the highest power of  $1.36\text{mW}/\text{cm}^2$  is however far from optimized [131]. Furthermore, heating has not been applied to the system due to a lack of time, but this should have a similar effect on performance as the flow rate. The higher power of the  $1\text{mL}/\text{min}$  could be attributed to a higher cell catalyst loading than the  $10\text{mL}/\text{min}$  cell and a higher concentration preceding test.

#### 4-4-4 Cell Stacking

Since most electrical devices require a higher potential to operate on than the maximum of  $0.9\text{V}$  OCP currently achieved, stacking of cells has to be applied. By attaching another MEA in series, the voltage rises by adding up the potential of each cell. This was demonstrated by adding multiple active cells after one another as shown in Figure 4-25a. A more ideal, compact, single structure as shown in Figure 4-25b represents better a stacked configuration, but this prototype ended up leaking too much and was thus not used for data acquisition. Its design can be optimized in many ways, such that external tubing and some internal end plates can be replaced with bipolar plates.

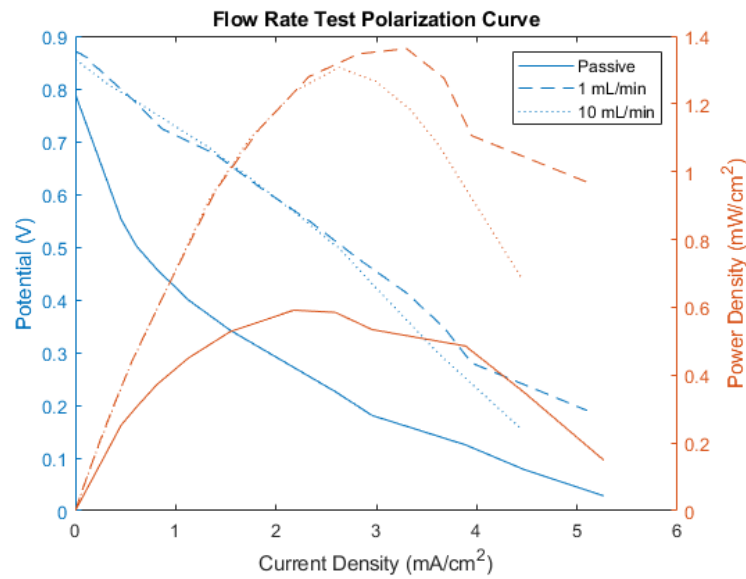
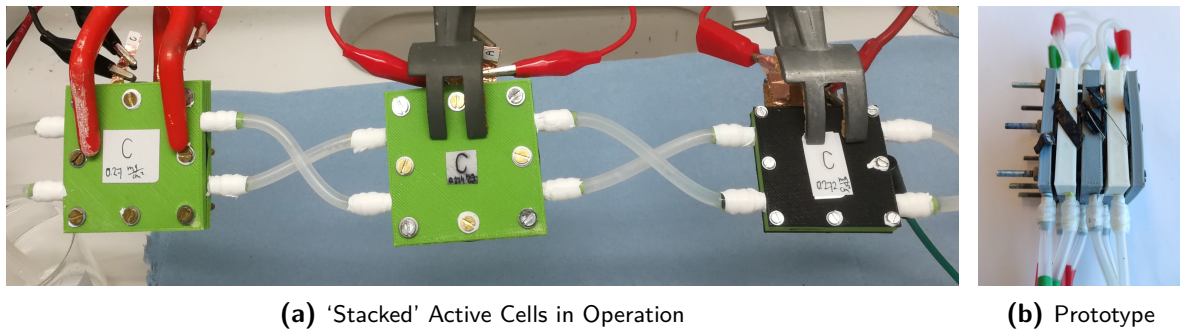


Figure 4-24: Fuel Cell Flow Rate Results



(a) 'Stacked' Active Cells in Operation

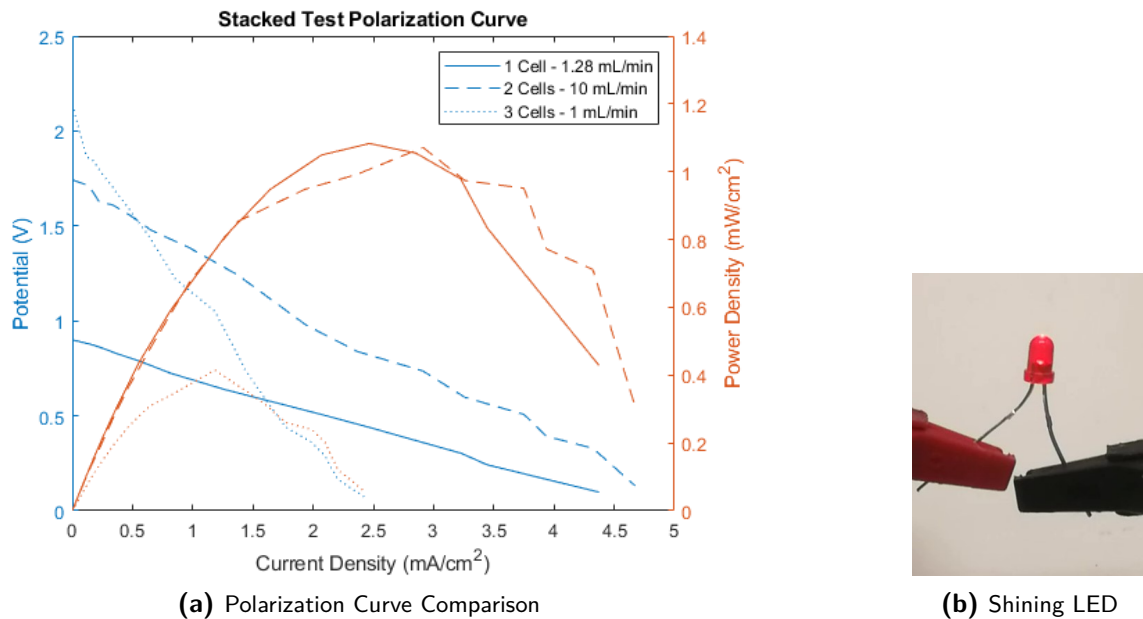
(b) Prototype

Figure 4-25: Active Cell Stack Setups

## Cell Stack Results

Regarding performance, the results for current density are about the same as single cells, since the circuit is limited by the cell MEA which creates the least current. Power is however far larger since the potential has gone up with the addition of each cell. Therefore, in the polarization curve comparison in Figure 4-26a, the power density is divided also by the number of cells. To demonstrate its use case, an LED requiring a minimum of 1.6V was attached instead of the usual resistances. This lit up instantly upon connection to the circuitry, which was experienced as quite a milestone in the project, as shown in Figure 4-26b.

An important notice about the results from Figure 4-26a is the difference in loading and even more influential, the flow rate. The single cell catalyst mass loading is the highest, which increases its potential and power output. Also, in this phase of the project where stacking was tested, obtaining a higher flow rate and method of supply for the electrolyte were experimented with simultaneously. Hence, the double cell which had a high flow rate and its tube with fresh electrolytes going in each compartment reaches a higher power density. In the triple cell, the occurrence of oxygen development as mentioned before in Section 4-3-4,



**Figure 4-26:** Active Cell 'Stacked' Results

was noticeably happening even more. After exiting each cell more oxygen was present in the outlet tube, which subsequently entered the next cell. This is likely to drastically influence the cell performance, as less concentrated  $\text{H}_2\text{O}_2$  is capable of reacting at the MEA surface in the last cell, which restricts the maximum current. Besides this, it causes the potential to go down since it is merely the ORR that happens instead of the Hydrogen Peroxide Reduction Reaction (HPRR).

#### 4-4-5 Electrolyte Composition

As shown in Section 4-4-2, changing the electrolyte concentrations up to stoichiometric ratio and more, already showed to have a clear effect. Additionally, some modifications to the both anolyte and catholyte were implemented, which had not yet been found to be tested in literature. First of which was the use of solely the  $\text{H}_2\text{SO}_4$  acid at the cathode and KOH base at the anode. The other was the use of high and low concentration  $\text{H}_2\text{O}_2$  in either cell compartment, as the difference should cause to solution to become equal as it is now the  $\text{H}^+$  which travels through the membrane. This way no additional electrolyte is required in the solutions, which makes the system less complex and harmful. The power density of all these tests turned out to be very low as expected and are shown in Figure 4-27.

Remarkable to see was the change in direction of electron flow whenever the two  $\text{H}_2\text{O}_2$  solutions changed compartments. High concentration  $\text{H}_2\text{O}_2$  as anolyte turned out to work best, whilst the other way around resulted in a power not even visible on the bottom left in the plot. Similarly, negligible power outputs are obtained whenever equal amounts of  $\text{H}_2\text{O}_2$  concentration are used as electrolyte on each side of the MEA. Interestingly enough, operation of the cell with KOH and  $\text{H}_2\text{SO}_4$  only, did give a noticeable OCP and power output. Despite no oxidiser and fuel being present, it is expected that the  $\text{K}^+$  is still able to travel through

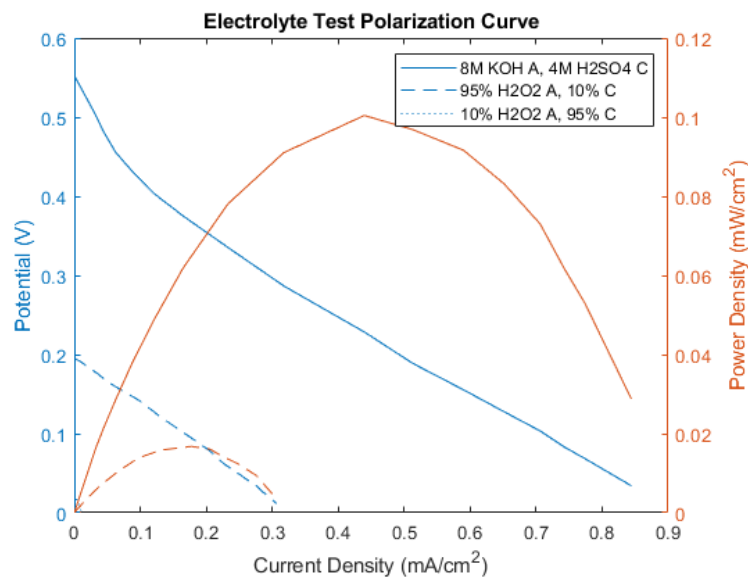


Figure 4-27: Active Cell Electrolyte Results

the membrane and react with the OH<sup>-</sup> lack of acid and base inside. Perhaps there was still some H<sub>2</sub>O<sub>2</sub> present inside the cell system despite thoroughly flushing beforehand, for example due to the membrane treatment before assembling the MEA.

Also interesting to see would have been the use of both high concentration H<sub>2</sub>O<sub>2</sub> and acid and base according to stoichiometric ratio, as well as, high concentration H<sub>2</sub>O<sub>2</sub> and lower quantities of acid and base. This was initially planned to do, but reconsidered after the mixing of KOH and H<sub>2</sub>O<sub>2</sub> caused an uncontrollable oxygen formation inside the beaker already. Besides this, the solution becomes quite aggressive, which is certainly the case with high concentration H<sub>2</sub>SO<sub>4</sub> and H<sub>2</sub>O<sub>2</sub> also known as the 'Piranha' solution. It is expected that having higher concentration H<sub>2</sub>O<sub>2</sub> will only keep the power production going on longer and decrease over time. Having also more acid and base however will simultaneously increase the power output and keep it at high level continuously, as it did slightly already in Figure 4-22.

## 4-5 Discussion & Recommendations

The effect of fuel cell changes on the results obtained from the experiments during this project show clear correspondence with the ones from literature. The power output range obtained however is far lower than expected, of which the cause is probably an accumulation of several aspects.

### 4-5-1 Reaction Kinetics

Presumably the reason for the resistance being lower in the first few seconds upon connecting to the circuitry as discussed in Section 4-3-3, is because of an overpotential, as described there already by the current building up on the electrode surface. Initially it felt unnatural



since the opposite was expected, where it would take time for the electrochemical reaction to start kicking in. It was found however that the same trend as in Figure 4-16a exists with the derivative of potential, also with fuel cells found in literature [45]. This transient response behaviour causes the current to go down rapidly as the fuel cell electrode surface acts in a same way as a capacitor. The phenomenon is clearly visible with the current interrupt technique, which is basically what was used in this study test procedure [64]. Double layer capacitance is thus the cause of the overshoot in current and the associated activation overpotential is apparently an issue in Direct Liquid Fuel Cell (DLFC). This happens mainly in the low current regime where you can see potential rising slowly over time, as was the case in this cell's study and thus has a larger influence than the Ohmic losses. The double layer capacitance and its effect on current is shown in Eq. (4-1).

$$C = \epsilon \frac{A}{d} \quad \& \quad I_{cap} = C \frac{dU}{dt} \quad (4-1)$$

In Eq. (4-1),  $\epsilon$  is the electrical permittivity of the medium,  $A$  is the surface area of the electrodes and  $d$  is the distance between the reacting surfaces. The product of the resulting capacitance  $C$  with the potential over time  $dU/dt$  forms the added capacitance current  $I_{cap}$ .

The development of oxygen in the cathode compartment is an indication of the mixed potential happening quite heavily. If only the HPOR would occur, there should namely be no gas development, hence the Hydrogen Peroxide Oxidation Reaction (HPOR) is taking place simultaneously. This is also the reason for the OCP reaching only around 0.85V and not 1.78V, as mentioned already in Section 2-3-2. This is also visible when the potential was taken as reversible cell voltage in the analytical model of Section 3-5-1. The voltage values derived and shown in the polarization curve corresponded more with experimentally derived ones. Having only the HPOR occur requires a more in depth study of the catalyst and electrode surface, which was not part of the scope of this research. Reducing the amount of gas that reaches the electrode and instead have more  $H_2O_2$  at its surface is however something that had to be looked into more. The MPL and PTFE present on the GDL are supposed to boost the performance of the cell by making sure the liquid does not get stuck inside. In this case however, where liquid is the energy carrier instead of the oxygen normally used in fuel cell, it could have been bringing down the performance. It namely prevents the liquid  $H_2SO_4$  and  $H_2O_2$  to even reach near the catalyst at the membrane as it is being repelled. On the other hand it does prevent reaction products to stay inside the GDL, which could have been a more influential factor at the nickel foam anode which has all this pores inside. It would thus be nice to investigate how the exact consistency of the GDL and its position and orientation effects the performance, for example by removing the PTFE treatment or using thinner foam layers.

Related to the capability of  $H_2O_2$  to react at the surface is the possibility of a thick boundary layer. In the active cell, the liquid at the surface will have a lower velocity then further away, which most likely effects the performance. Reducing the deepness of the flow fields trying different patterns or adding flow disturbances to make it mix better are possible other options to investigate. One does not want the flow to be too high however as it can cause the catalyst to wash away. Another noticeable change to the reaction product liquid was the formation of salts inside over time. Formation of  $K_2SO_4$  is inevitable as shown already in Figure 4-12, but its existence was confirmed after finding it building up on the bolts. EDS analysis showed it to



be indeed the salt, which indicated there were still some problems present. It should namely not be present on the outside, meaning the anolyte and catholyte most likely get in touch somewhere in the cell due to in proper sealing of the compartments. This fuel crossover also meant not all transfer happened through the membrane, hence a big loss in power generation is present as the protons and electrons can travel via a different path. Besides fuel crossover, the salts itself erode components and could clog the system after building up for example at the inside surfaces of the cell, tubes and pumps.

Then there were some concerns related to the resistance of the cell, which was found to be higher than expected. This resistance had to come from inside the cell and was presumably caused by the current collectors, its connection to the GDL, the GDL itself, or similar relations with the catalyst and electrolyte. Also when implemented in the analytical model, a higher resistance value in the cell, resulted in a perfect correspondence of the achieved current and power of the experiments with the model. Certainly when combined with the lowered reversible cell voltage caused by the mixed potential. Improving conductivity of the MEA components by its composition and orientation could help in reducing the resistance [29] [10]. Additionally, lowering the Charge Transfer Coefficient (CTC) and exchange current density value in the analytical model also caused a better match with the experimental data, by lowering the current and power output. Higher flow rates and less conducting metals as current collectors indeed raised resistance, which causes the transfer of electrons to happen less easily. Having the anolyte and catholyte in direct contact with the current collectors could solve this problem, but only when both are conducting well enough themselves. A possible solution is to have the cell compartments itself as current collectors, but only if it is made entirely sure that the two are properly electrically isolated and stay that way during operation.

#### 4-5-2 Setup Improvements

The setup itself has to be improved, such that the resistance due to instruments is not present anymore and data acquisition can be done with only one instrument. This way there would also be no offset anymore between measurement rate of the current and potential. Similarly the manual operation of changing resistance to obtain the polarization curve has to be excluded to get rid of the fluctuations in moment of switching. This would also help in increasing repeatability as the duration of each step is more controllable and there would be no sudden changes to the cell when the clamps are disconnected. Using the potentiostat as a measurement instrument would be the best, as it is made for obtaining electrochemical properties of the cell and thus solve the repeatability issue. With it, all parameters of the anode, cathode and electrolytes can be defined using cyclic and linear sweep voltammetry. Besides this, it excludes the resistances from cables and instrument because the measurement electrodes is placed inside the electrolyte itself. This is also what makes it difficult to use as the cell would have to be redesigned in order to make all required components fit inside.

Structural cell changes are however needed anyway due to more reasons than only changing the measurement instrument. Adding other instruments would namely be a great addition as well, mainly to constantly and more accurately measure temperature inside the structure and maybe even pH value of the liquids. This was now only done once using a handheld thermometer after operation, but should thus be checked more often to properly measure

heat development due to  $H_2O_2$  decomposition. A great addition to confirm if the reaction is running correctly would be to add a Gas Chromatography (GC) to the outlet of the cell. With this method the gas and liquid can be measured to check if the reaction products correspond with what was expected. As it measures the amount of oxygen released, an estimation can be done with the outcome on the efficiency of the cell. Lastly, changes are need to the structure to really prevent it from leaking and liquid crossover. These crossover losses were namely negatively influencing the current and power output drastically, as was confirmed by the analytical model and literature. Using a more rigid plastic such as Polyvinylidene Fluoride (PVDF) or Polyvinyl Chloride (PVC) or even stainless steel could help in properly sealing the cell.

**Table 4-3:** Fuel Cell Recommendations Overview

| Recommendation                    | Improves                  |
|-----------------------------------|---------------------------|
| Cell Structure & Instrumentation  | Repeatability & Accuracy  |
| MEA Composition & Test Conditions | Power Density Performance |
| Cell Stacking & Surface Area      | Voltage & Current Output  |

## 4-6 Conclusion

To electrochemically produce power with  $H_2O_2$  using fuel cell systems, a test campaign was set out. The first step in the process was the production of the components that worked best with the electrolyte and methods in mind. Conventional nickel foam was therefore used as anode and palladium catalyst electrodeposited on CFC turned out to be the optimal formula for the cathode. A treated Nafion membrane hot pressed between the two would complete the MEA, with the current collectors going out on either each electrode. This was then clamped between the two end plates, with Teflon tape, rubber foam and a ring to electrically and mechanically isolate the insides. The passive compartments were designed first, after which the many lessons learned mainly to prevent leakage are taken into account with the development of the subsequent active cell. In the production process continuous validation of components was performed, for example with SEM and XRD to check the electrode composition. During the actual experiments, obtaining proper results from the setup proved difficult, despite the simplicity of the passive system. The acid and base environment appeared to play the largest role in this, as they create an unsafe habitat, but are necessary to actually realize a meaningful power output. A rack of resistances and DMM's were used during these tests to acquire the data, with the addition of two syringe pumps in the active cell setup. After obtaining a maximum of  $0.59mW/cm^2$ ,  $0.92V$  in the passive and  $1.36mW/cm^2$ ,  $0.944V$  at  $1mL/min$  in the active structure, more time was spend on optimization and use-case of the cells. A higher flow rate by attaching multiple peristaltic pumps, wider MEA areas and stacking of cells, all proved to increased the performance. This led to demonstration by turning on an LED of  $1.6V$  and a maximum power density of  $3.2mW/cm^2$  with two cells in series. Changes to the robustness, accuracy and thus professionally of the setup and cell structure are most urgent and recommended as future improvements to continue testing different effects and optimizing its performance. Concluding, it can be said that obtaining power from  $H_2O_2$  with a fuel cell is definitely possible at relatively low power output levels, but has to be improved far more to actually be beneficial as power system.

# Decomposition Thruster

Now the generated achievable power using Hydrogen Peroxide ( $\text{H}_2\text{O}_2$ ) in a fuel cell is known from the research shown in Chapter 4, the required power needs to be investigated. The knowledge gained in Chapter 2 and the project plan provided in Chapter 3, will serve again as a guideline. This way, the goal of obtaining the minimum input power required for thermal decomposition of High-Test Peroxide (HTP) in a satellite thruster, was obtained. This was done by first investigating the decomposition requirements themselves more closely in a drop test study, from which a more clear overview of the accompanying challenges came to light. A small scale injection setup was developed subsequently, in which optimization of the decomposition method turned out to be necessary. The results of all of the experiments were closely analyzed, so a conclusion could be formed on its capability to decompose the  $\text{H}_2\text{O}_2$ . This chapter shows the process of development in chronological order, addressing the findings along the way, which appeared to be crucial for further success. The test setup is shown in great detail first, after which the experiments that were done and results coming from it were analyzed. Finally a conclusion and multiple recommendations based on the results could be given.

## 5-1 Experimental Preparation

During the thesis study there was no time to build an actual thruster system, which includes an injector, combustion chamber and nozzle. Instead, the experimental setup was kept simple and only a Proof of Concept (PoC) system was developed to check what power is required for decomposition. The focus lies thus on understanding the thermal decomposition process with mainly a heating wire and partly an arc. The setup therefore needed to be universal as well as safe and still be able to properly measure the relevant parameters.

Since decomposition of the  $\text{H}_2\text{O}_2$  can be quite dangerous, a safe working environment as explained in Section 3-3-2, was created first. A protective casing was thus constructed in which the decomposition could take place, as will be shown later in Section 5-2-1. Also, at all times, individual components and complete setups were tested with water beforehand to check for correct operation.

### 5-1-1 Instrumentation

Contrary to measuring thrust and pressure in a complete thruster system, only temperature and power are required in this study. Additionally, recordings are made from the decomposition to check if the process goes as expected.

Measuring the temperature as well as visual recordings of the decomposition simultaneously was expected to be done cleverly, using an infrared camera. Upon preliminary testing, however, it turned out that capturing the temperature of the liquid and gas was practically impossible this way. This was due to several reasons of which the first was a practical one; the glass used in the protective casing of the setup reflects the infrared radiation. Working without the glass would both be dangerous as well as risky for the camera since it can only withstand a certain temperature. Secondly, measurements appeared to be possible only with radiating solids, as the little amount of water and  $H_2O_2$  used in these tests are not recorded. Background radiation would namely interfere and the weak signal causes inaccurate and far too little temperature data.

#### Thermocouples

Hence the shift to thermocouples was logically made, despite their possibility to affect the flow when placing them in the setup. To make them disturb as little as possible, their size should be minimal and placement optimal. Multiple thermocouples were placed at known distances along the decomposition path of the  $H_2O_2$ , as is done in a preceding study [55]. Simultaneously, the thermocouple used should be as thin as possible to obtain a fast response time and high measurement accuracy considering only small amounts of  $H_2O_2$  are used. In addition, during the short but intense decomposition period, it should be able to withstand the high temperature which could reach up to  $1200K$ . A K-type thermocouple of  $0.125mm$  thickness should thus be sufficient for the short exposure times that were worked with in this research. This type, made of Nickel-Chromium / Nickel-Alumel, is compatible enough with  $H_2O_2$  and has an optimal response time and relative radiation harness [24]. It has a measurement accuracy of  $\pm 2.2^\circ C$  or  $\pm 0.75\%$  and its response time differs depending on the medium it is used for, ranging from  $1s$  in still air to  $0.04s$  in still water. Moving air also increases its response time to  $0.08s$ , which is defined as how long it takes to reach  $63.2\%$  of the new temperature [53]. The thermocouple should not be exposed to an oxidising atmosphere, but this unfortunately is inevitable and probably does not have a significant effect. Lastly, the maximum operating temperature of this thermocouple is  $593^\circ C$  but increases to  $982^\circ C$  with short exposures only, as is the case in these experiments. This limit might be reached with optimal conditions, but is not expected to be exceeded.

**Table 5-1:** K-type Thermocouple Specifications

| Thickness     | Accuracy $\pm$            | Response Time (63.2%)              | Maximum Temperature                         |
|---------------|---------------------------|------------------------------------|---|
| $d = 0.125mm$ | $2.2^\circ C$ or $0.75\%$ | $1s$ (Still), $0.08s$ (Moving) Air | $593^\circ C$ (long), $982^\circ C$ (Short) |

## Recordings

A Data Acquisition System (DAQ) was required for thermocouple results to be processed, preferably with a measurement frequency as high as possible. This could be done for example with an oscilloscope which has two inputs at most and an internal logging system. The signal would have to be amplified beforehand, to be able to measure the range of  $39\mu V$  that the K-type provides, which makes this method very inconvenient. This means only the DAQ cards from National Instruments (NI) remain as an option, which can be combined with a Labview program or Flexlogger in this case to process the raw data. Best suitable for this, is the NI DAQ-9219, plugged into the NI cRIO-9074, so multiple DAQ cards can easily be plugged in and processed by a laptop. The measurement setup was almost exactly the same as with a previous decomposition study, which means data comparison could be done [55]. These data, however, are from droplets falling on preheated plates, instead of injected on a different type of igniter. Other DAQ's are also investigated, but either do not support inputs (NI-9264), do not have a measurement frequency high enough (NI-9210), have too much noise added to the signal (NI-9201) or were simply broken and unavailable (NI-9205). The DAQ used, was set at its maximum measurement frequency of  $50HZ$  and had Cold Junction Compensation (CJC) switched on since the temperature at the cold end (which goes in the DAQ) of the thermocouple is not  $0^{\circ}C$ , but room temperature. Measuring voltage using a different model instead of temperature directly and converting the data does not increase measurement rate nor accuracy.

The other type of recording is a visual one, to optically measure the occurrences during decomposition. A Photron FASTCAM NOVA S high-speed camera was utilized for this, supported by an external light to create a high luminosity. The measurement frequency for the recordings was set at 6400 frames per second at a resolution of  $1024 \times 1024$  pixels. It is capable of filming for three seconds continuously, after which the video can be edited and is automatically saved. In addition, normal camera videos were taken for clarification, since the Photron is only able to film black and white. Unfortunately, the high-speed camera is also not capable to capture the arc discharge, hence those experiments rely solely on the color camera recordings.

## Other Parameters

Time, distance and mass are other important parameters to keep track of during the experiments. The time it takes for a specific volume of  $H_2O_2$  to decompose after being injected at a certain velocity is an important parameter. The moment a droplet is in first contact until it starts decomposing namely describes its Decomposition Delay Time (DDT), which is a crucial factor in propulsion system design. It however does not require extra instrumentation other than the already used high-speed camera besides a conventional ruler and volume indicating syringe. Since specifications of the igniter will be altered to optimize the setup, these characteristics have to be tracked as well. Similarly, the concentration was measured before inserting it into the syringe, as explained in Section 3-4-2. Lastly, is of course power, measured manually through the input screen of the lab power supply. It indicates both voltage as well as current that is being used during the operation of the components up to one digit in accuracy.

### 5-1-2 Heating Wire

Similarly to the reference study as discussed in Section 3-2-3, a heating coil was utilized for resistance decomposition. For experimental flexibility and cost-reducing reasons, however, it was decided not to add the insulation and casing around the resistance wire. Only the resistance wire itself was thus used since this is the component which consumes the power that causes it to reach a certain temperature. The amount of power needed depends on its electrical resistance, which in turn depends on the material type, diameter and length of the wire. The material used for the wire could be anything from copper up to stainless steel, although the following are most commonly used; Constantan (CuNi), Nichrome (NiCr), Kanthal (FeCrAl). From these, the Nichrome type American Wire Gauge (AWG)24 Nicr60, made of 60% nickel and 15% chromium and a remaining part iron, was used in this research. With a diameter of  $0.51\text{mm}$  it has a maximum continuous operating temperature of approximately  $1150^{\circ}\text{C}$  and electrical resistance of  $5.7\Omega/\text{m}$ . In general,  $0.4\text{W}/\text{g}$  is needed to increase the NiCr wire temperature by one degree Celsius, although its shape and environment have some influence on its actual measured value. Similarly as in the reference study, a coil formation was applied in each test to generate the most heat and contact area.

**Table 5-2:** Nichrome 60 AWG 24 Specifications

| $A_{\text{wire}}$ [ $\text{mm}^2$ ] | $d_{\text{wire}}$ [mm] | $T_{\text{max}}$ [ $^{\circ}\text{C}$ ] | $\rho_r$ [ $\Omega/\text{m}$ ] | $c_p$ [ $\text{W}/\text{g K}$ ] |
|-------------------------------------|------------------------|---|--------------------------------|---------------------------------|
| 0.205                               | 0.51                   | 1150                                    | 5.51                           | 0.4                             |

During experiments, multiple aspects related to the resistance wire were tested. This is because the exact specifications of the heating coil were expected to have a large effect on the minimum power required to start decomposition. Optimization of this wire is thus crucial and can be achieved in several ways. As indicated before, the type of material, length and thickness of the wire, all affect the current and voltage characteristics. Having short, thick wires, for example, drives down input power, whilst the current required to reach a temperature increases. This same temperature can be controlled and tested on what is minimally required for decomposition, so less power is needed for heating. Lastly, the effects coming from the shape and orientation of the coil are of interest, since less wire is needed to reach a temperature if they are close together. A dense mesh could thus work well, although in this case one should be careful since the wires are not isolated. The current chooses the least resisting path, which means a short circuit can easily be created this way.

## 5-2 Drop Test Study

To get a first impression of the energy needed to decompose the  $\text{H}_2\text{O}_2$  using igniters and a better understanding of the process, a drop test study was performed first.

### 5-2-1 Experimental Setup

The setup used was built up inside a fume hood and consisted of several instruments combined with some individual components and assemblies. The infrastructure of the first complete test setup is shown in Figure 5-1.

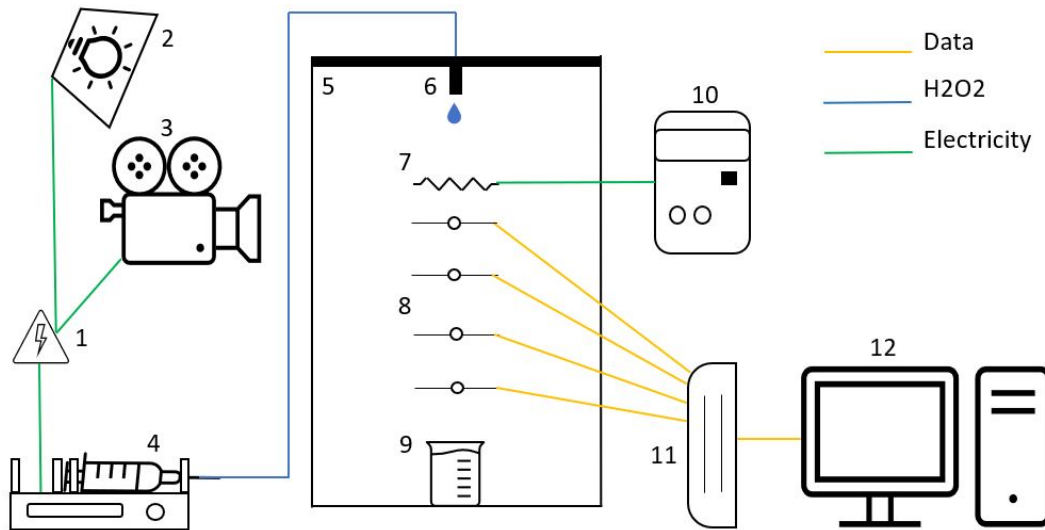


**Figure 5-1:** First Drop Test Study Setup Infrastructure

The infrastructure shows a wall plug (1) which provides power to multiple instruments of which it is not required to measure power usage. One of these is the extra light (2) required for the high-speed camera (3), both set up at a safe distance to record the complete falling distance or the impingement of the drop on the heating wire more closely. Recordings were sent to a different computer far away from the setup to later check and analyze the data. Another instrument is the syringe pump (4) with the syringe itself containing a low quantity of  $\text{H}_2\text{O}_2$ . It is the same one as used before in the fuel cell setup in Section 4-2-3, which is now set to only inject a known volume inside a chamber (5). This acts more like a protective casing in which the falling droplet is ignited. The box dimensions were approximately  $20\text{cm} \times 20\text{cm} \times 40\text{cm}$  and consisted of an additive manufactured Poly Lactic Acid (PLA) frame, with either steel or glass sheets in between. The droplet entered via tubing into a capillary tube (6) located at some distance, but directly above the coiled Nichrome heating wire (7). Similarly to the four k-type thermocouples (8), the wiring goes out via the back steel sheet of the protective box, sealed with sealant tape so it is properly electrically and thermally isolated. At the bottom of the box a collection beaker (9) is placed, to capture all liquid residue to check for concentration afterwards. Next to the setup is the power supply (10) which heats up the resistance wire is placed, which can be manually readout. Here the DAQ (11) is placed as well, where all thermocouples lead to from which the data can be subsequently stored on the computer (12) which contains all necessary software.

To improve decomposition results however, the setup as described by the infrastructure has been altered in several ways. Some instruments are left out whilst other components are added to the assembly as visible in the picture shown in Figure 5-2.

### 5-2-2 Results & Discussion

The experimental results and the alterations after their analysis is shown hereafter in chronological order. An overview of the performed tests is given already in Table 5-3.

Initial tests showed extremely bad results, as the injected droplet of  $\text{H}_2\text{O}_2$  would not de-

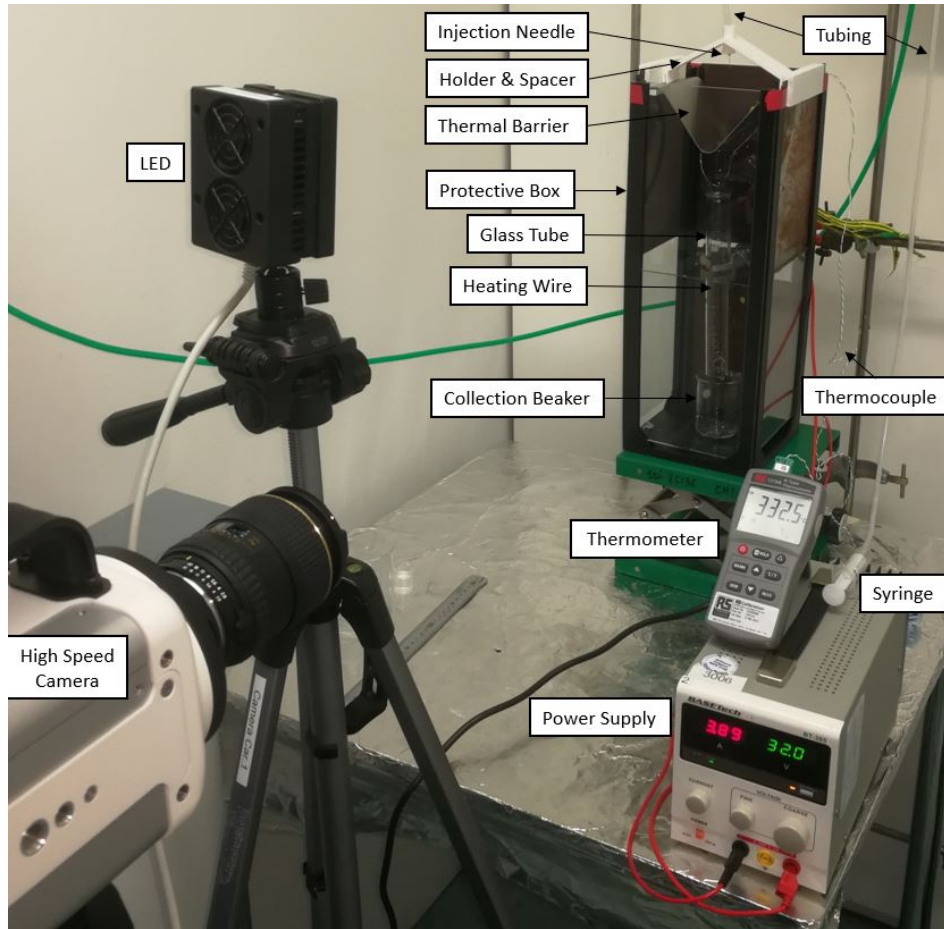


**Figure 5-2:** Final Drop Test Study Setup Overview

**Table 5-3:** Drop Experiment Settings Summary

| Heating Coil          | Test Settings                        | Remarks                  |
|-----------------------|--------------------------------------|--------------------------|
| Short Horizontal NiCr | 3 – 6A, 3 – 6V, 300 – 700°C, ±90%    | Failed Setup & Tests     |
| Long Vertical NiCr    | 2.5 – 4A, 32V, 300 – 600°C, 80 – 92% | Decomposition Achieved   |
| Curled Vertical NiCr  | 3.2A, 32V, ±650°C, 80 – 99%          | Repeatable Decomposition |

compose. Mainly the thermocouples turned out to be a hassle in many ways, whilst some clarification came forth from the high-speed recordings. A closeup of the droplet which is about to impact the short, horizontal, coiled Nichrome heating wire and the thermocouple placement is shown in Figure 5-3a. The temperature results from the first thermocouple in line with the heating wire are shown in Figure 5-3b for both a reference as well as an attempted decomposition test.

From Figure 5-3 it was concluded that the following issues caused the misreadings and problems with decomposition. First of which is related to the droplet to heating wire size ratio and the other to the heat loss.



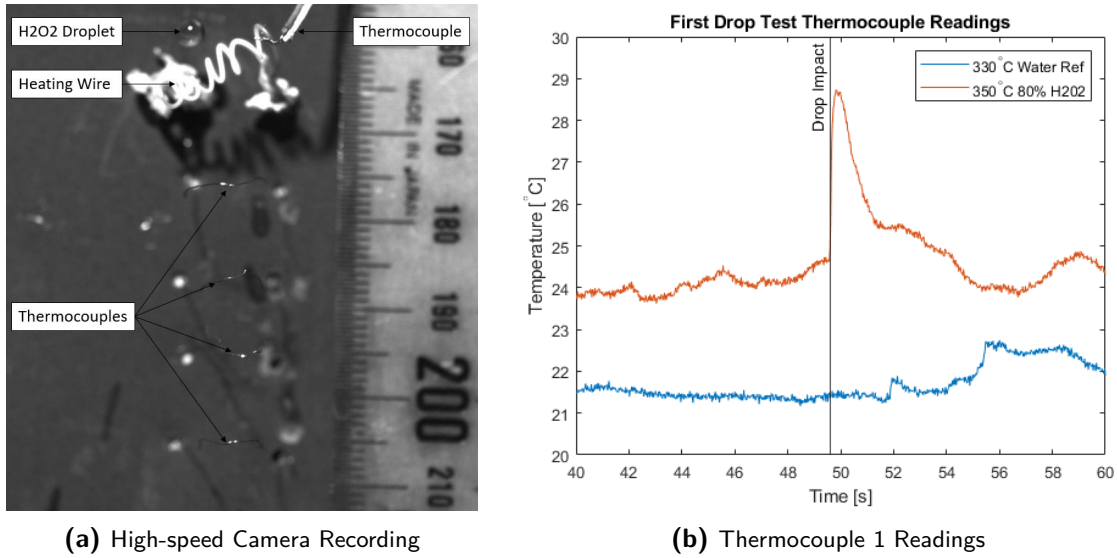


**Figure 5-3:** First Drop Test Setup Experimental Results

## Injection

The droplet created by the capillary tube that injected it is too large in comparison to the heating wire. Too much energy is therefore required to increase its temperature until decomposition will commence. Its mass can be approximated analytically with relation to the tube it is dispersed from, using Eq. (5-1).

$$m = \frac{\sigma_s d_{out}}{2g_0} f(d_{out}/2a_c) \quad \text{with } a_c = \sqrt{\frac{2\sigma_s}{\rho g_0}} \quad \text{and } f(d_{out}/2a_c) = 3.8 \quad (5-1)$$

Where  $\sigma_s$  is the surface tension for pure H<sub>2</sub>O<sub>2</sub> at ambient conditions, which is 80.4mN/m and  $d_{out}$  is the tube exit outer diameter. The droplet density  $\rho$  and gravitational acceleration  $g_0$  remain the same and thus constant  $a_c$  as well. Mass and size of the droplet can thus be reduced with a smaller outer diameter, which is why a needle was used for injection hereafter.

Also, the contact area with the heating wire needs improvement, so a longer, vertical heating wire would serve as a replacement. Unfortunately, this meant more power is required to heat an even smaller amount of propellant. This did however not solve another major issue, which was the dispersion of the droplet after collision with the wire. This made that the H<sub>2</sub>O<sub>2</sub> would touch the wire only once and it would go in any direction afterwards. This is the reason why only the first thermocouple was sometimes able to capture the droplet temperature since a fragment directly impacts the bead. Not even the reference case got impacted by the droplet whilst the other has a clear peak shown in Figure 5-3b.

The velocity of injection was hard to control as well since it would simply fall down and accelerate due to gravitational force. The distance from the heating wire is however desired to prevent the H<sub>2</sub>O<sub>2</sub> inside the injector to heat up or even decompose before injection. This is why a thermal barrier is placed in between the heating wire and injector, which would prevent the heat from going up too much and affecting the H<sub>2</sub>O<sub>2</sub>.

## Insulation

The thermal barrier also acted as a lid to somewhat keep the heat from dissipating into its surrounding. This heat loss had to be prevented, so more energy would go into the actual heating of the  $\text{H}_2\text{O}_2$ . A lab glass tube was thus inserted around the heating wire to act as insulation, which could withstand reasonable high temperatures. This way visual recordings could still be made of the decomposition process, although the thermocouples were harder to insert due to their length and obstruction of the glass insulation.

Only one thermocouple could now be inserted from the top, which had to be read manually. This was however not too bad, since the previous temperature recordings proved to be inaccurate due to poor electrical isolation since they were not shielded. The focus would thus from now on be on achieving actual decomposition instead of its temperature measurement. Still, an increase in temperature should be recorded more easily in the renewed setup, since the glass prevents it from dissipating too much into the surrounding. Instead, it is forced to leave through the opening on either the bottom or top and thus going past the one thermocouple left.

## Drop Decomposition

With the longer, vertical heating wire, partial insulation and smaller injected droplets decomposition happened every now and then. It would happen mainly whenever a secondary smaller drop or ligament would hit the heating wire a second time after the first collision. This  $\text{H}_2\text{O}_2$  namely has little mass, low velocity and would be heated for a longer period by the new heating wire. The cause is thus the increased contact area and time in which less energy would be needed. The actual power input, however, was far higher, up to  $124.48\text{W}$  due to the wire length causing the voltage to be  $32\text{V}$ , whilst only reaching a temperature of around  $350^\circ\text{C}$  with the accompanied  $3.89\text{A}$ . Despite not saving the peak temperatures, a clear increase of  $100^\circ\text{C}$  to  $200^\circ\text{C}$  was visible each time a satellite drop would explode. Stronger confirmation of decomposition was there from the loud popping sound it produced upon impact. Unfortunately, physically acquiring the reaction products with the beaker that is placed below turns out to be more difficult. Even if some liquid is captured inside, it could either be from the decomposed results as well as from droplets that simply fell down and thus did not give a definite answer.

With a shorter heating coil in a curled, more packed configuration using  $102.4\text{W}$ , with  $3.2\text{A}$  and  $32\text{V}$ , a higher decomposition repeatability was achieved. This was because it heated a more confined space and better intercepted the small droplets after first contact. This is captured by an orange glow circled in green in the coloured image shown in Figure 5-4b.

Even more obvious is it in the high-speed recordings where tiny droplets are flying away at high speed in every direction after the decomposition, shown inside the green circles in Figure 5-5b. This is clearly different from normal behaviour after impact on the wire, when the droplet would simply split up as it did already in Figure 5-5a.

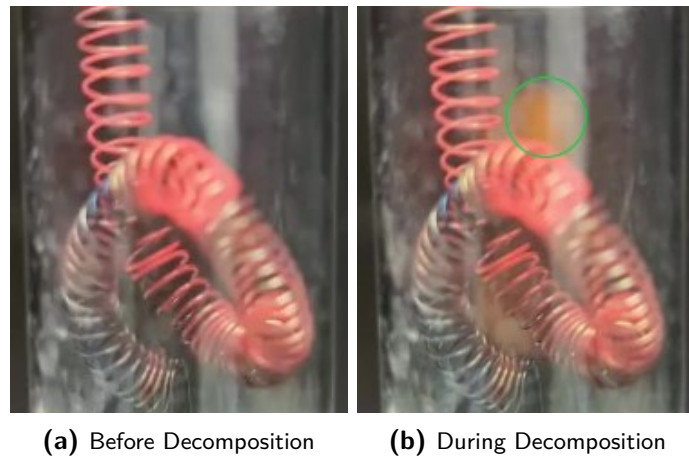


**Figure 5-4:** Color Visual 97% H<sub>2</sub>O<sub>2</sub> Decomposition Recording

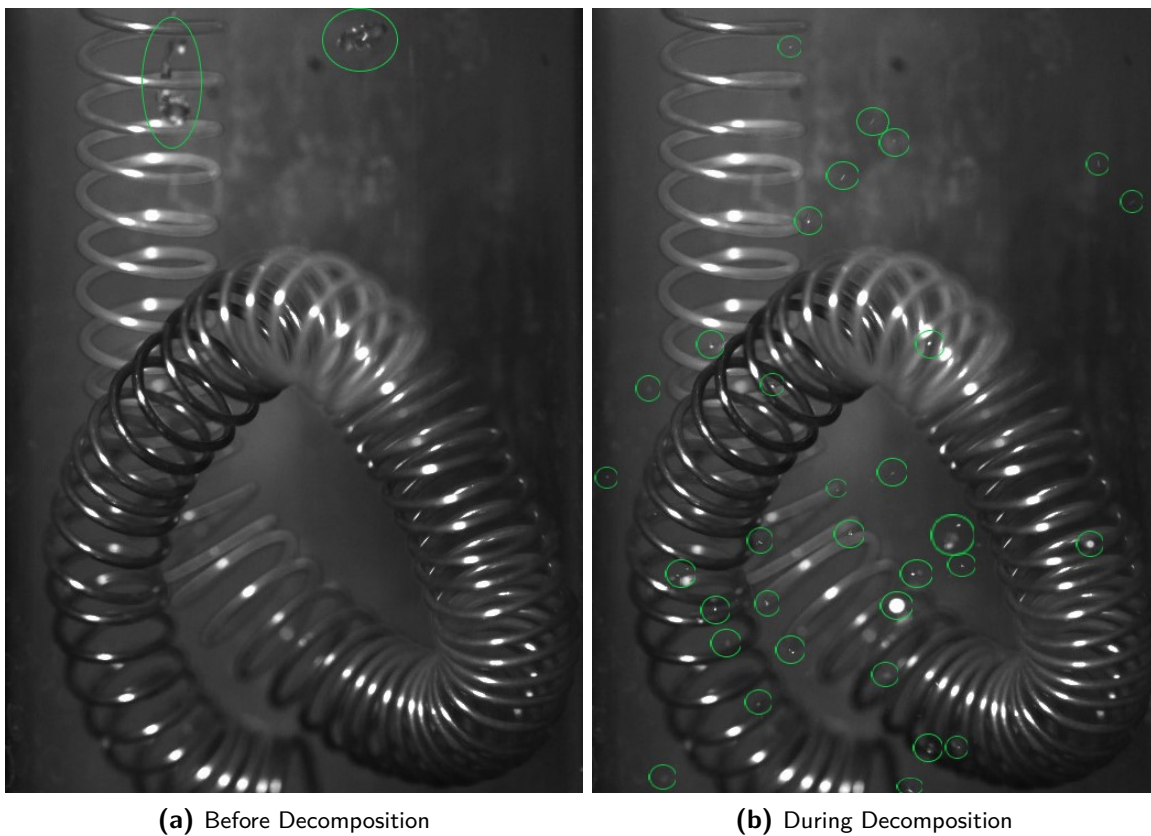


**Figure 5-5:** High Speed 97% H<sub>2</sub>O<sub>2</sub> Decomposition Recording

### Solution Summary

The drop test study showed to be far from ideal but does give some clear solutions on how to induce the decomposition. Efficient and sufficient energy transfer from the igniter to the propellant appears to be the crucial factor in this case. With the development of an improved setup, a closer look at the following points is essential.

- **Heating Coil Igniter**

- **Configuration:** the orientation and shape of the wire must not disturb the flow, whilst it does have to give away a lot of heat locally. A densely packed coil at a slight distance from the injection point would work best.
- **Dimensions:** length and thickness of the wire determine how much heat it can contain. Longer, thicker wires require more power but can transfer more of it to the propellant upon contact as well.
- **Temperature:** input current is directly related to this parameter, of which a known minimum of at least  $200^{\circ}\text{C}$  is needed to ignite the  $\text{H}_2\text{O}_2$ , but a higher value will help in initiating the decomposition.

- **Injected  $\text{H}_2\text{O}_2$  Propellant**

- **Insertion:** the velocity and path the  $\text{H}_2\text{O}_2$  has, determines its residence time on the wire or in the heated environment. Being distributed slowly over a larger area would help in making the energy transfer easier.
- **Proportion:** size and mass of the droplet showed to have a large effect, as it contributes to the contact area. Also, less energy is required to decompose smaller droplets, which is why these are preferred.
- **Temperature:** starting at an elevated temperature of the propellant, means less of an increase is required to reach decomposition. This could however become dangerous as it can induce unwanted boil off and is preferably not tested.

- **Environmental Conditions**

- **Insulation:** the experimental setup should hold the heat produced by the igniter, so only a minimum is lost to its environment. Building this type of combustion chamber is however outside the scope of this research.
- **Pressure:** not proven to work in this study, but it should help the process, although it can become quite dangerous.

Changing the test setup to a high pressure, isolated tank creates a dangerous high pressurized system, so this is not done hereafter. If properly build and well-sealed however, this type of bomb calorimeter is a good way to test the minimum energy required for decomposition. The main takeaway for the next study is that energy transfer can thus be increased by having little propellant injected under better conditions where it has more residence time and contact area.

### 5-3 Injected Flow Study

The lessons learned are taken into consideration when performing the flow study as far as possible. The goal now is to create a more comparable situation as in the combustion chamber, without the addition of high pressure and nozzle.

### 5-3-1 Injection Setup

The same instruments are used as before, but mainly the setup inside the protective box has changed, as shown by the infrastructure in Figure 5-6.

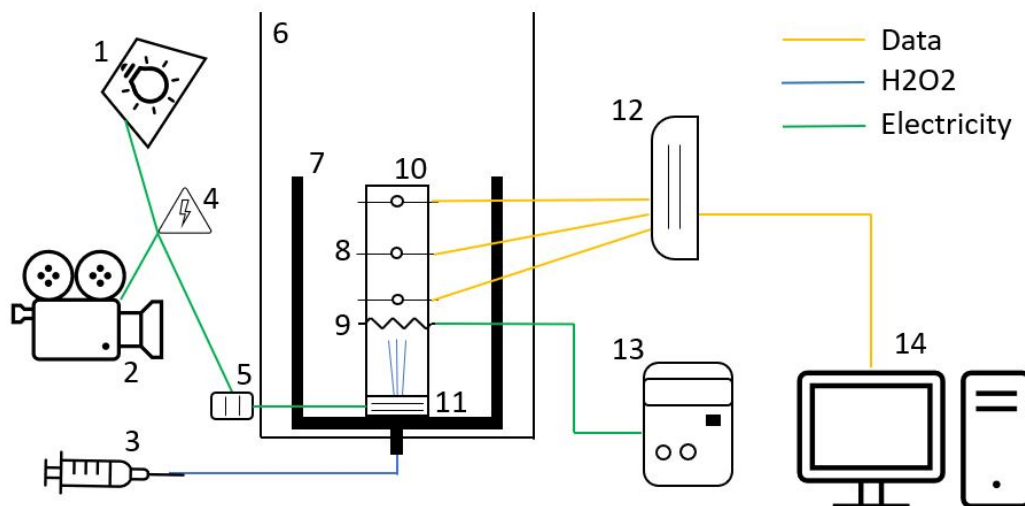


**Figure 5-6:** Injection Setup Infrastructure

Inside the protective box (6) an additive manufactured PLA decomposition stand (7) is now placed to hold everything in place at an equal distance. The stand has a nozzle on the bottom side where the  $\text{H}_2\text{O}_2$  can be inserted to go to the injector down below via its inside. In between the stand, thermocouples (8) are placed again, located above the heating wire (9) this time. They are placed inside a glass tube (10), to minimize the heat loss to the environment. Unlike with the drop tests, this is now possible because a technique is found on how to drill holes in the lab glass through which the thermocouples can enter. The same holds for the heating wire, which could easily be replaced with electrodes in the case of arc decomposition. Placement of the igniters is usually as follows, considering injection as a starting point. Heating wire bottom at  $25\text{mm}$  and top at  $35\text{mm}$  in case of vertical insertion, but this can differ with several  $\text{mm}$  in some cases. These locations are also the centre lines in case of two horizontal wires, whilst if only one horizontal wire is used, it would be placed at the  $25\text{mm}$  mark. Thermocouples are always placed horizontally at  $40\text{mm}$ ,  $50\text{mm}$  or  $80\text{mm}$  at the glass tube exit.

Then there is the nebulizer disc (11) which is the component that will inject the  $\text{H}_2\text{O}_2$ , powered by its microcontroller (5). It is placed at the bottom since it operates best if the propellant is supplied from below. On the decomposition stand, some aluminium tape is added to reflect the heat produced and prevent the plastic from melting. A picture of the setup is added in Figure 5-7, with a closeup of the decomposition stand in Figure 5-7b. Many problems preceded before obtaining this final configuration, although the hassle remains whenever something needs replacing inside the confined space of the decomposition stand.

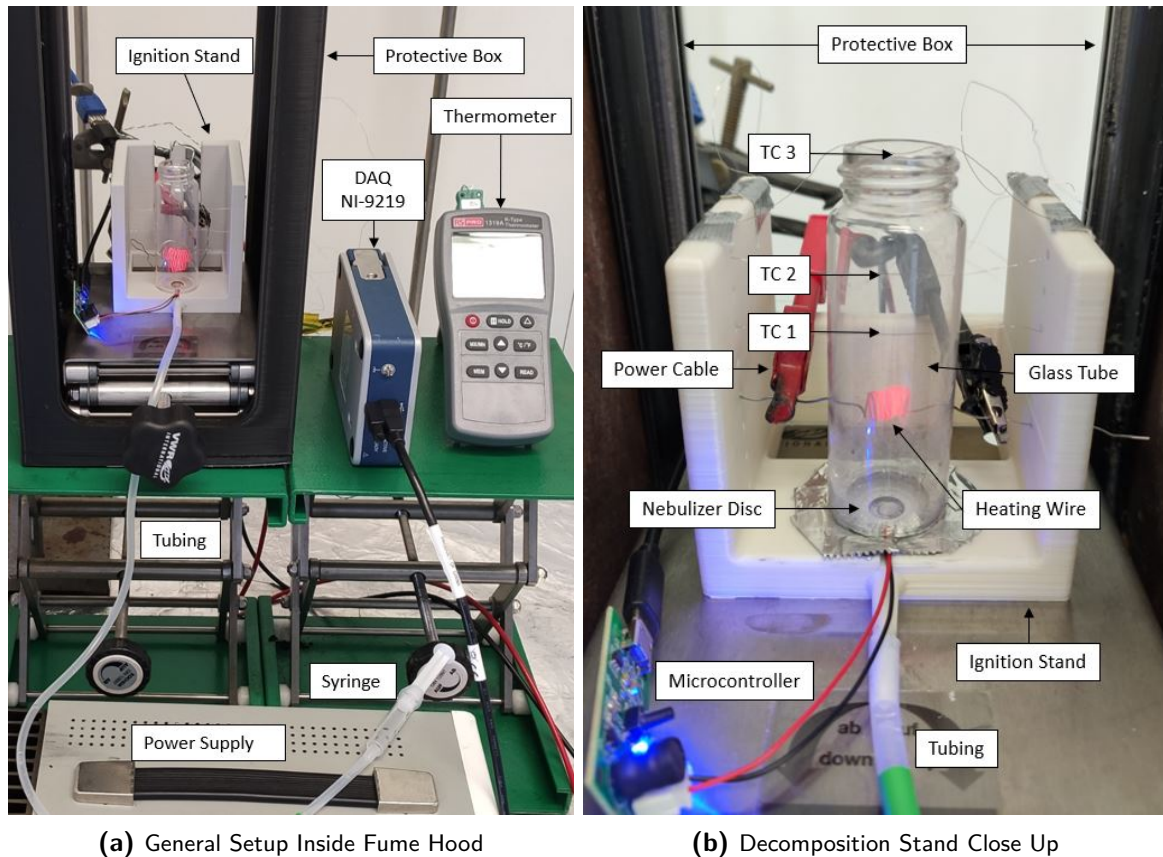


**Figure 5-7:** Final Injected Flow Study Setup Overview

### Injector Specifications

Since the setup is made in a reasonably short period, a pressurized injector is not part of the development. As instead, it is mimicked with a nebulizer disc, which is usually part of a mist maker. It uses high-frequency ultrasonic vibration which vaporizes a liquid on the bottom that is in contact with the mechanical vibration of a piezoelectric element. The droplet size obtained using this disc, could not be captured with the high-speed camera, but was found instead in literature. A median droplet size of  $9.5\mu\text{m}$  was found there, which means minimal mass and thus energy is required to induce decomposition [59]. There are however evaporation cooling characteristics which come into play when being injected, which are a disadvantage as the droplet temperature goes down.

Some additional tests revealed that the disc has a steady mass flow rate of approximately  $0.036\text{g/s}$  or  $1.5\text{ml/min}$  with  $\text{H}_2\text{O}_2$ . This stays unchanged when pressure is put on it with the syringe which inserts the approximately  $0.5\text{ml}$  of  $\text{H}_2\text{O}_2$  in each test. The velocity was measured to be approximately  $3\text{m/s}$  at the first  $20\text{mm}$ , after which the stream spread out and slowed down due to the drag. The initial straight column of  $3\text{mm}$   $\text{H}_2\text{O}_2$  in diameter, shown by the test in Figure 5-8, was taken into account with the placement of the igniters. Placement of the disk itself underneath the heating wire is beneficial since the hot air rises. The heating of the disk and the  $\text{H}_2\text{O}_2$  inside it was prevented this way, certainly when at a safe distance of  $25\text{mm}$  from the igniter. Droplets could however fall on the disc this way, if



liquid accumulates on the wires above. The specifications are summarized in Table 5-4.

**Table 5-4:** Nebuliser Disc Injector Specifications

| Mass Flow Rate       | Droplet Size         | Velocity         | Stream Width       | Wire Distance     |
|----------------------|----------------------|------------------|--------------------|-------------------|
| $\dot{m} = 0.036g/s$ | $d_{med} = 9.5\mu m$ | $v_{inj} = 3m/s$ | $d_{stream} = 3mm$ | $d_{wire} = 25mm$ |

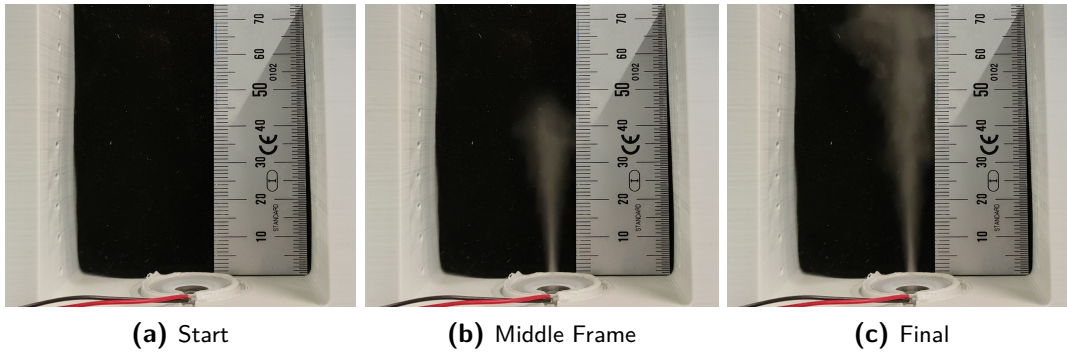


**Figure 5-8:** Injected  $H_2O_2$  Propagation Experiment

### 5-3-2 Decomposition Results

Despite the lessons learned from the drop test study, a continuation of failures was present using the renewed setup. Multiple heating wires differing in material type, thickness, length, shape and orientation were tried at first to obtain the same explosion as was the case with a drop. Only with prior injected  $H_2O_2$ , accumulating liquid on the wires and subsequent switching on the power, an explosion can be heard. Else, the small number of droplets that were injected did not sound different from the water reference case injection. The high-speed recordings already give some clues away on why this is happening as well as other effects the  $H_2O_2$  has inside the setup. Being able to tell if decomposition is happening is more difficult, which means most of the actual decomposition validation has to come from the thermocouple temperature data as shown later in Section 5-3-2. First, some high-speed camera recordings of trial experiments are shown in Figure 5-9 and are clarified hereafter.

Similarly as with the reference study, an vertically aligned double coil was mounted inside the glass, visible in Figure 5-9a. The method actually worked quite well, but only because of misalignment of the center line, which made the injected  $H_2O_2$  impact already at the bottom. Else, the outer coil would be a bit unnecessary in this case, since it does not directly contribute to the heating of the  $H_2O_2$ , while it does consume power. Besides this, the thick Constantan wire requires a lot of power to heat up and is therefore visibly not white glowing. It is also least compatible with the oxidising environment and will both erode as well as corrode fastest, making it less sustainable. The more packed, single, vertical, Nichrome coil configuration from Figure 5-9b, is performing better already as can be visually confirmed. The injected  $H_2O_2$  perfectly enters through its center, where it scrapes past the sides and heats up. However, it could also simply flow through if not enough power is applied, instead of in the ideal case expanding inside due to decomposition.

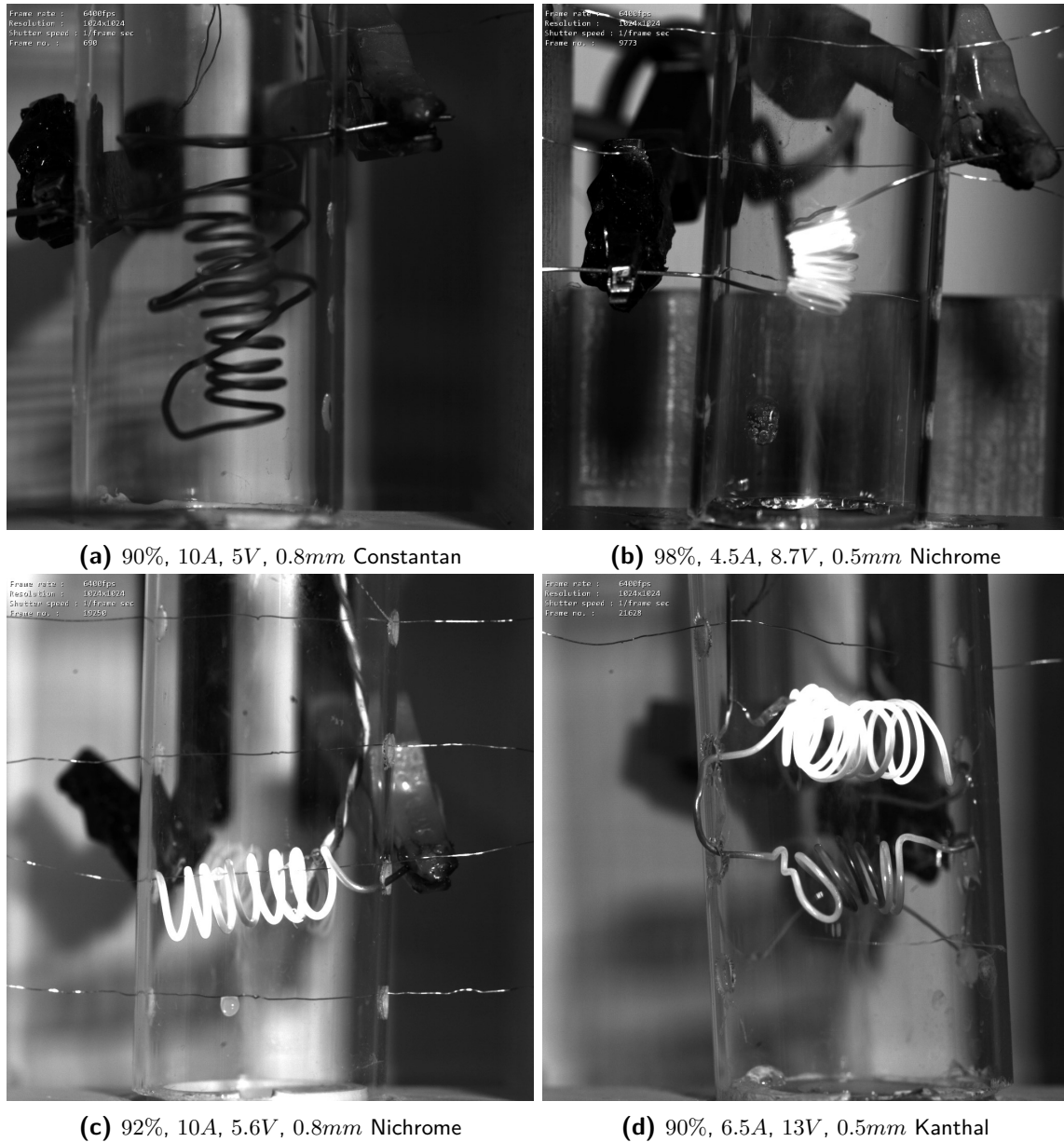


**Figure 5-9:** Heating Coil Configuration Test Recordings

Another method is the perpendicular alignment of the wire, where impingement of the injected  $H_2O_2$  is ensured and with it the interruption of the flow. In the early stage test with thicker Nichrome wire, as shown in Figure 5-9c, thermocouples were also placed underneath the igniter. This however obviously interfered with the flow, such that droplets would accumulate on all wires, amongst other problems. Although the impact of the propellant on the wire was clearly there, heating up turned out not to be sufficient either, due to the little contact time. A lot of energy was again wasted if the coil is not densely packed and used directly for heating the  $H_2O_2$ . The double, horizontally placed Kanthal coil would serve as the solution to this, as shown in Figure 5-9d. The first coil would act as a type of pre-heater when the  $H_2O_2$  continues to go upward and hit the second wire, which gives the last push to cause decomposition. The



main drawback is that hereby the flow has come to an almost complete standstill if too much wire is in its path. The material itself does seem to have the best qualifications as the igniter since it does not degrade a lot. There is however to speculate about the wire thickness since the thinner one disturbs less the incoming  $\text{H}_2\text{O}_2$  flow, but it is also less capable of holding the heat required to transfer into the propellant. This is visible in many of the tests and this exact picture, as it shows the difference in brightness between the bottom and top heating wire. The energy was being taken by the  $\text{H}_2\text{O}_2$  and the coil cools down, up until a point at which the temperature was too low to even cause decomposition. This is one of the outcomes that is also noticeable in the power output since the voltage gets lower due to the temperature decrease. On the other end, as the wires heat up, the voltage does the same up until a point at which the metal is more ductile and causes deformation of the coil. This is another outcome that came along with the difficult installation of the setup inside the glass in the beginning.

All in all, the number of tests performed are shown in Table 5-5, grouped per heating coil type, input power and  $\text{H}_2\text{O}_2$  concentration. Besides these, several non-registered preceding tests were done to check general setup functionality.

**Table 5-5:** Number Of Injected  $\text{H}_2\text{O}_2$  Experiments Performed (15-30W, 30-45W, 45-60W)

| Concentration      | $\leq 85\%$ |          |          | $\approx 90\%$ |          |          | $\geq 95\%$ |           |           |
|--------------------|-------------|----------|----------|----------------|----------|----------|-------------|-----------|-----------|
|                    | low         | med      | high     | low            | med      | high     | low         | med       | high      |
| Power              |             |          |          |                |          |          |             |           |           |
| Various Coil Types | 0           | 0        | 1        | 0              | 0        | 3        | 0           | 0         | 8         |
| 2 Horizontal NiCr  | 0           | 0        | 7        | 0              | 0        | 3        | 0           | 5         | 12        |
| 1 Horizontal NiCr  | 2           | 1        | 0        | 2              | 3        | 0        | 7           | 0         | 0         |
| 1 Vertical NiCr    | 0           | 0        | 0        | 0              | 4        | 0        | 0           | 7         | 1         |
| 1 Horizontal Ka    | 0           | 0        | 0        | 0              | 0        | 0        | 4           | 0         | 0         |
| <b>Total = 60</b>  | <b>2</b>    | <b>1</b> | <b>8</b> | <b>2</b>       | <b>7</b> | <b>6</b> | <b>11</b>   | <b>12</b> | <b>11</b> |

## Experimental Outcomes

In the end, the outcome of experiments can be divided into two groups, each consisting of three scenarios, which are shown below, substantiated by their corresponding data in the figures.

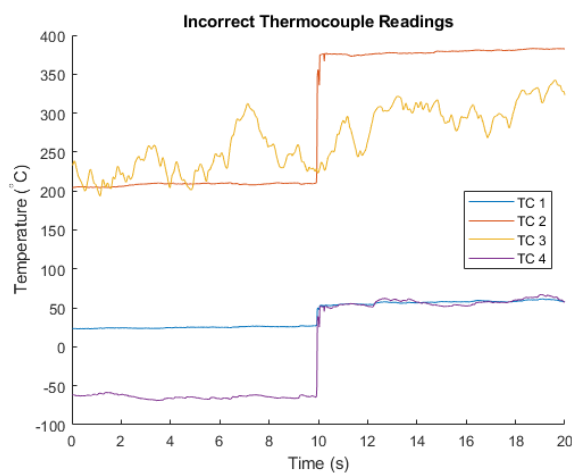
- **Failure:** this implies the experiment does not go according to plan. Mostly because of errors with the test setup, which could sometimes be very obvious, but also stayed unnoticed for quite a long time. Examples are shown in Figure 5-10.
  - **Measurement:** if one of the measurement instruments fails no validation can be done. This happens with the thermocouples as they are easily misplaced thermocouples inside and outside the glass. It can cause short-circuiting of the heating wire path because of contact with them or incorrect insertion in the DAQ. Touching other thermocouples or other conductive materials used in the setup via the back causes more subtle misreadings that are somewhat harder to discover.
  - **Igniter:** as mentioned before, the main errors here are short-circuiting with its wire, or changes in position. This is caused during instalment or more in the

process due to deformation, both causing improper alignment with the injected  $H_2O_2$ .

- **Injection:** the nebulizer disc often malfunctioned, due to its component quality as well as human error. Too much back pressure stops the outflow or moves the disc causing an incorrect injection. In the worst cases, accumulated droplets would fall on the disc again or it would heat up extremely due to the heating wire. If the hot air and liquid are sucked in the setup would catch fire with the  $H_2O_2$  inside and below, where the component itself would act as the fuel, destroying everything. Less noticeable is an offset in concentration, for example, due to refractometer misreading or the remaining liquid in the tubing, which is why the tubes are always flushed first and the tests are repeated.



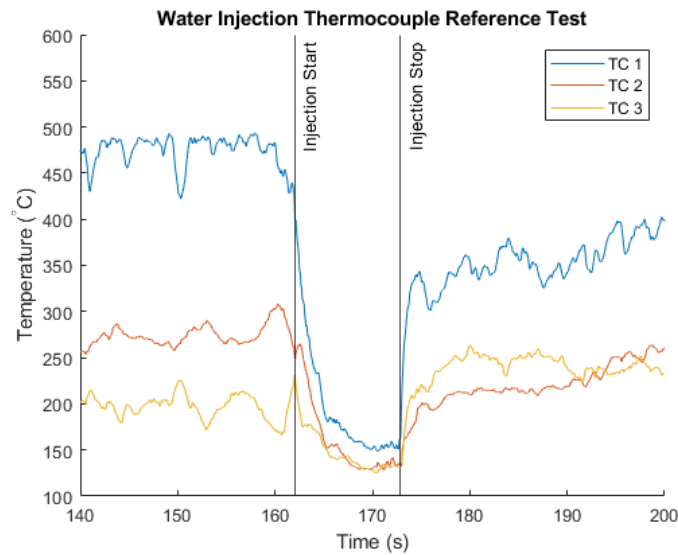
(a) Broken Jar After Injector Fire



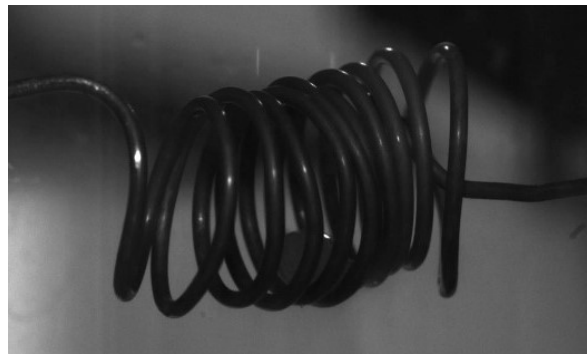
(b) Thermocouple Misreadings During Wire Heating

Figure 5-10: Setup Failure Examples

- **Success:** this is defined by an experiment where feasible data values are properly recorded when there is successful  $H_2O_2$  injection without any disruption.
  - **No decomposition:** a success does not necessarily have to mean there is decomposition. The data will for this case show a constant dip in temperature due to the colder  $H_2O_2$  contact. The best example for this situation is the water reference shown in Figure 5-11.
  - **Partial decomposition:** in which an increase in temperature due to decomposition is measured, but not kept constant during the whole injection period. This can be explained for different specific cases in its way but is often related to the accumulation of the liquid  $H_2O_2$ , as shown in Figure 5-12.
- (Par 1) A steady low-temperature value, followed by a peak is what occurred most frequently. This is because initially, not enough heat can be added to the  $H_2O_2$ , but as the liquid has built upon the wire or surrounding glass it can take in more energy over time, resulting in decomposition. To accumulate, a relatively long operation should thus have taken place, as shown in Figure 5-13a.



**Figure 5-11:** Water Reference Test Results



**Figure 5-12:** H<sub>2</sub>O<sub>2</sub> Droplet Accumulating Inside Heating Wire

- (Par 2) An alternating set of peaks and dips in temperature data, which is expected to be caused by a decomposition reaction followed up by the cold H<sub>2</sub>O<sub>2</sub> hitting the thermocouple and so on. The other cause could be the opposite of the previous item, in which the first impacting H<sub>2</sub>O<sub>2</sub> obtains enough energy to be able to decompose, after which the wire cooled down to such an extent that it is not capable of heating the newly incoming H<sub>2</sub>O<sub>2</sub>. This is however somewhat uncertain since one would expect the heat coming from the decomposition reaction to raise the heating wire temperature again quickly enough. An example of this unsteady behaviour is shown in Figure 5-13b.
- (Par 3) Best case scenario is the one where late decomposition with regards to distance is observed. This is visible in thermocouple data when the lower positioned thermocouple gives a decrease in temperature, whilst higher ones give an increase, as shown in Figure 5-13c. Optically visible in the case of heating coils when the lower one or inside of the wire loses its brightness, whilst the top one or the outside does not change colour or becomes whiter.

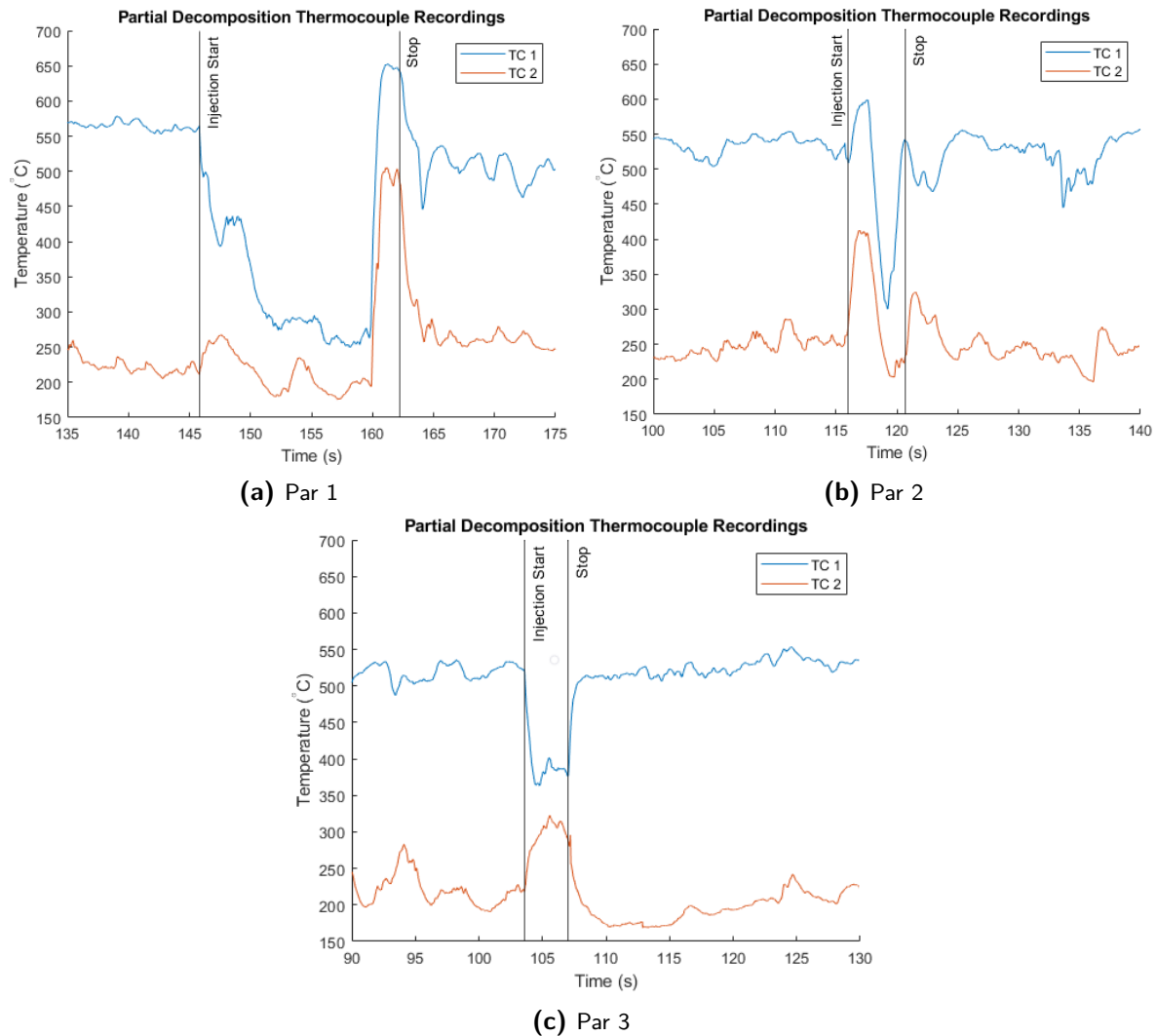
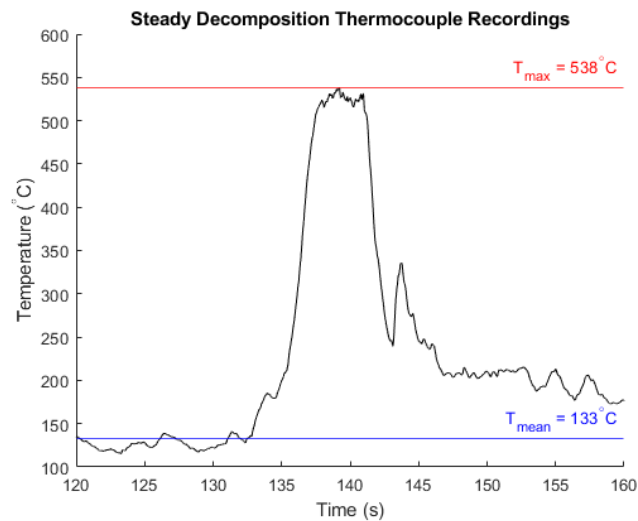


Figure 5-13: Partial Decomposition Test Result Cases

- **Decomposition:** solely an increase is measured, either in a short burst or a continuous high-temperature reading. The amount of decomposition can however still differ, as not all of the injected  $\text{H}_2\text{O}_2$  decomposes. This should be visible in the maximum achieved temperature, which is expected to be lower as it mixes with the remaining colder liquid and air. The mean temperature measured beforehand and maximum achieved during decomposition are important values for analysis, as shown in Figure 5-14.

Generally, whenever a higher heating wire temperature is used during the experiment, the peak temperature reached will be higher as well. The difference in temperature between the two, however, usually stays the same. This is expected to come from either the decomposed  $\text{H}_2\text{O}_2$  values being mixed with the ambient temperature or it simply decomposing less effectively, which makes the average temperature lower as it mixes in with the not decomposed  $\text{H}_2\text{O}_2$ .



**Figure 5-14:** Steady State Decomposition Test Results

It is not possible to measure DDT, since the droplets are either already decomposed as soon as they reach the thermocouple or will not do so at all. The high-speed camera recordings unfortunately do not give any clarification on this either.

### Heating Wire Results

All wires have an inner diameter of  $5\text{mm}$  and length of  $1.5\text{mm}$  and are furthermore sorted based on the material used and its orientation. The decomposition classification is based on the visual behaviour of the temperature during injection, as discussed in Section 5-3-2, with the failed tests left out. Another addition to these results is the registered injection time and its attempt number. For these, two influential cases apply such a short reaction that only an injection peak or dip is visible, without certainly knowing if it will continue as is. The second is a repetitive test, which is rated as a more reliable result, especially when the two sequential experiments give the same outcome.

The first result shown in Figure 5-15, is an overview per wire type, displaying whether or not decomposition is reached at all during the experiments. It shows the tests chronologically from left to right, where the 'various' bar represents multiple different wire types used in the first few successful exploratory experiments. The others indicate; the number of coils, horizontal or vertical orientation and Nichrome or Kanthal as the material used. All outcomes are represented in the figure and apart from the final set, no consistent results were obtained. This is partly because of the intended input parameter changes during tests but is also a consequence of inevitable changes to the setup in between the tests due to failures.

The amount of experiments done using the wire differs very much, as is displayed inside the bar. This is because, after having performed a full set of tests with the two horizontal coils trying different concentrations and power inputs, their effect did not seem to be the major influence. Instead, reducing power input by adjusting the wire itself and the way  $\text{H}_2\text{O}_2$  is injected into it, helped more in obtaining a minimum power required for achieving decomposition. This is clearly visible in Figure 5-16 which includes all wire types, as the

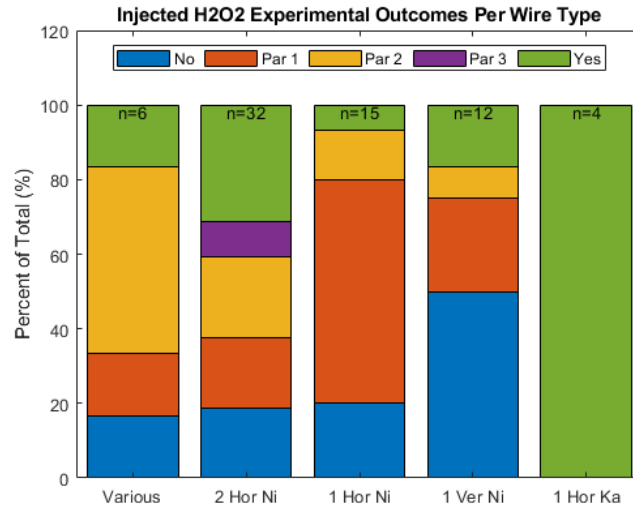


**Figure 5-15:** Wire Type and Outcome Dependency

lower power input tests achieved decomposition many times as well. This is mainly due to the few densely wound horizontal positioned Kanthal wire tests, which were performed in the final stage to prove that proper contact between the heat source and injected  $H_2O_2$  is very important here.

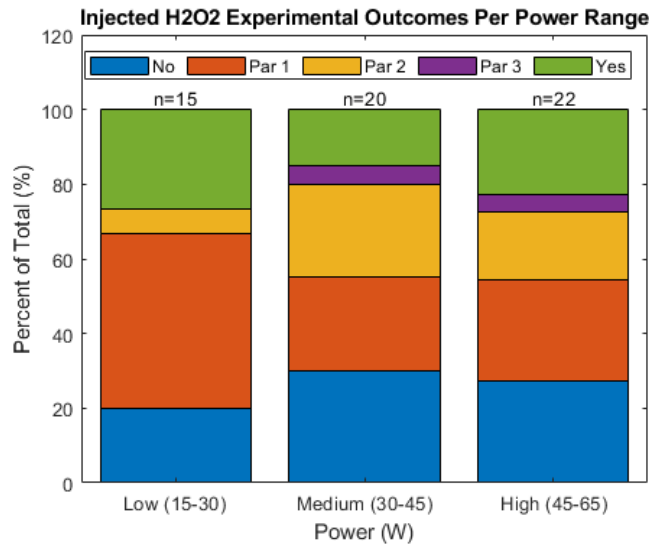


**Figure 5-16:** Power Range Outcome Classification

Whenever the wire was changed, the current was not changed that much, as it was known that with this set temperature, decomposition could be obtained. Apart from some exploratory tests, the changes in power come thus mostly from using the different wire itself, since, with that, more input power could be lost. Concentration was thus the other parameter that was changed to see if it had any significant effect on achieving decomposition. However, because decomposition could often not even be achieved with higher concentrations, not

many attempts were done on trying different ones. This can be seen in Figure 5-17, where again no direct relation comes forth from the outcomes, apart from the fact that the lower concentration tests have no decomposition cases.

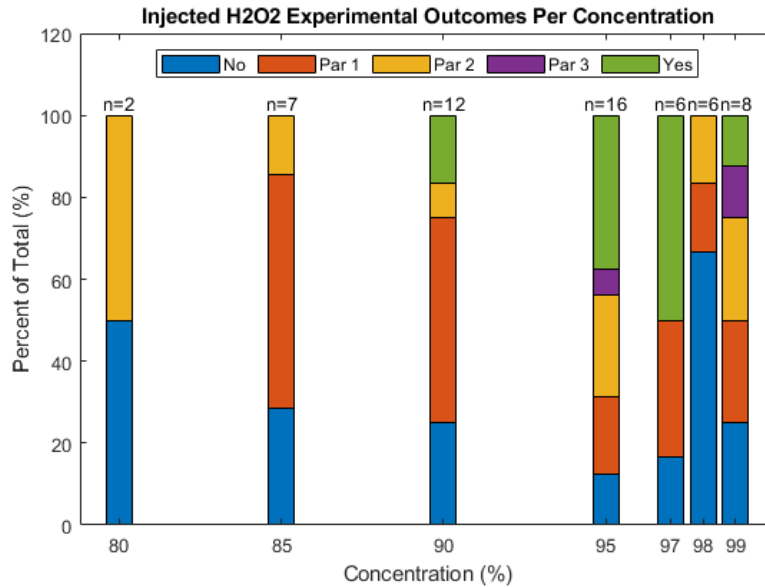


**Figure 5-17:** Concentration Outcome Classification

Apart from the classification based on the outcome, the results from actual temperature data should give a more distinct answer on what relations are present. To do so, all cases in which a decomposition peak was acquired, either due to steady-state or partial, are plotted against their corresponding input parameters in Figure 5-18 and Figure 5-19. The temperature readings from the thermocouple placed at  $50\text{mm}$  are used for this, as they were present during all tests and located somewhat further away from the heating wire. The straight horizontal lines indicate the maximum mean ambient temperature as measured just before injection for each corresponding wire type group. Unfortunately, results for both power and concentration are very much spread out. Whenever a fitting is executed however, a minor first-order polynomial trend is found, indicating an increase in temperature with both power as well as concentration. Coefficients for power are  $p_1 = 1.66$ ,  $p_2 = 349.8$  and that of concentration  $p_1 = 3.001$ ,  $p_2 = 138.9$ , which thus appears to have a greater influence on temperature than power in case of decomposition.

The mean temperature per wire type also tells something about the maximum one reached. It namely amplifies the differences in setup due to the resistance wire position and input power. For the 'various' case, where often almost direct contact with the thermocouple and a lot of power was used for input, this temperature is quite high. Similarly with the high location of the vertical and higher power of the double coiled, on the contrary to the small single horizontal coil cases. Then there are cases in which the maximum achieved temperature lies far below this set high mean temperature value, which indicates the fluctuations and instabilities that are present during the tests. This probably also slightly influences the maximum temperature reached in the case of decomposition, for example when the ambient air mixes in. The wire temperature itself however, does not necessarily influence the ability

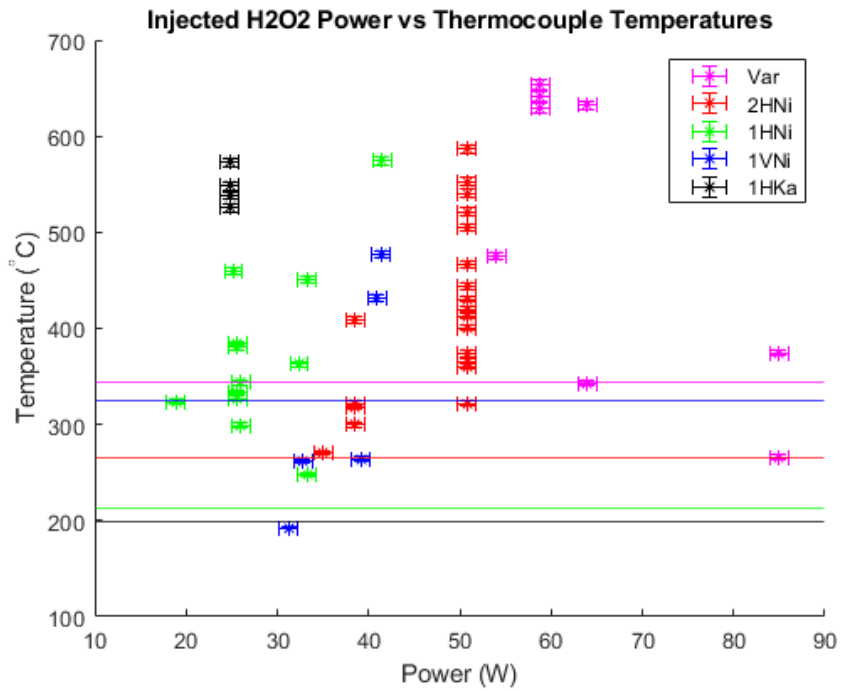


Figure 5-18: Power Range Decomposition Cases

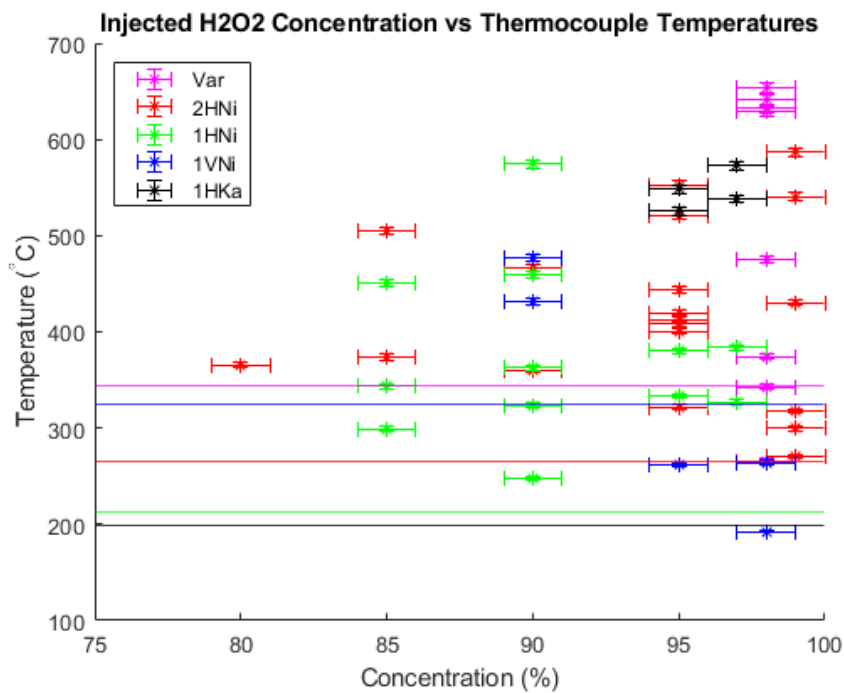


Figure 5-19: Concentration Decomposition Cases

to cause decomposition as was demonstrated already in the reference study [80]. As long as the initial temperature is high enough, the decomposition should simply take place.



To exclude most of the uncertainties related to input conditions, the maximum reached temperature of the constant decomposition tests of long duration only are plotted in Figure 5-20 and Figure 5-21.

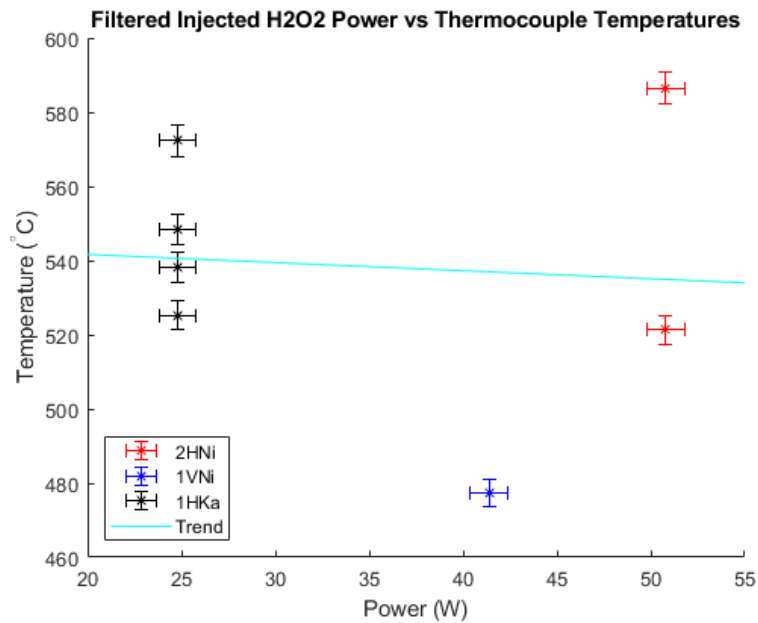


Figure 5-20: Power vs Temperature Filtered Decomposition Cases

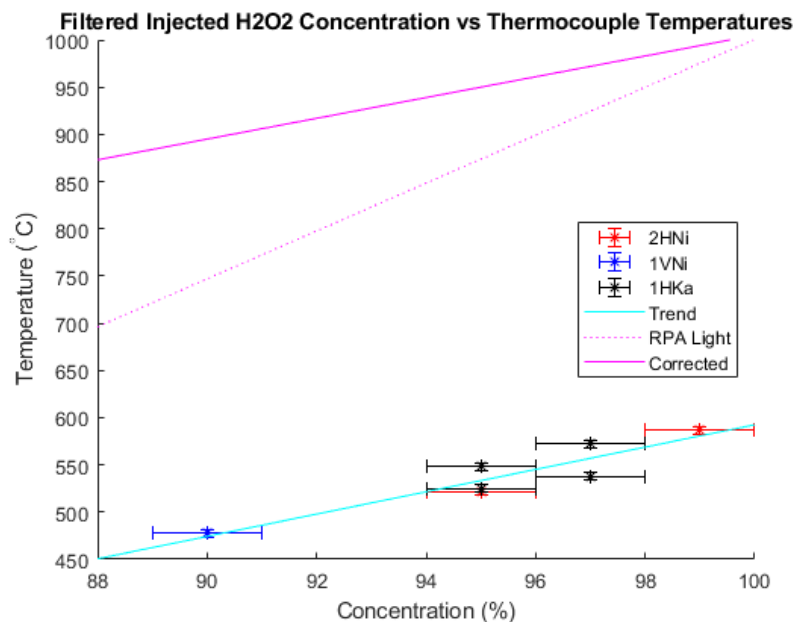


Figure 5-21: Concentration vs Temperature Filtered Decomposition Cases

As expected, input power shown in Figure 5-20 does not influence the maximum temperature reached. In the case  $H_2O_2$  fully decomposes it should namely go to its associated decomposi-

tion temperature anyway. When looking at the mean and maximum temperature difference per wire this occurrence can be proven. It shows a decreasing trend with increasing power, caused by the mean temperature rising whilst the maximum temperature stays approximately the same. Accordingly, the concentration for these decomposition cases is plotted as well in Figure 5-21. Here a more clear trend does show, corresponding roughly as before with how temperature should increase with increased concentration. Despite having a lower end temperature, the first coefficient of  $p_1 = 11.83$  seems to be an almost perfect fit with the analytical value from Section 3-5-2. Mainly the corrected value matches, where water evaporation was excluded, since it is expected to already be evaporated before decomposition or to not do so at all [55]. When looking at the temperature difference per wire again, but this time in relation with concentration, a similar increasing trend is visible. These analyses are however still slightly doubt full, because of the few useful data points. Also because of several shorter-duration experiments in which higher maximum decomposition temperatures were reached with lower concentrations.

## 5-4 Plasma Arc Decomposition

After the heating wire campaign, an arc generator was installed in both the drop decomposition as the injected flow setup to attempt decomposition with an arc igniter. The method of decomposition remains thermal still, but the physics involved differ since it now relies an electrical discharge similarly to an arcjet.

### 5-4-1 Electrical Discharge

Commonly used for ignition purposes is the electrical discharge, which will thus also be implement as igniter in these tests. This can be done similarly as with the heating wire, albeit that the  $\text{H}_2\text{O}_2$  not impacts the component itself, but merely the arc it creates. To get an arc to settle between two electrodes, proper isolation of the rest of the setup is crucial, making it only possible for the current to flow through the inserted medium. Besides this there are several more conditions to make the settling of the arc happen. The first being the breakdown voltage  $U_b$ , which is the voltage drop required for the electrons to jump over from one electrode to the other. The second is the pressure  $p$ , which can not be too high, since too much energy would then be required for ionization and neither too low as there would then be no medium to transfer the current. Lastly, there is the distance between electrodes  $d$ , which cannot be too large for the same reason as with high pressure, or too small would simply create a short circuit. The exact relation between these parameters is shown in Eq. (5-2) and described for various gasses by the Paschen curve.

$$V_b = \frac{B_{ex} \cdot p \cdot d}{\ln(A_{sat} \cdot p \cdot d) - \ln\left[\ln\left(1 + \frac{1}{\gamma_{se}}\right)\right]} \quad \& \quad p \cdot d = \frac{e \cdot \ln\left(1 + \frac{1}{\gamma_{se}}\right)}{A_{sat}} \quad (5-2)$$

In Eq. (5-2), coefficients  $A_{sat}$  and  $B_{ex}$  are the experimentally determined saturation ionization and excitation energy constants. These two in turn depend on the permittivity, atomic radius, heavy particle temperature, electron charge, ionization energy and the Boltzmann constant

$k_b$ . The second Townsend coefficient  $\gamma_{se}$  is also in the equation, which is dependent on the electrode material & shape as a work function of the surface and the kinetic energy, meaning the ions hitting the surface.

### High Voltage Generator

Ideally, the arc igniter requires as little power as possible, which is obtained with low pressure and gap distance. This is however not possible in the decomposition setup that was used in this study which operates at ambient pressure. Under these conditions, the electric field strength in this gap was somewhat more than  $3MV/m$  for air. Therefore, a very high voltage generator was required to create the arc between the air  $H_2O_2$  mixture. These full functional devices that are used for example in tasers and welding machines can be bought online and then include all necessary components, as shown in Figure 5-22.

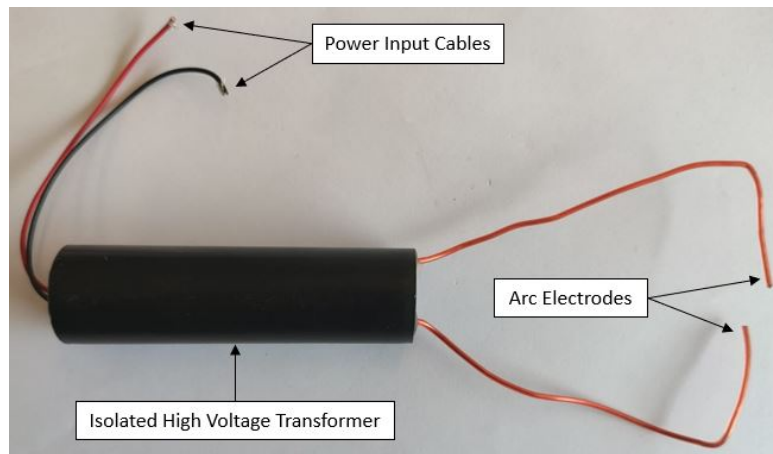


Figure 5-22: Commercial Arc Generator

This generator transforms  $3V$  to  $6V$  and  $1A$  to  $4A$  direct current input signal to a maximum of  $1MV$  and estimated maximum  $8mA$  output current. After the discharge has happened however, the voltage required to keep the arc stable will be smaller. Whenever the breakdown has occurred and no plasma is obtained, the voltage needs to build up again to discharge again. The frequency at which this happens with the high voltage generator used was not found in its specifications, since it depends on the situation and the parameters explained by Eq. (5-2). From all the obtained data during experiments however, the discharge frequency was measured to be approximately  $20Hz$  at high voltage and low distance and  $10Hz$  the other way around. Furthermore, the arc temperature itself can range from  $2000K$  to  $20000K$ , but is probably quite low in this case due to the low input power used. Regardless, upon discharge and contact with the  $H_2O_2$  the temperature should be sufficient to start decomposition. All its specifications are summarized in Table 5-6

#### 5-4-2 Arc Drop Test

The experiments in which an arc is used as an igniter, are executed in a later stage. Hence the setup is slightly different, as some of the solutions from Section 5-2-2 were taken into consideration already.

**Table 5-6:** Commercial Arc Generator Specifications

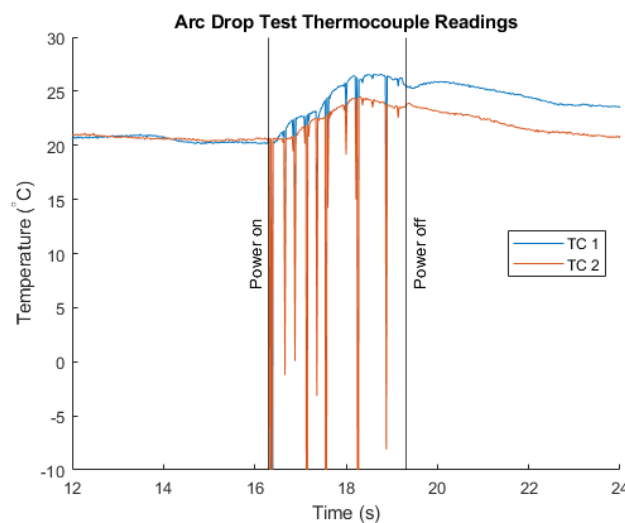
| Current Range [A] |                     | Voltage Range [V] |               | Frequency [Hz] | Temperature [K] |
|-------------------|---------------------|-------------------|---------------|----------------|-----------------|
| Input             | Output              | Input             | Output        | Discharge      | Arc             |
| 1 – 4             | $3e^{-6} - 8e^{-3}$ | 3 – 6             | $3e^2 - 1e^6$ | 10 – 20        | 2000 – 20000    |

### Arc Experimental Setup

The setup was similar to that as shown in Figure 5-1, but included some adjustment related to improved electrical isolation. The plastic decomposition stand and glass insulation were currently already present, in which the heating wire holes now served as entrance for the two electrode ends. The installation of the arc setup ended up as less of a difficulty and turned out to be better repeatable, due to the rigidity of the electrodes. Also safety was key here, since the high voltages that were generated were quite dangerous. Hence, even more electrical isolation was applied in the form of plastics and glass underneath the setup. Also, the distance between the electrodes was kept in mind, with each other metal or conductive component at least double the distance away. Therefore the electrodes were placed in the middle of the glass, one thermocouple at the bottom and the other at the top. Each component was subsequently checked with a multimeter on conductance to see if any short circuits were present. The high voltage generator itself is located next to the DAQ in the back as well, which is connected to the power supply. A normal camera with high-speed function was thus used to record the process, since the Photron high-speed camera was not able to capture the arc on video.

### Discharge Drop Results

The first component tests in ambient air, already showed some major issues related to the measurement. The arc and transformer create such a strong electric field that the temperature and visual recordings are visibly interrupted, as shown in Figure 5-23 by the deep dips.

**Figure 5-23:** Thermocouple 1 Readings During Arc Discharge

Ambient air temperature during arc operation itself only increased a little bit inside the glass, after which it gradually dropped again. Continuous operation of the generator to heat its surroundings was however not possible, as it would cause the components inside the device itself to overheat. After a while, the temperature recording even stopped working at all and would not measure anymore when near the arc and generator. Hence the normal color camera remained which was still capable of filming the experiments, as shown in Figure 5-24.

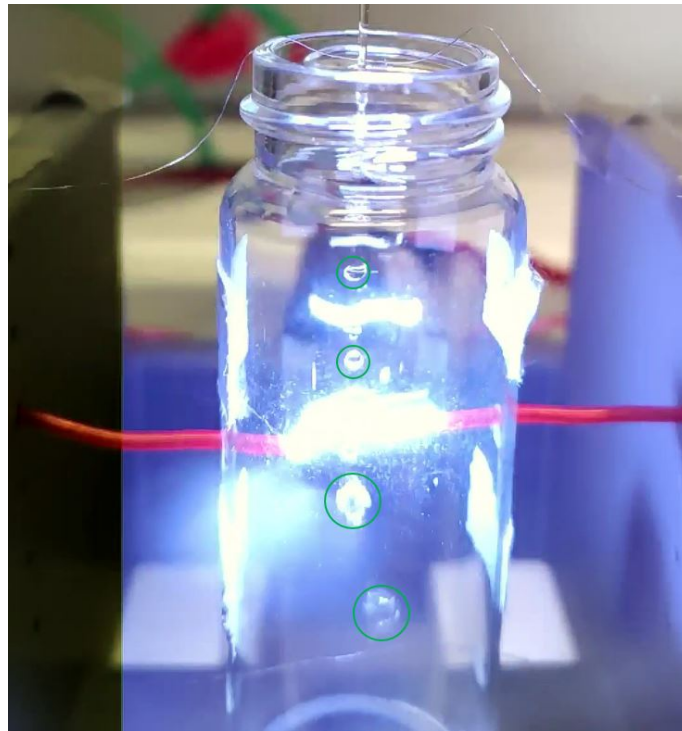


**Figure 5-24:** Camera Recording of 3V, 1.72A Arc Discharge 97% H<sub>2</sub>O<sub>2</sub> Drop Test

The H<sub>2</sub>O<sub>2</sub> droplets indicated in green were eventually injected almost as a constant stream. They were falling right between the two electrodes ends at fairly high velocity. This caused it to often miss the direct contact with the arc since its discharge frequency was so low. Even more so, it seemed to affect the settling of the arc negatively as it would discharge less frequently due to its interference between the electrodes. In the video recordings, arc impact on the droplet is however clearly visible due to smaller droplets deflecting from their path after the arc had settled. This was however far different in comparison with the droplets shooting away in the heating wire drop experiment in Figure 5-5b. Normally the sound produced by the decomposition of the H<sub>2</sub>O<sub>2</sub> gave the answer, but this was not possible with the arc, since the discharge produced a loud bang every time upon settling. Consequently, decomposition does not seem to be present as the H<sub>2</sub>O<sub>2</sub> simply continues to fall down. Presumably, this had the same cause as before, where not enough energy is present in the system to heat up the liquid in the short arc discharge contact time.

### 5-4-3 Injection Arc Experiments

The installation of the nebuliser disc for small droplet injection could solve the problem of heat transfer here as well. Initially the same setup as discussed in Figure 5-4-2 was used with the addition of the nebuliser disc and insertion of the propellant in the bottom. The insulating glass however appeared to be the problem in this setup, since the liquid film which was formed on it, acted as a shorter path for the current from each electrode end. During injection the  $\text{H}_2\text{O}_2$  namely accumulated on its surface and on the contrary to the hot glass when operating with a resistance wire, did not evaporate in this case. This even caused the arc generator to break down completely and it was decided to remove the glass during new attempts. Again, a thermocouple was installed at  $30\text{mm}$  above the electrode, and  $60\text{mm}$  above the injector.

Without the glass, the arc was still interrupted more than usual whenever the  $\text{H}_2\text{O}_2$  mist was injected, similarly to the drop test study. Since the arc settled at such a low frequency, the injected  $\text{H}_2\text{O}_2$  could simply continue upwards without decomposing. This is visible in Figure 5-25 by the build-up of liquid on the thermocouple. Nevertheless, the mist is clearly affected by the arc, since a big cloud forms differently from before, whenever the current flows through, as shown in Figure 5-25.

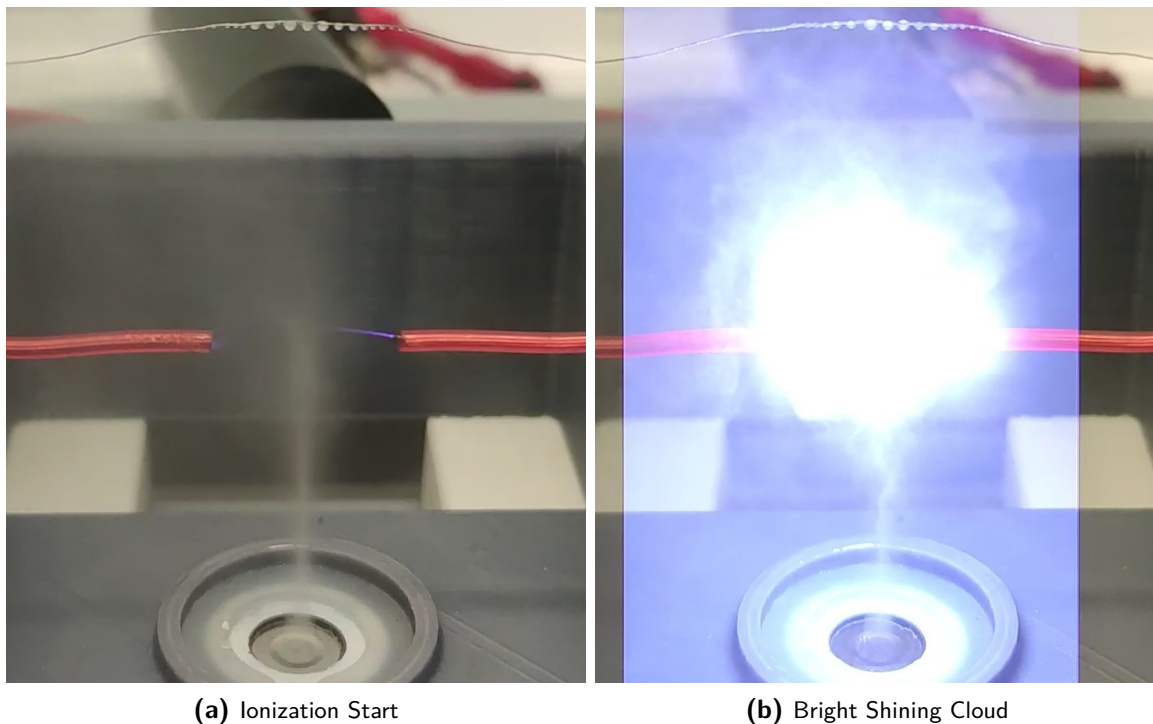


**Figure 5-25:**  $6\text{V}$ ,  $2.91\text{A}$ , Arc Discharge During  $97\%$   $\text{H}_2\text{O}_2$  Flow Injection

Unfortunately, during these experiments the DAQ would always stop recording completely and thus not register anything which can verify if this is decomposition. Even in the case in which metal shielding is placed around the DAQ to protect it from the electrical field. The formation of the bright shining cloud could be either due to the reflection of the droplets instead of due to the decomposition expansion. The few arc decomposition tests performed

only resulted in failed and non-decomposing experiments. Further analysis is thus needed as is explained in Section 5-5, leading up to several general recommendations.

The addition of nitrogen or electrodes placed such that the arc goes along with the injected propellant as done in some other studies could have helped the decomposition [111] [114]. With the currently used setup this was unfortunately not possible, which is why using only nitrogen gas at similar mass flow rates was attempted instead. This proved unsuccessful, since the arc would not even settle at this high volumetric flow rate, whilst using low volumetric flow rate caused the discharge to happen as it does normally in air.

## 5-5 Discussion & Recommendations

Most points were mentioned already during the explanation of the results. Still, there are some remarks left unsaid, mainly related to the way the setup is creating uncertainty in results.

Although the nebulizer disc steadily injected at a low and constant mass flow rate, it was still the cause of many problems. For example because of clogging of the flow and short-circuiting of its internal circuitry. Upon its destruction, the setup had to be rebuilt which inevitably caused changes. These minor differences for example with exact thermocouple bead orientation or heating wire density, have most likely contributed to the differences in temperature between two subsequent equal tests. The same holds for the often accompanied replacement of the lab glass used, due to shattering after an explosion or simply clumsy handling. Besides this the droplets would accumulate on the surface and slide down after injection, adding to the problem of the clogging injector. A more realistic test environment should resolve the above issues, as discussed later in Section 6-2-1.

Despite having little visuals of the decomposition, confirmation of it happening is definitely there. Not only because of the sudden increase in temperature but also because of tiny droplets flying away in unusual directions after impact on the heating wire. Still, some other methods could be attempted to capture with more accuracy what is exactly happening upon decomposition. The first would be via the pressure released, for example by adding pressure sensors inside the glass. Or alternatively use Schlieren imaging, as now already shock waves appeared to be visible in the high-speed recordings in the contours of the injected mist. With this photography style, the pressure waves coming from decomposition can most likely be captured even better. Or the complete setup has to be overhauled, in making it more about the power required and released upon decomposition. This is possible in a bomb calorimeter, in which the energy coming from a known quantity of propellant is measured in an isolated system as is done before with catalysts [17]. In it, all reaction products can be captured and subsequently measured with Gas Chromatography (GC), as is suggested with the fuel cell already in Section 4-5. Volume, mass, product ratio and concentration can subsequently be used again to calculate the efficiency of decomposition.

### 5-5-1 Heating Wire Improvements

Heat loss is still one of the major problems with the heating wire as igniter since it uses power even when  $\text{H}_2\text{O}_2$  is not yet being injected. Duration of operation was not even taken

into account with power consumption but does of course influence its capability to initiate decomposition, as it preheats the surroundings. The offset in the maximum decomposition temperature reached, as visible in Figure 5-21, is probably caused by the same heat loss. The air is namely capable of exiting the glass tube slightly through its sides, before encountering the thermocouple upon decomposition. The other reason could be the amount of  $\text{H}_2\text{O}_2$  which decomposes, which is first; not all of what is being injected, and secondly; too little to heat up the surrounding air as well. The similarities for concentration test temperature with the corrected results, are attributed to the lack of water taking in energy to evaporate. As the  $\text{H}_2\text{O}_2$  would namely decompose, liquid droplets are clearly shooting away in multiple directions. This is expected to consist of water as it is also the larger mass fraction in the reaction product. It is thus a good idea to try and capture the remaining liquids for subsequent analysis in a follow-up study, to determine their composition. The fact that the reaction product is partly liquid, does however substantiate the modelled values of Figure 3-7, in which the required input power to achieve decomposition is lower.

The same heat created by the wire, was also the cause of some problems, as the nebulizer disc would heat up too much due to its temperature. This made it stop injecting, or prematurely boil the  $\text{H}_2\text{O}_2$ , up to a point at which the  $\text{H}_2\text{O}_2$  underneath it started decomposing before injection. Injection could also be stopped due to droplets falling back onto the disc after accumulating on the wire. The resistance wire was thus obviously obstructing the flow, which can become a problem, as the liquids inside the chamber build up. Despite giving worse results regarding decomposition, vertical alignment might serve as one of the solutions as discussed later in Section 6-2-1.

Lastly, corrosion of resistance wire causes a black surface to appear after the first tests. This corrosion drives up the voltage required for heating but does stiffen the wire which is good for obtaining repetitive tests. Also, the maximum temperature reached after first use is measured to decrease at the same power input level. Good electrical and thermal insulation of these wires is thus a must to ensure durability by minimizing corrosion. The wire would become less ductile and hence less prone to position changes, again improving to obtain repetitive tests. This will also prevent the wires from short-circuiting, which opens up many possibilities to create a different type of mesh, more suitable to match the used injection.

### 5-5-2 Arc Improvements

Concerning arc decomposition, the main setup problem is obvious, as there are no measurements for the flow injected tests. The cause for this is the generated electric and magnetic field, of which the strength is described by the Biot-Savart law shown in equation 5-3 [87]. It shows that the field strength decreases proportionally with the distance squared, similarly to the inverse square law.

$$E = \frac{q}{4 \cdot \pi \cdot \epsilon_0} \cdot \frac{\hat{r}'}{|r'|^2} \quad \& \quad B = \frac{\mu_0 \cdot q}{4 \cdot \pi} \cdot v \times \frac{\hat{r}'}{|r'|^2} \quad (5-3)$$

In this equation  $E$  is the electric and  $B$  the magnetic field strength,  $q$  is the charged particle and  $v$  is its velocity. This gives an approximation of the actual field at location  $r$ , which basically means the DAQ should be located further away from the settling arc to avoid



interference of the induced fields. The same holds for the thermocouples, which is difficult since they should be located near the decomposing  $\text{H}_2\text{O}_2$  for correct measurements. Electrical isolation and shielding of the thermocouples could be one of the solutions but certainly affects its measurements accuracy and response time.

The cause for the droplets and presumably injected mist, not decomposing is expected to be due to a lack of energy transfer. The actual current going through the arc is too little to form a plasma which decomposes the  $\text{H}_2\text{O}_2$ . This will also partially come due to the low frequency at which the arc discharge was happening with the currently used high voltage transformer. One could better use a device more suitable for continuous operation at high input power. A plasma arc welding machine could for example be converted to operate with  $\text{H}_2\text{O}_2$  as well. Also, mixing in of a carrier gas might be required to form a plasma beforehand after which the  $\text{H}_2\text{O}_2$  can be injected, as is done in one of the reference studies discussed [9]. This environment consisting for example of nitrogen, will also prevent the electrodes from oxidising and corroding more.

Arc decomposition should be continued to be investigated, as it is expected to be beneficial in multiple areas in comparison with the heating wires. Mainly the combustion chamber volume required can be reduced, there is less disturbance of the injected  $\text{H}_2\text{O}_2$ , heat loss will be less of a problem and lastly, if correct components are used, the system should be more durable.

**Table 5-7:** Decomposition System Recommendations Overview

| <b>Recommendation</b>              | <b>Improves</b>                        |
|------------------------------------|--|
| Injector & Setup Instrumentation   | Repeatability & Measurement Accuracy   |
| Setup Insulation & Test Conditions | Decomposition Temperature & Efficiency |
| Heating Wire & Arc Generator       | Input Power & Decomposition Stability  |

## 5-6 Conclusion

To thermally decompose the injected  $\text{H}_2\text{O}_2$  using various igniters, a universal and inclusive test setup had to be constructed. Measurement instrumentation to do so is looked into first, resulting in thermocouples and visual imaging to acquire the data. Subsequently, this had to be integrated into an experimental setup that is capable of safely decomposing, yet precise enough to measure the injected  $\text{H}_2\text{O}_2$ 's reaction. A drop test study was thus performed to get a better understanding of the decomposition process and the challenges to obtaining this. A larger residence time and more energy transfer with less heat loss were found to be crucial besides the input pressure, temperature and concentration. These parameters were tweaked in the subsequent flow test study, by changing wire characteristics and injecting  $\text{H}_2\text{O}_2$  mist in a more confined area. Accurate impingement of the  $\text{H}_2\text{O}_2$  on the heating wire turned out to be of a big influence and difficult to repeat, due to the low durability of some of the experimental setup components. However, decomposition peaks of over  $650^\circ\text{C}$  with various  $\text{H}_2\text{O}_2$  concentrations were measured and a minimum of  $4\text{A}$ ,  $6.2\text{V}$  and thus  $24.8\text{W}$  input power was needed to achieve steady-state decomposition with a horizontal  $0.5\text{mm}$  Kanthal coil. Power was found to only influence whether or not decomposition can be reached at all in the current setup. A linear relation similar to the analytical one was however found between concentration and decomposition temperature. The little data points, where heat

loss and some contradicting values are present however make it hard to confirm this with full conviction. Finally, arc decomposition was attempted as well, which proved unsuccessful due to the negative effects it has on components of the experimental setup. Changes to the robustness and accuracy of the setup are thus most urgent and recommended as future improvements for both decomposition methods. Concluding, it can be said that thermal decomposition is definitely possible at relatively low power input levels, provided that the HTP is properly injected.

# Combined Satellite System

Now the pros and cons of the fuel cell from Chapter 4 and thermal decomposition system in Chapter 5 were experienced in person, a better decision could be made on how to combine the two. Such a combined system will not actually be developed, but merely suggestions are made on how their cooperation can take place most effectively based on the results of the individual tests. Regardless of the power and propulsion system not being fully optimized yet, a quick look is taken at what is needed and how they can be incorporated into a CubeSat. This chapter thus shows first what needs to be taken into account when combining the systems and subsequently what the possibilities of satellite incorporation are, based on several practical considerations.

## 6-1 Cooperative System

The only relation the two currently have is that the one provides power for the other by partially using the same propellant. Since structurally combining the two systems into one does not really seem to be possible, it is more a matter of making them work together as much as possible. To do so, certain crucial aspects such as power in- and output, propellant and usage have to be adjusted to fit one another.

### 6-1-1 Performance Evaluation

Since both experiments were performed at a smaller scale, the results have to be extrapolated to check if they can meet the requirements as set in Table 3-1.

#### Propulsion System

The mass flow rate of the injected Hydrogen Peroxide ( $H_2O_2$ ) in the experiments of this research was only  $0.036g/s$ , which is far from enough to meet the desired  $1N$  of thrust. In the reference study case 36 times as much is namely used;  $1.3g/s$  at  $5bar$  which resulted in just under  $0.9N$  [80]. Hence the power required for decomposition in the atmospheric condition of this project would become  $893W$ , which is still way too much for a satellite.

This is however far below the expected  $2500W$  mentioned in Section 3-5-2, presumably due to partially preheating the chamber before injection of the High-Test Peroxide (HTP). It does however match quite well already with the power required when the water reaction product in Figure 3-7 is in a liquid state. Under high pressure however, the power required for decomposition is expected to go down drastically as shown before in Figure 3-8. This shows already in the studies on more optimized thrusters still operating with a catalytic bed at mass flow rates more than half of  $1.3g/s$  [101]. Simultaneously, the heating wire currently used in the experiments was far from optimized, since the effective area on which the  $H_2O_2$  impinged was smaller. Voltage and thus power could go down whenever these useless areas, which were needed for clamping the power supply cables, are removed. Similarly when the heat loss to the surroundings is minimized less power would be needed. Regardless of these aspects, an obvious mismatch remains between the maximum Orbit Average Power (OAP) and the peak power required when the thruster is in operation.

A similar decrease in Decomposition Delay Time (DDT) would occur when operating in a more realistic environment, which can even halve the time at  $10bar$  [21]. Reaction kinetics are important and have to be very fast to reduce the length of the decomposition chamber. Similar  $H_2O_2$  thrusters using catalyst beds achieve  $1N$  at  $20bar$  with a flow rate of  $0.59m/s$  whilst only having a length of  $17.5mm$  [101]. In this project, a far larger distance was needed to decompose the  $H_2O_2$  as this was not the focus. If it would have been possible to place the injector closer to the heating wire, however, the distance required to impose decomposition would also be minimal. Since only one horizontal heating wire coil ended up being sufficient, a distance of  $5mm$  should already work, which was its inner winding diameter.

## Power System

The power produced in the fuel cell during this project was quite low in comparison with the theoretical one shown in Figure 3-6. To reach the maximum of  $60W$  required,  $9375$  of the developed cells are needed to obtain the necessary Membrane Electrode Assembly (MEA) surface area of approximately  $37500cm^2$ . Let alone the increase in surface area to reach the peak power upon operation of the thruster. The produced power can however be drastically improved when the electrochemical reaction at the electrode surface is optimized. Besides this, the area of the MEA can be made larger whilst the size of the cell structure can be minimized, by making thin stacks. If one would implement cells of  $100cm^2$  and  $1cm$  thickness with the maximum  $20mW/cm^2$  power density from the reference study, only 30 cells are needed [129]. The mass flow rate used for this case is  $10mL/min$ , or  $0.2417g/s$  for both anolyte and catholyte. Hence, only three cells would be needed to reach the same mass flow rate as used in the propulsion system. If only  $1mL/min$  would be used, the combination of 30 cells makes it match the propulsion system mass flow rate of  $1.3g/s$  in total. This decreased flow rate will simultaneously prevent the system from eroding too much over time due to the washing away of the catalyst. This way the  $H_2O_2$  output of the cell could directly serve as input for the propulsion system.

Another important factor is of course the maximum electrochemical energy that can be taken in from the  $H_2O_2$  until it is depleted. This is defined already for 100% efficiency by the decomposition energy released in Eq. (2-1). Translated to power this means that  $1kg$  of the liquid is capable to keep operating at  $60W$  for 7.3 hours at most. This is far from the

operational life cycle of a CubeSat, hence more conventional methods of power generation will have to be used still. The fuel cell would only serve as a backup similar to a battery, to supplement the existing power system.

### 6-1-2 Propellant Combination

Although both system processes are based on using the energy of  $\text{H}_2\text{O}_2$  decomposition, the propellant from which they do this has a different composition. The most beneficial would be to take the  $\text{H}_2\text{O}_2$  with the highest possible concentration since it contains the most energy for usage in thermal decomposition. This would then however have to be diluted and mixed with KOH and  $\text{H}_2\text{SO}_4$  separately to operate in the fuel cell as well. Instead, operation without the acid and base could be done, with high concentration  $\text{H}_2\text{O}_2$  only at the cathode and low concentration at the anode. By doing so reaction products would remain to be only water and oxygen, the propellants are safer and also fewer complications can arise. This comes at the price of performance going down drastically as demonstrated in Figure 4-27, were the cell reached only  $0.017\text{mW}/\text{cm}^2$  at max.

#### Reaction Products

As seen before, the fuel cell reaction will cause potassium sulfate salt ( $\text{K}_2\text{SO}_4$ ) to form in the catholyte solution. The same happens when the anolyte and catholyte are mixed in together according to the exothermic neutralization reaction in Eq. (6-1).



Whenever the two electrolytes would contain a high concentration  $\text{H}_2\text{O}_2$  they could be used in the thruster where this reaction should take place as well. This might give a kick start to the thermal decomposition due to the exothermic nature, but after decomposition make it reach a lower decomposition temperature as more salt and less  $\text{H}_2\text{O}_2$  is present. The salt has a melting temperature of  $1069^\circ\text{C}$  and thus remains after propellant decomposition. This might accumulate in the injector and decomposition chamber and affect the flow, as it did similarly already at the external surface of the cell structure. When the KOH and  $\text{H}_2\text{SO}_4$  are not able to fully react in the decomposition chamber, about the same will happen since the  $\text{H}_2\text{O}_2$  will evaporate and the acid and base will not. In this case, the remaining  $\text{H}_2\text{SO}_4$  would gradually decompose endothermically to  $\text{SO}_3$  and water. It does this from  $300^\circ\text{C}$  onward and will thus take in heat which was intended to start  $\text{H}_2\text{O}_2$  decomposition. Mainly the sulfate present as a reaction product is undesirable, as it contributes to acid rain and global dimming [35]. With the amounts used in the CubeSat however, this is not something to be very afraid of, since this process also happens naturally.

Ways to remove the salts and split them into acid and base are not that simple but might be needed to recycle them for use in the fuel cell. Distillation is not possible for example as it will cause the  $\text{H}_2\text{O}_2$  to decompose. Reverse osmosis and electrodialysis could be used to filter out pure  $\text{H}_2\text{O}_2$ , but require a whole system of their own. Similarly to the fuel cell, they both utilize a membrane and additional power is needed with electrodialysis. Besides this, they are often not capable of fully separating into a concentrate and water. Thus, the question remains;

what to do with the captured salts afterwards, since they cannot be distilled. Therefore, more experimental research should be done on both the reaction products of the compounds present in the  $\text{H}_2\text{O}_2$  as well as methods to effectively separate them for later reuse.

### 6-1-3 Effectiveness Increase

Similarly to propellant recirculation, some other methods are there to make the system more combined whilst simultaneously increase the efficiency of energy usage of the  $\text{H}_2\text{O}_2$ .

#### Heat Loss Minimizing

Experienced mainly in the decomposition experiments in Chapter 5, heat loss is a crucial aspect to work on. There are some standard methods to minimize the loss, such as regenerative cooling, in which the liquid flows along the outside of the decomposition chamber. This will simultaneously cool the metal on the outside, as well as pre-heat the  $\text{H}_2\text{O}_2$  propellant such that more power can be obtained from it in the fuel cell and less is needed to initiate decomposition. Less dispersion of the heat can of course already be achieved with thicker walls, but then nothing is done really with the heat contained in the metal chamber. As instead, installing a Thermoelectric Generator (TEG) to generate power from the temperature difference would be an ideal method to boost the efficiency, also in the fuel cell system [63] [74] [31]. Whether or not the mass added by all the suggested structures weighs up to the power gain should be further investigated.

#### Other Applications

By combining the fuel cell and thruster,  $\text{H}_2\text{O}_2$  would serve as a universal energy carrier. To make the process circular after filtering out the salts, electrolysis would have to be added to the infrastructure. This way the captured reaction products of water and oxygen can be transformed back into for example to produce the  $\text{H}_2\text{O}_2$  [38]. This would be needed in case the amount of oxygen and water in the  $\text{H}_2\text{O}_2$  fuel cell outlet is too high. Together with the neutralization reaction of the acid and base the increased amount of water could cause the desired decomposition conditions in the thruster can not be achieved anymore. Either this performance decrease in both systems due to high water content is accepted or the  $\text{H}_2\text{O}_2$  is thus regenerated. Ideally, more systems would be added to this infrastructure that are deemed useful as space applications. This would be more the case in larger satellites however, in which the resulting oxygen and water could be used for life support [68].

## 6-2 Spacecraft Incorporation

Physical implementation of the system structures in a CubeSat should be fairly simple. Fuel cells and thrusters are systems that are added to satellites more often but have not yet been properly downscaled to operate in nano-satellites. Still, the working principles stay the same, hence a lot of the incorporation should go similarly. The infrastructure of such a satellite is shown in Figure 6-1 and displays roughly how all components are connected.

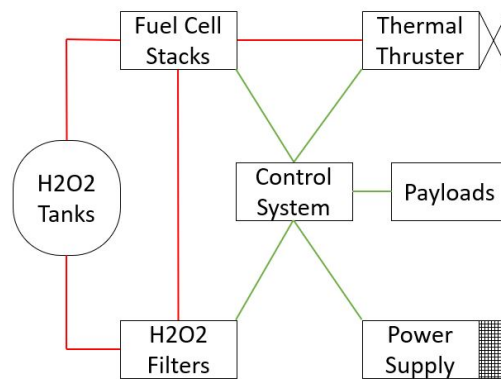


**Figure 6-1:** Combined Satellite System Infrastructure

The red line indicates propellant flow and the green one power. The  $\text{H}_2\text{O}_2$  flows through the fuel cell stack in the case extra power is required and goes either to the thruster directly after, or is recirculated back to the tank after going through a filter. Another power supply such as solar panels and ultracapacitors is present in the satellite as well. The control system is the one to determine if both power supplies need to be working simultaneously or only one to charge the other.

### 6-2-1 Thruster System

Regardless of the exact propellant composition, the thruster is build up of the distributor, injector, chamber and nozzle. There is not much to say about the nozzle yet, which should be dimensioned to work optimally under the conditions resulting from the decomposition. First the injector and decomposition system should be optimized as these gave enough problems in the experiments already. Comparable thruster system mass is around  $0.38\text{kg}$  with lengths of  $178\text{mm}$ , which is expected to be exceeded mainly in mass, since the heating wire has a slightly larger density and is less far developed [28].

#### Inlet & Injection

The feed of  $\text{H}_2\text{O}_2$  propellant can thus come directly from the outlet of the fuel cell stack elements via a capillary tube. Between the injector and feed, a thermal barrier and stand-off distance should be present, because otherwise the heat released in the decomposition process can cause the  $\text{H}_2\text{O}_2$  in the inlet to decompose prematurely. The outlet of the fuel cell will reach the injector either as two or one flow in case the anolyte and catholyte are mixed beforehand.

In order to have good atomization and distribution of the propellant it might be wise to use a shower head injector with many orifices or full cone injector. These are deemed best suitable for the application of monopropellant type thrusters, since they better cover the full decomposition chamber area. This more uniform spreading of the  $\text{H}_2\text{O}_2$  will increase the efficiency of the system by having more and faster decomposition [82]. The idea is to place a small heating coil directly aligned with each shower head orifice to maximize the contact area

and heat distribution inside the decomposition chamber. Having more smaller sized orifices will namely bring down the Sauter Mean Diameter (SMD) of the injected droplets which then have more surface area that can be heated [15]. Additionally the injection velocity  $v_{inj}$  and pressure drop  $\Delta p$  inside the chamber, should stay about the same when the number of orifices increase and their area decreases [34]. The pressure drop should stay relatively low with this configuration and is expected to be around  $3bar$ , similarly to catalyst bed studies [101].

## Decomposition Chamber

The high velocity at which the reaction products travel in the decomposition chamber require fast reaction kinetics for the  $H_2O_2$  or long decomposition systems. The faster the  $H_2O_2$  reacts and decomposes, the shorter the chamber length thus has to be to achieve the same outlet conditions. According to a previous drop test study, thermal decomposition has a shorter DDT, but a lower end temperature compared to catalytic decomposition [55]. This makes it possible for the chamber to be relatively short after having been in contact with the igniter. A cylindrical shaped chamber with a diameter of at least three times the nozzle throat area, could be helpful to achieve decomposition as much as possible [137]. This wide, but at the same time short design makes incorporation of the shower head injector with aligned heating coils more feasible and creates an interior which looks almost like a catalyst bed with many flow channels. The replacement of the heating wire on the location of the catalyst bed would thus be beneficial since the decomposition system does not degrade as much over time and should require less chamber length to achieve similar performance. Additional changes to the chamber would mainly be applied to its exterior, for example by having a double layered outer wall for insulation, electrical wiring, regenerative cooling or placement of a TEG.

### 6-2-2 Fuel Cell System

Besides the short operation time before depletion of the propellant, the system mass of the fuel cell is expected to exceed the set requirement. With the required surface area of the currently developed cell, the MEA will already weigh approximately  $5kg$ , but can be optimized to a feasible  $0.5kg$  with the optimized performance. This would also take down the mass of the cell structure as this requires less feed lines, end plates, connectors and predominantly; bipolar plates, which take up more than 80%, bringing the total mass to  $2.5kg$  [48]. Size wise, the structure is cubic and despite taking up a lot of space it should fit well in the  $10 \times 10 \times 10cm$  CubeSat units.

As mentioned before, the cell performance might not be sufficient to instantly power the thruster igniter, whilst an ultracapacitor might be better capable of doing so [110]. In a comparable study, ultracapacitors are advised as solution to store the energy whenever the fuel cell or solar arrays are running and discharge power all together during peak moments of operation [58]. A more extensive trade-off should be performed on what second power source to use in the satellite to be able to tell if it is beneficial, since it would also add mass to the CubeSat.



### Propellant Supply

Similarly to the thruster system, a supply of the propellant is needed in the fuel cell stack, strong enough to overcome the pressure drop that is formed due to all its layers. This was not tested during the experiments, but can be approximated with the Hagen-Poiseuille relation as shown in Eq. (6-2) [95].

$$\Delta p = \frac{8\pi\mu LQ}{A^2} \quad \rightarrow \quad P_p = Q\Delta p \quad (6-2)$$

The serpentine flow field of the bipolar plate can thus play a large role on the pressure difference depending on the length  $L$  and cross sectional surface area  $A$  of the channels. Since the dynamic viscosity  $\mu$  and volumetric flow rate  $Q$  are set, the flow field has to be designed accordingly such that the installed pump can overcome this difference. The type and amount of pumps needed are to be investigated further, since at least two are currently needed for each electrolyte and perhaps additional ones to build up the pressure again at the cell outlet and thruster system inlet. This is an aspect of concern, since the hydraulic pump power  $P_h$  will go up as well in relation to pressure, as shown in Eq. (6-2), where also efficiency should be taken in to account still. This was experienced in the experiments already since the power required to drive the pumps was far greater than what was generated in the cell. This, together with other auxiliary systems brings down the system efficiency drastically when looking at Eq. (2-10). Besides this, centrifugal pumps able to resist all the used chemicals are hard to find and peristaltic pumps tend to wear rapidly. However, using a pressurized blow down system which does not need power to transfer the propellant is not possible when the fuel cell electrolyte needs to be recirculated.

## 6-3 Conclusion

Besides transfer of power from the fuel cell to the igniter, the only resemblance between the two systems so far was the use of  $\text{H}_2\text{O}_2$ . Far more power was found to be needed to provide the energy required during operation of the thruster. Besides optimization of the individual systems, this power could come from cooperation and combining the two which increases the effectiveness. Mainly capturing heat loss and reusing the propellant are found as ways to do so. More experiments with the reaction products and the development of additional power generating systems are therefore needed. The infrastructure and structural design of all the components which could be added to the CubeSat is fairly straight forward, as it is mostly based on existing systems. Due to their sheer size and mass to performance relation however, downscaling and going under the  $10\text{kg}$  requirement set for the cell stack is difficult. The other parts such as casing, propellant tank, injector and nozzle should remain similar to those of the larger satellites, but the extra feed systems required can become quite challenging to find a suitable solution for.



---

# Chapter 7

---

## Summary

A recapitulation of the work done and its outcome is made first, by looking back into the research questions and objectives set up in Chapter 1. Then some suggestions are made on how to continue with the research and development based on some of the conclusions coming from this study.

### 7-1 Conclusions

One can say that by developing Proof of Concept (PoC)'s of both the power and propulsion system, the objectives as stated in Chapter 1 have been achieved. To be able to form a solid, single conclusion on the findings in this project however, the research question is revisited:

*How can Hydrogen Peroxide ( $H_2O_2$ ) be used in a satellite system to provide power as well as thrust most effectively and what would be the performance parameters?*

It was found that as of now,  $H_2O_2$  can be used most effectively in a satellite system with an active two compartment fuel cell and with heating wire induced thermal decomposition. The maximum power produced during the experiments of this research was  $4.5mW$ , whilst a minimum of  $24.5W$  was needed in the combustion chamber. However, many methods to optimise the performance still need to be implemented such that the combination and incorporation of the systems in a CubeSat becomes realistic.

With the literature overview on fuel cell and thruster functionalities, a better picture was attained of the options to use them with  $H_2O_2$ . The liquid was found to be very versatile, due to its properties as both an oxidiser and fuel, decomposing exothermically into water and oxygen. Therefore, some studies on thermal decomposition in a satellite and several on electrochemical decomposition in cell structures were gathered and summarized. More specific requirements of  $1N$  thrust and  $60W$  power for the use in a CubeSat were defined since this is the field of study where the systems could contribute the most. After comparing mostly their feasibility, a reference case was selected to narrow down the options and set a standard for the heating wire decomposition system and two compartment electrolyte structure developed during this research. Some groundwork was performed as well, by researching what materials

could be used with regard to the chemical and safety aspects, for which polymers tend to work best. Lastly, analytical models based on the Nernst equation showed that the current, voltage and thus power achieved can go up to almost  $200mW/cm^2$ . Whilst heat capacity based calculations indicated around  $2500W$  of power would be needed for thermal decomposition and reaching adiabatic flame temperatures.

Since a single compartment structure would not give enough power according to literature, a two compartment cell was developed. To do so, the Membrane Electrode Assembly (MEA) had to be produced first, which consisted of many intermediate treatment steps of each subcomponent to boost the final cell performance. A nickel foam anode, Nafion Polymer Exchange Membrane (PEM) and palladium electrodeposited on a Carbon Fiber Cloth (CFC) Micro Porous Layer (MPL) cathode was eventually chosen to work with. Scanning Electron Microscopy (SEM) and X-Ray Diffractometry (XRD) were used to validate if the process went correctly and a test setup with two Digital Multi Meter (DMM) and a resistance rack was used to do the subsequent experiments. A passive Poly Lactic Acid (PLA) cell prototype structure was used initially in which the MEA was clamped between gaskets and rubber, but leakage and fracturing were preventing the desired polarization curve to be obtained. The later used Acrylonitrile Butadiene Styrene (ABS) worked better, which resulted in a maximum power output of  $0.59mW/cm^2$  and constant degradation of performance over time for the passive cell. Hence an active cell was produced using syringes pumping at  $1mL/min$  to provide a larger power density of  $1.36mW/cm^2$  and moreover, better output stability. A higher flow rate using peristaltic pumps, wider MEA areas and stacking of cells, all proved to increase performance and applicability in a CubeSat.

To decompose the  $H_2O_2$  for subsequent use in a thruster, a heating wire was installed in a drop test chamber. In the safely designed setup, high-speed video recordings were used to get a better understanding of the thermal decomposition process. From these initial tests, it was concluded more efficient energy transfer to the droplets and less heat loss to surroundings were required since over  $100W$  of power was needed for decomposition. Hence an improved setup was developed in which smaller droplets were injected from below into a glass vessel with the heating wire and thermocouples inside. Various heating wire types and orientations were tested which caused full decomposition to be the case only occasionally, giving temperatures up to  $600^\circ C$  and over. Despite a clear increase in temperature readings, uncertainty in the amount of decomposition was still high and constant failure of the setup caused repeatable data to be hard to obtain. The minimum input power of  $4A$ ,  $6.2V$  and thus  $24.8W$  with direct impingement of the injected liquid on a horizontal  $0.5mm$  Kanthal coil was the best result. Input power did not show to have a relation with the temperature or decomposition cases reached, whilst  $H_2O_2$  concentration increase seemed to match linearly with the maximum temperature. The igniter itself thus turned out to be most influential as later attempted arc decomposition experiments proved unsuccessful due to its low energy transfer rate and the negative effects it has on components of the experimental setup.

Cooperation of the systems was currently only present in the sense that the power produced by the fuel cell is used by the thruster system. Combined utilization of the propellant flow and components would be the next step toward making a fully cooperative system for which another power supply and additional regenerating systems would have to be added to the infrastructure. By minimizing the heat loss and recirculating the propellant to make full use of the versatility of the  $H_2O_2$ , the unity and efficiency of the systems can be improved whilst simultaneously making the satellite self-sufficient. Incorporation of a fuel cell - thermal

thruster combination in a CubeSat is something which is deemed feasible only after optimizing the existing concepts, hence research on how to increase the performance of the individual systems has priority.

## 7-2 Recommendations

To continue this research on  $\text{H}_2\text{O}_2$  fuel cells and thrusters, four predominating improvements should be applied to fix both problems encountered during experiments in this study as well as to investigate other possible influences in future work. All the changes can be applied to both the power and the propulsion system since the difficulties encountered during the study often had a related cause.

First of which is related to obtaining more reliable and accurate measurement data. The instruments are important in this, as these have to be perfectly suited for the cause, which was currently not always the case. Higher frequency and more sensitive, but shielded temperature recordings or more goal specific energy measurements with a bomb calorimeter are options in the decomposition study. Whilst with the fuel cell, better matching current and potential Data Acquisition System (DAQ) or automated voltammetry measurement equipment such as the potentiostat can be used. The addition of several other passive instruments such as thermocouples, pH measurement, flow meters and potentially a Gas Chromatography (GC) can aid in this process by keeping track of the changes inside the operating system.

The second recommendation is to improve the experimental setup robustness and with it, the repeatability of the results. This can be done by making changes to the layout and components of the systems, and also to make the incorporation of the measurement instruments as discussed above possible. Since currently inevitable changes in the composition and design of the systems after operation caused the consistency to go down and hence influenced the results, also when this was unintended. For the fuel cell, this can be effectuated by constructing a properly sealed stainless steel stack together with bipolar plates and solid current collectors. This way, the cell components should not fail anymore and match better with the instruments, where the use of more suitable pumps is needed as well to control the flow rate. Similarly, for the decomposition system, the glass vessel currently used for trapping the heat should be replaced by a more robust combustion chamber material in which all other instruments can be firmly secured. Replacing the nebulizer disc with a small pressurized based atomizer for injection should fix the last inconsistency but requires quite some extra research and development. By implementing these changes, the power and propulsion systems are made more professional and simultaneously better represent how they would function in the satellite.

The third would be to improve the system's core components, which are the MEA and igniter, to actually optimize the power output from the fuel cell and reduce the power required by the thermal thruster. For the MEA, this could be done by checking the influence of fine-tuning its composition, since the method of production seems to be fairly optimised already. Hence, the thickness of the electrodes and membrane, catalyst material and loading, support structure characteristics and pre treatment of the sub components should all be looked at in more detail. Likewise, the heating wire specifications can be optimized, by adding electrical isolation and insulation or by looking into the material characteristics and thickness of the

resistance wire itself. As concluded in this research, however, the coil configuration might be more interesting to investigate and see the influence of its windings, orientation, dimensions and location in the combustion chamber. Physical interaction of these system surfaces with the propellant is important as well, which is altered for both cases by optimizing the contact between them, with is done in the cell with the flow field pattern and rate and injector with velocity and direction of the flow. Lastly, the long term effects of the operation of the core components on their durability and performance need to be looked into.

The fourth recommendation is to further investigate the aspects that can make it into a cooperative system in which the propellant and heat are the main interests. This relates mainly to the difference in chemical composition, hence the fuel cell solutions should be increased in concentration to subsequently try decomposition within the thruster system. Safety is crucial here since the  $\text{H}_2\text{SO}_4$ ,  $\text{KOH}$  and  $\text{H}_2\text{O}_2$  are all corrosive, if being used in the systems and not reacting to water, oxygen and salt. The other is thus the addition of several other systems, focusing more on heat and propellant regeneration and thus improving the system efficiency. To do so, more realistic testing conditions might however be needed, such as the combustion chamber environment with a higher mass flow rate and pressure discussed before. This will also help in simulating the possibility of incorporation into a true CubeSat system.

A different route could be taken by developing and testing alternative systems and broadening the knowledge instead of optimizing the above. This was also the reason to try and build a universal setup in the first place, which is modular enough to interchange the igniter and cell type. For the power generation, a  $\text{H}_2\text{O}_2$  redox couple cell could be installed and for the thruster, a more complicated laser decomposition system could be developed, besides the already attempted plasma arc. To boost performance another fuel such as ethanol can be added, as it is known to increase power output and specific impulse. Although the results of this research showed not enough power can yet be produced with the cell to operate the thruster with, it is expected that the above recommendations can lead to a sustainable, fully functional, combined power and propulsion CubeSat system that is capable of doing so.

---

## Bibliography

- [1] M. Abdolmaleki and M. G. Hosseini. A development in direct borohydride/hydrogen peroxide fuel cell using nanostructured ni-pt/c anode. *Fuel Cells*, 17(3):321–327, 2017.
- [2] Ramiz Akay and Ayse Bayrakceken Yurtcan. *Direct Liquid Fuel Cells; Fundamentals, Advances and Future*. Academic Press, 1 edition, 2020.
- [3] L An and T S Zhao. Performance of an alkaline-acid direct ethanol fuel cell. *International Journal of Hydrogen Energy*, 36:9994–9999, 2011.
- [4] L An, T S Zhao, Z H Chai, L Zeng, and P Tan. Modeling of the mixed potential in hydrogen peroxide-based fuel cells. *International Journal of Hydrogen Energy*, 39:7407–7416, 2014.
- [5] L. An, T. S. Zhao, X. L. Zhou, L. Wei, and X. H. Yan. A high-performance ethanol-hydrogen peroxide fuel cell. *RSC Advances*, 4:65031–65034, 2014.
- [6] Liang An, Tianshou Zhao, Xiaohui Yan, Zhou Xuelong, and Peng Tan. The dual role of hydrogen peroxide in fuel cells. *Science Bulletin*, 60:55–64, 2015.
- [7] Sungyong An, Hayoung Lim, and Sejin Kwon. Hydrogen peroxide thruster module for microsatellites with platinum supported by alumina as catalyst. In *43rd AIAA/ASME/SAE/ASEE Joint Propulsion Conference & exhibit, Cincinnati, OH*, volume 5, pages 4470–4477. American Institute of Aeronautics and Astronautics Inc., 2007.
- [8] William E Anderson, Kathy Butler, Dave Crocket, Tim Lewis, and Curtis McNeal. Peroxide propulsion at the turn of the century. Technical report, NASA MSFC, Boeing Rocketdyne power and propulsion, Orbital Sciences corp, 3 2000.
- [9] Junichiro Aoyagi, Kyoichi Kuriki, Haruki Takegahara, Jun Yokote, Akira Kakami, and Takeshi Tachibana. Feasibility study of plasma chemical thruster. In *The 30th International Electric Propulsion Conference, Florence, Italy*, 2007.
- [10] Scribner Associates. Through-plane & in-plane conductivity of polymer electrolyte membranes. Presentation, Scribner Associates Incorporated, 9 2010.
- [11] Allen J Bard, Joseph Jordan, and Roger Parsons. *Standard Potentials in Aqueous Solution*. CRC Press, 1st edition edition, 1985.

- [12] Y. Batonneau, R. Brahmi, B. Cartoixa, K. Farhat, C. Kappenstein, S. Keav, G. Kharchafi-Farhat, L. Pirault-Roy, M. Saouabé, and C. Scharlemann. Green propulsion: Catalysts for the european fp7 project grasp. *Topics in Catalysis*, 57:656–667, 2014.
- [13] J. Bouwmeester, G. F. Brouwer, E. K. A. Gill, G. L. E. Monna, and J. Rotteveel. Design status of the delfi-next nanosatellite project. In *61st International Astronautical Congress, Prague, Czech Republic*. TU Delft, 2010.
- [14] J Bouwmeester and J Guo. Survey of worldwide pico-and nanosatellite missions, distributions and subsystem technology. *Acta Astronautica*, 67:854–862, 2010.
- [15] Mohammed Bouziane, Artur Elias de Morais Bertoldi, Praskovia Milova, Patrick Hendrick, and Michel Lefebvre. Experimental investigation of showerhead injectors on performance of a 1-kn paraffin-fueled hybrid rocket motor. In *8th European Conference for Aeronautics and Space Sciences (EUCASS)*, 2019.
- [16] Guillaume Braesch, Zhongyang Wang, Shrihari Sankarasubramanian, Alexandr G. Oshepkov, Antoine Bonnefont, Elena R. Savinova, Vijay Ramani, and Marian Chatenet. A high performance direct borohydride fuel cell using bipolar interfaces and noble metal-free ni-based anodes. *Journal of Materials Chemistry A*, 8:20543–20552, 2020.
- [17] Cristina Bramanti, Angelo Cervone, Luca Romeo, Lucio Torre, Antony J Musker, and Giorgio Saccoccia. Experimental characterization of advanced materials for the catalytic decomposition of hydrogen peroxide. In *Conference: 42nd AIAA/ASME/SAE/ASEE Joint Propulsion Conference & Exhibit*, 7 2006.
- [18] Javier Brey, Delia Muñoz, Verónica Mesa, and Tamara Guerrero. Use of fuel cells and electrolyzers in space applications: From energy storage to propulsion/deorbitation. In *11th European Space Power Conference*, 2016.
- [19] David J Brodrecht and John J Rusek. Aluminum-hydrogen peroxide fuel-cell studies. *Applied Energy*, 74:113–124, 2003.
- [20] Chantal Cappelletti. Femto, pico, nano: Overview of new satellite standards and applications. In *Advances in the Astronautical Sciences*, volume 163, 2018.
- [21] David A Castaneda and Benveniste Natan. Experimental investigation of the hydrogen peroxide-solid hydrocarbon hypergolic ignition. In *7 TH EUROPEAN CONFERENCE FOR AERONAUTICS AND SPACE SCIENCES (EUCASS)*, 2017.
- [22] Angelo Cervone. *AE4S07 - Course Reader Micro-Propulsion*. Faculty of Aerospace Engineering, Delft University of Technology, 9 2018.
- [23] Angelo Cervone, Lucio Torre, Antony J Musker, Graham T Roberts, Cristina Bramanti, and Giorgio Saccoccia. Development of hydrogen peroxide monopropellant rockets. In *42nd AIAA/ASME/SAE/ASEE Joint Propulsion Conference & Exhibit, Sacramento, California*, 7 2006.
- [24] REOTEMP Instruments Corporation. Type k thermocouple. <https://www.thermocoupleinfo.com/type-k-thermocouple.htm>, 2011. Last accessed: 15-4-2022.



- 
- [25] Ian Coxhill and David Gibbon. A xenon resistojet propulsion system for microsattellites. In *41st AIAA/ASME/SAE/ASEE Joint Propulsion Conference & Exhibit, Tuscon, Arizona*. American Institute of Aeronautics and Astronautics (AIAA), 7 2005.
- [26] EC. REGULATION (EC) No 1907/2006 OF THE EUROPEAN PARLIAMENT AND OF THE COUNCIL concerning the registration, evaluation, authorisation and restriction of chemicals (REACH), establishing a european chemicals agency, amending directive 1999/45/ec and repealing council regulation (EEC) no 793/93 and commission regulation (EC) no 1488/94 as well as council directive 76/769/eec and commission directives 91/155/eec, 93/67/eec, 93/105/ec and 2000/21/ec. Legislation, European Chemicals Agency (ECHA), 12 2006.
- [27] EC. Final report summary - grasp (green advanced space propulsion). Technical report, European Communities, 2011. <https://cordis.europa.eu/project/id/218819/reporting> [last accessed 21-5-2021].
- [28] Bradford ECAPS. 1n hpgp thruster. <https://www.ecaps.space/products-1n.php>, 2022. Last accessed: 12-5-2022.
- [29] Asma A Eddib and D D L Chung. Electric permittivity of carbon fiber. *Carbon*, 143:475–480, 2019.
- [30] Theodore N. Edelbaum. Propulsion requirements for controllable satellites. In *ARS Semi-annual Meeting, Los Angeles, California*, volume 31, pages 583–589. American Rocket Society, 8 1961.
- [31] Diana Enescu. *Thermoelectric Energy Harvesting: Basic Principles and Applications*, pages –. IntechOpen, 2019.
- [32] K Essa, H Hassanin, M M Attallah, N J Adkins, A J Musker, G T Roberts, N Tenev, and M Smith. Development and testing of an additively manufactured monolithic catalyst bed for htp thruster applications. *Applied Catalysis A, General*, 542:125–135, 2017.
- [33] European Space Agency (ESA). Green hydrogen peroxide (h<sub>2</sub>o<sub>2</sub>) monopropellant with advanced catalytic beds, 2006. [http://www.esa.int/About\\_Us/Business\\_with\\_ESA/Small\\_and\\_Medium\\_Sized\\_Enterprises/SME\\_Achievements/Green\\_Hydrogen\\_Peroxide\\_H2O2\\_monopropellant\\_with\\_advanced\\_catalytic\\_beds](http://www.esa.int/About_Us/Business_with_ESA/Small_and_Medium_Sized_Enterprises/SME_Achievements/Green_Hydrogen_Peroxide_H2O2_monopropellant_with_advanced_catalytic_beds) [last accessed 10-6-2021].
- [34] Ewan Fonda-Marsland, Graham Roberts, Dave Gibbon, and Charlie Ryan. An investigation into injector architecture for sub-newton monopropellant propulsion. In *8th European Conference for Aeronautics and Space Sciences (EUCASS)*, 2019.
- [35] Agency for Toxic Substances and Disease Registry (ATSDR). Sulfur trioxide (so<sub>3</sub>) and sulfuric acid. Faq sheet, U.S. Department of Health and Human Services, 6 1999.
- [36] T. Franken. Design of a modular one newton hydrogen peroxide monopropellant thruster, including feed system and test setup. Master’s thesis, Delft University of Technology, 2020.

- [37] Thim Franken, Ferran Valencia-Bel, Botchu Vara Siva Jyoti, and B. T. C. Zandbergen. Design of a 1-n monopropellant thruster for testing of new hydrogen peroxide decomposition technologies. In *Aerospace Europe Conference 2020; BORDEAUX, FRANCE*. Delft University of Technology, 2020.
- [38] Shunichi Fukuzumi, Yusuke Yamada, and Kenneth D. Karlin. Hydrogen peroxide as a sustainable energy carrier: Electrocatalytic production of hydrogen peroxide and the fuel cell. *Electrochimica acta*, 82:493, 11 2012.
- [39] Paul A. Giguere and I. D. Liu. Kinetics of the thermal decomposition of hydrogen peroxide vapor. *Canadian Journal of Chemistry*, 35, 4 1957.
- [40] R J Gilliam, J W Graydon, D W Kirk, and S J Thorpe. A review of specific conductivities of potassium hydroxide solutions for various concentrations and temperatures. *International Journal of Hydrogen Energy*, 32:359–364, 2007.
- [41] Ulrich Gotzig. Challenges and economic benefits of green propellants for satellite propulsion. In *7TH EUROPEAN CONFERENCE FOR AERONAUTICS AND SPACE SCIENCES (EUCASS)*. ArianeGroup, 2017.
- [42] Franz Grafwallner. Hydrogen peroxide (hp) potential for space applications. Technical report, ET-EnergieTechnologie GmbH, 2004.
- [43] Sh L Guseinov, S G Fedorov, V A Kosykh, and P A Storozhenko. Hypergolic propellants based on hydrogen peroxide and organic compounds: historical aspect and current state. *Izvestiya Akademii Nauk. Seriya Khimicheskaya*, 67:1943–1954, 2018.
- [44] Sh L. Guseinov, S. G. Fedorov, V. A. Kosykh, and P. A. Storozhenko. Hydrogen peroxide decomposition catalysts used in rocket engines. *Russian Journal of Applied Chemistry*, 93:467–487, 2020.
- [45] Phuc Thi Ha, Hyunsoo Moon, Byung Hong Kim, How Yong Ng, and In Seop Chang. Determination of charge transfer resistance and capacitance of microbial fuel cell through a transient response analysis of cell voltage. *Biosensors and Bioelectronics*, 25:1629–1634, 3 2010.
- [46] Peter W Hart and Alan Rudie. Hydrogen peroxide-an environmentally friendly but dangerous bleaching chemical. In *Proceedings of TAPPI engineering, pulping and environmental conference*. Tappi Press, 10 2007.
- [47] Y. Haseli. Maximum conversion efficiency of hydrogen fuel cells. *International Journal of Hydrogen Energy*, 43:9015–9021, 5 2018.
- [48] Allen Hermann, Tapas Chaudhuri, and Priscila Spagnol. Bipolar plates for pem fuel cells: A review. *International Journal of Hydrogen Energy*, 30(12):1297–1302, 2005. Cancun 2003.
- [49] J. H. Hirchenhofer, D. B. Stauffer, R. R. Engleman, and M. G. Klett. *DOE Fuel Cell Handbook, fourth edition*, volume 4. Parsons Corporation, November 1998.

- 
- [50] Rachel M. E. Hjelm, Clémence Lafforgue, Robert W. Atkinson, Yannick Garsany, Richard O. Stroman, Marian Chatenet, and Karen Swider-Lyons. Impact of the anode catalyst layer design on the performance of h<sub>2</sub>o<sub>2</sub>-direct borohydride fuel cells. *Journal of The Electrochemical Society*, 166:F1218–F1228, 2019.
- [51] Jennifer Hudson, Sara Spangelo, Andrew Hine, Daniel Kolosa, and Kristina Lemmer. Mission analysis for cubesats with micropropulsion. *Journal of Spacecraft and Rockets*, 53:836–846, 2016.
- [52] Shin ichi Yamazaki, Zyun Siroma, Hiroshi Senoh, Tsutomu Ioroi, Naoko Fujiwara, and Kazuaki Yasuda. A fuel cell with selective electrocatalysts using hydrogen peroxide as both an electron acceptor and a fuel. *Journal of Power Sources*, 178:20–25, 3 2008.
- [53] OMEGA Engineering Inc. Unsheathed fine diameter thermocouples with bead-welded junction. j, k, t, n, e, r, s & b. [https://www.omega.nl/pptst/IRCO\\_CHAL\\_P13R\\_P10R.html](https://www.omega.nl/pptst/IRCO_CHAL_P13R_P10R.html), 2022. Last accessed: 15-4-2022.
- [54] ISECG. The global exploration roadmap. Roadmap, National Aeronautics and Space Administration, 1 2018.
- [55] J. Quesada Mañas. Propellant grade hydrogen peroxide production and thermo pseudo hypergolicity investigation for dual mode green propulsion systems. Master’s thesis, Delft University of Technology, 2020.
- [56] Ma Jia, Yogeshwar Sahai, and Rudolph G Buchheit. Direct borohydride fuel cell using ni-based composite anodes. *Journal of Power Sources*, 195:4709–4713, 2010.
- [57] Craig W. Jones and James H. Clark. Introduction to the preparation and properties of hydrogen peroxide. In *Applications of Hydrogen Peroxide and Derivatives*, pages 1–36. The Royal Society of Chemistry, 1999.
- [58] Jan Kindracki, Przemysław Paszkiewicz, and Łukasz Mężyk. Resistojet thruster with supercapacitor power source – design and experimental research. *Aerospace Science and Technology*, 92:847–857, 2019.
- [59] Stefan Kooij, Alina Astefanei, Garry L Corthals, and Daniel Bonn. Size distributions of droplets produced by ultrasonic nebulizers. *Scientific Reports*, 9(6128), 4 2019.
- [60] David Krejci and Paulo Lozano. Space propulsion technology for small spacecraft. *Proceedings of the IEEE*, 106:362–378, 3 2018.
- [61] David Krejci, Alexander Woschnak, Carsten Scharlemann, and Karl Ponweiser. Structural impact of honeycomb catalysts on hydrogen peroxide decomposition for micro propulsion. *Chemical Engineering Research and Design*, 90:2302–2315, 2012.
- [62] Erik Kulu. Nanosats database, 2021. [www.nanosats.eu](http://www.nanosats.eu) [last accessed 3-6-2021].
- [63] V. Lappas, V. Kostopoulos, A. Tsourdos, and S. Kindylides. A low cost thermoelectric generator for small satellites. In *AIAA Scitech Forum, San Diego, California*. American Institute of Aeronautics and Astronautics Inc, AIAA, 2019.

- [64] James Larminie and Andrew L. Dicks. *Fuel Cell Systems Explained*. J. Wiley, second edition edition, 2003.
- [65] Heng Yi Lee, Yi Hsuan Hsu, Po Hong Tsai, Jiunn Yih Lee, and Yong Song Chen. The performance of a direct borohydride/peroxide fuel cell using graphite felts as electrodes. *Energies*, 10, 8 2017.
- [66] Kristina Lemmer. Propulsion for cubesats. *Acta Astronautica*, 134:231–243, 5 2017.
- [67] Mirko Leomanni, Andrea Garulli, Antonio Giannitrapani, and Fabrizio Scortecci. Propulsion options for very low earth orbit microsattelites. *Acta Astronautica*, 133:444–454, 4 2017.
- [68] Craig M. Lewandowski and David L. Akin. Development of a single-fluid consumable infrastructure for life support systems. In *37th International Conference on Environmental Systems (ICES)*, Chicago, Illinois. SAE International, 2007.
- [69] Yinshi Li. A liquid-electrolyte-free anion-exchange membrane direct formate-peroxide fuel cell. *International Journal of Hydrogen Energy*, 41:3600–3604, 2 2016.
- [70] Yinshi Li, Hao Wu, Yaling He, Yue Liu, and Lei Jin. Performance of direct formate-peroxide fuel cells. *Journal of Power Sources*, 287:75–80, 2015.
- [71] Chunmei Liu, Canxing Sun, Yanjun Gao, Weijuan Lan, and Shaowei Chen. Improving the electrochemical properties of carbon paper as cathodes for microfluidic fuel cells by the electrochemical activation in different solutions. *ACS Omega*, 6:19153–19161, 7 2021.
- [72] J G Liu, T S Zhao, Z X Liang, and R Chen. Effect of membrane thickness on the performance and efficiency of passive direct methanol fuel cells. *Journal of Power Sources*, 153:61–67, 2006.
- [73] Biaowu Lu, Wei Yuan, Xiaoqing Su, Ziyi Zhuang, Yuzhi Ke, and Yong Tang. Passive direct methanol–hydrogen peroxide fuel cell with reduced graphene oxide–supported prussian blue as catalyst. *Energy Technology*, 8:1901360, 3 2020.
- [74] Marian Von Lukowicz, Elisabeth Abbe, Tino Schmiel, and Martin Tajmar. Thermoelectric generators on satellites—an approach for waste heat recovery in space. *Energies*, 9(7), 2016.
- [75] J. Ma, N. A. Choudhury, Y. Sahai, and R. G. Buchheit. Performance study of direct borohydride fuel cells employing polyvinyl alcohol hydrogel membrane and nickel-based anode. *Fuel Cells*, 11:603–610, 10 2011.
- [76] Benjamin K. Malphrus, Anthony Freeman, Robert Staehle, Andrew T. Klesh, and Roger Walker. *Interplanetary CubeSat missions*, pages 85–121. Academic Press, 2021.
- [77] V K Mani, F Topputo, and A Cervone. Dual chemical-electric propulsion systems design for interplanetary cubesats. In *ESA Space Propulsion 2018 Conference, Seville, Spain*, 2018.

- [78] R. F. Martins, D. A.A. Martins, L. A.C. Costa, T. Matencio, R. M. Paniago, and L. A. Montoro. Copper hexacyanoferrate as cathode material for hydrogen peroxide fuel cell. *International Journal of Hydrogen Energy*, 45:25708–25718, 9 2020.
- [79] B. M. Melof and M. C. Grubelich. Investigation of hypergolic fuels with hydrogen peroxide. In *37th AIAA/ASME/SAE/ASEE Joint Propulsion Conference and Exhibit, Salt Lake City, Utah*. American Institute of Aeronautics and Astronautics Inc., 2001.
- [80] Lukasz Mezyk, Zbigniew Gut, Przemyslaw Paszkiewicz, Piotr Wolanski, and Grzegorz Rarata. Possibility of using thermal decomposition of hydrogen peroxide for low thrust propulsion system application. In *7TH EUROPEAN CONFERENCE FOR AERONAUTICS AND SPACE SCIENCES (EUCASS)*, 2017.
- [81] D. W. Miller and John Keesee. *Spacecraft power systems*, 2003.
- [82] T. R. Nada and A. A. Hashem. Geometrical characterization and performance optimization of monopropellant thruster injector. *The Egyptian Journal of Remote Sensing and Space Science*, 15:161–169, 12 2012.
- [83] L. Napoli, J. Franco, H. Fasoli, and A. Sanguinetti. Conductivity of nafion® 117 membrane used in polymer electrolyte fuel cells. *International Journal of Hydrogen Energy*, 39:8656–8660, 5 2014.
- [84] NASA. Nasa technology roadmaps - ta 3: Space power and energy storage. Roadmap, National Aeronautics and Space Administration, 7 2015.
- [85] NASA. Nasa technology roadmaps ta 2: In-space propulsion technologies. Roadmap, National Aeronautics and Space Administration, 7 2015.
- [86] NASA. State-of-the-art small spacecraft technology. Technical report, National Aeronautics and Space Administration, 10 2020.
- [87] R Nave. Biot-savart law, 2016. <http://hyperphysics.phy-astr.gsu.edu/hbase/magnetic/Biosav.html> [last accessed 12-5-2022].
- [88] NFPA 704. *Standard System for the Identification of the Hazards of Materials for Emergency Response*. National Fire Protection Association, 2017.
- [89] Bao Nguyen, Neal Kuperman, Gary Goncher, and Raj Solanki. Membraneless h<sub>2</sub> o<sub>2</sub> fuel cells driven by metallophthalocyanine electrocatalysts. *ECS Journal of Solid State Science and Technology*, 9:061009, 7 2020.
- [90] NIST Chemistry WebBook, SRD 69. Hydrogen peroxide, 2018. <https://webbook.nist.gov/cgi/cbook.cgi?ID=7722-84-1> [last accessed 26-5-2021].
- [91] Ahmed E.S. Nosseir, Angelo Cervone, and Angelo Pasini. Review of state-of-the-art green monopropellants: For propulsion systems analysts and designers. *Aerospace*, 8:1–21, 1 2021.
- [92] Robert K Palmer and John J Rusek. Low toxicity reactive hypergolic fuels for use with hydrogen peroxide. Technical report, Swift Enterprises, Ltd, 2004.

- [93] Zhefei Pan, Yanding Bi, and Liang An. Performance characteristics of a passive direct ethylene glycol fuel cell with hydrogen peroxide as oxidant. *Applied Energy*, 250:846–854, 2019.
- [94] Enza Passalacqua, Rolando Pedicini, Alessandra Carbone, Irene Gatto, Fabio Matera, Assunta Patti, and Ada Saccà. Effects of the chemical treatment on the physical-chemical and electrochemical properties of the commercial nafion™ nr212 membrane. *Materials*, 13:1–16, 11 2020.
- [95] J Pfitzner. Poiseuille and his law. *Anaesthesia*, 31:273–275, 1976.
- [96] PubChem. Compound summary for cid 784, hydrogen peroxide, 2021. <https://pubchem.ncbi.nlm.nih.gov/compound/Hydrogen-peroxide> [last accessed 25-5-2021].
- [97] Sri Pujiastuti and Holia Onggo. Effect of various concentration of sulfuric acid for nafion membrane activation on the performance of fuel cell. In *AIP Conference Proceedings 1711*, volume 1711. American Institute of Physics Inc., 2 2016.
- [98] Paulina Pędziwiatr, Filip Mikołajczyk, Dawid Zawadzki, Kinga Mikołajczyk, and Agnieszka Bedka. Decomposition of hydrogen peroxide-kinetics and review of chosen catalysts. *Acta Innovations*, 26:45–52, 2018.
- [99] S. Radu, S. Uludag, S. Speretta, E. K. A. Gill, J. Bouwmeester, and N. Chronas Foteinakis. Delfi-pq: The first pocketcube of delft university of technology. In *Proceedings of 69th International Astronautical Congress: Bremen, Germany*. International Astronautical Federation (IAF), 2018.
- [100] John J Rusek. Hydrogen peroxide for propulsion and power applications: a swift perspective. In *Int. Conference on Green Propellants for Space Propulsion*. European Space Agency, 2004.
- [101] Charles N. Ryan, Ewan Fonda-Marsland, Graham T. Roberts, Alan Lear, Edward Fletcher, Lee Giles, Matthew J. Palmer, and David Gibbon. Experimental validation of a 1-newton hydrogen peroxide thruster. *Journal of Propulsion and Power*, 36:158–166, 2020.
- [102] Thomas Saaty and T Mathot. Ahp trade-off tool users manual v2.7. Manual, Dutch Space B.V., 2007.
- [103] A. E. Sanli and Aylin Aytaç. Response to disselkamp: Direct peroxide/peroxide fuel cell as a novel type fuel cell. *International Journal of Hydrogen Energy*, 36:869–875, 1 2011.
- [104] Ayse Elif Sanli. A possible future fuel cell: the peroxide/peroxide fuel cell. *International journal of energy research*, 37:1488–1497, 2013.
- [105] Megan B. Sassin, Yannick Garsany, Benjamin D. Gould, and Karen E. Swider-Lyons. Fabrication method for laboratory-scale high-performance membrane electrode assemblies for fuel cells. *Analytical Chemistry*, 89:511–518, 1 2016.
- [106] Walter C Schumb, Charles N Satterfield, and Ralph L Wentworth. *Hydrogen Peroxide*. Reinhold Publishing Corporation, 1955.

- [107] Debasis Sengupta, Sandip Mazumder, J Vernon Cole, and Samuel Lowry. Controlling non-catalytic decomposition of high concentration hydrogen peroxide. Technical report, CFD Research Corporation, 2004.
- [108] Seyed Ali Mousavi Shaegh, Nam Trung Nguyen, Seyyed Mohsen Mousavi Ehteshami, and Siew Hwa Chan. A membraneless hydrogen peroxide fuel cell using prussian blue as cathode material. *Energy and Environmental Science*, 5:8225–8228, 2012.
- [109] Omar Z Sharaf and Orhan F Mehmet. An overview of fuel cell technology: Fundamentals and applications. *Renewable and sustainable energy reviews*, 32:810–853, 2014.
- [110] Tatsuo Shimizu and Craig Underwood. Super-capacitor energy storage for micro-satellites: Feasibility and potential mission applications. *Acta Astronautica*, 85:138–154, 4 2013.
- [111] Takahiro Shindo, Asato Wada, Hiroshi Maeda, Hiroki Watanabe, and Haruki Takegahara. Performance of a green propellant thruster with discharge plasma. *Acta Astronautica*, 131:92–95, 2017.
- [112] Chaozhu Shu, Erdong Wang, Luhua Jiang, Qiwen Tang, and Gongquan Sun. Studies on palladium coated titanium foams cathode for mg - h<sub>2</sub>o<sub>2</sub> fuel cells. *Journal of Power Sources*, 208:159–164, 6 2012.
- [113] George P Sutton and Oscar Biblarz. *Rocket Propulsion Elements*. John Wiley & Sons, 7 edition, 2001.
- [114] Mitsutoshi Tsuchiya and Hideyuki Horisawa. A chemically augmented arcjet thruster with exotic propellants. In *The 36th International Electric Propulsion Conference, University of Vienna, Austria*, 2019.
- [115] TU Delft. Delfi space, 2021. <https://www.tudelft.nl/lr/delfi-space> [last accessed 3-6-2021].
- [116] Akshay Reddy Tummala and Atri Dutta. An overview of cube-satellite propulsion technologies and trends. *Aerospace*, 4, 2017.
- [117] USP Technologies. H<sub>2</sub>o<sub>2</sub> self-accelerated decomposition, 2021. <https://www.h2o2.com/technical-library/physical-chemical-properties/thermodynamic-properties/default.aspx?pid=42&name=Self-Accelerated-Decomposition> [last accessed 9-6-2021].
- [118] USP Technologies. Hydrogen peroxide is a powerful oxidizer, 2021. <https://www.h2o2.com/products-and-services/us-peroxide-technologies.aspx?pid=112&name=Hydrogen-Peroxide> [last accessed 26-5-2021].
- [119] Guiling Wang, Dianxue Cao, Cuilei Yin, Yinyi Gao, Jinling Yin, and Lin Cheng. Nickel foam supported-co<sub>3</sub>o<sub>4</sub> nanowire arrays for h<sub>2</sub>o<sub>2</sub> electroreduction. *Chemistry of Materials*, 21:5112–5118, 11 2009.
- [120] Zhongyang Wang, Javier Parrondo, Cheng He, Shrihari Sankarasubramanian, and Vijay Ramani. Efficient ph-gradient-enabled microscale bipolar interfaces in direct borohydride fuel cells. *Nature Energy* 2019 4:4, 4:281–289, 2 2019.

- [121] Adam Z. Weber and John Newman. Effects of microporous layers in polymer electrolyte fuel cells. *Journal of The Electrochemical Society*, 152:A677, 3 2005.
- [122] V Weiser, J Hürttlen, U Schaller, A Imiolek, and S Kelzenberg. Green liquid oxidizers basing on solutions of adn and an in hydrogen peroxide for hypergolic propellants with high performance. In *7th european conference for aeronautics and space sciences. EUCASS*, 2017.
- [123] Eric J Wernimont. System trade parameter comparison of monopropellants: Hydrogen peroxide vs hydrazine and others. In *42nd AIAA/ASME/SAE/ASEE Joint Propulsion Conference & Exhibit, Sacramento, CA. American Institute of Aeronautics and Astronautics (AIAA)*, 7 2006.
- [124] J C Whitehead. Hydrogen peroxide propulsion for smaller satellites. In *Conference: 12th Annual American Institute of Aeronautics and Astronautics/Utah State University Conference on Small Satellite, Logan, UT*, 1998.
- [125] Fred Wilson. In-space propulsion data sheets. Technical report, Aerojet Rocketdyne, 2020.
- [126] Xue Xiao, Fan Yang, Kui Cheng, Xin Wang, Hongyu Zhang, Ke Ye, Guiling Wang, and Dianxue Cao. Enhanced performance of direct peroxide/peroxide fuel cell by using ultrafine nickel ferric ferrocyanide nanoparticles as the cathode catalyst. *International Journal of Hydrogen Energy*, 42:22856–22865, 9 2017.
- [127] Yusuke Yamada, Masaki Yoneda, and Shunichi Fukuzumi. High power density of one-compartment h<sub>2</sub>o<sub>2</sub> fuel cells using pyrazine-bridged fe[m c (cn) 4 ] (m c = pt 2+ and pd 2+ ) complexes as the cathode. *Inorganic Chemistry*, 53:1272–1274, 2014.
- [128] Fan Yang, Bo Cao, Yue Tao, Dianxue Cao, and Ying Zhang. Nicotinamide-assisted fabrication of high-stability gold-palladium nanoparticles on carbon fiber cloth for hydrogen peroxide electroreduction. *Electrochimica Acta*, 210:199–205, 2016.
- [129] Fan Yang, Kui Cheng, Xiuling Liu, Sha Chang, Jingling Yin, Chunyu Du, Lei Du, Guiling Wang, and Dianxue Cao. Direct peroxide-peroxide fuel cell - part 2: Effects of conditions on the performance. *Journal of Power Sources*, 217:569–573, 11 2012.
- [130] Fan Yang, Kui Cheng, Yinghua Mo, Liqiu Yu, Jingling Yin, Guiling Wang, and Dianxue Cao. Direct peroxide-peroxide fuel cell - part 1: The anode and cathode catalyst of carbon fiber cloth supported dendritic pd. *Journal of Power Sources*, 217:562–568, 11 2012.
- [131] Fan Yang, Kui Cheng, Tianhao Wu, Ying Zhang, Jinling Yin, Guiling Wang, and Dianxue Cao. Dendritic palladium decorated with gold by potential pulse electrodeposition: Enhanced electrocatalytic activity for h<sub>2</sub>o<sub>2</sub> electroreduction and electrooxidation. *Electrochimica Acta*, 99:54–61, 2013.
- [132] Fan Yang, Kui Cheng, Xue Xiao, Jinling Yin, Guiling Wang, and Dianxue Cao. Nickel and cobalt electrodeposited on carbon fiber cloth as the anode of direct hydrogen peroxide fuel cell. *Journal of Power Sources*, 245:89–94, 2014.



- 
- [133] Puqing Yang, Ying Zhu, Pei Zhang, Houcheng Zhang, Ziyang Hu, and Jinjie Zhang. Performance evaluation of an alkaline fuel cell/thermoelectric generator hybrid system. *International Journal of Hydrogen Energy*, 39:11756–11762, 7 2014.
- [134] Ersin Yener Yazıcı and Hacı Deveci. Factors affecting decomposition of hydrogen peroxide. In Ozcan Y Gulsoy, S Levent Ergun, N Metin Can, and ilkay B Celik, editors, *Proceedings of the 12th international mineral processing symposium*. Hacettepe University, 10 2010.
- [135] Ke Ye, Fen Guo, Yinyi Gao, Dongming Zhang, Kui Cheng, Wenping Zhang, Guiling Wang, and Dianxue Cao. Three-dimensional carbon- and binder-free nickel nanowire arrays as a high-performance and low-cost anode for direct hydrogen peroxide fuel cell. *Journal of Power Sources*, 300:147–156, 2015.
- [136] Lanhua Yi, Bin Yu, Wei Yi, Yuanqing Zhou, Rui Ding, and Xianyou Wang. Carbon-supported bimetallic platinum–iron nanocatalysts: Application in direct borohydride/hydrogen peroxide fuel cell. *ACS Sustainable Chemistry & Engineering*, 6(7):8142–8149, 2018.
- [137] B.T.C. Zandbergen. *Thermal Rocket Propulsion (Course AE4S01)*, volume 2.07. Delft University of Technology, Faculty of Aerospace Engineering, August 2018.



---

# Appendices

## -1 SEM, EDS & XRD Manual

### SEM & EDS Procedure

#### Sample Preparation

- Reserve SEM in online system beforehand
- The maximum sample size is approximately 2.5x4cm
  - Use extra samples, since they can be damaged by the instrument
  - If lightweight or thin, use the copper plate as base
  - Use carbon double sided tape to attach sample to the plate

**Note** Sample must be conductive or it must be coated with gold nanoparticles in advance

- Place copper plate in holder to clamp the sample plate

**Note** Smaller samples & powder need different specific clamp

- Make sure the sample is horizontally flat and straighten with gloves
- Check if sample is attached properly and does not fall off easily
- Take sample to computer monitors
  - Left: SEM software & control + physical panels to control the brightness, contrast, focus
  - Right: Energy Dispersive X-Ray Spectroscopy (EDS) analyser, which needs SEM images first to analyse
- If a specific region on the sample needs to be magnified, mark the spot with a marker
  - The same might be needed if a small shiny metal is used as sample to distinguish from sample holder

#### Gold Coating

- Use in case the sample material is not conductive

- If material is heavy, can be placed inside directly
- If material is light, use small rack to place in apparatus
- Turn on the device right side at the back
- Open top lid, use black handle to lift
- Open up until locked in safety, visible by a metal part clicking in the lid
- Note** Do not press down once in lock, this will break the lid
- In the lid, make sure a plate is bolted on tightly by checking in the centre.
- Place plate over the ‘Gold’ side (side B)
- Place sample in the centre of the sample holder in the device
- Once sample is placed, grab lid, unlock it (bottom left on lid) and bring back down slowly
- Select ‘Au 15 nm’ program
  - use pen attached to the side of the machine to select programs
- Open nitrogen gas top valve until a ‘medium’ hissing sound can be heard
  - Gas is located in the left corner, next to door when entering)
- If an error occurs on screen, press ‘Abort’ and restart the program with more or less nitrogen gas supply
  - The whole process takes about six minutes
- Note** If process goes well, plasma can be seen from within the chamber
- Once finished and not able to lift the lid, run venting program ‘QT Cent Chamber’
- Open lid, lock door and take out sample
- Unlock door, bring back down and turn off device on the back

### SEM Preparation

- Switch on Infrared (IR) camera
  - A small screen now shows the SEM chamber

#### Software setup related tasks

- Check if the time clock is running in the software, ask for help if not the case
- Check ‘LC/HC’, make sure it is set at 8
- Set magnification to x25 with control panel next to monitor

- Set voltage to 5 kV on top left
  - Check the 'Conditions' button on the right of the SEM software
  - Change 'Sample Holder' selected to the one that will be used
- Sample insertion related tasks
- Hold the 'VENT' button for six seconds, located at the side of the opening
  - Detach the clip on the opening and slowly open the door with two hands
  - Place the copper plate holder on the tray in the door
    - The circular button (silver coloured) on the copper plate holder should be pointed directly away from the door and into the chamber once closed
    - Push the sample holder down & backwards to lock in place, check if properly fixed
  - Close the door, re-attach clip and hold 'EVAC' for six seconds
    - Evacuation of the chamber will take approximately 90 seconds
  - Pull black handle on the door upwards and turn to a horizontal position, push the rod into the SEM door until it halts and then retreat the handle to its original vertical position
- Note** Operate the rod with two hands, but do not touch the metallic part of the handle
- Via the IR camera screen, you should now be able to see the sample
  - Wait for pressure to reach  $10^{-4} Pa$  or lower

Software setup related tasks

- click on 'Z' to change height of sample and insert value close to  $17mm$
- Note** Physical white round button next to monitor is the emergency button, use to stop sample height if necessary
- Cool the setup with the EDS software on the bottom right needle logo
    - At 'Thermal', click 'Operate' and at 'Insertion' click 'In'
  - Cooling takes a few minutes, but can be sped up by adding nitrogen
  - Click 'ON' button at top left once available
  - Wait until current increases to  $10\mu A$  (top left panel, next to voltage)

### Cooling Process

- Take isolation container bucket located next to SEM and take it outside to the nitrogen tank
- Remove container cap and place tube nozzle with black handle of the tank inside

**Note** Wear thermal resistive gloves when handling the liquid nitrogen, not the blue chemical lab gloves

- Open blue top valve of large liquid nitrogen storage tank to let out the N<sub>2</sub>
  - In case the liquid nitrogen does not flow, open the lower valve until the liquid starts running inside container
- Leave running until container is half full and then close top valve as well
- Put back the nozzles and bring container to SEM
- Insert funnel into tube on left hand side of the SEM
- Gradually pour in the liquid nitrogen until the container is empty

**Note** Do not worry when steam and or liquid flows out of this hole since it will evaporate immediately and is no harm to the system

- Return the container, funnel and gloves next to SEM

### SEM Operation

- Once the sample is visible on screen, hit 'ACB' button on physical panel to auto-adjusts the brightness of the sample
- If the magnification > x500, switch to SEM on bottom right
- Select LEI or SEI to change contrast & focus, where LM & LEI best for carbon material
- Use mouse to move around by dragging on image as well as other controls indicated on screen
- Use control panel with buttons to focus and magnify the image, up to x800 or more
- For images, focus on a spot then go back to half the magnification and take the picture for best quality
- Press 'FREEZE' and subsequently 'PICTURE' on the control panel or on screen with the mouse to take a photo

**Note** Loading the picture could take some time and if not visible after a minute it can be found in the pre-designated folder

- Save the image as TIFF or other extension in a folder with your name
- To continue, press again 'FREEZE' on the control panel
- Use 'Quick 2' on SEM software for a possibly more stable image
- For better quality images set to 15kV on top left corner
  - Works only on metals and high temperature resistant materials, not composites, since they will melt

**Note** Shut down IR camera if  $> 5kV$  is used

- Start at low magnification to get a good sample overview and focus at every step
- If looking for other spots, zoom out first find other spot and zoom in again

### EDS & Data Handling

- For EDS open a folder in the D database on the right screen
  - Perform a 'map' for surface measurement or 'point id' for point measurement
  - Make 'new specimen' and add notes on magnification, sample specification, etc
  - Ex- or include gold coating at 'Describe Specimen' interface depending on the coating
  - Set the potential at  $15kV$  for image quality increase and turn off IR camera
  - Set the input to output rate between 1000 and 2000 by increasing 'Probe Current' at the bottom
  - Click 'start' in 'Scan Image', then 'Acquire map' and start
    - Wait longer than one minute to analyze more of the surface and increase composition points measured
  - Click 'stop' and wait until finished
  - Go to next tab to see the composition at 'Analyze' on the top left
    - There you can right click on peaks to show more detailed information
    - Remove elements that are found but most expected not to be present
      - \* The case when gold coated and it is certain no gold should be in the sample
      - \* Elements that have 0% or low % occurrence but high error count
  - Go to 'Construct map' to see elements, which again can be removed before saving
  - Predefine the sample in this screen when the composition is known, 'Auto-ID' otherwise
- Note** Predefining could have been done by previous user, so check if this is the case
- If registered materials are coloured the same, it can be fixed by going to 'Acquire' and changing the material color code
- Save the file as report template depending on which information you want displayed

### Shutting Down SEM & EDS

- EDS software can be left as it is
- Set SEM LC/HC to 8, magnification to x25 and in LM and LEI mode

- Change voltage back to  $5kV$  if needed and make sure IR camera is turned on
- Click 'Exchange position' to bring sample back to initial position
- When returned, click OFF top left of SEM software
- Switch off cooling, by at 'Thermal' switch to 'Standby' and at 'Insertion set to 'Out'
- Wait and pull out the sample with the black handle exactly the same way as inserted.
  - Use two hands to control black handle and still do not touch metallic parts
- Press 'VENT' for six seconds and detach clip at the door
  - Use two hands to slowly open the small door
- Take out sample by slightly pressing down and outwards
- Close door, attach the door clip and press 'EVAC' again for six seconds
- Switch of the IR camera of the SEM and leave on the computer
- Clean sample holder afterwards, if tape has been used for sample fixation
- When transferring the saved files, insert USB at the appropriate input cables on desk
- Properly remove USB by ejecting on bottom right of windows control beforehand



## XRD Procedure

### Sample Preparation

- Reserve XRD in online system and start heating laser before usage
- Cut the samples at the appropriate sizes ( $\pm 1 \times 1 \text{ cm}$ )
  - Use extra samples, since they can be damaged by the instrument
- Place sample in disk holder with the best suitable height
  - To fixate the sample on place, clay can be used in the holder

**Note** The disk edge height should be aligned with the sample

### XRD Operation

- Set lower angle to 0 or 10 and upper angle to 80 or 90 degrees
- Set measuring speed at approximately 1 deg/min for a 90 minute measurement
  - A higher speed goes faster, but is also less accurate and visa versa
  - Use a step size that is low enough as well, for example 0.05 degrees
- When multiple samples are used, check all the corresponding boxes
  - If the same setting are used as with the first sample, select 'tr1' as program
  - Give each sample a unique name and description, based on its type
  - Place the sample discs in their allocated slots, indicated on the wheel numbers
- Set the file in the location that you want it to be saved in
  - Name it according to the sample and measurement settings

### Shutting Down

- When the program is finished, click 'ok' and export file on top left
- Turn of the x-ray on top left as well and wait a minute at least
- Press 'lock door' to open door, after which an interval beep will sound
  - This will keep on beeping until the door is closed again by pressing the button
  - Remove holders from the machine first and then samples from the holders
- Shut down XRD and computer after transferring files

## -2 Keithley Measurement Manual

### Keithley 2701 DMM Measurement Procedure

#### DMM Installation

- Connect power, ethernet and TP link to DMM at location of measurement
- Plug TP link in laptop for storage with Keithley Kickstart software installed (v2.5.0)
- Go to laptop configuration panel and click on ethernet in network centre to obtain details
- Turn on Keithley and set ethernet details; shift > ethernet set > ethernet on > DHCP off > insert
- Laptop IP address > insert laptop gateway address > enter
- Insert set IP address in Kickstart software under instruments, advanced discovery tab
- Click on found instrument to control using DMM app after setting up configuration

#### Measuring U & I

- Attach measuring cables from DMM to cell and press front input button on DMM
  - Front panel; 2 upper right most for voltage, 2 lower right most for current
  - OCP measurement can be done via direct parallel connection over cell MEA
- Set measurement function and range in Kickstart software according to desired input
- Set NPLC high for accurate, but slow measurement and visa versa
- Leave, rel, filter, math and limits off and set infinite measure count on with small delay
- Run program to record and show live data at table and graph tab (check viability)
- Use aluminum for low resistance 0 V reference and battery for 1.4 V reference
- Export and name files after test as .csv, found at documents > Kickstart > projects

## -3 High-Speed Recording Camera Manual

### High-Speed Recording Measurement Procedure

#### Setup Preparation

- Reserve Photron High Speed Camera; LED's and computer software are included
    - Additional light can be found next to the camera car, with an extra stand
  - Place camera at approximately one meter distance from experimental setup
    - Attach power and ethernet cable directly to the computer inputs
    - Make sure the camera is horizontal and at the same height as the test stand
  - Place light at similar distance with light shining from behind the camera
    - Make sure no shadow is created behind the object that is filmed
    - Ethernet cable goes in the port panel, where multiple can be attached
- Note** Both the light as well as the fans should work immediately

**Note** When working with dangerous chemicals, keep both instruments at a safe distance

#### Tests Procedure

- Start the recording software, which can be controlled with the buttons on top
  - Connecting with the camera in software often requires multiple restarts
  - Set frame rate ( $\pm 6200 fps$ ) and other specifications at the right hand side, such as comments and resolution
  - Focus by turning the camera lens itself, after setting zoom to 100%
- Control the light at the corresponding port with the panel black button
  - Changing power adjusts the luminosity of the LED'S

**Note** A higher framerate requires a higher brightness and takes more time to save

- Record by pressing the record button twice in the live tab on the right hand side
  - Recording will start immediately and stay for three second or stop sooner when either of the two buttons are pressed
- Recorded data can be cut to a smaller size and saved under your own subfolder, after naming it accordingly
  - 'Year/month/day – decomposition method – propellant – test settings'

## -4 Thermocouple Measurement Manual

### NI DAQ & Thermocouple Measurement Procedure

- Reserve DAQ NI 9219 and use thermocouples of choice without connector plugs
  - Insert up to four thermocouples at one of the inputs in port 4 and 5
    - A very thin screwdriver is required to open the ports
  - Open the accompanied software on the laptop and plug in the DAQ
  - Set the measurement and export rate at  $50Hz$  and export backup files as .csv automatically
  - Link each thermocouple to its port on the DAQ in the software
    - Specify its type, Cold Junction Compensation and temperature range
  - Check the validity of the data using numerical and longer duration graphical interfaces

**Note** In case no temperature increase is present when touching the thermocouple bead, the connections or software link must be revised

**Note** In case the temperature decreases the thermocouple wires need to be switched between port 4 and 5 inputs
  - Calibrate the thermocouple by holding it in boiling water to verify if  $100^{\circ}C$  is reached
  - Recording of data can be done by setting a trigger such as minimum temperature reached or by pressing record on top left
  - Recorded data is saved according in designated subfolder of software by name set in advance
- ‘Year/month/day – decomposition method – propellant – test settings’

## **-5 Material Compatibility Sheet**

# COMPATIBILITY

---

## CHEMICAL COMPATIBILITY

### Chemical Compatibility Guide

The following information is intended to be used as a general guideline for pump material selection. The information accuracy of these ratings cannot be guaranteed, nor is it a complete list due to the extensive area of this field. Materials used in the pump and pumping systems must be chemically compatible. The data provided for the chemicals is at 70°F (21°C), unless otherwise noted. If your temperature differs from this, it may affect the compatibility of the fluid with the given pump materials by accelerating the reaction.

If you are unsure of the compatibility of your chemical, we recommend testing a sample of the material in question with the chemical.

Updated 7/2/13



# CHEMICAL COMPATIBILITY

| CHEMICALS                       | METALS   |              |                   |                     |                     | PLASTICS, ELASTOMERS & LEATHER |      |               |           |              |                       |                                |             |     |         |              |               |       |                 |               |      |      |                                   |        |          |   |
|---------------------------------|----------|--------------|-------------------|---------------------|---------------------|--------------------------------|------|---------------|-----------|--------------|-----------------------|--------------------------------|-------------|-----|---------|--------------|---------------|-------|-----------------|---------------|------|------|-----------------------------------|--------|----------|---|
|                                 | Aluminum | Carbon Steel | Cast/Ductile Iron | 304 Stainless Steel | 316 Stainless Steel | Acetal                         | Buna | CSM (Hypalon) | EPR, EPDM | Fluorocarbon | Fluoroelastomer (FKM) | Geolast (Buna & Polypropylene) | Hastelloy C | TPE | Leather | Nitrile (TS) | Nitrile (TPE) | Nylon | Polychloroprene | Polypropylene | PTFE | PVDF | Santoprene (EPDM & Polypropylene) | UHMWPE | Urethane |   |
| Acetaldehyde                    | B        | D            | C                 | A                   | A                   | A                              | D    | C             | A         | D            | D                     | D                              | A           | B   | B       | D            | D             | B     | D               | C             | A    | D    | B                                 | B      | D        |   |
| Acetamide                       | A        | D            | D                 | D                   | A                   | A                              | B    | B             | A         | B            | B                     | A                              | A           | D   | -       | A            | A             | B     | B               | A             | A    | D    | A                                 | A      | A        | D |
| Acetate Solvents                | B        | D            | D                 | D                   | A                   | A                              | D    | C             | B         | D            | D                     | D                              | D           | D   | -       | D            | D             | A     | D               | D             | A    | D    | B                                 | B      | D        |   |
| Acetic Acid                     | B        | D            | D                 | D                   | B                   | D                              | C    | C             | A         | -            | C                     | -                              | A           | D   | D       | C            | C             | D     | C               | B             | A    | C    | C                                 | B      | C        |   |
| Acetic Acid — 20%               | B        | D            | D                 | B                   | A                   | C                              | C    | A             | A         | C            | B                     | D                              | C           | -   | -       | -            | -             | D     | B               | B             | A    | B    | B                                 | A      | -        |   |
| Acetic Acid — 30%               | D        | -            | A                 | A                   | -                   | B                              | C    | -             | A         | D            | -                     | -                              | C           | -   | -       | -            | -             | -     | B               | B             | A    | B    | B                                 | A      | -        |   |
| Acetic Acid — 50%               | D        | -            | A                 | A                   | -                   | B                              | C    | -             | A         | C            | -                     | -                              | C           | -   | -       | -            | -             | -     | C               | B             | A    | B    | B                                 | A      | -        |   |
| Acetic Acid — 80%               | B        | D            | D                 | D                   | B                   | D                              | C    | C             | A         | -            | B                     | D                              | A           | -   | -       | -            | -             | D     | C               | A             | A    | C    | -                                 | -      | -        |   |
| Acetic Acid — Glacial           | B        | D            | D                 | C                   | A                   | D                              | D    | C             | B         | D            | D                     | B                              | A           | C   | -       | -            | -             | D     | D               | C             | A    | A    | D                                 | B      | -        |   |
| Acetic Acid Vapors              | A        | -            | -                 | -                   | A                   | -                              | -    | -             | -         | -            | -                     | -                              | -           | D   | D       | -            | -             | D     | -               | -             | A    | D    | -                                 | -      | -        |   |
| Acetic Anhydride                | D        | D            | D                 | D                   | B                   | D                              | D    | A             | D         | D            | D                     | D                              | A           | C   | B       | D            | D             | D     | B               | D             | A    | D    | D                                 | D      | B        |   |
| Acetone                         | B        | A            | A                 | A                   | A                   | B                              | D    | C             | A         | D            | D                     | D                              | A           | C   | -       | D            | D             | B     | D               | D             | A    | D    | B                                 | A      | D        |   |
| Acetone 120° F                  | -        | -            | -                 | -                   | -                   | B                              | -    | -             | -         | -            | -                     | -                              | -           | -   | -       | -            | -             | B     | -               | A             | A    | D    | -                                 | A      | -        |   |
| Acetone 140° F                  | -        | -            | -                 | -                   | -                   | -                              | -    | -             | -         | -            | -                     | -                              | -           | -   | -       | -            | -             | -     | -               | A             | A    | D    | -                                 | D      | -        |   |
| Acetone 70° F                   | A        | -            | B                 | A                   | A                   | -                              | D    | -             | A         | -            | D                     | -                              | -           | C   | -       | -            | -             | A     | -               | A             | A    | D    | A                                 | A      | -        |   |
| Acetone Cyanohydrin             | B        | -            | B                 | B                   | -                   | -                              | D    | -             | D         | D            | -                     | D                              | -           | -   | -       | -            | -             | -     | B               | -             | A    | -    | A                                 | -      | -        |   |
| Acetonitrile (Methyl Cyanide)   | A        | A            | A                 | A                   | A                   | A                              | C    | -             | A         | D            | D                     | D                              | B           | -   | -       | D            | D             | A     | D               | D             | A    | B    | A                                 | -      | B        |   |
| Acetophenone                    | B        | A            | A                 | A                   | B                   | -                              | D    | -             | B         | D            | D                     | D                              | B           | -   | -       | D            | D             | A     | D               | C             | A    | B    | B                                 | -      | -        |   |
| Acetyl Acetone                  | D        | -            | B                 | B                   | -                   | -                              | D    | -             | A         | D            | D                     | D                              | -           | -   | -       | D            | D             | -     | D               | -             | A    | -    | B                                 | -      | D        |   |
| Acetyl Bromide                  | -        | -            | -                 | -                   | -                   | -                              | -    | -             | -         | -            | -                     | -                              | -           | -   | -       | -            | -             | D     | -               | -             | A    | -    | -                                 | -      | -        |   |
| Acetyl Chloride                 | D        | B            | B                 | B                   | B                   | D                              | D    | D             | D         | B            | B                     | D                              | A           | D   | -       | D            | D             | D     | D               | D             | A    | A    | B                                 | -      | D        |   |
| Acetyl Salicylic Acid (Aspirin) | D        | -            | B                 | B                   | -                   | -                              | -    | -             | B         | -            | A                     | -                              | -           | -   | -       | A            | -             | -     | D               | -             | A    | -    | C                                 | A      | -        |   |
| Acetylene                       | A        | A            | A                 | A                   | A                   | A                              | B    | B             | A         | -            | A                     | B                              | A           | B   | A       | A            | A             | B     | B               | D             | A    | A    | -                                 | -      | D        |   |
| Acetylene Tetrabromide          | D        | -            | A                 | -                   | -                   | -                              | D    | -             | -         | A            | -                     | D                              | -           | -   | -       | -            | -             | -     | D               | -             | A    | -    | D                                 | -      | -        |   |
| Acid (Concentrated)             | -        | -            | -                 | -                   | -                   | -                              | -    | -             | B         | -            | A                     | -                              | -           | -   | -       | -            | -             | -     | -               | -             | A    | -    | -                                 | -      | -        |   |
| Acid (Mild)                     | -        | -            | -                 | -                   | -                   | -                              | A    | -             | B         | -            | A                     | -                              | -           | -   | -       | -            | -             | -     | -               | -             | A    | -    | -                                 | -      | -        |   |
| Acid Mine Water                 | -        | -            | -                 | -                   | -                   | A                              | -    | -             | -         | -            | -                     | -                              | -           | -   | -       | -            | -             | A     | -               | A             | A    | A    | -                                 | A      | -        |   |
| Acrolein (Acryaldehyde)         | B        | -            | B                 | B                   | -                   | -                              | B    | -             | A         | A            | B                     | B                              | -           | D   | -       | C            | -             | -     | D               | -             | A    | -    | A                                 | -      | D        |   |
| Acrylonitrile                   | B        | A            | A                 | A                   | A                   | -                              | D    | C             | D         | D            | D                     | D                              | B           | D   | -       | D            | D             | B     | D               | B             | A    | B    | D                                 | -      | D        |   |
| Adipic Acid                     | B        | A            | B                 | B                   | B                   | B                              | C    | -             | A         | A            | A                     | A                              | A           | D   | -       | A            | B             | A     | D               | B             | A    | B    | B                                 | A      | -        |   |
| Aero Lubriplate                 | A        | A            | A                 | A                   | A                   | A                              | A    | -             | D         | -            | A                     | -                              | A           | D   | -       | A            | A             | -     | A               | A             | A    | A    | C                                 | -      | -        |   |
| Aerosafe 1Ac                    | -        | -            | -                 | -                   | -                   | A                              | A    | -             | D         | -            | A                     | -                              | -           | -   | -       | -            | -             | -     | B               | -             | A    | -    | -                                 | -      | -        |   |

# CHEMICAL COMPATIBILITY

| CHEMICALS                           | METALS   |              |                   |                     |                     | PLASTICS, ELASTOMERS & LEATHER |      |               |           |              |                       |                                |             |     |         |              |               |       |                 |               |      |      |                                   |        |          |
|-------------------------------------|----------|--------------|-------------------|---------------------|---------------------|--------------------------------|------|---------------|-----------|--------------|-----------------------|--------------------------------|-------------|-----|---------|--------------|---------------|-------|-----------------|---------------|------|------|-----------------------------------|--------|----------|
|                                     | Aluminum | Carbon Steel | Cast/Ductile Iron | 304 Stainless Steel | 316 Stainless Steel | Acetal                         | Buna | CSM (Hypalon) | EPR, EPDM | Fluorocarbon | Fluoroelastomer (FKM) | Geolast (Buna & Polypropylene) | Hastelloy C | TPE | Leather | Nitrile (TS) | Nitrile (TPE) | Nylon | Polychloroprene | Polypropylene | PTFE | PVDF | Santoprene (EPDM & Polypropylene) | UHMWPE | Urethane |
| Aerosafe 2300                       | A        | A            | A                 | A                   | A                   | A                              | D    | -             | A         | -            | D                     | -                              | -           | B   | -       | D            | D             | -     | D               | -             | A    | -    | B                                 | -      | A        |
| Aerosafe 2300F                      | A        | A            | A                 | A                   | A                   | -                              | -    | -             | -         | -            | -                     | -                              | -           | -   | -       | -            | -             | -     | -               | -             | -    | -    | -                                 | -      | -        |
| Aerosafe 2300W                      | A        | -            | A                 | A                   | -                   | A                              | D    | -             | A         | -            | D                     | -                              | -           | A   | -       | D            | D             | -     | D               | -             | A    | -    | B                                 | -      | D        |
| Aeroshell 17 Grease                 | A        | A            | A                 | A                   | A                   | A                              | A    | -             | D         | -            | A                     | -                              | -           | D   | -       | A            | A             | -     | B               | -             | A    | -    | D                                 | -      | A        |
| Aeroshell 1Ac                       | A        | A            | A                 | A                   | A                   | A                              | -    | -             | D         | -            | A                     | -                              | A           | D   | -       | A            | A             | -     | B               | A             | A    | B    | D                                 | -      | B        |
| Aeroshell 750                       | A        | A            | A                 | A                   | A                   | A                              | B    | -             | D         | -            | A                     | -                              | -           | D   | -       | B            | C             | -     | D               | -             | A    | -    | D                                 | -      | A        |
| Aeroshell 7A Grease                 | A        | A            | A                 | A                   | A                   | A                              | A    | -             | D         | -            | A                     | -                              | -           | D   | -       | A            | A             | -     | B               | -             | A    | -    | D                                 | -      | D        |
| Alcohol                             | A        | A            | A                 | A                   | A                   | B                              | A    | -             | B         | -            | A                     | -                              | -           | B   | A       | -            | -             | D     | -               | B             | A    | A    | A                                 | A      | -        |
| Alcohol: Allyl                      | -        | -            | -                 | -                   | -                   | -                              | -    | -             | -         | -            | -                     | -                              | -           | -   | -       | -            | -             | -     | -               | -             | -    | -    | -                                 | -      | -        |
| Alcohol: Amyl                       | B        | B            | B                 | A                   | A                   | A                              | B    | A             | A         | -            | B                     | B                              | A           | A   | -       | B            | B             | A     | B               | B             | A    | A    | A                                 | A      | D        |
| Alcohol: Benzyl                     | B        | B            | B                 | B                   | B                   | A                              | D    | C             | C         | -            | A                     | -                              | A           | D   | -       | D            | D             | D     | C               | A             | A    | A    | A                                 | A      | C        |
| Alcohol: Butyl                      | B        | B            | B                 | A                   | A                   | A                              | C    | A             | A         | -            | A                     | -                              | A           | D   | -       | A            | B             | D     | A               | B             | A    | A    | A                                 | A      | D        |
| Alcohol: Diacetone                  | B        | A            | B                 | A                   | A                   | A                              | D    | D             | B         | -            | D                     | -                              | A           | D   | -       | D            | D             | A     | D               | B             | A    | A    | C                                 | -      | B        |
| Alcohol: Ethyl                      | B        | B            | B                 | A                   | A                   | A                              | C    | A             | A         | -            | A                     | -                              | A           | A   | -       | A            | A             | B     | A               | A             | A    | A    | B                                 | A      | D        |
| Alcohol: Hexyl                      | A        | A            | A                 | A                   | A                   | A                              | A    | B             | C         | -            | C                     | -                              | A           | D   | -       | A            | A             | A     | B               | A             | A    | A    | B                                 | -      | D        |
| Alcohol: Isobutyl                   | B        | C            | C                 | A                   | A                   | A                              | C    | A             | B         | -            | A                     | -                              | A           | B   | -       | C            | C             | B     | A               | A             | A    | A    | A                                 | -      | D        |
| Alcohol: Isopropyl                  | B        | A            | C                 | B                   | B                   | A                              | C    | A             | B         | -            | A                     | -                              | A           | A   | -       | C            | C             | D     | B               | A             | A    | A    | B                                 | -      | D        |
| Alcohol: Methyl                     | B        | A            | A                 | A                   | A                   | A                              | A    | A             | B         | -            | D                     | -                              | A           | B   | -       | A            | A             | B     | A               | A             | A    | A    | A                                 | A      | D        |
| Alcohol: Octyl                      | A        | A            | A                 | A                   | A                   | A                              | B    | B             | A         | -            | B                     | -                              | C           | D   | -       | B            | -             | A     | B               | -             | A    | -    | B                                 | -      | D        |
| Alcohol: Propyl                     | A        | A            | A                 | A                   | A                   | A                              | A    | A             | B         | -            | A                     | -                              | A           | D   | -       | A            | A             | B     | A               | A             | A    | A    | A                                 | A      | D        |
| Alcohols R-OH                       | -        | -            | -                 | -                   | -                   | A                              | -    | -             | -         | -            | -                     | -                              | A           | -   | -       | -            | -             | A     | -               | A             | -    | A    | -                                 | A      | -        |
| Alkaline Solutions                  | -        | -            | -                 | A                   | A                   | A                              | A    | -             | A         | -            | A                     | -                              | -           | -   | -       | -            | -             | -     | A               | -             | A    | -    | -                                 | A      | -        |
| Alkazene                            | -        | -            | -                 | -                   | -                   | -                              | D    | -             | -         | A            | A                     | -                              | -           | D   | -       | D            | D             | -     | D               | -             | A    | -    | D                                 | B      | D        |
| Allyl Alcohol                       | B        | A            | A                 | A                   | A                   | -                              | A    | -             | A         | B            | B                     | -                              | A           | D   | -       | A            | A             | A     | A               | B             | A    | A    | B                                 | A      | B        |
| Allyl Bromide                       | D        | -            | A                 | -                   | -                   | -                              | D    | -             | D         | B            | B                     | -                              | -           | D   | -       | D            | D             | -     | D               | -             | A    | -    | -                                 | -      | A        |
| Allyl Chloride                      | D        | -            | D                 | B                   | B                   | -                              | D    | -             | D         | B            | B                     | D                              | -           | D   | -       | B            | C             | -     | D               | A             | A    | A    | -                                 | B      | D        |
| Almond Oil (Artificial)             | -        | -            | -                 | B                   | B                   | -                              | D    | -             | B         | D            | D                     | -                              | -           | D   | -       | D            | D             | -     | D               | -             | A    | -    | C                                 | -      | D        |
| Alum (Aluminum Potassium Sulfate)   | C        | -            | D                 | B                   | -                   | A                              | A    | -             | A         | D            | A                     | -                              | B           | D   | -       | A            | A             | C     | A               | A             | A    | A    | A                                 | A      | D        |
| Aluminum Acetate (Burov's Solution) | A        | -            | D                 | C                   | B                   | A                              | C    | -             | A         | D            | D                     | D                              | B           | -   | -       | B            | -             | A     | C               | A             | A    | -    | A                                 | A      | D        |
| Aluminum Ammonium Sulfate           | -        | -            | -                 | -                   | -                   | -                              | -    | -             | A         | -            | A                     | -                              | -           | -   | -       | A            | A             | -     | A               | A             | A    | A    | B                                 | -      | -        |
| Aluminum Bromide                    | -        | -            | -                 | -                   | -                   | -                              | A    | -             | A         | -            | A                     | A                              | -           | D   | -       | A            | B             | -     | A               | -             | A    | A    | B                                 | -      | D        |
| Aluminum Chloride                   | D        | D            | D                 | D                   | C                   | B                              | A    | B             | A         | A            | A                     | A                              | A           | C   | -       | A            | A             | D     | A               | A             | A    | A    | A                                 | A      | B        |



# CHEMICAL COMPATIBILITY

| CHEMICALS                       | METALS   |              |                   |                     |                     | PLASTICS, ELASTOMERS & LEATHER |      |               |           |              |                       |                                |             |     |         |              |               |       |                 |               |      |      |                                   |        |          |   |
|---------------------------------|----------|--------------|-------------------|---------------------|---------------------|--------------------------------|------|---------------|-----------|--------------|-----------------------|--------------------------------|-------------|-----|---------|--------------|---------------|-------|-----------------|---------------|------|------|-----------------------------------|--------|----------|---|
|                                 | Aluminum | Carbon Steel | Cast/Ductile Iron | 304 Stainless Steel | 316 Stainless Steel | Acetal                         | Buna | CSM (Hypalon) | EPR, EPDM | Fluorocarbon | Fluoroelastomer (FKM) | Geolast (Buna & Polypropylene) | Hastelloy C | TPE | Leather | Nitrile (TS) | Nitrile (TPE) | Nylon | Polychloroprene | Polypropylene | PTFE | PVDF | Santoprene (EPDM & Polypropylene) | UHMWPE | Urethane |   |
| Hydrofluoric Acid (Hot)         | D        | D            | D                 | D                   | B                   | D                              | D    | -             | D         | -            | C                     | -                              | -           | -   | -       | -            | -             | D     | D               | D             | D    | A    | A                                 | -      | D        | - |
| Hydrofluoric Acid 100%          | D        | D            | D                 | D                   | B                   | D                              | D    | B             | D         | -            | D                     | D                              | D           | -   | D       | D            | D             | D     | D               | D             | D    | A    | A                                 | D      | -        | D |
| Hydrofluoric Acid 20%           | D        | D            | D                 | D                   | D                   | D                              | D    | B             | D         | -            | A                     | D                              | D           | D   | -       | D            | D             | C     | D               | A             | A    | A    | D                                 | A      | D        |   |
| Hydrofluoric Acid 50%           | D        | D            | D                 | D                   | D                   | D                              | D    | B             | D         | -            | B                     | D                              | D           | D   | -       | D            | D             | D     | D               | B             | A    | A    | D                                 | A      | D        |   |
| Hydrofluoric Acid 75%           | D        | D            | D                 | D                   | D                   | D                              | D    | B             | D         | -            | D                     | D                              | D           | D   | -       | D            | D             | D     | D               | C             | A    | A    | D                                 | -      | D        |   |
| Hydrofluosilicic Acid 100%      | D        | D            | D                 | D                   | A                   | B                              | B    | B             | B         | -            | A                     | B                              | B           | B   | -       | B            | D             | D     | B               | A             | A    | A    | B                                 | A      | D        |   |
| Hydrofluosilicic Acid 20%       | D        | B            | D                 | C                   | D                   | B                              | B    | B             | A         | -            | A                     | B                              | B           | -   | -       | -            | -             | D     | B               | A             | A    | A    | -                                 | -      | -        |   |
| Hydrogen Chloride Gas           | D        | -            | A                 | A                   | -                   | -                              | -    | -             | A         | -            | A                     | -                              | A           | -   | -       | D            | B             | -     | B               | A             | A    | A    | B                                 | -      | -        |   |
| Hydrogen Chloride Gas Dry       | D        | -            | B                 | A                   | A                   | -                              | -    | -             | -         | -            | -                     | -                              | -           | -   | -       | -            | -             | -     | -               | A             | A    | A    | -                                 | -      | -        |   |
| Hydrogen Chloride Gas Wet       | D        | -            | B                 | D                   | B                   | -                              | -    | -             | -         | -            | -                     | -                              | -           | -   | -       | -            | -             | -     | -               | A             | A    | A    | -                                 | -      | -        |   |
| Hydrogen Cyanide                | A        | B            | B                 | B                   | A                   | -                              | -    | -             | -         | -            | -                     | -                              | -           | D   | -       | -            | -             | B     | -               | A             | A    | A    | A                                 | -      | -        |   |
| Hydrogen Cyanide Gas            | D        | -            | A                 | B                   | -                   | -                              | -    | -             | A         | -            | A                     | -                              | -           | D   | -       | B            | A             | -     | D               | A             | A    | A    | A                                 | -      | D        |   |
| Hydrogen Fluoride               | D        | -            | -                 | D                   | -                   | -                              | D    | -             | C         | A            | A                     | -                              | A           | D   | -       | D            | D             | D     | C               | A             | B    | A    | -                                 | D      |          |   |
| Hydrogen Fluoride Anhydrous     | D        | D            | D                 | B                   | A                   | -                              | -    | -             | -         | -            | -                     | -                              | -           | -   | -       | -            | -             | D     | -               | A             | A    | A    | -                                 | -      |          |   |
| Hydrogen Gas                    | A        | A            | A                 | A                   | A                   | C                              | A    | A             | B         | -            | A                     | A                              | A           | A   | -       | A            | A             | B     | A               | A             | A    | A    | A                                 | A      | A        |   |
| Hydrogen Peroxide - 10%         | A        | C            | C                 | B                   | B                   | D                              | D    | D             | B         | A            | A                     | -                              | A           | D   | -       | -            | -             | D     | D               | A             | A    | A    | -                                 | A      | -        |   |
| Hydrogen Peroxide - 100%        | A        | B            | D                 | B                   | A                   | D                              | D    | D             | D         | -            | A                     | D                              | A           | D   | -       | B            | C             | D     | D               | B             | A    | A    | A                                 | A      | C        |   |
| Hydrogen Peroxide - 3%          | A        | -            | -                 | -                   | -                   | D                              | B    | -             | B         | A            | A                     | -                              | -           | D   | -       | -            | -             | D     | D               | A             | A    | A    | A                                 | A      | -        |   |
| Hydrogen Peroxide - 30%         | A        | B            | D                 | B                   | B                   | D                              | D    | D             | B         | A            | A                     | D                              | A           | D   | -       | -            | -             | D     | D               | B             | A    | A    | -                                 | A      | -        |   |
| Hydrogen Peroxide - 5%          | -        | -            | -                 | -                   | -                   | -                              | -    | -             | -         | -            | -                     | -                              | -           | -   | -       | -            | -             | -     | -               | -             | -    | -    | -                                 | -      | -        |   |
| Hydrogen Peroxide - 50%         | A        | -            | -                 | B                   | A                   | D                              | D    | D             | B         | -            | A                     | D                              | A           | -   | -       | -            | -             | D     | D               | B             | A    | A    | -                                 | -      | -        |   |
| Hydrogen Peroxide - 90%         | A        | -            | D                 | A                   | -                   | D                              | D    | -             | C         | A            | A                     | -                              | -           | D   | -       | -            | -             | D     | D               | A             | A    | A    | -                                 | A      | -        |   |
| Hydrogen Sulfide (dry)          | B        | D            | D                 | C                   | A                   | -                              | D    | B             | B         | -            | D                     | -                              | A           | A   | -       | -            | -             | C     | A               | A             | A    | A    | -                                 | -      | -        |   |
| Hydrogen Sulfide (wet)          | D        | D            | D                 | C                   | A                   | C                              | D    | D             | B         | D            | D                     | D                              | A           | A   | -       | D            | D             | D     | C               | A             | A    | A    | A                                 | A      | D        |   |
| Hydrogen Sulfide (Wet) (Cold)   | D        | -            | D                 | -                   | A                   | -                              | C    | -             | -         | -            | A                     | -                              | A           | -   | -       | -            | -             | C     | B               | A             | A    | A    | -                                 | -      | -        |   |
| Hydrogen Sulfide (Wet) (Hot)    | D        | -            | D                 | -                   | A                   | -                              | D    | -             | -         | -            | B                     | -                              | A           | -   | -       | -            | -             | D     | C               | A             | A    | A    | -                                 | -      | -        |   |
| Hydrogen Sulfide Dry            | B        | B            | D                 | C                   | A                   | A                              | -    | -             | A         | -            | D                     | -                              | A           | A   | A       | A            | D             | C     | A               | A             | A    | A    | A                                 | A      | A        |   |
| Hydrolube-Water/Ethylene Glycol | A        | -            | A                 | A                   | -                   | D                              | -    | -             | A         | -            | A                     | -                              | A           | B   | -       | A            | A             | -     | B               | A             | A    | A    | A                                 | -      | D        |   |
| Hydroquinone                    | B        | -            | B                 | B                   | B                   | A                              | D    | D             | D         | C            | C                     | D                              | B           | -   | -       | D            | C             | D     | D               | A             | A    | A    | A                                 | A      | -        |   |
| Hydroxyacetic Acid              | D        | -            | B                 | B                   | -                   | C                              | -    | -             | A         | -            | D                     | A                              | -           | -   | -       | D            | D             | -     | D               | -             | A    | -    | A                                 | -      | D        |   |
| Hydroxyacetic Acid --- 10%      | B        | -            | -                 | B                   | -                   | -                              | D    | -             | -         | -            | -                     | -                              | -           | -   | -       | -            | -             | -     | D               | -             | A    | -    | A                                 | -      | -        |   |
| Hydroxyacetic Acid 70%          | D        | B            | B                 | -                   | -                   | A                              | A    | -             | A         | -            | A                     | -                              | -           | -   | -       | -            | -             | -     | A               | -             | A    | A    | -                                 | -      | -        |   |
| Hydlyne                         | -        | -            | -                 | -                   | -                   | -                              | -    | -             | A         | -            | D                     | -                              | -           | -   | -       | B            | B             | -     | B               | -             | A    | -    | D                                 | -      | -        |   |
| Hypochlorous Acid               | D        | D            | D                 | D                   | D                   | D                              | D    | -             | B         | A            | A                     | D                              | A           | -   | -       | D            | D             | D     | D               | A             | A    | A    | A                                 | A      | D        |   |

# CHEMICAL COMPATIBILITY

| CHEMICALS                    | METALS   |              |                   |                     |                     | PLASTICS, ELASTOMERS & LEATHER |      |               |           |              |                       |                                |             |     |         |              |               |       |                 |               |      |      |                                   |        |          |   |
|------------------------------|----------|--------------|-------------------|---------------------|---------------------|--------------------------------|------|---------------|-----------|--------------|-----------------------|--------------------------------|-------------|-----|---------|--------------|---------------|-------|-----------------|---------------|------|------|-----------------------------------|--------|----------|---|
|                              | Aluminum | Carbon Steel | Cast/Ductile Iron | 304 Stainless Steel | 316 Stainless Steel | Acetal                         | Buna | CSM (Hypalon) | EPR, EPDM | Fluorocarbon | Fluoroelastomer (FKM) | Geolast (Buna & Polypropylene) | Hastelloy C | TPE | Leather | Nitrile (TS) | Nitrile (TPE) | Nylon | Polychloroprene | Polypropylene | PTFE | PVDF | Santoprene (EPDM & Polypropylene) | UHMWPE | Urethane |   |
| Polyvinyl Acetate Emulsion   | -        | -            | B                 | -                   | -                   | A                              | -    | -             | A         | -            | D                     | -                              | -           | -   | -       | -            | A             | B     | -               | C             | B    | A    | A                                 | A      | -        | - |
| Potash (Potassium Carbonate) | D        | C            | C                 | B                   | B                   | B                              | A    | -             | A         | -            | A                     | A                              | B           | D   | -       | -            | -             | A     | B               | A             | B    | A    | A                                 | A      | -        | - |
| Potassium Acetate            | D        | B            | B                 | B                   | B                   | A                              | B    | -             | A         | D            | D                     | A                              | B           | -   | -       | B            | B             | B     | B               | A             | A    | A    | A                                 | A      | A        | D |
| Potassium Aluminum Sulfate   | C        | -            | D                 | D                   | B                   | A                              | -    | -             | -         | -            | -                     | -                              | -           | -   | -       | -            | D             | -     | A               | A             | A    | A    | -                                 | A      | -        |   |
| Potassium Bicarbonate        | D        | B            | B                 | B                   | B                   | C                              | A    | -             | A         | A            | A                     | A                              | B           | -   | A       | A            | A             | A     | A               | A             | A    | A    | B                                 | A      | A        | D |
| Potassium Bichromate         | B        | -            | B                 | B                   | B                   | C                              | -    | -             | -         | -            | -                     | -                              | -           | B   | -       | -            | -             | D     | -               | A             | A    | B    | A                                 | -      | -        |   |
| Potassium Bisulfate          | A        | -            | D                 | A                   | -                   | A                              | -    | -             | A         | -            | A                     | -                              | -           | -   | -       | -            | -             | -     | A               | A             | A    | A    | -                                 | A      | -        |   |
| Potassium Bisulfite          | B        | -            | -                 | B                   | -                   | A                              | -    | A             | A         | A            | A                     | A                              | B           | -   | -       | A            | A             | -     | A               | A             | A    | -    | -                                 | -      | A        |   |
| Potassium Bromide            | D        | D            | D                 | D                   | B                   | A                              | A    | -             | A         | A            | A                     | A                              | B           | -   | A       | A            | A             | A     | A               | A             | A    | A    | A                                 | A      | D        |   |
| Potassium Carbonate (Potash) | D        | B            | B                 | B                   | B                   | B                              | A    | -             | A         | A            | A                     | -                              | B           | D   | -       | A            | A             | C     | B               | A             | A    | A    | A                                 | A      | D        |   |
| Potassium Chlorate           | D        | C            | C                 | B                   | B                   | B                              | A    | -             | A         | A            | A                     | A                              | B           | -   | A       | A            | A             | D     | A               | A             | A    | A    | A                                 | A      | A        |   |
| Potassium Chloride           | D        | D            | D                 | C                   | C                   | B                              | A    | A             | A         | A            | A                     | A                              | B           | D   | A       | A            | A             | B     | A               | A             | A    | A    | A                                 | A      | A        |   |
| Potassium Chromate           | B        | B            | B                 | B                   | B                   | D                              | A    | -             | A         | A            | A                     | A                              | A           | -   | A       | A            | A             | B     | A               | A             | A    | B    | A                                 | A      | B        |   |
| Potassium Copper Cyanide     | -        | -            | -                 | -                   | -                   | A                              | -    | A             | A         | -            | -                     | -                              | -           | -   | -       | -            | -             | -     | A               | A             | A    | A    | -                                 | -      | -        |   |
| Potassium Cupro Cyanide      | -        | -            | -                 | -                   | -                   | C                              | A    | -             | B         | -            | A                     | -                              | -           | -   | -       | A            | -             | -     | A               | A             | A    | A    | A                                 | -      | -        |   |
| Potassium Cyanide            | D        | B            | B                 | B                   | B                   | C                              | A    | A             | A         | A            | A                     | A                              | B           | B   | A       | A            | A             | A     | B               | A             | A    | A    | A                                 | A      | A        |   |
| Potassium Dichromate         | B        | B            | B                 | B                   | B                   | D                              | A    | A             | A         | A            | A                     | A                              | B           | C   | -       | A            | A             | D     | A               | A             | A    | A    | A                                 | A      | B        |   |
| Potassium Ferricyanide       | B        | C            | C                 | B                   | B                   | B                              | D    | A             | A         | -            | A                     | D                              | B           | -   | -       | C            | -             | B     | A               | A             | A    | A    | -                                 | A      | -        |   |
| Potassium Ferrocyanide       | B        | C            | C                 | B                   | B                   | B                              | D    | -             | A         | -            | A                     | D                              | B           | -   | -       | -            | -             | B     | A               | A             | A    | A    | -                                 | -      | -        |   |
| Potassium Hydrate            | D        | -            | B                 | A                   | B                   | -                              | -    | -             | -         | -            | -                     | -                              | -           | -   | -       | -            | -             | -     | -               | -             | A    | -    | -                                 | -      | -        |   |
| Potassium Hydroxide          | D        | B            | C                 | B                   | A                   | C                              | B    | A             | A         | B            | D                     | -                              | B           | D   | -       | B            | A             | D     | B               | A             | A    | A    | A                                 | A      | B        |   |
| Potassium Hypochlorite       | D        | A            | D                 | D                   | B                   | D                              | A    | A             | A         | -            | D                     | A                              | B           | -   | -       | B            | B             | B     | B               | D             | B    | B    | -                                 | -      | B        |   |
| Potassium Iodide             | B        | A            | A                 | B                   | A                   | -                              | A    | A             | A         | A            | A                     | A                              | B           | -   | -       | A            | B             | A     | A               | A             | A    | A    | -                                 | B      | -        |   |
| Potassium Nitrate            | B        | A            | B                 | B                   | B                   | B                              | A    | A             | A         | A            | A                     | A                              | B           | B   | A       | A            | A             | D     | A               | A             | A    | A    | A                                 | A      | A        |   |
| Potassium Nitrite            | B        | -            | B                 | B                   | -                   | A                              | -    | A             | A         | A            | -                     | B                              | -           | -   | -       | -            | -             | -     | A               | -             | A    | -    | -                                 | -      | -        |   |
| Potassium Oxalate            | B        | A            | A                 | B                   | B                   | -                              | -    | -             | -         | -            | -                     | -                              | A           | -   | -       | -            | -             | -     | -               | -             | A    | -    | -                                 | -      | -        |   |
| Potassium Permanganate       | B        | B            | B                 | B                   | B                   | C                              | C    | -             | A         | B            | A                     | D                              | A           | D   | -       | B            | D             | D     | C               | B             | A    | A    | A                                 | A      | B        |   |
| Potassium Phosphate          | D        | -            | D                 | B                   | -                   | A                              | -    | A             | A         | A            | A                     | -                              | B           | -   | -       | A            | -             | -     | A               | -             | A    | -    | -                                 | -      | C        |   |
| Potassium Salts              | -        | -            | -                 | -                   | -                   | -                              | -    | -             | A         | -            | A                     | -                              | -           | -   | -       | A            | A             | -     | A               | -             | A    | -    | -                                 | -      | A        |   |
| Potassium Silicate           | B        | -            | B                 | B                   | -                   | A                              | -    | A             | A         | A            | -                     | B                              | -           | -   | -       | -            | -             | -     | A               | -             | A    | -    | -                                 | -      | -        |   |
| Potassium Silicide           | -        | -            | -                 | -                   | -                   | -                              | -    | -             | -         | -            | -                     | -                              | -           | -   | -       | -            | -             | -     | -               | -             | -    | -    | -                                 | -      | -        |   |
| Potassium Sulfate            | C        | A            | B                 | B                   | B                   | B                              | A    | A             | A         | A            | A                     | A                              | B           | B   | -       | A            | A             | B     | A               | A             | A    | A    | A                                 | A      | A        |   |
| Potassium Sulfide            | D        | B            | B                 | B                   | B                   | -                              | A    | B             | A         | A            | A                     | A                              | B           | -   | -       | A            | A             | A     | A               | A             | A    | A    | A                                 | -      | A        | A |
| Potassium Sulfite            | A        | A            | D                 | B                   | A                   | -                              | A    | -             | A         | A            | A                     | -                              | -           | -   | -       | A            | A             | -     | A               | A             | A    | A    | -                                 | A      | A        |   |

# CHEMICAL COMPATIBILITY

| CHEMICALS                           | METALS   |              |                   |                     |                     | PLASTICS, ELASTOMERS & LEATHER |      |               |           |              |                       |                                |             |     |         |              |               |       |                 |               |      |      |                                   |        |          |   |
|-------------------------------------|----------|--------------|-------------------|---------------------|---------------------|--------------------------------|------|---------------|-----------|--------------|-----------------------|--------------------------------|-------------|-----|---------|--------------|---------------|-------|-----------------|---------------|------|------|-----------------------------------|--------|----------|---|
|                                     | Aluminum | Carbon Steel | Cast/Ductile Iron | 304 Stainless Steel | 316 Stainless Steel | Acetal                         | Buna | CSM (Hypalon) | EPR, EPDM | Fluorocarbon | Fluoroelastomer (FKM) | Geolast (Buna & Polypropylene) | Hastelloy C | TPE | Leather | Nitrile (TS) | Nitrile (TPE) | Nylon | Polychloroprene | Polypropylene | PTFE | PVDF | Santoprene (EPDM & Polypropylene) | UHMWPE | Urethane |   |
| Sulfur Dioxide (dry)                | B        | A            | A                 | D                   | A                   | B                              | D    | -             | A         | -            | A                     | -                              | B           | C   | -       | -            | -             | B     | D               | A             | A    | A    | -                                 | -      | -        |   |
| Sulfur Dioxide Gas Dry              | D        | -            | B                 | A                   | A                   | B                              | D    | -             | A         | -            | A                     | -                              | -           | D   | -       | -            | -             | B     | D               | C             | A    | A    | -                                 | -      | A        | - |
| Sulfur Dioxide Gas Wet              | -        | -            | -                 | -                   | -                   | C                              | D    | -             | A         | -            | A                     | -                              | -           | D   | -       | -            | -             | C     | B               | D             | A    | A    | -                                 | -      | A        | - |
| Sulfur Hexafluoride                 | D        | -            | D                 | -                   | -                   | D                              | B    | B             | B         | A            | C                     | B                              | D           | B   | -       | B            | C             | B     | B               | -             | A    | -    | B                                 | A      | B        |   |
| Sulfur Molten                       | -        | -            | -                 | -                   | -                   | D                              | -    | -             | -         | -            | -                     | -                              | -           | -   | -       | -            | -             | D     | -               | D             | A    | -    | -                                 | D      | -        |   |
| Sulfur Trioxide                     | D        | B            | D                 | B                   | C                   | -                              | D    | D             | C         | A            | A                     | D                              | B           | D   | -       | D            | D             | D     | D               | D             | A    | D    | D                                 | C      | C        |   |
| Sulfur Trioxide (dry)               | A        | A            | A                 | D                   | C                   | D                              | D    | -             | C         | -            | A                     | -                              | B           | -   | -       | -            | -             | A     | D               | D             | A    | D    | -                                 | -      | -        |   |
| Sulfuric Acid - (To 75%)            | D        | -            | D                 | C                   | -                   | D                              | -    | -             | C         | -            | A                     | -                              | A           | B   | -       | D            | D             | -     | D               | A             | A    | A    | A                                 | -      | D        |   |
| Sulfuric Acid - 10%                 | D        | -            | D                 | A                   | -                   | D                              | B    | -             | A         | A            | A                     | -                              | A           | D   | -       | -            | -             | D     | A               | A             | A    | A    | A                                 | D      | -        |   |
| Sulfuric Acid - 25%                 | D        | -            | D                 | B                   | -                   | D                              | C    | -             | B         | A            | A                     | -                              | A           | D   | -       | -            | -             | D     | B               | A             | A    | A    | A                                 | D      | -        |   |
| Sulfuric Acid - 50%                 | D        | -            | D                 | D                   | -                   | D                              | C    | -             | B         | A            | A                     | -                              | A           | D   | -       | -            | -             | D     | B               | A             | A    | A    | A                                 | D      | -        |   |
| Sulfuric Acid - 60%                 | D        | -            | D                 | D                   | -                   | D                              | D    | -             | C         | A            | A                     | -                              | A           | D   | -       | -            | -             | D     | C               | A             | A    | A    | A                                 | D      | -        |   |
| Sulfuric Acid - 75%                 | D        | -            | C                 | C                   | -                   | D                              | D    | -             | C         | A            | A                     | -                              | A           | D   | -       | -            | -             | D     | D               | A             | A    | A    | C                                 | D      | -        |   |
| Sulfuric Acid - 95%                 | D        | -            | B                 | A                   | -                   | D                              | D    | -             | C         | A            | A                     | -                              | A           | D   | -       | -            | -             | D     | D               | D             | A    | A    | C                                 | D      | -        |   |
| Sulfuric Acid - Concentrated        | -        | -            | -                 | -                   | -                   | D                              | D    | -             | D         | -            | A                     | -                              | -           | D   | -       | -            | -             | D     | D               | B             | A    | A    | D                                 | D      | -        |   |
| Sulfuric Acid (<10%)                | D        | C            | D                 | D                   | C                   | D                              | D    | A             | A         | -            | A                     | B                              | B           | A   | -       | D            | D             | C     | D               | A             | A    | A    | A                                 | A      | D        |   |
| Sulfuric Acid (10-75%)              | D        | D            | D                 | D                   | D                   | D                              | D    | B             | B         | -            | A                     | D                              | B           | -   | -       | -            | -             | D     | D               | A             | A    | A    | -                                 | -      |          |   |
| Sulfuric Acid (20% Oleum)           | D        | -            | D                 | -                   | -                   | D                              | -    | -             | -         | B            | -                     | -                              | -           | -   | -       | -            | D             | D     | D               | A             | -    | -    | -                                 | -      |          |   |
| Sulfuric Acid (75-100%)             | D        | D            | D                 | C                   | D                   | -                              | C    | C             | B         | -            | A                     | -                              | B           | C   | -       | -            | -             | D     | D               | C             | A    | A    | -                                 | -      |          |   |
| Sulfuric Acid (cold concentrated)   | B        | D            | D                 | C                   | B                   | -                              | D    | C             | C         | -            | B                     | -                              | A           | B   | -       | -            | -             | D     | D               | A             | A    | A    | -                                 | -      |          |   |
| Sulfuric Acid (Conc.)               | -        | -            | D                 | B                   | -                   | D                              | D    | -             | C         | A            | -                     | -                              | B           | -   | -       | -            | D             | D     | A               | A             | A    | B    | -                                 |        |          |   |
| Sulfuric Acid (Concentrated To 98%) | D        | -            | D                 | -                   | B                   | -                              | D    | -             | -         | -            | A                     | -                              | -           | -   | -       | -            | D             | D     | C               | A             | A    | -    | -                                 |        |          |   |
| Sulfuric Acid (Concentrated)        | D        | -            | D                 | C                   | -                   | D                              | -    | -             | C         | -            | A                     | -                              | B           | C   | -       | D            | D             | -     | D               | C             | A    | A    | B                                 | -      |          |   |
| Sulfuric Acid (Dilute)              | D        | -            | D                 | -                   | B                   | -                              | D    | -             | -         | -            | A                     | -                              | -           | -   | -       | -            | C             | C     | A               | A             | A    | -    | -                                 |        |          |   |
| Sulfuric Acid (Fuming)              | C        | -            | D                 | C                   | -                   | D                              | D    | -             | D         | -            | A                     | -                              | D           | D   | -       | D            | D             | D     | D               | A             | A    | D    | D                                 | D      |          |   |
| Sulfuric Acid (hot concentrated)    | D        | D            | D                 | D                   | C                   | -                              | D    | D             | D         | -            | A                     | -                              | D           | -   | -       | -            | D             | D     | D               | A             | C    | -    | -                                 |        |          |   |
| Sulfuric Acid Aerated               | -        | -            | -                 | -                   | -                   | D                              | -    | -             | -         | -            | -                     | -                              | -           | -   | -       | -            | D             | -     | C               | A             | D    | -    | D                                 |        |          |   |
| Sulfuric Acid Air Free              | -        | -            | -                 | -                   | -                   | D                              | -    | -             | -         | -            | -                     | -                              | -           | D   | -       | -            | -             | D     | -               | C             | A    | D    | A                                 | D      |          |   |
| Sulfuric Acid Boiling               | -        | -            | -                 | -                   | -                   | D                              | -    | -             | -         | -            | -                     | -                              | -           | -   | -       | -            | D             | -     | D               | A             | D    | -    | D                                 |        |          |   |
| Sulfuric Acid -Dilute               | D        | -            | D                 | B                   | -                   | D                              | -    | -             | A         | -            | A                     | -                              | A           | A   | -       | D            | D             | -     | C               | A             | A    | A    | A                                 | C      |          |   |
| Sulfuric Acid Fuming Oleum          | B        | D            | D                 | B                   | B                   | D                              | D    | -             | D         | -            | A                     | -                              | -           | D   | -       | -            | -             | D     | D               | D             | A    | D    | -                                 | D      |          |   |
| Sulfurous Acid                      | D        | D            | D                 | D                   | B                   | D                              | C    | A             | B         | -            | A                     | A                              | B           | C   | -       | -            | -             | D     | C               | A             | A    | A    | -                                 | A      |          |   |
| Sulfurous Acid                      | B        | -            | D                 | B                   | -                   | D                              | B    | -             | C         | A            | -                     | -                              | B           | -   | -       | -            | -             | D     | D               | A             | A    | A    | A                                 | A      |          |   |
| Sulfuryl Chloride                   | -        | -            | -                 | -                   | -                   | A                              | -    | -             | -         | -            | -                     | -                              | -           | -   | -       | -            | -             | -     | -               | -             | A    | -    | -                                 | -      |          |   |

# Hydrogen Peroxide Material Compatibility Chart

All wetted surfaces should be made of materials that are compatible with hydrogen peroxide. The wetted area or surface of a part, component, vessel or piping is a surface which is in permanent contact with or is permanently exposed to the process fluid (liquid or gas).

Less than 8% concentration H<sub>2</sub>O<sub>2</sub> is considered a non-hazardous substance. Typically encountered versions are baking soda-peroxide toothpaste (0.5%), contact lens sterilizer (2%), over-the-counter drug store Hydrogen Peroxide (3%), liquid detergent non-chlorine bleach (5%) and hair bleach (7.5%).

At 8% to 28% H<sub>2</sub>O<sub>2</sub> is rated as a Class 1 Oxidizer. At these concentrations H<sub>2</sub>O<sub>2</sub> is usually encountered as a swimming pool chemical used for pool shock treatments.

In the range of 28.1% to 52% concentrations, H<sub>2</sub>O<sub>2</sub> is rated as a Class 2 Oxidizer, a Corrosive and a Class 1 Unstable (reactive) substance. At these concentrations, H<sub>2</sub>O<sub>2</sub> is considered industrial strength grade.

Concentrations from 52.1% to 91% are rated as Class 3 Oxidizers, Corrosive and Class 3 Unstable (reactive) substances. H<sub>2</sub>O<sub>2</sub> at these concentrations are used for specialty chemical processes. At concentrations above 70%, H<sub>2</sub>O<sub>2</sub> is usually designated as high-test peroxide (HTP).

Concentrations of H<sub>2</sub>O<sub>2</sub> greater than 91% are currently used as rocket propellant. At these concentrations, H<sub>2</sub>O<sub>2</sub> is rated as a Class 4 Oxidizer, Corrosive and a Class 3 Unstable (reactive) substance.

| Material   | Compatibility<br>10% H <sub>2</sub> O <sub>2</sub> | Compatibility<br>30% H <sub>2</sub> O <sub>2</sub> | Compatibility<br>50% H <sub>2</sub> O <sub>2</sub> | Compatibility<br>100% H <sub>2</sub> O <sub>2</sub> (HTC) |
|--|--|--|--|---|
| <b>Chemical resistance data is based on 72° F (22° C) unless otherwise noted</b> |  |  |  |   |
| <b>A- Suitable</b>   |  |  |  |   |
| <b>B - Good, minor effect, slight corrosion or discoloration</b>                 |  |  |  |   |
| <b>F - Fair, moderate effect, not recommended for continuous use;</b>            |  |  |  |   |
| <b>softening, loss of strength, and/or swelling may occur</b>                    |  |  |  |   |
| <b>X - Do Not Use - severe effect, not recommended for ANY use</b>               |  |  |  |   |
| <b>NA - Information Not Available</b>  |  |  |  |   |
| 304 stainless steel  | B <sup>1</sup>                                     | B <sup>1</sup>                                     | B <sup>1</sup>                                     | B <sup>1</sup>  |
| 316 stainless steel  | B  | B  | A <sup>1</sup>                                     | A <sup>1</sup>  |
| 416 stainless steel  | B  | B  | F  | X   |
| 440C stainless steel   | B  | B  | A  | X   |
| ABS plastic  | A  | A  | A  | A   |

*It is the sole responsibility of the system designer and user to select products suitable for their specific application requirements and to ensure proper installation, operation, and maintenance of these products. Material compatibility, product ratings and application details should be considered in the selection. Improper selection or use of products described herein can cause personal injury or product damage. In applications where exposure to harmful chemicals is frequent, of long duration or in high concentrations, additional testing is recommended.*



End your search, simplify your supply chain  
ISO 9001:2015 Certified Companies

4091 S. Eliot St., Englewood, CO 80110-4396  
Phone 303-781-8486 | Fax 303-761-7939  
Ismedspec.com

© Copyright 2020 IS MED Specialties

# Hydrogen Peroxide Material Compatibility Chart

ver 09-Jul-2020

| Material   | Compatibility<br>10% H <sub>2</sub> O <sub>2</sub> | Compatibility<br>30% H <sub>2</sub> O <sub>2</sub> | Compatibility<br>50% H <sub>2</sub> O <sub>2</sub> | Compatibility<br>100% H <sub>2</sub> O <sub>2</sub> (HTC) |
|--|--|--|--|---|
| <b>Chemical resistance data is based on 72° F (22° C) unless otherwise noted</b> |  |  |  |   |
| <b>A- Suitable</b>   |  |  |  |   |
| <b>B - Good, minor effect, slight corrosion or discoloration</b>                 |  |  |  |   |
| <b>F - Fair, moderate effect, not recommended for continuous use;</b>            |  |  |  |   |
| <b>softening, loss of strength, and/or swelling may occur</b>                    |  |  |  |   |
| <b>X - Do Not Use - severe effect, not recommended for ANY use</b>               |  |  |  |   |
| <b>NA - Information Not Available</b>  |  |  |  |   |
| <b>1 - Satisfactory to 120°F (48° C)</b>   |  |  |  |   |
| <b>2 - Satisfactory for O-rings, diaphragms or gaskets</b>                       |  |  |  |   |
| <b>3 - Temporary use only</b>  |  |  |  |   |
| Acetal (Delrin®)   | X  | X  | X  | X   |
| Acrylic (PMMA)   | B  | F  | NA   | X   |
| Alloy 20 (Carpenter 20)  | F  | B  | B  | X   |
| Aluminum   | A  | A  | A  | A   |
| Brass  | X  | X  | X  | X   |
| Bronze   | B  | B  | B  | B   |
| Buna N (Nitrile)   | X  | X  | X  | X   |
| Carbon graphite  | F  | F  | F  | F   |
| Carbon steel   | X  | X  | X  | X   |
| Cast iron  | F  | X  | X  | X   |
| Ceramic Al <sub>2</sub> O <sub>3</sub>   | A  | A  | A  | A   |
| Ceramic magnet   | A  | A  | A  | A   |
| Copper   | X  | X  | X  | X   |
| CPVC   | A  | A  | A  | A   |
| EPDM   | A  | B  | B  | X   |
| Epoxy (epoxide polymers)   | F  | B  | B  | X   |
| FKM (fluoroelastomers, Viton®)   | A  | A  | A  | A   |
| Hastelloy-C®   | A  | A  | A  | A   |
| HDPE   | A  | A  | A  | X   |
| Hypalon®   | X  | X  | X  | X   |
| Hytre® (polyester elastomer)   | X  | X  | X  | X   |
| LDPE   | A  | F <sup>1</sup>                                     | F <sup>1</sup>                                     | F <sup>1</sup>  |
| Natural rubber   | B  | F  | F  | F   |
| Neoprene   | X  | X  | X  | X   |
| NORYL®   | A <sup>1</sup>                                     | A <sup>1</sup>                                     | A  | A   |

*It is the sole responsibility of the system designer and user to select products suitable for their specific application requirements and to ensure proper installation, operation, and maintenance of these products. Material compatibility, product ratings and application details should be considered in the selection. Improper selection or use of products described herein can cause personal injury or product damage. In applications where exposure to harmful chemicals is frequent, of long duration or in high concentrations, additional testing is recommended.*



End your search, simplify your supply chain  
ISO 9001:2015 Certified Companies

4091 S. Eliot St., Englewood, CO 80110-4396  
Phone 303-781-8486 | Fax 303-761-7939  
Ismedspec.com

© Copyright 2020 IS MED Specialties

# Hydrogen Peroxide Material Compatibility Chart

ver 09-Jul-2020

| Material   | Compatibility<br>10% H <sub>2</sub> O <sub>2</sub> | Compatibility<br>30% H <sub>2</sub> O <sub>2</sub> | Compatibility<br>50% H <sub>2</sub> O <sub>2</sub> | Compatibility<br>100% H <sub>2</sub> O <sub>2</sub> (HTC) |
|--|--|--|--|---|
| <b>Chemical resistance data is based on 72° F (22° C) unless otherwise noted</b>   |  |  |  |   |
| <b>A- Suitable</b>   |  |  |  |   |
| <b>B - Good, minor effect, slight corrosion or discoloration</b>   |  |  |  |   |
| <b>F - Fair, moderate effect, not recommended for continuous use; softening, loss of strength, and/or swelling may occur</b> |  |  |  |   |
| <b>X - Do Not Use - severe effect, not recommended for ANY use</b>   |  |  |  |   |
| <b>NA - Information Not Available</b>  |  |  |  |   |
| Nylon (polyamides)   | F  | X  | X  | X   |
| PCTFE (Kel-F® and Neoflon®)  | A <sup>1</sup>                                     | A <sup>1</sup>                                     | A <sup>1</sup>                                     | X   |
| PFA (perfluoroalkoxy alkanes)  | A  | A  | A  | A   |
| Polycarbonate  | A <sup>1</sup>                                     | A <sup>1</sup>                                     | A <sup>1</sup>                                     | A   |
| Polypropylene  | A  | B  | B  | B   |
| PP-363 (plasticized vinyl) <sup>2</sup>  | A  | A  | A  | X   |
| PPS (Ryton®)   | A  | A  | F  | F   |
| PTFE (Garlock Glyon® 3500) <sup>2</sup>  | A  | A  | A  | X   |
| PTFE (Teflon®), virgin <sup>2</sup>  | A  | A  | A  | A   |
| PVC  | A  | A  | A  | A   |
| PVDF (Hylar®)  | A <sup>1</sup>                                     | A <sup>1</sup>                                     | X  | X   |
| PVDF (Kynar®)  | A  | A  | A  | A   |
| PVDF (Solef®)  | A <sup>1</sup>                                     | A <sup>1</sup>                                     | X  | X   |
| Silicone   | A  | B  | B  | B   |
| SPR (styrene butadiene rubber)   | X  | X  | X  | X   |
| Thiokol™ (polysulfide polymers)  | X  | X  | X  | X   |
| Titanium <sup>3</sup>  | A  | B  | B  | B   |
| TPE (thermoplastic elastomers)   | X  | X  | X  | X   |
| TPU (thermoplastic polyurethanes)  | X  | X  | X  | X   |
| Tygon®   | B  | B  | B  | B   |
| Tungsten carbide   | X  | X  | X  | X   |
| Viton® A <sup>2</sup>  | A  | A  | A  | A   |

*It is the sole responsibility of the system designer and user to select products suitable for their specific application requirements and to ensure proper installation, operation, and maintenance of these products. Material compatibility, product ratings and application details should be considered in the selection. Improper selection or use of products described herein can cause personal injury or product damage. In applications where exposure to harmful chemicals is frequent, of long duration or in high concentrations, additional testing is recommended.*



End your search, simplify your supply chain  
ISO 9001:2015 Certified Companies

4091 S. Eliot St., Englewood, CO 80110-4396  
Phone 303-781-8486 | Fax 303-761-7939  
Ismedspec.com

© Copyright 2020 IS MED Specialties

## **-6 90% Hydrogen Peroxide Safety Sheet**

# SAFETY DATA SHEET

## Hydrogen Peroxide 90% HTP

SDS # : 7722-84-1-90-60  
Revision date: 2015-05-28  
Format: NA  
Version 1



### 1. PRODUCT AND COMPANY IDENTIFICATION

#### Product Identifier

**Product Name** Hydrogen Peroxide 90% HTP

#### Other means of identification

**CAS-No** 7722-84-1

#### Recommended use of the chemical and restrictions on use

**Recommended Use:** Monopropellant and bipropellant systems; fuel for rocket engines; rocket boosters / propellants / power source for aircraft; steam generation; rapid source of heat; electronics IC circuits and other military uses

**Restrictions on Use:** Use as recommended by the label.

#### Manufacturer/Supplier

PeroxyChem LLC  
2005 Market Street  
Suite 3200  
Philadelphia, PA 19103  
Phone: +1 267/ 422-2400 (General Information)  
E-Mail: sdsinfo@peroxychem.com

PeroxyChem Canada  
PG Pulp Mill Road  
Prince George, BC V2N2S6  
1+ 250/ 561-4200 (General Information)

#### Emergency telephone number

For leak, fire, spill or accident emergencies, call:  
1 800 / 424 9300 (CHEMTREC - U.S.A.)  
1 703 / 527 3887 (CHEMTREC - Collect - All Other Countries)  
1 613/ 996-6666 (CANUTEC - Canada)  
1 303/ 389-1409 (Medical - U.S. - Call Collect)

1 281 / 474-8750 (Bayport, Texas Plant)  
1 250 / 561-4221 (Prince George, BC, Canada Plant)

### 2. HAZARDS IDENTIFICATION

#### Classification

#### **OSHA Regulatory Status**

This material is considered hazardous by the OSHA Hazard Communication Standard (29 CFR 1910.1200).

|                                      |                           |
|--------------------------------------|---------------------------|
| Acute toxicity - Oral                | Category 4                |
| Acute toxicity - Inhalation (Vapors) | Category 4                |
| Skin corrosion/irritation            | Category 1 Sub-category A |



# Hydrogen Peroxide 90% HTP

SDS # : 7722-84-1-90-60  
Revision date: 2015-05-28  
Version 1


|  |            |
|--|------------|
| Serious eye damage/eye irritation                | Category 1 |
| Specific target organ toxicity (single exposure) | Category 3 |
| Oxidizing Liquids                                | Category 1 |

## GHS Label elements, including precautionary statements

### EMERGENCY OVERVIEW

**Danger**

**Hazard Statements**  
H314 - Causes severe skin burns and eye damage  
H302 - Harmful if swallowed  
H332 - Harmful if inhaled  
H335 - May cause respiratory irritation  
H272 - May intensify fire; oxidizer



#### **Precautionary Statements - Prevention**

- P271 - Use only outdoors or in a well-ventilated area
- P260 - Do not breathe mist, vapours or spray.
- P280 - Wear protective gloves/ protective clothing/ eye protection/ face protection
- P283 - Wear fire/ flame resistant/ retardant clothing
- P210 - Keep away from heat/sparks/open flames/hot surfaces. - No smoking
- P220 - Keep/Store away from clothing/flammable materials/combustibles
- P221 - Take any precaution to avoid mixing with combustibles/flammables

#### **Precautionary Statements - Response**

- P305 + P351 + P338 - IF IN EYES: Rinse cautiously with water for several minutes. Remove contact lenses, if present and easy to do. Continue rinsing
- P310 - Immediately call a POISON CENTER or doctor
- P303 + P361 + P353 - IF ON SKIN (or hair): Take off immediately all contaminated clothing. Rinse skin with water/ shower
- P306 + P360 - IF ON CLOTHING: rinse immediately contaminated clothing and skin with plenty of water before removing clothes
- P304 + P340 - IF INHALED: Remove person to fresh air and keep comfortable for breathing
- P312 - Call a POISON CENTER or doctor if you feel unwell
- P301 + P330 + P331 - IF SWALLOWED: rinse mouth. Do NOT induce vomiting
- P310 - Immediately call a POISON CENTER or doctor
- P370 + P378 - In case of fire: Use water for extinction
- P371 + P380 + P375 - In case of major fire and large quantities: Evacuate area. Fight fire remotely due to the risk of explosion

#### **Hazards not otherwise classified (HNOC)**

No hazards not otherwise classified were identified.

#### **Other Information**

Keep container in a cool place out of direct sunlight. Store only in vented containers. Do not store on wooden pallets. Do not return unused material to its original container. Avoid contamination - Contamination could cause decomposition and generation of oxygen which may result in high pressure and possible container rupture. Empty drums should be triple rinsed with water before discarding. .

**3. COMPOSITION/INFORMATION ON INGREDIENTS**

Formula HO - OH

| Chemical name     | CAS-No    | Weight % |
|-------------------|-----------|----------|
| Hydrogen peroxide | 7722-84-1 | 90       |
| Water             | 7732-18-5 | 10       |

Occupational exposure limits, if available, are listed in section 8

**4. FIRST AID MEASURES**

|   |   |
|---|---|
| <b>Eye Contact</b>  | Rinse immediately with plenty of water, also under the eyelids, for at least 15 minutes. Remove contact lenses, if present, after the first 5 minutes, then continue rinsing. Seek immediate medical attention/advice.  |
| <b>Skin Contact</b>   | Take off contaminated clothing. Rinse skin immediately with plenty of water for 15-20 minutes. Call a poison control center or doctor for further treatment advice.   |
| <b>Inhalation</b>   | Move to fresh air. If person is not breathing, contact emergency medical services, then give artificial respiration, preferably mouth-to-mouth if possible. Call a poison control center or doctor for further treatment advice.  |
| <b>Ingestion</b>  | Rinse mouth. Do not induce vomiting. If conscious, give 2 glasses of water. Get immediate medical attention. Never give anything by mouth to an unconscious person.   |
| <b>Most important symptoms and effects, both acute and delayed</b>                          | Hydrogen Peroxide irritates respiratory system and, if inhaled, may cause inflammation and pulmonary edema. The effects may not be immediate. In case of accidental ingestion, necrosis may result from mucous membrane burns (mouth, esophagus and stomach). Oxygen rapid release may cause stomach swelling and hemorrhaging, which may produce major, or even fatal, injury to organs if a large amount has been ingested. Corneal lesions and irreversible damage if contact with the eyes  |
| <b>Indication of immediate medical attention and special treatment needed, if necessary</b> | Hydrogen peroxide at these concentrations is a strong oxidant. Direct contact with the eye is likely to cause corneal damage especially if not washed immediately. Careful ophthalmologic evaluation is recommended and the possibility of local corticosteroid therapy should be considered. Because of the likelihood of corrosive effects on the gastrointestinal tract after ingestion, and the unlikelihood of systemic effects, attempts at evacuating the stomach via emesis induction or gastric lavage should be avoided. There is a remote possibility, however, that a nasogastric or orogastric tube may be required for the reduction of severe distension due to gas formation. |

**5. FIRE-FIGHTING MEASURES**

|   |  |
|---|--|
| <b>Suitable Extinguishing Media</b>               | Water. Do not use any other substance.   |
| <b>Specific Hazards Arising from the Chemical</b> | In closed unventilated containers, risk of rupture due to the increased pressure from decomposition. Contact with combustible material may cause fire. Non-flammable but vapor phase decomposition occurs at 7.6 vol. % for 90% based on flash point.  |
| <b>Hazardous Combustion Products</b>              | A severe detonation hazard when mixed with organics. Contact with combustibles will cause fire. While not flammable by OSHA and DOT definitions, contamination, contact with incompatible materials, or high temperatures could cause a rapid decomposition that yields heat and oxygen, which support combustion and will cause a rapid overpressure if confined. |
| <b>Explosion data</b>                             |  |
| <b>Sensitivity to Mechanical Impact</b>           | Not sensitive.   |
| <b>Sensitivity to Static Discharge</b>            | Static discharge can potentially initiate decomposition in vapor mixtures.   |
| <b>Protective equipment and</b>                   | Use water spray to cool fire exposed surfaces and protect personnel. Move containers from  |

**precautions for firefighters** fire area if you can do it without risk. As in any fire, wear self-contained breathing apparatus and full protective gear.

**6. ACCIDENTAL RELEASE MEASURES**

**Personal Precautions** Avoid contact with skin, eyes and clothing. Wear personal protective equipment. Isolate and post spill area. Keep people away from and upwind of spill/leak. Eliminate all sources of ignition and remove combustible materials.

**Other** Combustible materials exposed to hydrogen peroxide should be immediately submerged in or rinsed with large amounts of water to ensure that all hydrogen peroxide is removed. Residual hydrogen peroxide that is allowed to dry (upon evaporation hydrogen peroxide can concentrate) on organic materials such as paper, fabrics, cotton, leather, wood or other combustibles can cause the material to ignite and result in fire.

**Environmental Precautions** Prevent material from entering into soil, ditches, sewers, waterways, and/or groundwater. See Section 12, Ecological Information for more detailed information.

**Methods for Containment** Dike to collect large liquid spills. Stop leak and contain spill if this can be done safely. Small spillage: Dilute with large quantities of water.

**Methods for cleaning up** Flush area with flooding quantities of water. Hydrogen peroxide may be decomposed by adding sodium metabisulfite or sodium sulfite after diluting to about 5%.

**7. HANDLING AND STORAGE**

**Handling** CONSULT PEROXYCHEM FOR APPROVED PERSONAL PROTECTIVE EQUIPMENT AND HANDLING AND STORAGE PROCEDURES. Wear chemical splash-type monogoggles and full face shield, Gortex®, polyester or acrylic full cover clothing and approved rubber or nitrile gloves and shoes. Do not use cotton, wool or leather for these materials react rapidly with hydrogen peroxide concentrations greater than 90%. Avoid contamination and heat as these will cause decomposition and generation of oxygen gas which will result in high pressures and possible container rupture. Hydrogen peroxide should be stored only in vented containers and transferred only in a prescribed manner (contact Peroxychem for procedures). Never return unused hydrogen peroxide to original container. Empty aluminum drums should be returned to Peroxychem. Utensils used for handling hydrogen peroxide should be made only of clean glass, pre-approved passivated aluminum or stainless steel, or approved plastics such as polytetrafluoroethylene. Do not discard 90% or higher concentrations without first diluting to less than 5%.

**Storage** Keep containers in cool areas out of direct sunlight and away from combustibles. Provide mechanical general and/or local exhaust ventilation to prevent release of vapor or mist into work environment. Containers must be vented. Keep/store only in original container. Store rooms or warehouses should be made of non-combustible materials with impermeable floors. In case of release, spillage should flow to safe area. Containers should be visually inspected on a regular basis to detect any abnormalities (swollen drums, increases in temperature, etc.).

**Incompatible products** Combustible materials. Copper alloys, galvanized iron. Strong reducing agents. Heavy metals. Iron. Copper alloys. Contact with metals, metallic ions, alkalis, reducing agents and organic matter (such as alcohols or terpenes) may produce self-accelerated thermal decomposition.

**8. EXPOSURE CONTROLS/PERSONAL PROTECTION**

Control parameters

**Exposure Guidelines** Ingredients with workplace control parameters.

| Chemical name                  | ACGIH TLV  | OSHA PEL                                 | NIOSH  | Mexico   |
|--------------------------------|------------|--|--|--|
| Hydrogen peroxide<br>7722-84-1 | TWA: 1 ppm | TWA: 1 ppm<br>TWA: 1.4 mg/m <sup>3</sup> | IDLH: 75 ppm<br>TWA: 1 ppm<br>TWA: 1.4 mg/m <sup>3</sup> | Mexico: TWA 1 ppm<br>Mexico: TWA 1.5 mg/m <sup>3</sup><br>Mexico: STEL 2 ppm |

## Hydrogen Peroxide 90% HTP

SDS # : 7722-84-1-90-60  
Revision date: 2015-05-28  
Version 1

| Chemical name                  | British Columbia | Quebec                                   | Ontario TWAEV | Mexico: STEL 3 mg/m <sup>3</sup><br>Alberta |
|--------------------------------|------------------|--|---------------|---|
| Hydrogen peroxide<br>7722-84-1 | TWA: 1 ppm       | TWA: 1 ppm<br>TWA: 1.4 mg/m <sup>3</sup> | TWA: 1 ppm    | TWA: 1 ppm<br>TWA: 1.4 mg/m <sup>3</sup>    |

### Appropriate engineering controls

**Engineering measures** Showers. Eyewash stations. Ventilation systems.

### Individual protection measures, such as personal protective equipment

**Eye/Face Protection** Use chemical splash-type monogoggles and a full-face shield made of polycarbonate, acetate, polycarbonate/acetate, PETG or thermoplastic.

**Skin and Body Protection** For body protection wear impervious clothing such as an approved splash protective suit made of SBR rubber, PVC (PVC Outershell w/Polyester Substrate), Gore-Tex (Polyester trilaminate w/Gore-Tex), or a specialized HAZMAT Splash or Protective Suite (Level A, B, or C). DO NOT wear any form of splash suit or rainwear made of nylon or nylon-blends. For foot protection, wear approved boots made of NBR, PVC, Polyurethane, or neoprene. Overboots made of Latex or PVC, as well as firefighter boots or specialized HAZMAT boots are also permitted. DO NOT wear any form of boot or overboot made of nylon or nylon blends. DO NOT USE cotton, wool or leather as these materials react RAPIDLY with 90% or higher concentrations of hydrogen peroxide. Completely submerge hydrogen peroxide contaminated clothing or other materials in water prior to drying. Residual hydrogen peroxide, if allowed to dry on materials such as paper, fabrics, cotton, leather, wood or other combustibles, can cause the material to ignite and result in a fire.

**Hand Protection** For hand protection, wear approved gloves made of nitrile, PVC, or neoprene. DO NOT use cotton, wool or leather for these materials react RAPIDLY with higher concentrations of hydrogen peroxide. Thoroughly rinse the outside of gloves with water prior to removal. Inspect regularly for leaks.

**Respiratory Protection** If concentrations in excess of 10 ppm are expected, use NIOSH/DHHS approved self-contained breathing apparatus (SCBA) or other approved air-supplied respirator (ASR) equipment (e.g., a full-face airline respirator (ALR)). DO NOT use any form of air-purifying respirator (APR) or filtering facepiece (dust mask), especially those containing oxidizable sorbants such as activated carbon.

**Hygiene measures** Avoid breathing vapors, mist or gas. Clean water should be available for washing in case of eye or skin contamination.

**General information** Protective engineering solutions should be implemented and in use before personal protective equipment is considered.

## 9. PHYSICAL AND CHEMICAL PROPERTIES

### Information on basic physical and chemical properties

|                                     |   |
|-------------------------------------|---|
| <b>Appearance</b>                   | Clear, colorless liquid   |
| <b>Physical State</b>               | Liquid  |
| <b>Color</b>                        | Colorless   |
| <b>Odor</b>                         | odorless  |
| <b>Odor threshold</b>               | Not applicable  |
| <b>pH</b>                           | <= 1  |
| <b>Melting point/freezing point</b> | -12 °C  |
| <b>Boiling Point/Range</b>          | 141 °C  |
| <b>Flash point</b>                  | Seta Closed Cup: (90% ) 82 - 85°C. No visible flame observed. Reaction attributed to rapid decomposition. |
| <b>Evaporation Rate</b>             | > 1 (n-butyl acetate=1)   |
| <b>Flammability (solid, gas)</b>    | Non-flammable but vapor phase decomposition occurs at 7.6 vol. % for 90 % based on flash point.           |
| <b>Flammability Limit in Air</b>    | Not applicable  |
| <b>Upper flammability limit:</b>    |   |

## Hydrogen Peroxide 90% HTP

SDS # : 7722-84-1-90-60  
Revision date: 2015-05-28  
Version 1

|                                     |  |
|-------------------------------------|--|
| <b>Lower flammability limit:</b>    |  |
| <b>Vapor pressure</b>               | 5 mm Hg @ 30 °C  |
| <b>Vapor density</b>                | No information available   |
| <b>Density</b>                      | 1.39 g/cm <sup>3</sup> @ 20°C  |
| <b>Specific gravity</b>             | 1.39   |
| <b>Water solubility</b>             | completely soluble   |
| <b>Solubility in other solvents</b> | No information available   |
| <b>Partition coefficient</b>        | No data available  |
| <b>Autoignition temperature</b>     | ASTM E 659-78: 99% - 210°C (in air) 169°C (in oxygen). Reaction was attributed to rapid decomposition of vapors. |
| <b>Decomposition temperature</b>    | 740 °C   |
| <b>Viscosity, kinematic</b>         | 1.15 cP @ 25 °C  |
| <b>Viscosity, dynamic</b>           | No information available   |
| <b>Explosive properties</b>         | No information available   |
| <b>Oxidizing properties</b>         | Powerful oxidizer  |
| <b>Molecular weight</b>             | 34   |
| <b>Bulk density</b>                 | Not applicable   |

## 10. STABILITY AND REACTIVITY

|   |  |
|---|--|
| <b>Reactivity</b>                         | Reactive and oxidizing agent.  |
| <b>Chemical Stability</b>                 | Stable under normal conditions. Decomposes on heating. Stable under recommended storage conditions.  |
| <b>Possibility of Hazardous Reactions</b> | A severe detonation hazard when mixed with organics. Contact with combustibles will cause fire. While not flammable by OSHA and DOT definitions, contamination, contact with incompatible materials, or high temperatures could cause a rapid decomposition that yields heat and oxygen, which support combustion and will cause a rapid overpressure if confined. |
| <b>Hazardous polymerization</b>           | Hazardous polymerization does not occur.   |
| <b>Conditions to avoid</b>                | Excessive heat; Contamination; Exposure to UV-rays; pH variations.   |
| <b>Incompatible materials</b>             | Combustible materials. Copper alloys, galvanized iron. Strong reducing agents. Heavy metals. Iron. Copper alloys. Contact with metals, metallic ions, alkalis, reducing agents and organic matter (such as alcohols or terpenes) may produce self-accelerated thermal decomposition.   |
| <b>Hazardous Decomposition Products</b>   | Oxygen which supports combustion. Liable to produce overpressure in container.   |

## 11. TOXICOLOGICAL INFORMATION

### Product Information

|                        |   |
|------------------------|---|
| <b>LD50 Oral</b>       | 50% solution: LD50: > 225 mg/kg bw (rat)<br>35 % solution: LD50 1193 mg/kg bw (rat)<br>70 % solution: LD50 1026 mg/kg bw (rat)  |
| <b>LD50 Dermal</b>     | 35% solution: LD50 > 2000 mg/kg bw (rabbit)<br>70 % solution: LD50 9200 mg/kg bw (rabbit)   |
| <b>LC50 Inhalation</b> | 50% solution: LC50 > 170 mg/m <sup>3</sup> (rat) (4-hr)<br>Hydrogen Peroxide vapors: LC0 9400 mg/m <sup>3</sup> (mouse) (5 - 15 minutes)<br>Hydrogen Peroxide vapors: LC50 > 2160 mg/m <sup>3</sup> (mouse) |
| <b>Sensitization</b>   | Did not cause sensitization on laboratory animals.  |

### Information on toxicological effects

|                 |   |
|-----------------|---|
| <b>Symptoms</b> | Vapors, mists, or aerosols of hydrogen peroxide can cause upper airway irritation, inflammation of the nose, hoarseness, shortness of breath, and a sensation of burning or tightness in the chest. Prolonged exposure to concentrated vapor or to dilute solutions can |
|-----------------|---|

## Hydrogen Peroxide 90% HTP

SDS # : 7722-84-1-90-60  
Revision date: 2015-05-28  
Version 1

cause irritation and temporary bleaching of skin and hair. Exposure to vapor, mist, or aerosol can cause stinging pain and tearing of eyes.

### Delayed and immediate effects as well as chronic effects from short and long-term exposure

**Carcinogenicity** This product contains hydrogen peroxide. The International Agency for Research on Cancer (IARC) has concluded that there is inadequate evidence for carcinogenicity of hydrogen peroxide in humans, but limited evidence in experimental animals (Group 3 - not classifiable as to its carcinogenicity to humans). The American Conference of Governmental Industrial Hygienists (ACGIH) has concluded that hydrogen peroxide is a 'Confirmed Animal Carcinogen with Unknown Relevance to Humans' (A3).

| Chemical name                  | ACGIH | IARC | NTP | OSHA |
|--------------------------------|-------|------|-----|------|
| Hydrogen peroxide<br>7722-84-1 | A3    | 3    |     |      |

**Mutagenicity** This product is not recognized as mutagenic by Research Agencies  
In vivo tests did not show mutagenic effects

**Reproductive toxicity** This product is not recognized as reprotox by Research Agencies.

**STOT - single exposure** May cause respiratory irritation.  
**STOT - repeated exposure** Not classified.

**Target organ effects** Eyes, Respiratory System, Skin.

**Aspiration hazard** Aspiration risk: may cause lung damage if swallowed.

## 12. ECOLOGICAL INFORMATION

### Ecotoxicity

**Ecotoxicity effects** Hydrogen peroxide is naturally produced by sunlight (between 0.1 and 4 ppb in air and 0.001 to 0.1 mg/L in water). Not expected to have significant environmental effects.

| Hydrogen peroxide (7722-84-1) |           |                            |       |       |
|-------------------------------|-----------|----------------------------|-------|-------|
| Active Ingredient(s)          | Duration  | Species                    | Value | Units |
| Hydrogen peroxide             | 96 h LC50 | Fish Pimephales promelas   | 16.4  | mg/L  |
| Hydrogen peroxide             | 72 h LC50 | Fish Leuciscus idus        | 35    | mg/L  |
| Hydrogen peroxide             | 48 h EC50 | Daphnia pulex              | 2.4   | mg/L  |
| Hydrogen peroxide             | 24 h EC50 | Daphnia magna              | 7.7   | mg/L  |
| Hydrogen peroxide             | 72 h EC50 | Algae Skeletonema costatum | 1.38  | mg/L  |
| Hydrogen peroxide             | 21 d NOEC | Daphnia magna              | 0.63  | mg/L  |

**Persistence and degradability** Hydrogen peroxide in the aquatic environment is subject to various reduction or oxidation processes and decomposes into water and oxygen. Hydrogen peroxide half-life in freshwater ranged from 8 hours to 20 days, in air from 10 - 20 hours, and in soils from minutes to hours depending upon microbiological activity and metal contamination.

**Bioaccumulation** Material may have some potential to bioaccumulate but will likely degrade in most environments before accumulation can occur.

**Mobility** Will likely be mobile in the environment due to its water solubility but will likely degrade over time.

**Other Adverse Effects** Decomposes into oxygen and water. No adverse effects.

**13. DISPOSAL CONSIDERATIONS**

|                               |  |
|-------------------------------|--|
| <b>Waste disposal methods</b> | Dispose of in accordance with local regulations. Can be disposed as waste water, when in compliance with local regulations.  |
| <b>US EPA Waste Number</b>    | D001 D002  |
| <b>Contaminated Packaging</b> | Dispose of in accordance with local regulations.<br>Drums - Empty as thoroughly as possible. Triple rinse drums before disposal. Avoid contamination; impurities accelerate decomposition. Never return product to original container. |

**14. TRANSPORT INFORMATION**

DOT

|                             |   |
|-----------------------------|---|
| <b>UN/ID no</b>             | 2015  |
| <b>Proper Shipping Name</b> | HYDROGEN PEROXIDE, AQUEOUS SOLUTION, STABILIZED |
| <b>Hazard class</b>         | 5.1 (Oxidizer)                                  |
| <b>Subsidiary class</b>     | 8   |
| <b>Packing Group</b>        | I   |

TDG

|                             |   |
|-----------------------------|---|
| <b>UN/ID no</b>             | UN 2015   |
| <b>Proper Shipping Name</b> | HYDROGEN PEROXIDE, AQUEOUS SOLUTION, STABILIZED |
| <b>Hazard class</b>         | 5.1 (Oxidizer)                                  |
| <b>Subsidiary class</b>     | 8   |
| <b>Packing Group</b>        | I   |

ICAO/IATA

Hydrogen peroxide (>40%) is forbidden on Passenger and Cargo Aircraft.

IMDG/IMO

|                                |   |
|--------------------------------|---|
| <b>UN/ID no</b>                | 2015  |
| <b>Proper Shipping Name</b>    | HYDROGEN PEROXIDE, AQUEOUS SOLUTION, STABILIZED |
| <b>Hazard class</b>            | 5.1   |
| <b>Subsidiary Hazard Class</b> | 8   |
| <b>Packing Group</b>           | I   |

**OTHER INFORMATION**

Protect from physical damage. Keep drums in upright position. Drums should not be stacked in transit. Do not store drums on wooden pallets.

**15. REGULATORY INFORMATION**

**U.S. Federal Regulations**

**SARA 313**

Section 313 of Title III of the Superfund Amendments and Reauthorization Act of 1986 (SARA). This product does not contain any chemicals which are subject to the reporting requirements of the Act and Title 40 of the Code of Federal Regulations, Part 372

**SARA 311/312 Hazard Categories**

|  |     |
|--|-----|
| <b>Acute health hazard</b>               | Yes |
| <b>Chronic health hazard</b>             | No  |
| <b>Fire hazard</b>                       | Yes |
| <b>Sudden release of pressure hazard</b> | No  |
| <b>Reactive Hazard</b>                   | No  |

**Clean Water Act**

This product does not contain any substances regulated as pollutants pursuant to the Clean Water Act (40 CFR 122.21 and 40 CFR 122.42)

# Hydrogen Peroxide 90% HTP

SDS # : 7722-84-1-90-60  
Revision date: 2015-05-28  
Version 1

## CERCLA

This material, as supplied, contains one or more substances regulated as a hazardous substance under the Comprehensive Environmental Response Compensation and Liability Act (CERCLA) (40 CFR 302):

| Chemical name                  | Hazardous Substances RQs | Extremely Hazardous Substances RQs | SARA RQ |
|--------------------------------|--------------------------|------------------------------------|---------|
| Hydrogen peroxide<br>7722-84-1 |                          | 1000 lb                            |         |

Hydrogen Peroxide RQ is for concentrations of > 52% only

## International Inventories

| Component                             | TSCA<br>(United States) | DSL<br>(Canada) | EINECS/EL<br>INCS<br>(Europe) | ENCS<br>(Japan) | China<br>(IECSC) | KECL<br>(Korea) | PICCS<br>(Philippines) | AICS<br>(Australia) | NZIoC<br>(New Zealand) |
|---------------------------------------|-------------------------|-----------------|-------------------------------|-----------------|------------------|-----------------|------------------------|---------------------|------------------------|
| Hydrogen peroxide<br>7722-84-1 ( 90 ) | X                       | X               | X                             | X               | X                | X               | X                      | X                   | X                      |

Mexico - Grade Serious risk, Grade 3

## CANADA

WHMIS Hazard Class C - Oxidizing materials  
D1B - Toxic materials  
E - Corrosive material  
F - Dangerously reactive material



## 16. OTHER INFORMATION

|      |                  |                |                   |                       |
|------|------------------|----------------|-------------------|-----------------------|
| NFPA | Health Hazards 3 | Flammability 0 | Stability 3       | Special Hazards OX    |
| HMIS | Health Hazards 3 | Flammability 0 | Physical hazard 3 | Special precautions H |

### NFPA/HMIS Ratings Legend

Severe = 4; Serious = 3; Moderate = 2; Slight = 1; Minimal = 0

Special Hazards: OX = Oxidizer

Protection = H (Safety goggles, gloves, apron, the use of supplied air or SCBA respirator is required in lieu of a vapor cartridge respirator)

Uniform Fire Code Oxidizer: Class 3--Liquid

Revision date: 2015-05-28  
Revision note Initial Release

### Disclaimer

PeroxyChem believes that the information and recommendations contained herein (including data and statements) are accurate as of the date hereof. **NO WARRANTY OF FITNESS FOR ANY PARTICULAR PURPOSE, WARRANTY OF MERCHANTABILITY OR ANY OTHER WARRANTY, EXPRESSED OR IMPLIED, IS MADE CONCERNING THE INFORMATION PROVIDED HEREIN.** The information provided herein relates only to the specified product designated and may not be applicable where such product is used in combination with any other materials or in any process. Further, since the conditions and methods of use are beyond the control of PeroxyChem, PeroxyChem expressly disclaims any and all liability as to any results obtained or arising from any use of the products or reliance on such information.

Prepared By:

PeroxyChem  
© 2015 PeroxyChem. All Rights Reserved.

End of Safety Data Sheet